Pharmacokinetic/pharmacodynamic modelling to optimize the dose of analgesics and sedatives in children

A dissertation submitted in partial fulfillment of the requirements for the degree of Doctor of Philosophy of Univerity College London

Maddlie Bardol

Primary supervisor: Dr Joseph Standing

Secondary supervisor: Dr Suellen Walker

UCL Great Ormond Street Institute of Child Health

July 2021

I, Maddlie Bardol, confirm that the work presented in this thesis is my own. Where information has been derived from other sources, I confirm that this has been indicated in the work.

Abstract

Analgesic and sedative drugs are mostly used in an "off label" fashion in children. The pharmacokinetic-pharmacodymamic (PK/PD) approach is useful in order to determine the dose-concentration-response relationship and therefore the optimal dose regimens in different populations. However, this approach has not been fully explored for all analgesics and sedatives. This is mostly due to the complex and multidimentional nature of pain, making it challenging to evaluate objectively their effect particularly in neonates and infants. Hence, there is an important need for PK/PD studies in pain and sedation. This thesis focuses on analysing clinical trial results on specific areas that lack good quality PK/PD data in order to optimise the dose of analgesic and sedative agents in children.

The studies described in this thesis aimed to address the following questions: what is the optimal dose of fentanyl for procedural pain in preterm infants (NEOFENT study); what is the adequate dose regimen of fentanyl and clonidine to provide an adequate pain and sedation management in asphyxiated newborns receiving hypothermic treatment (SANNI study); and finally what is the optimal dose of clonidine and midazolam in the PICU (CloSed study). In order to address these questions, PK and PK/PD models were developed in order to describe the relationship between drug concentration and analagesic/sedative effect using pain and sedation scores. These models were used to define target concentrations and perform simulations to determine the optimal dose.

The results of the NEOFENT study showed that three genetic variants had a significant influence on the fentanyl clearance and suggested an IV dose of 2 $\mu g/kg$ for procedural pain in preterm infants. The results of the SANNI analysis showed that the hypothermic treatment significantly decreased the clearance of both fentanyl and clondine. Finally, the models developed for the CloSed and SANNI studies suggested that the dose routinely prescribed in clinical practice should be increased in order to provide an adequate pain and sedation management.

IMPACT STATEMENT

The findings of this thesis improve our knowledge on the adequate use of sedatives and analgesics in children using non-linear mixed effect modelling. The PK/PD models developed in the different chapters provide information on the optimal dose of analgesics and sedatives necessary to provide adequate pain and sedation in specific paediatric populations. In addition, subgroups that require dose adjustments were determined by identifying covariates that affect the PK of the drugs.

The results of the NEOFENT chapter highlight the influence of genetic variants on the fentanyl elimination in preterm infants. The PK/PD model developed in this chapter was also used to suggest an optimal dose of fentanyl that could be given to this population in clinical practice. The results of the SANNI chapter show that hypothermia affects clonidine and fentanyl elimination by reducing the clearance of both drugs in asphyxiated newborns receiving hypothermic treatment. The findings of the CloSed and SANNI chapters support the hypothesis that the dose of clonidine alone should be increased in children in order to provide adequate pain/sedation management and therefore suggest that clonidine should be given in combination with other sedatives.

In this thesis, target concentrations for fentanyl, clonidine and midazolam were defined in specific peadiatric populations using PK/PD models and optimal doses for these drugs were suggested using simulations. Together these findings could be used in clinical practice to improve pain and sedation management in children.

ACKNOWLEDGEMENTS

There are many people who I would like to thank for their support during my PhD.

First, I would like to thank Joseph Standing for his great supervision during these three years as well as his guidance and patience. And Suellen Walker for her help and support.

I would also like to thank all the participating children, their parents and the hospital staff as well as the Neofent, CloSed and SANNI teams for trusting me with these projects.

To the students and staff of the Institute of Child Health for their help and making this PhD a pleasant experience in the office.

Finally, I would also like to thank Iris Condamine, Ana Nehvonen and Leonard Dubois for their support during my PhD and my family who always believes in me.

Contents

List of Figures

List of Tables

1 Introduction

1.1 Pain and sedation in children

Pain is defined as "an unpleasant sensory and emotional experience associated with actual or potential tissue damage, or described in terms of such damage" (1). Recognising and treating pain early in children is essential in order to limit distress and avoid physical and psychological outcomes (2, 3). However assessing pain in children is a complicated task especially in infants and neonates. This is due to the multidimensional nature of pain perception which differs for each child and their difficulty to express their distress in a way well understood by adults who have to learn the language of the child's pain expression. Hence, pain is frequently inadequately treated (2, 4).
Infants and neonates are particularly vulnerable to pain and stress exposure because pain mechanisms are still in development during the first years of life (3). Thus, there is a risk of adverse consequences later in life on both mental and physical health. Reports have shown that repeated painful stimuli during the neonatal period might influence normal brain development (5). As a consequence, somatosensory processes might alter pain sensitivity later in life (6, 7, 8, 3). For example, it has been observed that term newborns who had undergone circumcision without analgesia were more sensitive to immunization than the uncircumcised infants (9). Studies have also shown a higher risk of cognitive development alteration in preterm infants and newborns who experienced neonatal intensive care (10).

Sedation and change in level of consciousness can be caused by administration of sedative and analgesic medications (11, 12). Levels of sedation can be ranked as follows (11):

- Minimal sedation: anxiolysis is provided but the patient is still conscious.
- Moderate sedation: at this state, a depression of consciousness is observed but the patient can breathe independently and respond to verbal commands.
- Deep sedation: the child has difficulties to stay awake but reacts to appropriate stimulations. At this state, the patient might need ventilatory support.

- General anaesthesia: the child looses consciousness. This is a state during which the patient is unresponsive to stimulations and may need breathing assistance.

The level of sedation needed is different for each child and depends on the desired effect which can be anxiety relief, pain or agitation control. For this reason, individualized care and identification of the child's needs are essential in order to provide an appropriate sedation (13, 14). However, several studies have shown that in many cases, patients do not receive adequate sedation (15).

1.1.1 Developmental pathophysiology

Pain stimuli (mechanical, thermal or chemical) leads to activation of peripheral pain receptors called nociceptors. The signal is conducted to the spinal cord via different primary afferent nerves which undergo anatomical changes after birth. The nerve distribution and functionality are developing with age changing the balance between excitatory and inhibitory signalling. As a result, the spinal reflex is more generalized in newborns increasing their sensitivity to less intense stimuli (3, 7). Due to the maturation of these pain mechanisms, the degree of pain response changes with age. Physiological and behavioural pain responses are different for each child since it depends on age, sleep state, previous pharmacological treatments and experiences (16).

Furthermore, invasive medical care such as surgery can induce "trauma" and thus a stress response leading to changes in their metabolism, endocrinology and immunology. Stress response is the result of the activation of both the hypothalamic–pituitary–adrenal (HPA) axis and the sympathetic-adrenal-medullary (SAM) axis in the central nervous system (CNS) as well as the action of cytokines produced locally which act in the CNS (17). Because of the developmental differences discussed above, it has been argue that the children might need a higher dose of sedatives in order to reduce this stress response and maintain the physiological stability (avoid fluctuation of blood pressure, heart rate, oxygen saturation and intra-cranial pressure) (18, 19).

Before administering analgesics and sedatives in young infants and neonates, it is essential to evaluate the potential risks and benefits individually for each child. The

analgesic effect has to be balanced against the potential drug adverse reactions (acute and long term) which depend on the dose and type of agent. Studies have shown that general anaesthetics and analgesics may have adverse neurodevelopmental effects when they are administered in a prolonged way during the neonatal period (7, 20). Agents that have been associated with such neurotoxic effects in laboratory animals are primarily barbiturates, propofol and ketamine (2, 13).

1.1.2 Pharmacological treatments

In PICU, sedatives and analgesics are used alone or in combination in order to relieve the pain and stress in various situations such as procedural pain (e.g. endotracheal intubation), perioperative and postoperative pain management (21). Relatively few pharmacological trials have been conducted in children particularly in neonates and infants for analgesics and sedatives (22). Many of these drugs are prescribed in an "off label" fashion. In USA, only 30% of the medications prescribed in children were properly studied in paediatric population (23). In Europe, more than 90% of the newborns are exposed to drugs prescribed "off-label" in neonatal intensive care units (NICU) (24). In this case, "Off-label" use means that the drug is licensed in adults but is still prescribed in children outside the group age (e.g neonatal group) defined by the license terms of the product. However, because of differences in pharmacokinetics (PK) and pharmacodynamics (PD) due to developmental changes, children can't be considered like small adults and therefore it is not accurate to assume that the drug effect is the same in adults and children (8). Inadequate extrapolation can lead to under and overdosing which can cause side-effects especially in neonates (25). The risk of adverse effect is different for each drugs. Respiratory events are the most common and dangerous adverse reactions of both analgesics and sedatives when prescribed in peadiatric population and therefore should be carefully monitored (26). When possible, a single drug should be prescribed in order to improve the child safety (26).

Paracetamol is the analgesic most commonly used in children to relief pain. Correct dosing associated with a favourable safety profile and efficacy has now been elucidated

(27, 28, 29). In addition, paracetamol presents the advantage of reducing the need of opioids. Studies have shown that when prescribed in combination with paracetamol, the dose of morphine could be significantly reduced in term neonates and preterm infants (21).

Similarly, non-steroidal anti-inflammatory drugs can provide benefits alone or as part of multimodal analgesia if there are no contraindications in the individual patient (28, 29). However, the use of these drugs have been limited because of their adverse reactions which include gastric irritation, haemorrhage and kidney lesion (21).

In children as in adults, opioids remain the gold standard treatment for moderate and severe pain during postoperative settings and invasive procedures (30). Morphine is the most prescribed opioid for perioperative pain in infants and children followed by fentanyl. Although the benefit of opioids in preterm infants is clear for acute pain, its long term use in NICU may be associated with adverse effects that may be exacerbated by dose-dependent hypotension (20, 7). For this reason, the use of opioids should be as short as possible and carefully monitored by the carers. There is a clear need for additional PK/PD data to inform opioid use in neonates, infants and children. In addition, pharmacogenetic differences may also need to be considered. For instance, ultra rapid metaboliser phenotypes of CYP2D6, one of main enzyme in charge of the codeine and tramadol metabolism have been associated with several deaths related to respiratory depression. As a result, the FDA no longer recommends the use of codeine for children under 12 years old (31, 32, 33).

With regard to sedation and until recently, benzodiazepines such as midazolam and lorazepam were the first line agents. They are routinely prescribed in combination with opioids for post-operative pain management. Midazolam is the most common benzodiazepine used in children because it induces anterograde amnesia in addition to anxiolysis and sedation. This effect is particularly convenient in PICU and NICU since it minimizes the recall of unpleasant events. However, midazolam might cause many adverse effects such as agitation, tolerance, dependence and withdrawal symptoms (34). Moreover, studies have shown that its long term use may alter the brain development

(34, 35).

For these reasons, the use of alpha-2-adrenergic receptor agonists such as clonidine and dexmedetomidine has been increasing in recent years (36). These drugs present a clear advantage in terms of safety with lower incidence of withdrawal, respiratory depression as well as agitation and delirium (13). In addition, several studies show that both drugs reduce the need of opioids in children. Dexmedetomidine has been described as effective as benzodiazepine in term of anxiolysis and sedation, therefore it can be used as sole agent to provide adequate short term and long term sedation in non intubated children. Alpha-2-adrenergic receptor agonists can cause hypotension and bradycardia which might limit their use particularly in cardiac patients, however safety studies report a low incidence of such adverse reactions in peadiatric population (4).

Propofol is the most common drug used for procedural sedation in infants and children (37). Since propofol was one of the first anesthetics commercialized, many studies including several PK/PD modelling analysis have been published. Hence, its safety and efficacy are well documented for children over 3 years old (38, 39, 40, 41). Among other adverse reactions, propofol can cause cardiovascular instability (hypotension) and respiratory effects (desaturation and apnoea) (42).

Ketamine is widely used in emergency department setting and for procedural pain management in children (13). The popularity of this drug has been increasing recently because it provides anxiolysis and analgesia with a low risk of respiratory depression while maintaining stable hemodynamics (4). However, ketamine might cause neurodegenerative effects in the developing brain. Therefore, it should be used with caution in neonates and infants (43).

1.1.3 Role of Pharmacokinetic/Pharmacodymamic modelling

The pharmacokinetic/pharmacodymamic (PK/PD) approach is used to develop mathematical models which describe and predict the relationship between drug exposure and response intensity (desired effect and/or a toxic effect) (44, 45). Population PK is the approach most commonly used because it provides population PK and PD

estimates and describes the interindividual variability for each parameter which allows the identification of subgroups (e.g responder *vs* no responder). In addition it allows the analyse of unbalanced data with different number of samples by patients (46, 45, 47). In recent years, PK/PD modelling for analgesics and sedatives has been increasing. However, due to the complex and multidimentional nature of pain, it is challenging to evaluate objectively the sedative and analgesic effect particularly in young children. This issue explains why the PK/PD approach has not been fully explored for all drugs (44). PK/PD modelling is an essential tool in pain and sedation, which informs on the appropriate use of analgesic and sedative agents by determining the optimal dose and studying their interaction with complex pain processes (45). There are various application of PKPD modelling in clinical practice; PK/PD models are used for target controlled infusion (TCI), drug interaction models describe the effect of drugs given simultaneously and simulations inform trial design and dose optimisation after commercialisation (47).

1.1.4 Challenge of paediatric clinical trials

Clinical studies conducted in paediatric populations present some challenges for the clinicians. These challenges include ethical considerations, study design, safety, patient recruitment, product formulation and economic considerations (48, 49).

ETHICAL CONSIDERATIONS

When conducting research in children, important ethical implications have to be taken into account. Documents produced by organisations such as World Health Organisation (WHO) and European Medicines Agency (EMA) describing these implications state that children should be included in research studies only if there is no other population in which the drug can be studied. For ethical reasons, clinicians also have to monitor closely pain and discomfort experienced by children during the trials in order to provide adequate care and avoid distress when feasible (48, 49).

STUDY DESIGN

Planning the study design of a paediatric trial is an important step. Factors specific

to the paediatric population must be taken into account such as early stopping, smaller sample size and impact of rescue medications. For this reason, flexible designs which allow sample size re-estimation and adaptive randomisation should be considered. Blood sampling also need to be adapted to the population. The frequency, volume, timing, and type of blood sampling have to be carefully considered when planning the trial since these procedures are more invasive in young children. Moreover unlike adult studies, the trials performed in children do not include healthy volunteers. Therefore most patients receive concomitant medications that must be closely monitored since they might interact with the drug studied (48, 49).

When planning clinical trials in pharmacometrics, additional factors need to considered. The number of subjects and measurements which are reduced in children trials have a high impact in pharmacometric analyses and therefore are an essential part of the study design (48).

SAFETY

In all clinical trials, it is important to measure and monitor the drug toxicity. However, safety assessment in children can be challenging for different reasons. First, adverse effects that do not occur in adults can be observed in children. Secondly, adverse effects might not be detectable in young children because they are not able to express their symptoms. In addition, safety assessment tools might not be validated in children. As a consequence, adverse effects can be under or over-interpreted which can lead to a misinterpretation of the results (48).

PATIENT RECRUITMENT

Patient recruitment is a critical stage of paediatric studies because it presents numerous challenges. Studies have shown that up to 19% of trials conducted in children are terminated early because of issues in the patient recruitment. In addition, there is a large percentage of patient withdrawal that occurs during paediatric studies compared to adult trials. In most cases, the recruitment issues are compensated by using different sites for the study. However, a multicenter study increases the cost and time since regulatory approvals are needed in different regions and/or countries (49).

Several factors explain why patient recruitment is challenging in paediatric studies. Parents can be reluctant to give their consent because of the lack of knowledge about the drug studied and the risks that clinical studies present. It has been shown that even though the benefices and risks of a study are explained to the parents prior their consent, it does not ensure that the parents are making their choice objectively. In addition, the consent process is different across countries (48, 49).

DRUG FORMULATION

In paediatric clinical studies, the drug formulation needs to be adapted to the population. For most studies, the children included are divided by age groups and each group receives a different formulation based on their age and weight. Therefore more than one formulation are needed which can increase the time, cost and resources required. Product availability can also be a challenge particularly if the trial is not done using a pharmaceutical industry as partner. These issues can be reduced if the drug studied is routinely given at the site of investigation (49).

ECONOMIC CONSIDERATIONS

Clinical studies in children are economically challenging for the following reasons. First, the number of patients targeted is smaller compared to a drug given to adults which reduces the market's size. Secondly, the investigators and carers might need to be trained in order to be able to conduct a study in children. As mentioned previously, the formulations need to be adjusted depending on age or weight. In addition, the risk of short and long-term adverse reactions is unpredictable. All these factors explain why clinical trials in paediatric populations are less profitable than in adults and therefore are not conducted as frequently (49).

1.1.5 Clinical challenge in drug dosing

Once a pharmacometric paediatric trial is conducted, one of the main challenges for the clinicians is to apply the findings in clinical practice. This is partly due to the large interindividual variability observed in children. Ideally, the dosage regimens should be adapted to each child individually based on the covariates influencing the

drug PK and PD that can be identified using pharmacometric models. However, this is not always feasible. In clinical practice, some covariates can be challenging to measure routinely (e.g. genetic variants) making it difficult for the clinician to adjust the dose based on such covariates. Most pharmacometric studies suggest doses regimens that differ depending on age/weight groups which is not always easy to apply in clinical practice since it requires to sub-classify the patients. One of the systems that can facilitate this issue is the Target-Controlled Infusion (TCI) system (50). The TCI presents the advantage to administer the drug based on real time PK calculation and to maintain the therapeutic levels within the efficacy/safety margin. It takes into account developmental age and weight and therefore allows to adjust the dose to the individual patient (50). Although TCI systems are used for propofol administration, it has not been developed for most analgesics and sedatives. This can be explained by the lack of PK and PD data available for these drugs. In addition, a robust PK/PD model needs to be developed in order to be able to implement a TCI system. However, this can be a challenging task in children due to the small sample size of patients, the large unexplained interindividual variability, the need of rescue medications and the lack of validated objective tools that can be used as PD endpoints (51).

1.2 Developmental pharmacology

1.2.1 Developmental differences in pharmacokinetics

In paediatric pharmacology, children may not be seen as "small adults". Their response differs in terms of efficacy but also toxicity (52). During childhood, they undergo developmental changes which affects the pharmacokinetic and pharmacodynamic profile of analgesic and sedative drugs . Hence, the dose cannot be simply scaled using linear weight (53). These changes include physical growth, maturation of organs and biochemical mechanisms and they vary considerably between age groups (25).

ABSORPTION

Absorption is the first PK phase for all non intravenous drug administrations. This

process is altered in children. The gastric pH varies after birth and that can affect the drug absorption. The pH is neutral at birth but decreases to 1 within 2 days after birth before gradually returning to neutral at day 8. The pH reaches the adult value only by age 2-3 (54, 55, 56). As a result, the bioavailability of weakly basic drugs is increased and the bioavailability of weakly acidic drugs is reduced (57). Bile acid synthesis and pancreatic lipase function are low during the first year of life, which might affect the absorption of some lipophilic drugs that can't be solubilized properly. In addition, the prolonged time of gastric emptying in neonatal population can cause a delay in the absorption of some orally administered drugs (56).

DISTRIBUTION

The distribution phase is also affected by developmental maturation. The volume of distribution depends on tissue binding, plasma protein binding and properties of the drugs, all different aspects that are affected by developmental changes early in life (56). The weight fluctuates considerably after birth. Newborn infants lose weight during the first days following the birth, then they return to their initial birth weight during the second week of postnatal life and reach a 50% increase weight compared to their birth weight at 6 weeks of life (58). In term newborns, the percentage of body water is high (70% of the body weight) and it progressively decreases to reach 60% around the second year of life. This percentage is even higher in preterm infants (80-90%) (59, 54). On the opposite, body fat increases with age from 10% in term neonates to 20% after the first year of life (56). Compared to adults, the neonates volume of distribution (Vd) is larger for water soluble drugs and smaller for lipophilic compounds (57).

The distribution in children is also affected by a higher membrane permeability. As a consequence, the penetration in the CNS is easier due to the immaturity of the blood-brain barrier (BBB). This may lead to toxicity if the doses are not adapted (54, 59). These physiological changes are particularly important to consider for analgesics and sedatives since these drugs target the CNS.

In addition, infants and neonates have lower concentration of plasma proteins and lower binding capacity which affect both distribution and elimination rate. The active

drugs are able to diffuse more easily in the body resulting in higher Vd and clearance (59, 57). For example, the concentration of alpha-1-acid glycoprotein in neonates corresponds to half of the adult concentration. However, it is important to note that this number increases when the child undergoes surgery inducing stress (56).

METABOLISM

Most drugs are metabolised in the liver although metabolism can also take place in the kidney, gastrointestinal tract and lung (55). The metabolism depends on several factors: blood flow, extraction rate and drug-metabolizing enzyme capacity.

There are two phases in the hepatic metabolism (54). Phase I reactions include oxidation (CYP450), reduction, and hydroxylation whereas phase 2 involves reactions of glucuronidation (UGT), sulfation, and acetylation (57). Organ maturation may impact the efficiency of these reactions by changing hepatocellular distribution and expression of the enzyme involved in both phases (57). Studies suggest three different categories of metabolism enzymes based on their patterns of development; the class 1 corresponds to the enzymes with a high foetal concentration that significantly decreases at birth, class 2 represents the enzymes that stay stable during the development and the class 3 corresponds to the enzymes which have a low concentration during the gestation and increase substantially after birth (58). Most enzymes of phase I are 50% mature at birth and reach adult activity at the end of the first year of life. Regarding the enzymes of phase two, there is a large variability of maturation depending on the type of enzymes (55). For example, UGT enzymes reach their adult activity at the end of the infancy whereas sulfotransferases are already active at birth (57). These enzyme deficiencies early in life can increase the risk of toxicity and should therefore be taken into account when defining the safe dose for young infants.

The drug distribution can also be affected by uptake and efflux transporters of the hepatocytes such as anion transporting polypeptides (OATPs) and P-gp, respectively. The developmental expression of such transporters has not been well described in the literature. However, studies suggest that P-gp expression increases gradually to reach the adult levels after 2 years of life (56).

ELIMINATION

Most of the drugs are excreted though urine and faeces although other routes of elimination are possible (i.e. saliva, sweat, breast milk) (55). Renal elimination depends on three processes: glomerular filtration, tubular secretion, and tubular re-absorption (54). These processes are reduced at birth, which explains why newborn renal activity is only of 35% (25). Functional renal development is associated with an improvement of these three processes, an increase of renal blood flow and a maturation of renal tubules. Glomerular filtration undergoes rapid maturation during the first two weeks whereas maturation of tubular secretion occurs later in life around 15 months. Tubular secretion is reduced at birth to 20-30% of the adult values. Unfortunately, there are limited data describing the maturation of renal tubular transporters (58). Tubular re-absorption (which is an important function for the lipophilic and non metabolised drugs) reaches adult function only after 2 years of age (59). As a result, drug renal clearances are reduced in young infants (57).

In addition, anatomic formation of the kidney occurs during the gestational period *in utero*, between the week 6 and 36. Hence, elimination pathways might be more immature in preterm infants than in term newborns. This also explains why it is more appropriate to use the postmentrual age (PMA) instead of postnatal age (PNA) to describe the renal maturation function (60).

The developmental change in the kidney should be taken into consideration to determine the optimal dose of drugs eliminated in the urine in neonatal population. Because of the immaturity of the kidney, drugs are not eliminated efficiently and therefore the elimination half life is prolonged leading to an increase of risk of toxicity. In that case, the dose can be adjusted either by increasing the dosing intervals or decreasing the dose (56).

1.2.2 Developmental differences in pharmacodynamics

Ontogeny also applies to therapeutic targets that act as mediators of the drug response. Since the biological systems depend on organ maturation, it is challenging to

extrapolate pharmacodynamic profile from adults to children. Unfortunately, very little is known about developmental pharmacodynamics in humans to date (59, 61). However, ontogeny can affect the affinity, density and signal transduction of the receptors as well as biochemical pathways. Therefore it can have a high impact on the drug response and should be taken into account when developing PK/PD models in children. Furthermore, the pathophysiology of certain diseases might be different in children and neonates, and it can therefore impact the drug response (62).

Developmental pharmacodymamics also affect the adverse reactions. As a consequence, young children can have smaller therapeutic windows and therefore be more vulnerable to adverse effects than older children. Although there is a lack of knowledge about the developing brain, it has been shown that some neurotransmitters play a different role in children and in adults. They can act through the same second messenger system than in the mature brain but as developmental regulators (63).

The interindividual variability in children of the PD parameters is expected to be much larger than for the PK parameters (63). However, due to the limited knowledge on the developmental pharmacodymamics, it is challenging to identify and include the covariates that could explain a part of this variability in the PK/PD models (64). Improving our understanding of developmental physiology that leads to PD differences between age groups would help to develop adequate and robust PK/PD models that could be used to determine the optimal dose for different sub-populations (63).

PD changes can also be due to other factors than physiological development which can lead to an overestimation of "real" PD differences. For example, PK differences can cause changes in drug response. As described in the previous section, PK changes with age due to organ maturation and as a consequence, the same dose might result in smaller concentrations in infants and thus, smaller effect. Another factor is the difficulty in adequately measuring a significant effect in children because this effect is too small and the assessment of pain and sedation is challenging in young infants and neonates (62).

Animal models can be used to improve our understanding of developmental pharma-

codymamics. However, such models are challenging to translate to humans for different reasons. First, there is no certainty that the ontogeny of the receptors and pathways is similar in animals and humans. Secondly, animals undergo maturation faster than humans (65).

For instance, animal models have been used to study the developmental response to opioids. These studies show that the expression of opioid receptors as well as opioid binding vary with postnatal age. A rapid increase was observed during the first three weeks following birth. In addition, studies in rats showed that the morphine effect assessed using mechanical sensors was higher in neonates compared to older rats. These findings could explain why the sensibility and selectivity of the opioid response observed in human change with age. A better understanding of opioid receptor density and function in neonates and young infants would help to optimise the dose of opioids in this population particularly vulnerable to opioids adverse effects (63).

1.3 Pharmacokinetic/pharmacodymic modelling in pain and sedation

1.3.1 Pharmacodynamic tools in pain and sedation

Pain assessment is an essential step in order to provide optimal pain management. A regular measure of pain intensity improves pain management and thus the satisfaction of both patients and carers (37). However, it is a complex task particularly in infants and neonates because of the lack of specificity and sensitivity of the available assessment tools for this population. An ideal pain assessment should take into account all factors which influence pain perception including a description of the pain by the child and their parents, the sociocultural context, physical evaluation and individual characteristics such as age, gender and pathology. However, there is no such perfect standard tool.

Three fundamental approaches can be used to assess pain in children. First, self-report which measures the experience of pain as described by the patient. Secondly, observation/behavioural measures, which report the experience of pain as observed by

the medical staff or patient's family. Finally, the physiological approach which measures the physiological body reactions caused by the pain (66).

Self report is the gold standard tool. However, in intensive care, a verbal response may be limited by communication, ability to describe pain, or developmental stage. Hence, it is not always possible to use self report particularly in neonates, infants and young children (37). To provide the most accurate measure, the tool has to be carefully described and explained to the child by the carer. It is essential to make sure that the patient fully understands how the tool works before the assessment (67). Behavioural indicators require the presence and expertise of a caregivers. Hence, a large individual variability might be observed depending on the knowledge and observational skills of the carer in charge of the report. In addition, the behaviour can be different for each child making the interpretation of the pain tool challenging (66).

The choice of the approach is different for each child and it is based on clinical setting, available resources and characteristics of the patient. When feasible, self report should be preferred as assessment tool alone or in combination with other approaches because it provides the most accurate description of the pain experience (68). For children between 3 and 5 years old, it has been shown that the self report may be unreliable in certain cases. For this reason, it is recommended to use a behavioural measure in addition with the self report (69).

Physiological measures such as heart rate variability and blood pressure, should not be used alone to asses pain due to the lack of evidence regarding their reliability and validity (66).

Assessment tools from these approaches can be used in PK/PD modelling in order to relate concentration to sedative/analgesic effect. These tools can be divided in two categories: those which evaluate pain and sedation based on human judgement such as self report and behavioural measures and those which monitor it, such as physiological measures. They can be unidimentional if they include only behavioural observations for example or multidimentional if they incorporate a combination of behavioural, physiological and contextual factors (66).

1.3.2 Evaluating pain and sedation

Depending on their age, their ability to communicate and their development status, there are many reliable and valid scales available for children which can be used as PD endpoints to evaluate pain and sedation (70).

For children older than 8 years old and able to communicate, the Visual analogue scale (VAS) and the Numerical rating scale (NRS) are the pain scales of first choice (71, 67, 69). The use of these scales requires a level of development to be able to translate and express the pain in abstract concept such as numbers or distances (71, 70).

For children between 3 and 8 years old, the revised version of Faces Pain Scale (FPS-R) is more appropriate (69). The original FPS which incorporated seven faces was revised by Hicks and al. (72) in order to provide a score which can be easily compared and combined with other pain assessment tools such as NRS scale (73).

Several scales have been validated for younger children (under 3 years old) and/or children not able to express verbally their pain in order to assess pain and sedation. Among them, the Faces, Legs, Arms, Cry and Consolability (FLACC) and COMFORT-behavioural (COMFORT-B) scales are widely used because of their excellent reliability (71). These tools are both based on observations by a carer of behavioural items which reflect the pain intensity and sedation levels (71). The original COMFORT scale was developed by Ambuel *et al.* (74) and includes eight items: alertness, calmness/agitation, respiratory response, physical movement, blood pressure, heart rate, muscle tone, and facial muscle tension. Each item has five possible responses rated from 1 to 5 which provides a total score from 8 to 40 (75). Even though the validity of the COMFORT scale for assessing pain in children has been well established over the years (74, 76, 77), studies have shown that the validity of the scale was improved by excluding blood pressure and heart rate, two items which can be affected by other factors than pain and sedation (75). Hence, Ista *et al.* (78) developed the COMFORT-B score in 2005, a tool derived from the COMFORT score excluding these two physiological items. The COMFORT-B score is widely used in clinical trials for infants between 0 and 3 years old (79). It shows a better validity than the original COMFORT score without losing

information. This scale has later been modified by Van Dijk *et al.* (80) resulting in the COMFORT-neo, a scale able to assess pain and sedation in preterm infants. Both COMFORT-B and COMFORT-neo provide a score between 6 to 30. Thanks to their good reliability, COMFORT-B and COMFORT-neo become the gold standard of pain assessment tool in young children (78, 79, 81). In addition, researches have shown that these scales assess effectively pain changes due to analgesic and sedative administration making it a reliable tool for PD modelling (79).

Many pain scales more specific to newborns are available such as Behavioural Indicators of Infant Pain (BIIP) and the Astrid Lindgren and Lund Children's Hospitals Pain and Stress Assessment Scale (ALPS-neo). ALPS-Neo is a new Swedish scale developed and validated for the first time by Lundqvist *et al.* in 2014 (82). The advantage of this scale is that it evaluates stress in addition to pain for both term and preterm infants. ALPS-neo is an unidimensional scale including 6 behavioural items (facial expression, breathing pattern, tone of extremities, hand and foot activity and level of activity). Each item can take a number between 0 and 2 which gives a total pain score between 0 and 10, 0 being a state with no pain or stress (82). Another tool validated in newborns is the BIIP scale which has been validated for procedural pain assessment. It combines four sleep/wake state indicators, 5 facial actions and 2 hand actions. Each behavioural item takes a score of 1 if it is observed or 0 if not. Hence, the total score can reach 11 (worst pain). The BIIP has been originally developed and validated in preterm infants by holsti *et al.* (83).

Among the scales for assessing pain in newborns, two tools have been validated particularly in preterm infants, Premature Infant Pain Profile (PIPP) and Échelle Douleur Inconfort Nouveau-Né (EDIN) (82). The EDIN scale was originally developed and validated by Debillon *et al.* in 2001. It aims to assess prolonged pain in preterm newborns and includes 5 items: facial expression, body movements, quality of sleep, quality of contact with nurses or sociability, and consolability; each item given a score between 0 (no pain) and 3 (worst prolonged pain) (84). The PIPP score is using physiological (heart rate and oxygen saturation) and contextual factors (gestational age

and behavioural state) in addition to behavioural indicators (brow bulge, eye squeeze and nasolabial furrow) to describe pain in preterm infants. With a total of 7 items, the PIPP gives a score between 0 and 21. The PIPP was developed in 1996 by Stevens and al, and has becoming a reliable and valid tool (70). However, the inclusion of the contextual factors is controversial. For example, a state of deep sleep doesn't relate to pain intensity in every cases (83).

The pain and sedation scales used in this thesis as PD endpoints are summarised in Table 1.

Table 1: Table describing the 4 scales used as PD endoint in this thesis.

	ALPS-neo	EDIN	COMFORT-B	COMFORT-neo
Name	Astrid Lindgren and Lund Children's Hospitals Pain and Stress Assessment Scale	Échelle Douleur Inconfort Nouveau-Né	COMFORT-behavioural	COMFORT-neo
Pain assessed	Continuous	Continuous	Continuous	Continuous
Validated population	Term/preterm newborns	Term/preterm newborns	Term newborns/ children	Term/preterm newborns
Item	Facial expression, breathing pattern, tone of extremities, hand and foot activity-level of activity	Facial expression, body movements, quality of sleep, Sociability, Consolability	alertness, calmness/agitation, respiratory response, physical movement, muscle tone, facial tension	alertness, calmness/agitation, respiratory response, physical movement, muscle tone, facial tension
Score item	0-2	0-3	0-5	0-5
Score total	0-10	0-15	0-30	0-30

1.3.3 Monitoring physiological effects of pain and sedation

There are different tools which monitor pain and sedation and can be used as PD endpoints.

Firstly, it is possible to measure physiological changes due to the autonomic response

to stress induced by pain. This includes measures of heart rate, blood pressure, oxygen saturation, respiratory rate, galvanic skin response and pupillary changes (85, 86). However, heart rate as well as blood pressure, oxygen saturation and respiratory rate have not been validated for pain assessment because of their lack of specificity. It has been shown that changes in these variables can be the consequence of different pathological and psychological conditions other than pain (85). Biomarkers such as cortisol can also be used to evaluate pain (85) . For a better specificity and reliability of the pain assessment, it is recommended to use these physiological measures in combination with behavioural indicators (87).

Quantitative EEG is the most frequent tool used in PK/PD modelling for analgesics and sedatives (38, 39, 40, 41). EEG signal reflects the neuron voltage fluctuation caused by the pain process. The signal is obtained via electrodes placed on the patient scalp and can be analysed using Bispectral index (BIS) or State Entropy (SE) (88, 89). Both BIS and SE scores are correlated to a level of pain/sedation and can be used in PK/PD modelling to evaluate the analgesic/sedative effect (90).

The use of magnetic resonance imaging (MRI) and Near Infrared Spectroscopy (NIRS) to monitor pain and sedation has been increasing in recent years (85, 26) mostly because it is non invasive and provides information about location and intensity of pain. Both MRI and NIRS assess pain by detecting changes of cerebral blood flow (91, 85).

1.4 Aim of the thesis

The overall aim of this thesis was to optimise the dose of analgesics and sedatives in children using non-linear mixed effect modelling. More specifically, the aims were to suggest regimen dosages using pain scales to assess efficacy in different specific paediatric populations for which the drugs are prescribed “off-label”.

In the second chapter, the methods used to estimate the PK and PK/PD parameters in this thesis are described. In the third chapter describing the NEOFENT study, the goal was to determine the optimal dose of IV bolus fentanyl for procedural pain in preterm infants. The fourth chapter focused on newborns who received hypothermic

treatment for asphyxia. This study called SANNI1 aimed to determine the optimal dose combination of fentanyl and clonidine in this specific population. The fifth chapter presents a study called CloSed that aimed to compare clonidine and midazolam and suggest an adequate dose regimen for both sedatives in children.

In order to determine the optimal dose of fentanyl for the NEOFENT study, a PK model was first developed for fentanyl in preterm infants and this model was then used to develop PK/PD models using four different pain scales: ALPS-neo, EDIN, BIIP and PIPP scores. For the SANNI1 chapter, a PK model was developed for both clonidine and fentanyl in order to identify the covariates influencing their PK and then PK/PD models were developed for both drugs using ALPS-neo and COMFORT-neo in order to determine the optimal dose of both drugs in newborns receiving hypothermia to treat asphyxia. To achieve the aim of the CloSed chapter, the first objective was to develop PK models for clonidine, midazolam and morphine. The second objective was to build PK/PD models for clonidine and midazolam in children using the COMFORT-B scale.

The structure of the chapters 3, 4 and 5 is similar; each chapter starts with an introduction describing the background of the subject, then the methods and results to achieve the main goal are presented. The chapters end with a discussion of the results and a summary of the findings. For each chapter of this thesis, the method and result parts first present the PK model built for the drugs studied describing the effect of covariates followed by a description of the PK/PD models developed in order to establish the relationship between PK and pain scales and determine a target concentration. The last part of the results corresponds to the simulations performed in order to establish the adequate dose of each population using the PK and PK/PD models developed.

2 Parameter estimation

2.1 Modelling approaches

PK data can be analysed using two different approaches: non compartmental or compartmental analysis. Non compartmental analysis (NCA) is a model-independent method which estimates parameters such as maximum drug concentration (C_{max}) and area under curve (AUC). NCA presents some benefits: it is simple, fast, and few assumptions are required. In contrast, the compartmental analysis represents the body using compartments connected to each other and kinetically homogeneous. One of the advantages of this approach compared to NCA is that it can analyse sparse data. This is particularly useful for PK studies in the paediatric population (e.g neonates, infants) for which it is challenging to collect a large number of samples for ethic or medical reasons. In addition, it is easier to analyse PK data after complex infusion administration using the compartmental analysis. Another advantage is that this approach can be used to investigate the influence of various covariates on the PK variability (92).

2.2 Statistical modelling

There are four main methods which can be used to model PK and PD data: naïve pooled data, naïve average data, two-stages and non linear mixed effect approach (NLME). Both naive pooled data and naive average data methods estimate population parameters in ignoring the correlation within individual's data points. Naïve average data is the simplest method, it fits a model to mean values of concentrations calculated for all individuals at each sampling time in order to estimate the PK and PD parameters. This method requires identical sampling times for all individuals and therefore is not ideal to analyse sparse data. The naïve pooled data method pools together all data from all individuals and fits all data at once as if it was only one individual. This model is able to estimate parameters with sparse data, however it performs poorly if the interindividual variability is important leading to an over-estimation of the variability.

Two-stages approach and NLME take into account the correlation within individuals. The two stages approach consists in first, estimate individual parameters by fitting each individual data and then estimate population parameters.

The NLME approach fits a model to all data from all individuals simultaneously in order to estimate PK parameters. However, the model allows the parameters to vary between individuals and therefore it is able to estimate the variability. There are two different sources of variability: interindividual variability (IIV) which is the variance of parameters between subjects and the unexplained variability called residual variability due to noise or model misspecification. The model generates population parameters, their interindividual variability and the variance of residual variability unexplained by the model. This approach is preferred to analyse PK data particularly in the paediatric population since it is appropriate for sparse data and it can be used to investigate the covariates (e.g. age, weight) which can partly explain the interindividual variability estimated by the model. The NLME approach requires modelling software (93).

The software most commonly used in PK studies is the non-linear mixed-effect modelling (NONMEM) which maximizes the likelihood function in order to estimate the population parameters that are most likely to occur. NONMEM provides an objective function value (OFV) which corresponds to the minus 2 log likelihood with a chi-squared distribution. The difference between two OFV can be used to compare nested models (a difference of 3.84 and 6.63 corresponding to a p-value of 0.05 and 0.01 respectively). In NONMEM, IIV and residual errors are assumed to follow a normal distribution of mean 0 and variance estimated by the model.

2.3 Pharmacokinetic models in children

In paediatric population modelling, it is necessary that the model accounts for changes in size and age due to the growth and development of organs over time. For children older than 2 years, a scaling based only on size usually adequately describes the PK parameters. However for younger infants, maturation of glomerular filtration and enzymes involved in drug metabolism should be taken into account since organs such as

the liver and kidneys are still in development during the first months of gestation (94, 95). A standard method of scaling for size and maturation is to fix the allometric weight exponent to 0.75 and use a sigmoidal maturation function driven by post menstrual age (PMA) to estimate the fractional decrease in allometrically scaled clearance with decreasing age (95):

$$CL_i = CL_T \cdot \left(\frac{WT_i}{70}\right)^n \cdot \frac{PMA_i^{Hill}}{PMA_{50}^{Hill} + PMA_i^{Hill}}$$

Where CL_i is the drug clearance in an individual, CL_T is the typical CL for a 70 kg adult, WT is the body weight, n the allometric weight exponent, PMA_{50} is the PMA (weeks) when the maturation has reached 50%, and $Hill$ is the shape parameter.

However, there are other methods of scaling for size and different types of maturation functions that have been used (96, 97, 98). Germovsek *et al.* (99) compared the fit of all the major types of published model for size and age scaling of clearance in children and found that no model gave superior fit to this standard model describe above. In addition, this method presents the advantage to be suitable for the analyse of PK studies that include different age populations and to allow the the comparison of clearance estimated by the model with values previously published in the literature.

2.4 Pharmacokinetic/pharmacodynamic models

There is no standard method to develop a PK/PD model. Either PK and PD can be estimated simultaneously ("simultaneous" method), or first the PK model is built, then the PD is estimated with the PK parameters fixed if the model is unstable ("sequential" method) (100). There are different ways to model the PD variables depending on whether the variables are continuous or categorical. For continuous PD variables such as VAS scale or EEG index signal (BIS and SE), linear, log linear and $Emax$ models are usually used (38, 101). Often a delay between observed concentration and effect occurs, in which case effect compartment models and indirect response models can be used to describe the data (102). For categorical PD variables, the data are analyzed

with logistic regression. A model of cumulative probabilities can be used to describe ordinal categorical data such as the COMFORT scale. However Peeters *et al.* in their PK/PD study of propofol in children modelled the COMFORT score as a continuous variable with an $Emax$ value corresponding to the maximum score of the scale (103).

2.4.1 Models for continuous response variables

Continuous variables are numeric variables that can take on any score or value within a measurement scale. The difference between each of the values has a real meaning. There are two main types of continuous variables, interval and ratio. Interval variables have numerical values which can be ordered and the distance between each score is equal and static (e.g temperature). If this variable has a clear 0 point which indicates that there is none of that variable and the ratio of the scores make sense, this variable is called ratio (e.g weight, age, distance). For instance, if respondents were being surveyed about their pain levels on a scale of 0-10, a respondent with a pain level of 10 should have twice the pain experienced as a respondent who selected a pain level of 5.

2.4.1.1 Direct models

Firstly, it is important to define the PD model which describes the response data. The direct models are the most commonly used PD models in the literature due to its simplistic but also mechanistic nature (102). In these models, a change in blood drug concentration causes an effect which can be observed instantaneously. These models can be linear and log linear which suppose a proportional relationship between concentration or log-transformed concentration and effect as described by the following equations (102):

$$E = m \cdot C_p + E_0$$

$$E = m \cdot \log(C_p) + E_0$$

Where E is the effect, C_p is drug plasma concentration, E_0 the baseline effect, m is

the slope.

The linear model may provide a good description of concentration-effect for small concentration ranges. However, the log linear model is more appropriate for concentrations that produce effects between 20% and 80% of the maximum effect (E_{max}). These models have some disadvantages since they are not able to predict a saturated E_{max} for high concentrations. This issue is removed in the E_{max} model:

$$E = \frac{E_{max} \cdot C_p}{EC_{50} \cdot C_p}$$
$$E = E_0 + \frac{E_{max} \cdot C_p}{EC_{50} \cdot C_p}$$

Where E is the observed effect, E_{max} the maximum effect, EC_{50} is the drug concentration for 50% Emax effect observed, E_0 the baseline effect and C_p the drug concentration.

The limited resources of biological systems (e.g. receptor protein) are taken into account in this model by the notion of maximum effect (104). When the effect is between 20% and 80%, the relationship between Cp and effect is log linear. The slope of this log linear function can be controlled by adding an exponent to the Emax model; this model is called sigmoidal Emax model:

$$E = E_0 + \frac{E_{max} \cdot C_p^n}{EC_{50}^n \cdot C_p^n}$$

When n >1 , the hyperbolic function becomes sigmoidal hyperbolic. However in PK/PD this n parameter has no real physiological meaning. For n<1, Emax/2 is reached quickly then the evolution to Emax is slow whereas for n>1 Emax is reached more rapidly with lower concentration (Figure 1).

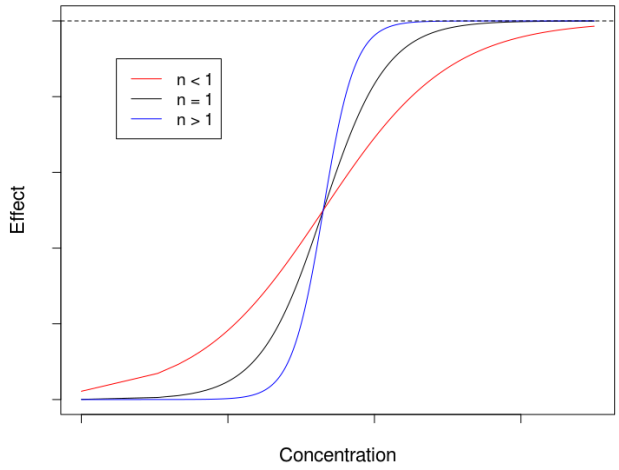

Figure 1: Plot of a sigmoidal Emax model with a logarithmic abscissa and three different values of n

It is common to observe a time delay between a dose given and the observed effect. In this case the PK and PD don't belong to the same compartment. A plot of the effect versus concentration would show a hysteresis which is the typical curve observed in indirect response models. Hysteresis describes the time delay between plasma concentration and effect and can be caused by different physiological mechanisms such as sensitisation or formation of active metabolites (105).

2.4.1.2 Effect compartment model

In case of hysteresis, the PK/PD model commonly used is the biophase model also called effect compartment model. The concept is to integrate a hypothetical effect compartment to the PK compartment models as described in the Figure 2.

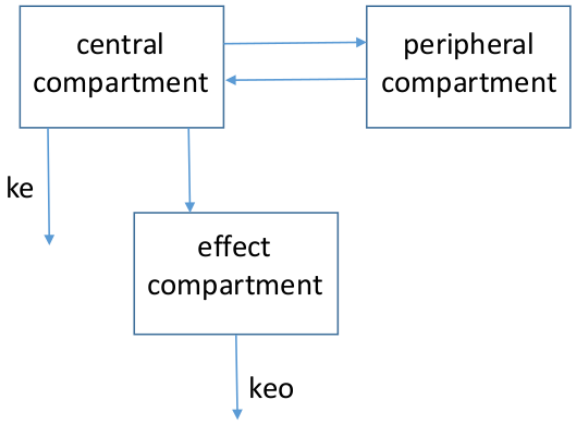

Figure 2: Representation of a biophase model

It is assumed that the amount of drug in the effect compartment is negligible and therefore the mass balance in the system is not affected. By adding the hypothetical effect compartment, the drug concentration in the effect compartment is then linked with observed PD effect.

K_{eo} is the equilibrium rate constant and determines alone the time delay between observed drug concentration and PD effect. Thus it is essential to estimate this parameter. At an extreme scenario where K_{eo}. is estimated as a very large value, this suggests a fast equilibrium between plasma and effect compartments and therefore the effect compartment can be removed without a delay in effect. In case of a delay in effect, the effect compartment can be then regarded as a direct model making possible the use of direct pharmacodynamic models such as a E_{max} sigmoid model to describe the effect.

2.4.1.3 Indirect response model

The indirect response corresponds to the PD response caused by the drug which alters the production (K_{in}) or dissipation (K_{out}) process of endogenous factors. Drugs are able to inhibit or stimulate these processes. For example, the NSAIDs inhibit the production of endogenous pain mediators which results in pain reduction. Although this model is frequently used in PK/PD modelling within other therapeutic areas for adult

and paediatric populations, it assumes the measurement and inclusion of a biomarker which is rarely used to assess pain and sedation. Hence, there is no indirect model published to date describing the effect of analgesics and sedatives in children.

2.4.2 Models for categorical PD variables

A categorical variable is a measurement scale composed of a set of finite number of categories or distinct groups which can be ordinal or nominal. A nominal variable does not have an intrinsic order and is called binary or dichotomous if it has only two possible outcomes such as gender or awake versus asleep. However in clinical practice, variables are commonly rank ordered as in sedation and pain scores (e.g COMFORT scale) . In this instance, the data is described as ordinal categorical data.

2.4.2.1 PK/PD analysis of binary data

The analysis of binary endpoints involves logistic regression. To model this type of data, it is important to understand the statistical basis. The two categories can be quantified as "success" (S) and "failure" (F). The response R is denoted by 1 for S and 0 for F. The corresponding proportion or probability P has a Bernouilli distribution as described in the following equations (102):

$$P(S) = \pi$$

$$P(F) = 1 - \pi$$

$$P(R = r) = \pi^r (1 - \pi)^{1-r}$$

Since the response changes with time following drug administration, the goal of PK/PD is to describe the relationship between those binary endpoints Y and variables x ($E(Y|x)$), such as dose and time. This expectation is expressed as a linear function $E(Y|x) = \beta_0 + \beta 1_1 x$ where *beta* are constants. Because of the binary nature of the data, π can take values only between 0 and 1. To ensure this, it is necessary to transform p from onto a $-\infty$ to $+\infty$ which is done using the logistic transformation or *logit*. The *logit* transforms the 0 to 1 probability scale to a $-\infty$ to $+\infty$ scale and is expressed as

a function of pi (102):

$$logit(\pi_i) = ln\left(\frac{\pi_i}{1-\pi_i}\right)$$

In PK/PD modeling, many strategies can be adopted to evaluate the influence of the PK (exposure) and covariates on this response. These variables have to be implemented on transformed scales, as is shown is the following example (102):

$$Logit(\pi_i(t_j)) = \theta_1 + \theta_2 C_e(t_j) + \eta_i$$
$$P_j = \frac{e^{Logit_j}}{1 + e^{Logit_j}}$$

Where $C_e(t)$ represents the drug concentration at effect site at time point t for the jth patient j which can be linear or folow an E_{max} model, $thetas$ are the $Logit$ baseline, η the residual error for the observation which is independent and follows a normal distribution with mean 0 and variance ω^2 and P is the predicted probability of success S in the jth patient.

2.4.2.2 PK/PD analysis of ordinal categorical data

To analyse ordinal categorical data, the probability of an observation instead of the numerical value of this observation is used. Several approaches can be used to model these data. The most common method is called the proportional odds model (PO) which is a logit model for cumulative probabilities (106). Recently, more sophisticated approaches have been developed such as the bounded integer (BI) which respect the bounded nature of such data using a probit-based approach.

2.4.2.2.1 Proportional odds model (PO)

This model has been described for the first time in PK/PD modelling by Lewis Sheiner in 1994 (107). Since then, this approach has been applied widely to model ordinal categorical data in various therapeutic areas such as pain and sedation. If necessary, it is possible to merge original categories into a lesser number of categories, especially when a small number of observations are available for each category.

The proportional odds model is parametrized in order to estimate the cumulative probabilities in the logit scale. The response is able to take different values Y of probability $P(Y)$. If we consider a trichotomous variable $Y = 1, 2$ or 3 the probabilities can be modelled as following:

$$P(Y = 1) = 1 - P(Y > 1)$$

$$P(Y = 2) = P(Y > 1) - P(Y > 2)$$

$$P(Y = 3) = P(Y > 2)$$

For this model, the probability needs to be transformed in logit function in order to ensure the probability to be between 0 and 1.

$$Logit[P(Y >= j)] = \alpha_j + \beta x$$

Where α represents the logit baseline probability for each category ($\alpha_1 < \alpha_2 < ....\alpha_j$), β is the parameter identical for all categories and x is the effect of explanatory factors called predictors which can be the drug effect, dose effect, biomarkers and other variables (106).

It is important to note that the parameters are estimated on the logit scale and therefore can't be compared with the values estimated by a continuous model (106, 108).

In the proportional odds model, time effect can also be a significant predictor, however the potential relationship between a current observation and the previous one is not taken into account (no Markov element) (109).

An important assumption of the proportional odds model is that the predictor effect is the same for all the categories which might be inaccurate when analysing complex categorical scales with composed scores.

2.4.2.2.2 Bonded integer model (BI)

The BI model which has been developed in 2019 by Wellhagen *et al.* uses a probit-based approach to provide the probability of the scores. The concept of this model is

to assume a grid defined by quantiles of the normal distribution in which each patient has a location described by its mean and variance over time (110).
More precisely, the model uses cut-off values to divide the area under a standard normal distribution (of mean 0 and variance 1) into areas of same size. The number of sub-areas corresponds to the number of categories of the scale. The cut-off values are defined using the probit (or quantile function of the standard distribution). The probability of each score corresponds to the the area under a variable defined function within the interval defined by the cut-offs.

The BI model is a flexible model in which a markov element can easily be added in order to allow the model to take into account the correlation between two consecutive observations (110).

2.5 Model evaluation

The model evaluation of a model includes the assessment of goodness of fit, stability and reliability. The methods of model evaluation can be divided in two categories: internal (basic and advanced) and external.

Basic internal methods include mostly goodness of fit (GOF) and the reliability of parameter estimation using relative standard error (RSE) for example. The standard estimate used to calculate the RSE can be obtained using a bootstrap analysis or the covariance step in NONMEM. If the parameters are adequately estimated by the model, the RSE should not exceed 50%.

The typical diagnostic plots used as goodness-of-fit are population predictions (PRED) and individual predictions (IPRED) versus observations (DV). If the model describes well the data, a symmetry should be observed around the unit slope line. Plot of conditional weighted residuals (CWRES) or weighted residuals (WRES) versus PRED or TIME are also commonly checked to investigate the distribution of standardized residuals. If the residuals are following a normal distribution N (0,1) indicating that the model fits well the data, the CWRES should be dispersed between -2 and 2 and no pattern should be observed over time. The plot of IWRES versus TIME or

IPRED can be used to analyse if the error model is adequate. When the data are treated as categorical using for instance the proportional odds model or BI model, the PK/PD models predict probabilities rather than the actual values so the residual does not represent a link between model and data. Therefore, residual errors described above cannot be calculated and residual plots cannot be generated. For the BI model, the goodness of fit can be analysed using diagnostic plot of the Pearson residual for categorical data (PWRES) versus time. As the CWRES, the PWRES should ideally be between the interval [-2, 2] and no trend should be observed over time (110).

Advanced internal techniques include resampling techniques (bootstrap) and simulation-based diagnostics such as visual predictive check (VPC) and normalised prediction distribution errors (NPDE). The bootstrap tests the robustness of the model by generating new samples (ideally 1000) in resampling with replacement from the entire database and then fitting the model to each of these new samples in order to generate multiple parameter estimates. If the model describes well the data, the parameter estimates should fall within the 95% confidence interval produced by the bootstrap evaluation and the median should be close to the estimates obtained with the final model. The VPC simulates a large number of datasets using the parameter estimates of the final model. The model fits the data if at least 90% of the observations are captured by the prediction interval 95%. More recently Bergstrand *et al.* (111) developed a modified version of the VPC called prediction-corrected visual predictive checks (PC-VPC) that corrects the prediction taking into account independent variables such the dose.

External evaluation methods consist in testing the final model using a different dataset to the one used to develop the final model (92).

2.6 Systematic verification and validation of the models

In addition of the main evaluation methods presented in the previous section, different aspects were systematically verified after running a model in order to validate it. First, it was checked that NONMEM provided the message “optimisation successful”

meaning that the model ran successfully. Secondly, we verified that non of the parameter gradient was equal to 0 which would mean that the model was not able to estimate these parameters. Thirdly, we ensured that the parameter estimated were biologically plausible. Finally, the shrinkage for each parameter estimate was checked to ensure that they were all below 30%.

3 Pharmacokinetic/pharmacodynamic modelling of the results of the NEOFENT trial

3.1 Introduction

3.1.1 Fentanyl pharmacology

Fentanyl is widely used in children. It is the opioid the most prescribed in the NICU in the United Kingdom (UK) (112, 113). Fentanyl is a synthetic opioid first synthesized in 1960 in Belgium (114). The drug binds both μ and κ opioid receptors and has analgesic, sedative and aesthetic properties (112). Its molecular formula is C22H28N20 and its molecular weight is 336.5 g/mol. Fentanyl is prescribed in children for invasive surgery or painful procedures such as intubation (21). Fentanyl is commercialised in various forms such as IV formulations, sublingual tablets, nasal sprays and transdermal patches (115). Fentanyl is often prescribed with sedatives such as midazolam. The combination midazolam/fentanyl has been shown more efficient than midazolam alone in mechanically ventilated children (116). In several clinical studies, pain scores as well as heart and hormone rates have been shown significantly reduced in infants after administration of fentanyl proving the efficacy of the drug in this population (113).

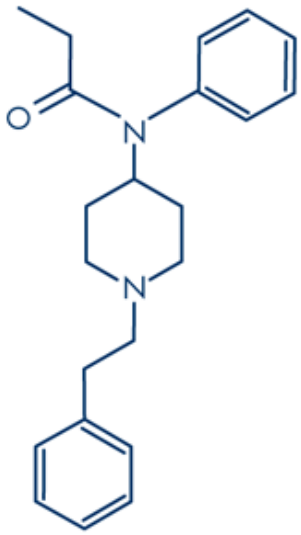

Figure 3: Fentanyl structure

3.1.1.1 Fentanyl toxicity

As all the μ receptor opioids, fentanyl presents numerous adverse reactions such as fatigue, sedation, nausea, vomiting, dizziness, respiratory depression and bradycardia (115). Depending on the dose, fentanyl can cause chest wall rigidity and respiratory depression (117, 113). Chest wall rigidity is a well known severe adverse reaction of bolus IV administration of fentanyl that can be better controlled when the drug is given via slow infusion (21). In addition, prolonged administration of fentanyl can lead to dependence and tolerance which result in withdrawal syndrome, a adverse reaction particularly undesired in young children (113).

In preterm infants, it has been shown that fentanyl can be associated with a decrease of reflex, impairment of motor skills and brain size reduction (118). These effects seem to be more important in case of high cumulative doses (119).

3.1.1.2 Fentanyl pharmacokinetics

Fentanyl has a high gastrointestinal permeability, but it has a low bioavailability (30%) due to a high first pass metabolism (120). As a result, there is no oral formulation available (120).

Fentanyl has a high volume of distribution between 5 and 17 L/kg in young children. Because of its lipophilic properties (log P = 4), it is rapidly distributed to muscles and fat tissues. The compound crosses the BBB by both diffusion and active transport mechanisms to reach the CNS, the principal target of the drug (112). Around 80-85% of the drug binds to plasma proteins, mainly alpha-1-acid glycoprotein.

Fentanyl is metabolised in the liver by the CYP3A4. The drug undergoes a N-dealkylation to provide its main inactive metabolite, norfentanyl. A minor metabolite is produced as well following a N-hydorxylation (117). 75% of the drug is eliminated in the urine, of which 10% corresponds to unchanged fentanyl (112). The half life is very variable between patients, it has been observed that the half life is longer in newborns (6-32h for preterm infants) compared to older children (2-3h) (121, 112).

Due to their organ immaturity, newborns and particularly preterm infants have higher

blood flow and altered protein binding that affect both distribution and elimination of fentanyl. As a result, the volume of distribution is higher in this population and fentanyl clearance varies widely in young children following the maturation of the organs involved in the drug elimination. In noenates, clearance is significantly reduced compared to adults even when scaling for body size with allometric scaling (112,122).

3.1.2 Previously published models

Fentanyl pharmacokinetics have been well described in the literature by compartmental and non compartmental analyses (123, 124, 121, 125). A large interindividual variability on the fentanyl clearance was observed in children particularly in newborns and preterm infants (126). The majority of the previous PK studies explained a part of this variability using age and weight as covariates. Table 2 summarize the clearances estimated in neonates by PK analyses published in the literature.

Table 2: Table summarising the fentanyl clearances found in the literature for neonates and preterm infants.

Author	n	Age	Weight (kg)	Clss (L/h)
Völler (2019)	98	Preterm	0.90	0.42
Encinas (2013)	-	Full term	3.0	1.68
Saarenmaa (1999)	38	Preterm, full term	1.8	2.1
Gauntlett (1988)	14	Preterm, full term	2.7	2.2
Johnson (1984)	2	-	3.2	3.1
Koehntop (1886)	14	-	2.9	4.1

Most of the fentanyl compartmental PK studies in children included the effect of weight using an allometric weight scaling with an allometric exponent fixed to 0.75 for the clearances and 1 for volumes (127, 128). Age was included in the majority of the models using postnatal age as covariate. However, it has been shown that the postmentrual age is highly correlated to the CYP3A4 activity in newborn infants since the enzyme is still in development during the the neonatal period (117). No model has

been published to date using a PMA-based maturation function to describe the effect of age on clearance.

Table 1 shows that the clearance of preterm infants is reduced compared to the clearance of term newborns and older children. This is probably due to the immaturity of the elimination pathways which is more important in preterm infants. Recently, two analyses have been published that describe specifically the fentanyl PK in preterm infants: a non compartmental analysis published by Norman *et al.* (124) in 2019 and a compartmental PK model developed by Völler *et al.* (123) in 2018.

In their model, Völler *et al.* (124) included the effect of age on the clearance using both postnatal age (PNA) and gestational age (GA) as follows:

$$CL_i = CL_T \cdot \left(\frac{PNA_i}{PNA_{median}}\right)^{\theta PNA} \cdot \left(\frac{GA_i}{GA_{median}}\right)^{\theta GA}$$

Where CL is the clearance, GA the gestational age, PNA the postnatal age, GA_i individual GA, PNA_i individual PNA, θGA is the exponent for the influence of GA on CL and θPNA is the exponent for the influence of PNA on CL.

The authors found a significant effect of weight only on the central volume of distribution. Each covariate (PNA, GA and weight) was included in the model using a centred multiplicative covariate model. Although the model seemed to adequately describe the fentanyl PK in a large population of approximatively 100 preterm infants, it is not ideal for extrapolation purposes since the authors did not use an allometric weight scaling nor a PMA-based maturation function to describe the influence of weight and age, respectively.

Norman *et al.* (124) used a non compartmental analysis to describe the fentanyl PK in 14 preterm infants receiving fentanyl for procedural pain. These patients were included in the compartmental model described in this chapter. With this approach, the authors weren't able to explain the interindividual variability on the clearance. In addition, they weren't able to find a correlation between pain score and fentanyl concentration.

Only one PK/PD model describing the relationship between analgesic effect and fentanyl PK in children has been published in the literature. This model developed by Encinas *et al.* (129) was a predictive model based on a semi physiologic approach using adult data. In this study, the level of sedation expressed in percentage (100% being the maximum effect) was modelled using a predictive sigmoidal *Emax* model. Based on their results, the authors suggested a new regimen of continuous infusion in newborns. However, there is no PK/PD model in the literature which describing the relationship between fentanyl concentration and analgesic effect using a paediatric cohort.

3.1.3 Rationale

Preterm infants are particularly vulnerable to pain since their brain and pain mechanisms are still in development after birth (119). Compared to older children, preterm infants experience a higher hormonal and physiological response following painful stimuli leading to hyperalgesia, allodynia and prolonged periods of stress (130). In addition, studies have reported evidences that repeated and prolonged expositions to pain early in life could cause alterations in the brain development resulting in neurological impairments in the long term (124, 119). Preterm babies stay in the NICU longer than term newborns and are therefore more exposed to painful procedures such as blood sampling, intubation or line insertion (124).

For this reason, it is fundamental to provide adequate pain management in this population in order to decrease the risk of pain adverse effects. However, drug safety should be carefully considered since the preterm infants are more sensitive to the drug adverse reactions due to the immaturity of their brain and elimination pathways. Hence, it is essential to administer the adequate dose of analgesics in order to provide an optimal effect at the lowest dose possible to avoid adverse reactions (124).

Opioids such as morphine and fentanyl are routinely prescribed for procedural pain management in preterm infants. Their use in newborns should be closely monitored because they might affect normal brain development. Studies in animals have shown that such medications can lead to apoptotic neurodegeneration in newborns. Fentanyl

might be the most adequate opioid for analgesic treatment in preterm infants. It presents numerous advantages in terms of efficacy and safety compared to morphine which might cause a prolonged decrease of brain activity (131, 132). Fentanyl has a faster onset of action and shorter effect duration (132). For these reasons, fentanyl is the opioid most commonly prescribed in the NICU. However, its optimal dose has not been determined in preterm infants.

Additional PK studies are needed in order to describe the fentanyl PK in preterm newborns and determine the covariates that explain the large interindividual variability observed on the parameters. The influence of age and weight on fentanyl PK have been previously described by published PK models. However, only one recent model studied a cohort of preterm infants (123). This model did not include an allometric weight scaling nor a PMA-based maturation function, making the model difficult to extrapolate.

Ontogeny is not the only factor that can influence the drug response (59). Genetic polymorphisms can explain a part of the interindividual variability on the PK and PD parameters. For instance, studies have reported that mutations in genes coding for metabolism enzymes such as CYP450 can cause an induction or inhibition of that metabolism and therefore explain a part of the variability on the clearance. In addition, it has been shown that single nucleotide polymorphisms (SNPs) in genes involved in the opioid mechanisms can also affect the drug response. These mutations might alter the sensitivity of opioid receptors or enzymes and therefore the drug pharmacokinetics (62). More PK/PG studies are needed in order to identify the SNPs which affect the fentanyl PK and determine the optimal dose of fentanyl in these sub-populations.

Because fentanyl might cause significant adverse reactions even at low doses, it is essential to evaluate the PK/PD relationship of fentanyl in this vulnerable population in order to determine the optimal dose. One predictive semi-physiologic model using extrapolation data from adults to predict the PK and PK/PD relationship in term and preterm infants has been published (129). However, there is no previous PK/PD model including clinical data from a neonatal cohort. The target concentration or optimal IV

bolus dose for procedural pain in preterm infants has not been determined.

3.1.4 Aim

The aim of the NEOFENT project was to study the PK and the PK/PD relationship of a new formulation of fentanyl 5 $\mu g/mL$ for procedural pain in preterm infants. This study was used to improve our understanding of dose-concentration-effect relationship of fentanyl and therefore optimize the dose in preterm infants. The other objective of this chapter was to determine if certain gene polymorphisms can explain a part of the interindividual variability observed on the pharmacokinetic parameters and identify subgroups of patients which will need a dose adaptation.

3.2 Methods

3.2.1 Data

The data used for this study have been collected from September 2012 to November 2014 in two Swedish university centres, the NICUs at Skåne University Hospital and at Karolinska University Hospital in Stockholm. The study was registered as EUDRACT (number 2011-000310-19) and monitored by the Unit for Clinical Study Support within Clinical Studies Sweden Forum South. For both investigation sites, the study was approved by the Regional Ethical Review Board for Southern Sweden in Lund. In addition, The European Medicines Agency (EMA) and the Swedish Medical Products Agency both approved the protocol.

A fentanyl formulation of 5 $\mu g/mL$ was produced in Sweden by Apotekarnas laboratorium (manufacturing authorisation number 24;2011/500192). The formulation was suitable for preterm infants and based on the commercially manufactured fentanyl formulation available (Janssen-Cilag AB, Solna, Sweden). It was confirmed that the dilution was stable with a shelf life up to 36 months.

Thirty perterm infants born between 24 and 34 weeks of gestation with a postnatal age below 28 days were included in the study. The exclusion criteria were: concurrent

or previous opioid administration, congenital anomaly, neonatal encephalopathy and renal/hepatic failure. They received 0.5 $\mu g/kg$ during 1 minute within 10 minutes before skin-breaking procedure or 2 $\mu g/kg$ over 5 minutes before tracheal intubation with other short acting drugs (atropine, suxamethonium and thiopentone). Depending on the pain score, a second similar bolus was allowed after 15 minutes.

Blood samples of 0.8 mL used to measure fentanyl concentrations were collected at 10 minutes and 2, 4, 6, 8h post-administration. The number of samples collected was adapted to the patient weight; 3 samples if the body weight was between 600g and 1000g and 2 samples if body weight was inferior to 600g.

The genetic variants tested in the PK/PG study came from genes expressing enzymes involved in the metabolism (UGT2B7, OPRM1, CYP3A7, CYP3A4, COMT, CYP2D6) and opioid receptors (SLC22A1, ABCC1, ABCC3, KCNJ6). The choice of the genetic variants to test was based on the paper published by Matic *et al.* (133). The genotypes of patients were obtained by whole-exome sequencing performed at the Center for Translational Genomics, Lund University and Clinical Genomics Lund, SciLifeLab. In total, 153 different genotypes were analysed.

Pain and stress were assessed using four different pain scales: Échelle de douleur et d'inconfort du nouveau-né (EDIN), Astrid Lindgren and Lund Children's Hospitals Pain and Stress Assessment Scale for Preterm and sick Newborn Infants (ALPS-neo), Premature Infant Pain Profile (PIPP), and the Behavioural Indicators of Infant Pain (BIIP). EDIN and ALPS-neo scores were evaluated every hour for 48h in order to assess continuous pain. PIPP and BIIP scores were used to assess procedural pain.

3.2.2 Fentanyl pharmacokinetic modelling

The data were analysed using NONMEM (version 7.4) and the plots were obtained using R (version 3.4.4).

A NLME model was built to describe the fentanyl concentration data. First, a one-, two- and three-compartment models were tested to define the basic structural model. In order to describe the residual variability, an additive, proportional, and a combined

additive with proportional error model were tested.

Body weight and postmenstrual age (PMA) were included in the model using an allometric weight scaling standardized to a body weight of 70 kg and a sigmoidal maturation function, respectively, as described by the following equation:

$$CL_i = CL_T \cdot \left(\frac{WT_i}{70}\right)^n \cdot \frac{PMA_i^{Hill}}{PMA_{50}^{Hill} + PMA_i^{Hill}}$$

Where CL_i is the drug clearance in an individual, CL_T is the typical CL for a 70 kg adult, WT is the body weight, n the allometric weight exponent, PMA_{50} is the PMA (weeks) when the maturation has reached 50%, PMA_i is the individual postmentrual age and $Hill$ is the shape parameter.

The allometric weight exponent was fixed to 0.75 for the clearances and 1 for the volumes of distribution. The parameters of the sigmoidal maturation function (PMA50 and Hill) were estimated by the model or fixed to values estimated by a previous model published by Anderson *et al.* (134).

Interindividual variability was tested on each parameter in a stepwise fashion using a multiplicative model and included in the model if the objective function decreased of at least 3.84 points.

The concentration values below the limit of quantification (BLQ) corresponding to 0.05 $\mu g/mL$ ($> 10\%$) were included in the model using the M3 method. With this method, the BLQ values are treated as categorical data. Their likelihood functions are maximized with respect to the model parameters but the model assumes that the values are below the limit of quantification (LOQ) (135).

3.2.3 Fentanyl pharmacokinetic/pharmacogenetic modelling

The genetic variants with no minor allele detected or with a minor allelic frequency (MAF) below 5% were excluded of the PK/PG analysis. The remaining genetic markers were tested for Hardy-Weinberg equilibrium in order to detect genotyping errors.

To test the influence of the genotypes on the PK, a screening process was conducted

in order to increase the power of the analysis and avoid false positives since 153 SNPs were tested and only 25 patients were included in the study. The concept was to test the genetic association between variants and fentanyl individual clearances (CLi) extracted from the final PK model using multiple linear regression. This screening was done with the software Plink 1.9 and an additive genetic model was used to test the SNPs. A Bonferroni correction was applied with a p-value of 0.2 in order to select the significant genotypes and avoid false positives due to multiple testing.

Once the SNPs have been selected with the screening process, they were tested one by one as covariate on the clearance using the final PK model with NONMEM. In the dataset, the genotypes for each patient were coded with three variables: 0 (homozygous wild type), 1 (heterozygous type), 2 (homozygous mutant type). In the model, the heterozygous type and homozygous mutant type were grouped and included as follows:

$$CL_i = CL_T \cdot \left(\frac{WT_i}{70}\right)^n \cdot \frac{PMA_i^{Hill}}{PMA_{50}^{Hill} + PMA_i^{Hill}} \cdot (1 + H1)$$

Where $H1$ is equal to 0 for the wild homozygous type and is estimated for the others (mutant type). CL_i is the drug clearance in an individual, CL_T is the typical CL for a 70 kg adult, WT is body weight, n the allometric weight exponent, PMA_{50} is the PMA (weeks) for CL to reach 50% mature, and $Hill$ is the shape parameter.

3.2.4 Fentanyl pharmacokinetic/pharmacodynamic modelling

The PK/PD models were developed using a sequential method. Four different models (one for each pain scale: ALPS-neo, EDIN, BIIP, PIPP) were built in order to describe the relationship between fentanyl concentration and analgesic effect.

First, a continuous Emax model with and without effect compartment was tested to link the fentanyl PK and PD. Then the scores were treated as categorical and a proportional odds model was tested for each scale.

In the proportional odds model, if we consider a vector of categorical response Y_{in} for the ith patient with N observations, the probability that Y_{in} is superior or equal to

the score m can be calculated with the following equations:

$$Logit[P(Y_{in} \geq m|\eta_i)] = f_m + \eta_i$$

$$P(Y_{in} \geq m|\eta_i) = \frac{e^{(f_m+\eta_i)}}{1 + e^{(f_m+\eta_i)}}$$

where $Logit[P(Y_{in} \geq m|\eta_i)]$ is the logit function of the probability $P(Y_{in} \geq m|\eta_i)$. η_i is a normally distributed random variable of mean 0 and variance estimated by the model describing the interindividual variability. f_m denote the function of baseline conditions and predictors.

This function f_m can be described as follows:

$$f_1 = B_1 + f(predictor)$$

$$f_2 = B_1 + B_2 + f(predictor)$$

$$f_3 = B_1 + B_2 + B_3 + f(predictor)$$

where B_1, B_2, B_3 is the baseline probability of a score >= to 1, 2 and 3, respectively. The baseline probabilities of all the categories except the lowest one are estimated by the model and limited to negative values. For the highest category there is no need to estimate this parameter since it is equal to one by definition of the cumulative probabilities. $f(predictor)$ corresponds to the function describing the effect of a predictor.

In this chapter, the predictors evaluated were the drug effect (using the predicted concentration), age (using PMA) and weight. For each predictor, a linear and Emax model was tested.

The objective function of the baseline model without predictor was first estimated. The predictor effect was then added in the model and found significant if it induced a decrease of the baseline OFV of at least 3.84 points.

The categories of score missing in the databases were ignored in the proportional odds model. If the model was not able to find a relationship between fentanyl concentration and pain scores, a proportional odds model in which the scores were grouped into 3 equal categories was tested. These categories can be described as low pain, middle pain

and high pain level.

The target concentration was then graphically determined using the results of the PK/PD model.

3.2.5 Simulations

Simulations were performed with NONMEM in order to determine the optimal dose to reach the target concentration defined by the PK/PD model. A database of 1000 patients with different demographic characteristics (PMA, weight and sex) was generated with R using the Sumpter function (136). This function uses an equation which takes into account the change of weight with PMA to simulate patients with demographic characteristics similar to the population studied. The database generated was then used with the final PK model to performed simulations with different doses of fentanyl (0.5, 1 ,1.5, 2, 3 and 4 $\mu g/kg$). The simulations were limited to 2h which corresponds approximately to the procedure time during which fentanyl is used in preterm infants.

3.2.6 Model evaluation

For all the models developed, the RSE were calculated using the standard error from NONMEM covariance step.

Goodness-of-fit plots were produced in order to evaluate graphically if the PK model adequately described the data. The goodness-of-fit includes the following plots: DV *vs.* PRED, DV *vs.* IPRED, CWRES *vs.* time after dose, and CWRES *vs.* PRED. In addition, a histogram and a QQ-plot of the CWRES distribution were done to ensure the normality and homogeneity of the residual error.

The final PK model was also evaluated using a bootstrap analysis based on 1000 samples of the data using Perl-speaks-NONMEM (PsN).

Both PK and PK/PD models was evaluated using visual predictive check (VPC). 1000 simulations from the final PK model were performed in order to produce the VPC. VPC was done using PsN and the plot was generated using the package Xpose4 in R.

The categorical VPC for the proportional odds model were stratify by score categories for a better visualisation.

3.3 Results

3.3.1 Data

Twenty five preterm infants born with a gestational age between 23.3 and 30.7 weeks were included in the final dataset of the PK study. The demographic data of the patients are summarized in Table 3. 18 patients received 0.5 $\mu g/kg$ before skin-breaking procedures and 7 children received 2 $\mu g/kg$ before tracheal intubation. Only one patient included received a second dose after 15 min.

Table 3: Table summarising the demographic characteristics of the NEOFENT cohort.

	Range	Median
Birth weight (kg)	0.56 - 1.37	0.83
Gestational age (weeks)	23.3 - 34.1	26.7
Postnatal age (days)	0.25 - 28.2	6.90
Postmenstrual age (weeks)	24.5 - 28.2	27.5

In total, 107 samples were used to build the model. Around 13% of the observations were below the limit of quantification. The relationship between concentration and time are presented on Figure 4.

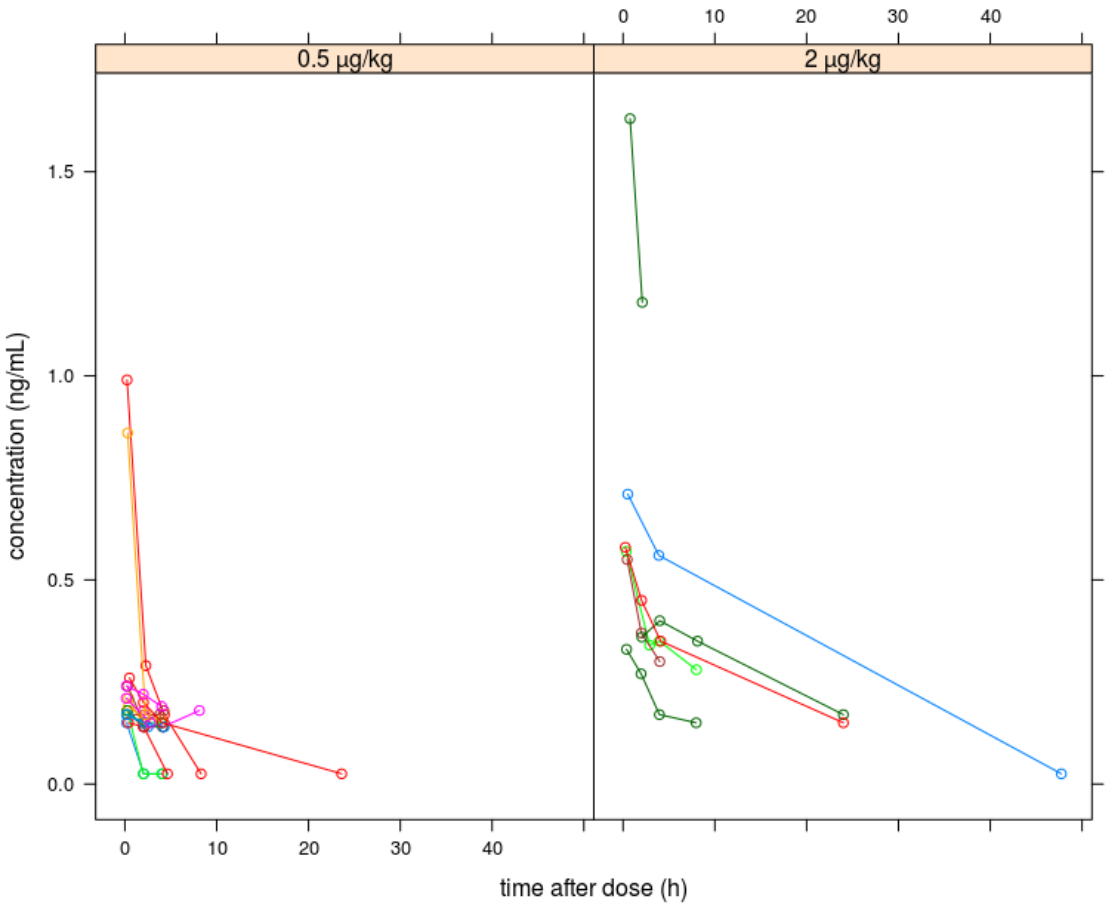

Figure 4: plots of the concentration observed vs time from the final dataset after administration of 0.5 mcg/kg (left) and 2 mcg/kg of fentanyl (right). Each line represents a patient.

The plot shows that higher concentrations were observed for a patient receiving 2 $\mu g/kg$ compared to the others. This patient is the only one who received a second dose after 15 min which explains why its profile is different. The graph shows that the data are limited with a number of samples between 2 and 5 by patient.

The 25 patients were included in the PK/PG analysis. Eleven SNPs were excluded because no minor allele was detected and 30 were excluded because the minor allele frequency was below 5%. Therefore, in total the effects of 112/153 genetic variants were tested on the PK.

To increase the relevance of the PK/PD models, the observation time of the scores were fixed to 12h for continuous pain scale (ALPS-neo and EDIN) and 6h for procedural pain scale (BIIP and PIPP). All patients for which the pain was assessed during this

time were included in the PK/PD models. Hence, the 25 preterm infants were included in the models for ALPS-neo and EDIN whereas only 21 and 16 of them were included in the analyses of BIIP and PIPP, respectively.

3.3.2 Fentanyl pharmacokinetic modelling

The PK data were best described by a two-compartment model with interindividual variability on clearance (CL) and central volume of distribution (V1). The residual model was a proportional error model. The inclusion of a peripheral compartment induced an OFV decreased corresponding to 148.4 points.

When trying to estimate the parameters of the maturation function, the model estimated PK parameters to non plausible values. Therefore the clearance was best described by fixing these parameters to values estimated by the midazolam model published by Anderson *et al.* (134). This maturation model could be used for fentanyl since both drugs are mainly metabolised by the same enzyme: CYP3A4.

The estimates of the final PK parameters and the RSE corresponding are presented in Table 4.

Table 4: Estimates from the final PK model.

Parameter	Estimate	RSE (%)	Bootstrap estimate (95% CI)
CL (L/h/70kg)	94.0	18	95.3 (32.6 - 158.4)
V1 (L/70kg)	175.1	12	171.8 (121.9 - 208.2)
Q (L/h/70kg)	6.01	37	7.4 (2.3 - 92.1)
V2 (L/70kg)	17.1	28	20.4 (9.3 - 82.3)
IIV CL (%)	95.1	28	94.3 (48.5 - 187.8)
IIV V1 (%)	60.2	54	59.1 (21.3 - 88.6)
Err prop (%)	46.9	31	0.13 (0.089 - 0.18)
PMA_50	73.6 FIX	-	-
Hill	3 FIX	-	-

CL is the clearance, V1 is the central volume of distribution, Q is the inter-compartmental clearance, V2 is the peripheral volume of distribution, RSE is the relative standard error (from NONMEM covariance step), IIV is the interindividual variability. PMA_50 is the PMA (weeks) for CL to reach 50% maturity, and Hill is the shape parameter. FIX means that the value of the parameter was fixed a priori in the model.

Basic goodness-of-fit plots are presented in Figure 5.

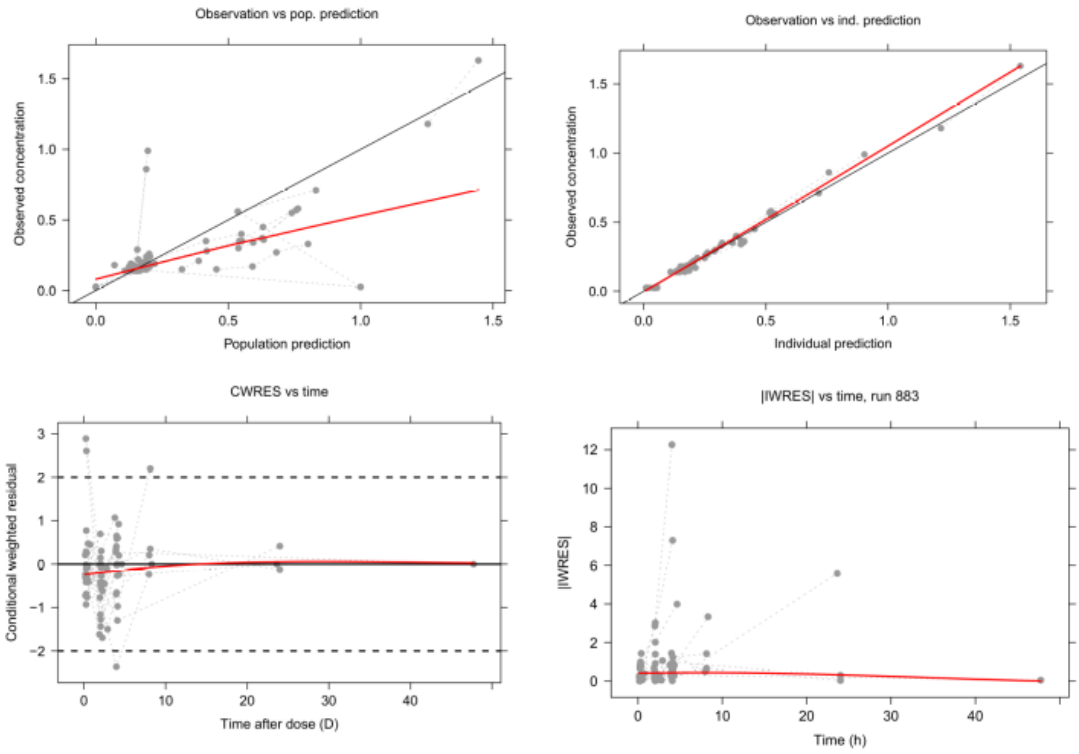

Figure 5: Goodness-of-fit plots of the final PK model. Plots of the observed concentration vs population predicted concentration (top left) and vs individual predicted concentration (top right), the CWRES versus time after dose (bottom left) and plot of the IWRES vs time after dose (bottom right) from the final fentanyl population PK model. The red line is the lowess line and the black line is the line of unity.

The distribution of the conditional weighted residuals are shown in Figure 6.

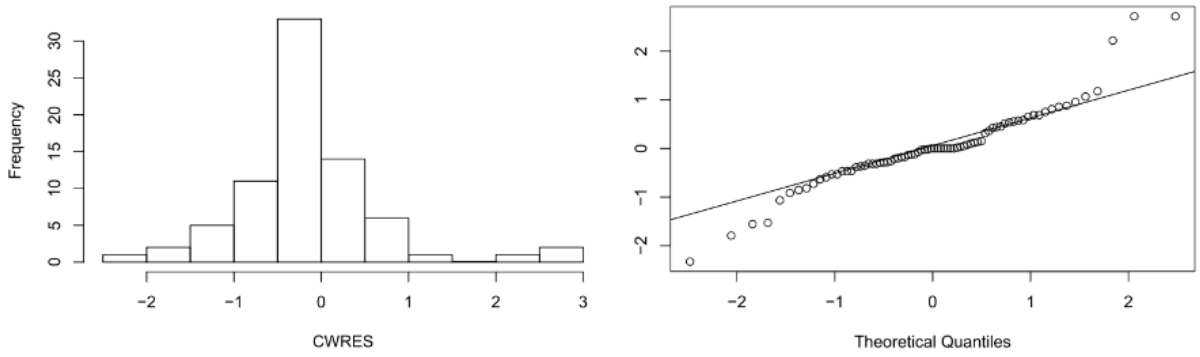

Figure 6: Distribution of conditional weighted residuals presented by a histogram (left) and a QQ plot (right)

The VPC are presented in Figure 7.

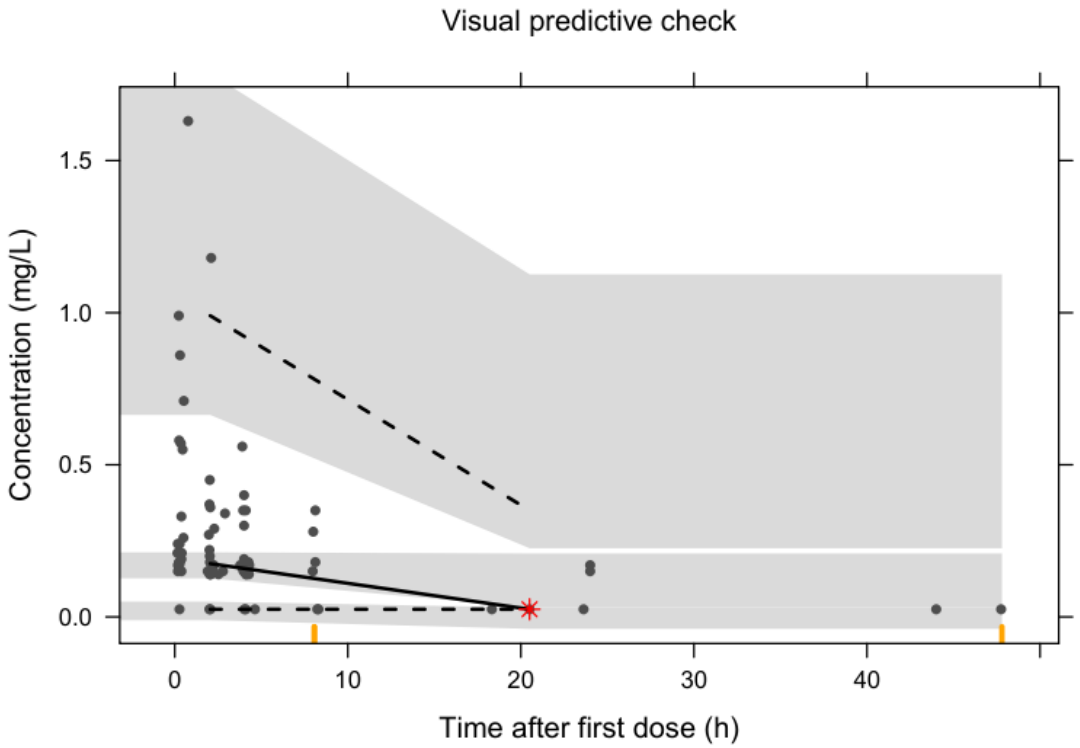

Figure 7: Visual Predictive Check produced using the parameters estimated by the final PK model. The shaded grey area is the 95 percent prediction interval. The black solid line is the median of the observed data; the black dashed lines are the 5 th and 95 th percentiles of the observed data.

3.3.3 Fentanyl pharmacokinetic/pharmacogenetic modelling

All the variants were in Hardy-Weinberg equilibrium based on the statistic test conducted using a Bonferroni adjusted p-value.

The results of linear regression analysis used for the screening process to test the association between the variants and individual clearances (CL_i) are summarized in Table 5.

Table 5: Results of the linear regression analyses used for the screening process of the SNPs

Conditioning variant		Variant	beta	p-value
1	2			
Model 1				
-	-	rs111517339	0.74	5.1 x 10-5
-	-	rs11079921	1.01	1.4 x 10-4
		rs8077268		
-	-	rs11079922	0.77	6.6 x 10-4
Model 2				
rs111517339	-	rs4780592	0.33	5.3 x 10-4
rs111517339	-	rsrs4238623	0.29	1.2 x 10-3
Model 3				
rs111517339	rs4780592	rs11079921	0.60	1.2 x 10-3
		rs8077268		

Four genetic variants had a significant relationship with CL_i after correcting the p-value using Bonferroni: rs111517339, rs4780592, rs11079921 and rs8077268. The effect of these 4 SNPs was then tested in the final PK model. The model showed that 3 of these genetic variants significantly increased the clearance. Table 6 summarises the characteristics of these 3 SNPs as well as the parameters estimated by the model with the RSE corresponding.

Table 6: Estimates of the final PK/PG model

Variant	Receptor coded	Alteration	n	Estimate (CL increase-fold)	RSE (%)
rs111517339	ABCC1	T/TA	8/25	1.6	61
rs11079921	ABCC3	T/C	4/25	4.3	38
rs8077268	ABCC3	C/T	4/25	4.3	38

n is the number of patients that carry the minor alleles and the parameter estimates corresponds to the clearance increase expressed using a multiplication factor.

A significant influence of the genetic variant rs111517339 T/TA in the gene coding for the receptor ATP Binding Cassette Subfamily C Member 1 (ABCC1) was found. This mutation is the result of an insertion in position 16146287 on the chromosome 16. Two variants coding for the receptor ATP Binding Cassette Subfamily C Member 3 (ABCC3) had a significant impact on the CL: rs11079921 T/C and rs8077268 C/T. Both genotypes are the consequences of a single nucleotide variant (SNV) on the chromosome 17 in position 48752379 and 48753522, respectively.

In total, the 3 genetic variants explained 15% of the IIV estimated on the clearance by the final PK model.

3.3.4 Fentanyl pharmacokinetic/pharmacodynamic modelling

No significant relationship between fentanyl PK and the four scales was found using a continuous Emax model.

When the scores were treated as categorical, the proportional odds model was not able to describe the effect of fentanyl concentration on any of the four scales when the scores were not grouped. However when the scores were grouped into 3 equal categories, the model established a significant relationship between fentanyl concentration and

EDIN scale with an OFV decrease corresponding to 5.06 points. This model used a linear model to describe the drug effect on EDIN score. No other predictor was found significant when the scores were grouped.

In the final PK/PD model, the EDIN scores were grouped as follows:

- Group 1 (P0): scores between 0 and 3 (“low pain”)
- Group 2 (P1): scores between 4 and 6 (“middle pain”)
- Group 3 (P2): scores between 7 and 9 (“high pain”)

The estimates of the final PK/PD parameters and the RSE corresponding are presented in Table 7.

Table 7: Estimates of the final PK/PD model

Parameter	Estimate	RSE (%)
B1	-1.86	31
B2	-2.23	34
ETA(1)	2.03	50
SLOPE	-4.51	60

B1 and B2 are the baseline values, ETA (1) is the variance of the random effect and SLOPE corresponds to the slope of the linear drug effect.

The model was evaluated using categorical VPC presented in Figure 8 and Figure 9. Figure 8 shows the proportion of the observed scores plotted against time whereas Figure 9 presents the proportion plotted against fentanyl concentration. The categorical VPC were stratified in three different graphs by observed scores (=DV).

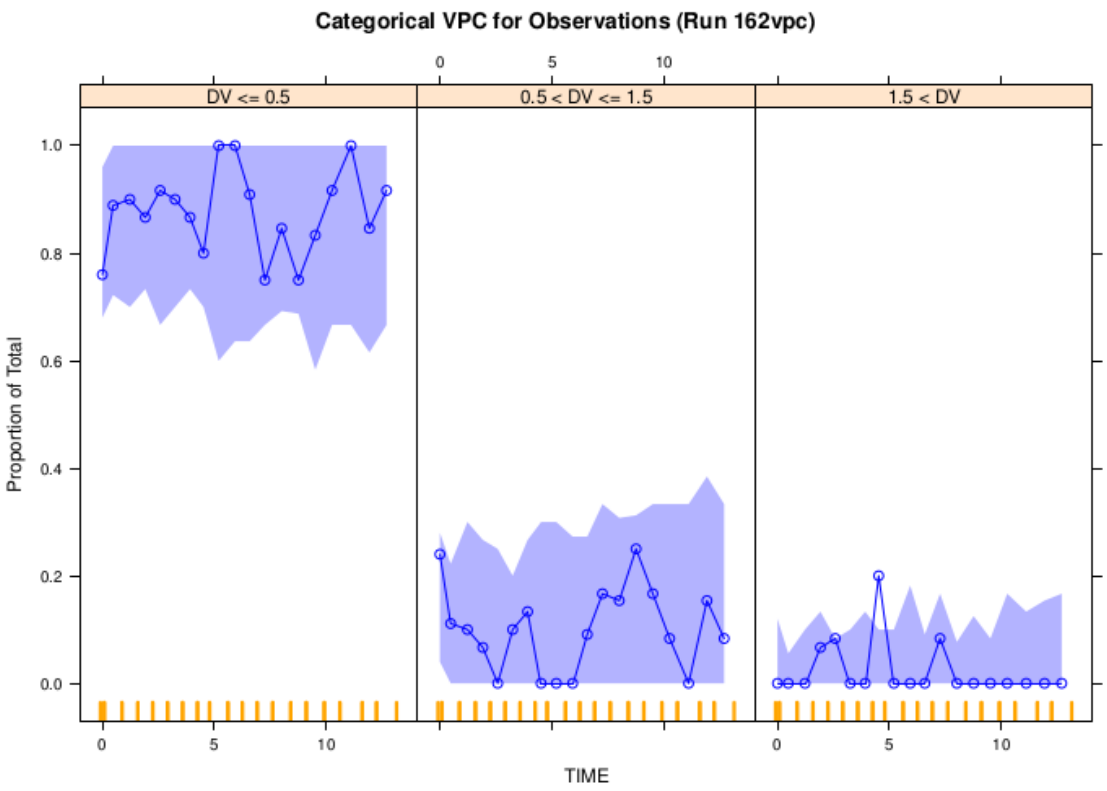

Figure 8: Categorical VPC (proportion vs time) produced using the parameters estimated by the final PK/PD model. The shaded blue area is the 95 percent prediction interval. The blue solid line is the median proportion of the observed scores. DV corresponds to the observed scores and the VPC were stratified by scores.

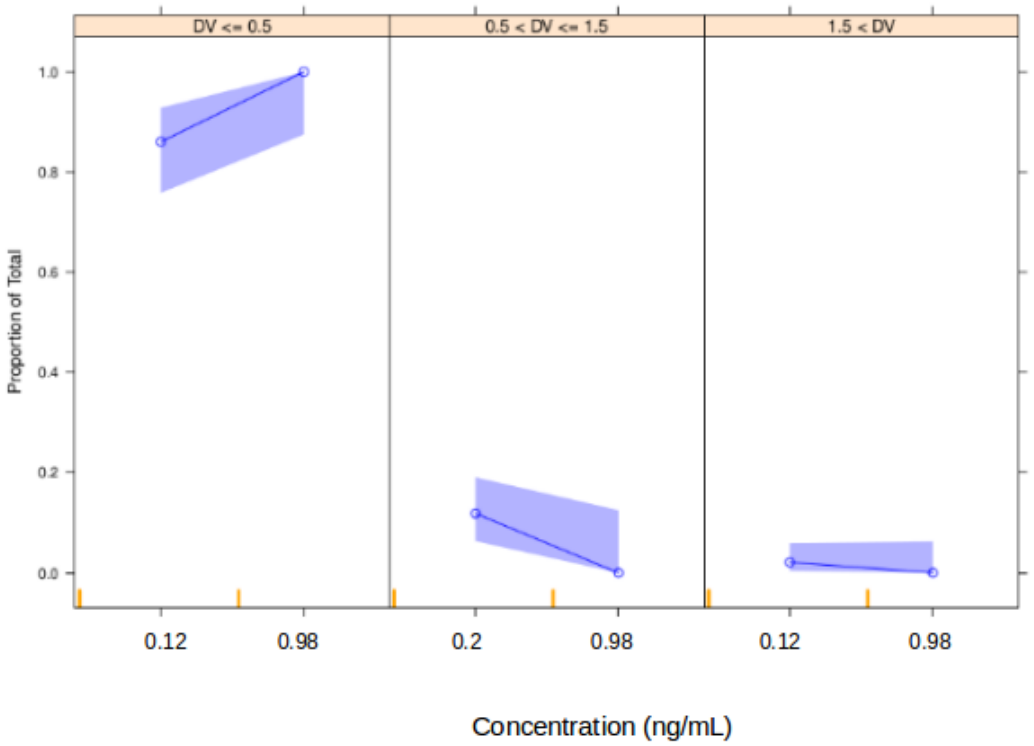

Figure 9: Categorical VPC (proportion vs concentration) produced using the parameters estimated by the final PK/PD model. The shaded blue area is the 95 percent prediction interval. The blue solid line is the median proportion of the observed scores. DV corresponds to the observed scores and the VPC were stratified by scores.

The relationship between fentanyl concentration and the probabilities to observe a score is presented Figure 10.

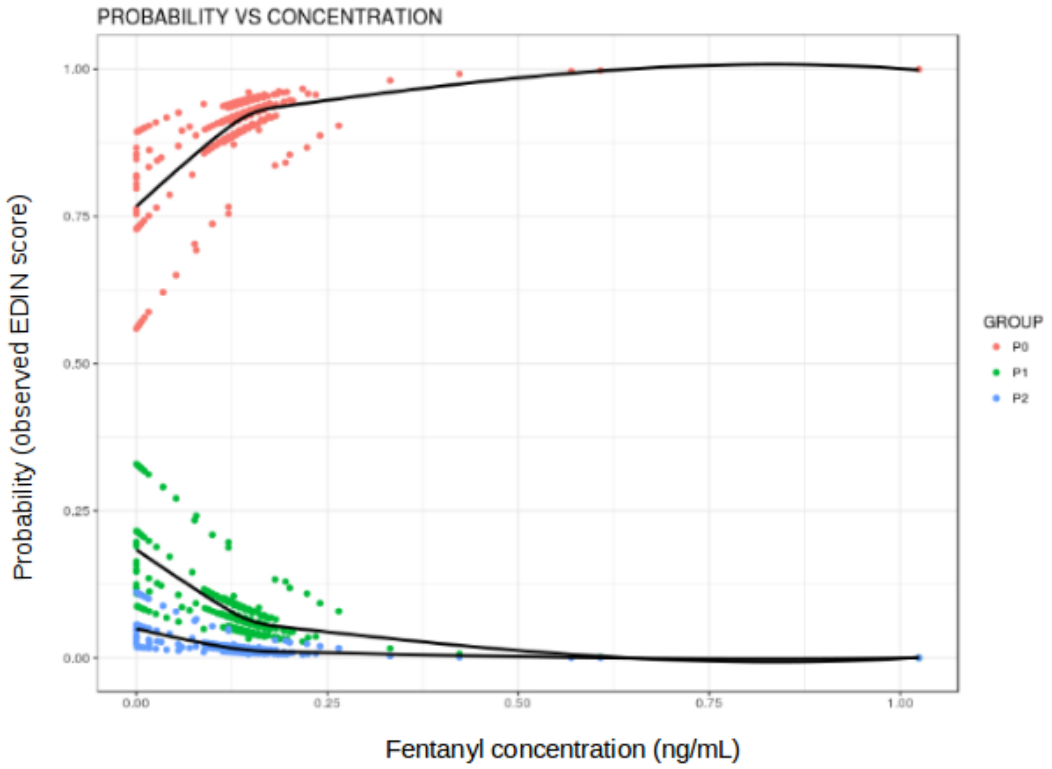

Figure 10: Probability to observe a score plotted against fentanyl concentration. The red point corresponds to the proportions of the scores observed in the group P0, the green points to the scores in the group P1 and the blue points the scores in the group P2. The black solid lines are smooth lines for each category.

The graph shows that the probability to have a score in the category P0 corresponding to a low pain level increases gradually to reach 100% around 0.6 ng/mL and 95% around 0.3 ng/mL. The probability to have a score higher or equal to 4 (categories P1 or P2) corresponding to a higher pain level decreases gradually to reach 0% around 0.6 ng/mL. Therefore, target concentrations of 0.6 ng/mL and 0.3 ng/mL were graphically chosen to perform simulations.

3.3.5 Simulation

The simulated concentrations for the dose of 1.5, 2 and 3 $\mu g/kg$ are presented in Figure 11, 12, and 13, respectively.

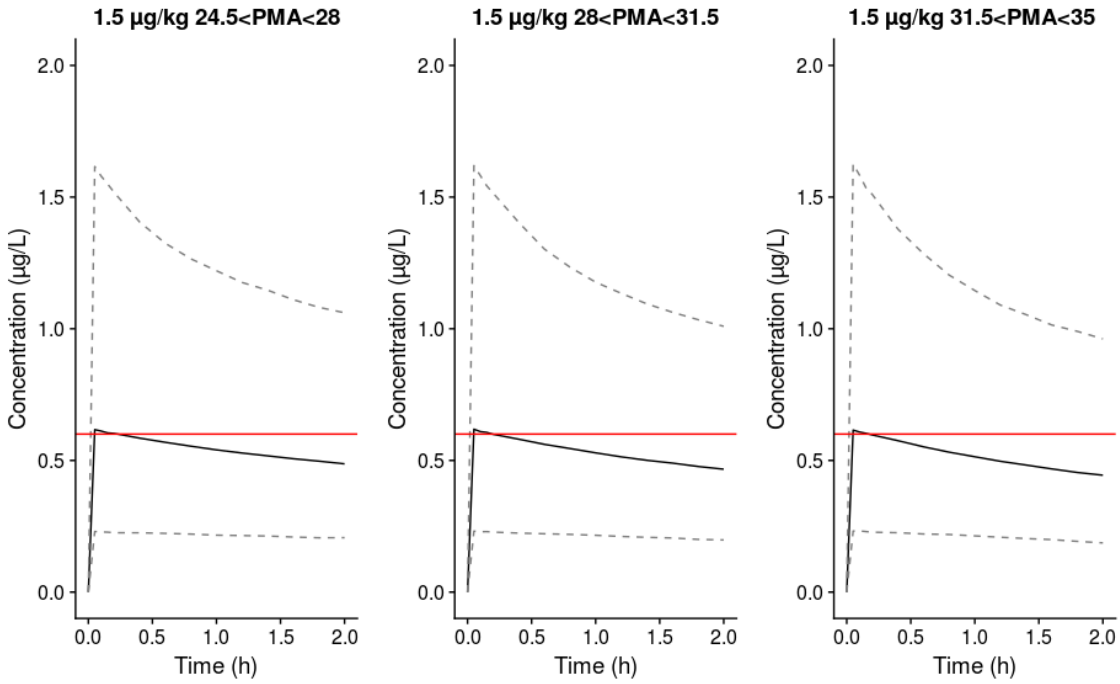

Figure 11: Simulated plasma fentanyl concentrations for a dose of 1.5 mcg/kg. The red line represents the target concentration of 0.6 ng/mL defined using the PK/PD model. The black line is the predicted median concentration and the dotted line represents the 95 percent prediction interval. The simulation graph was stratified by PMA.

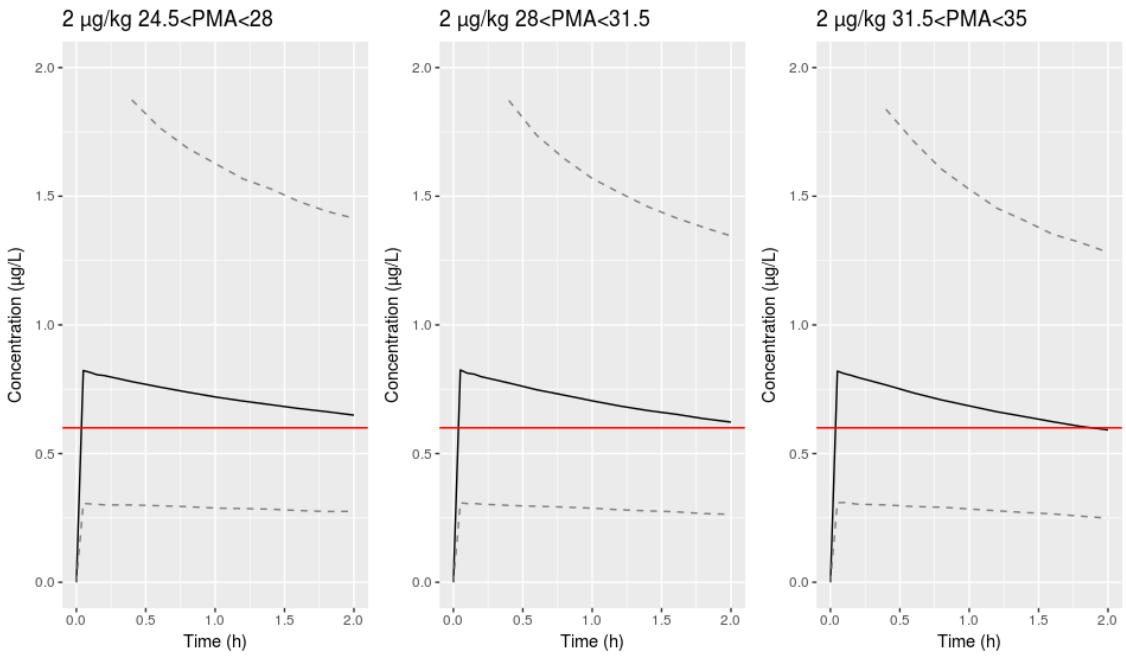

Figure 12: Simulated plasma fentanyl concentrations for a dose of 2 mcg/kg. The red line represents the target concentration of 0.6 ng/mL defined using the PK/PD model. The black line is the predicted median concentration and the dotted line represents the 95 percent prediction interval. The simulation graph was stratified by PMA.

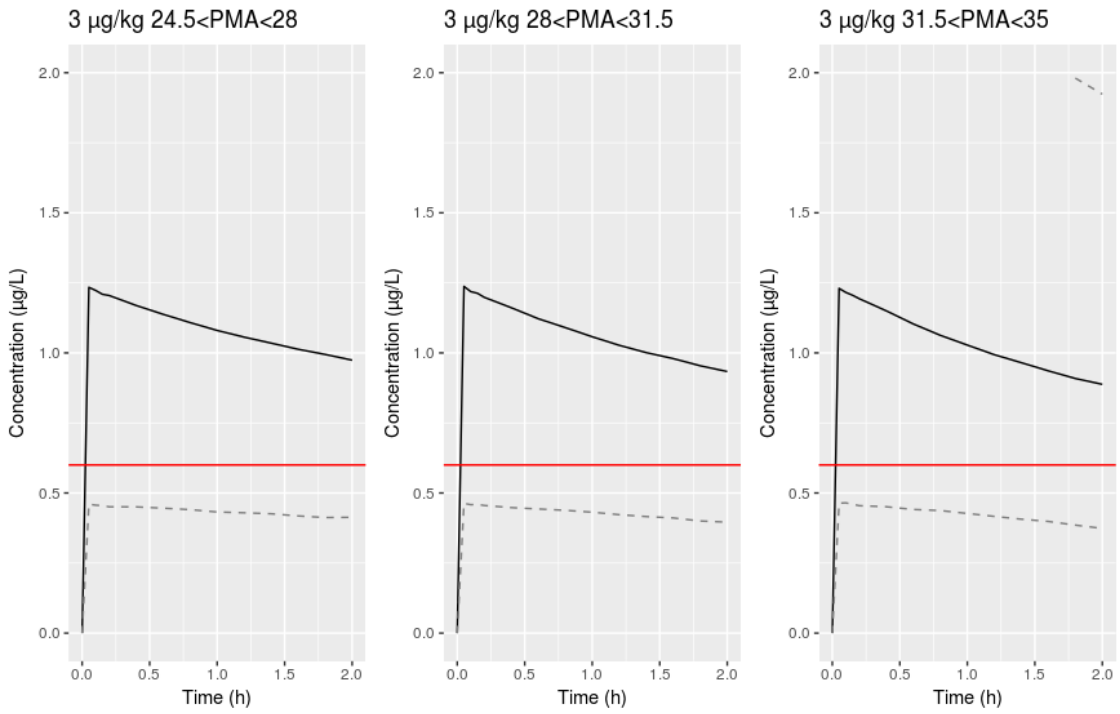

Figure 13: Simulated plasma fentanyl concentrations for a dose of 3 mcg/kg. The red line represents the target concentration of 0.6 ng/mL defined using the PK/PD model. The black line is the predicted median concentration and the dotted line represents the 95 percent prediction interval. The simulation graph was stratified by PMA.

The simulated concentration plots presented in Figure 11, 12 and 13 show that there is a high interindividual variability in preterm patients receiving fentanyl IV bolus. For a dose of 1.5 $\mu g/kg$, the predicted median reaches the target concentration of 0.6 ng/mL only during the first minutes post-administration whereas for the dose of 2 $\mu g/kg$ and 3 $\mu g/kg$, this target concentration is reached by the median during the 2h following fentanyl administration.

Figure 14 and 15 show the probability of achieving the target concentration of 0.6 ng/mL and 0.3 ng/mL, respectively for the dose of 1.5, 2 and 3 $\mu g/kg$ by PMA range. After a rapid increase to reach its maximum few minutes after the dose administration, the probability of target achievement deceases progressively over time. This decrease varies between PMA groups. The probability of achieving the target concentration decreases faster with age.

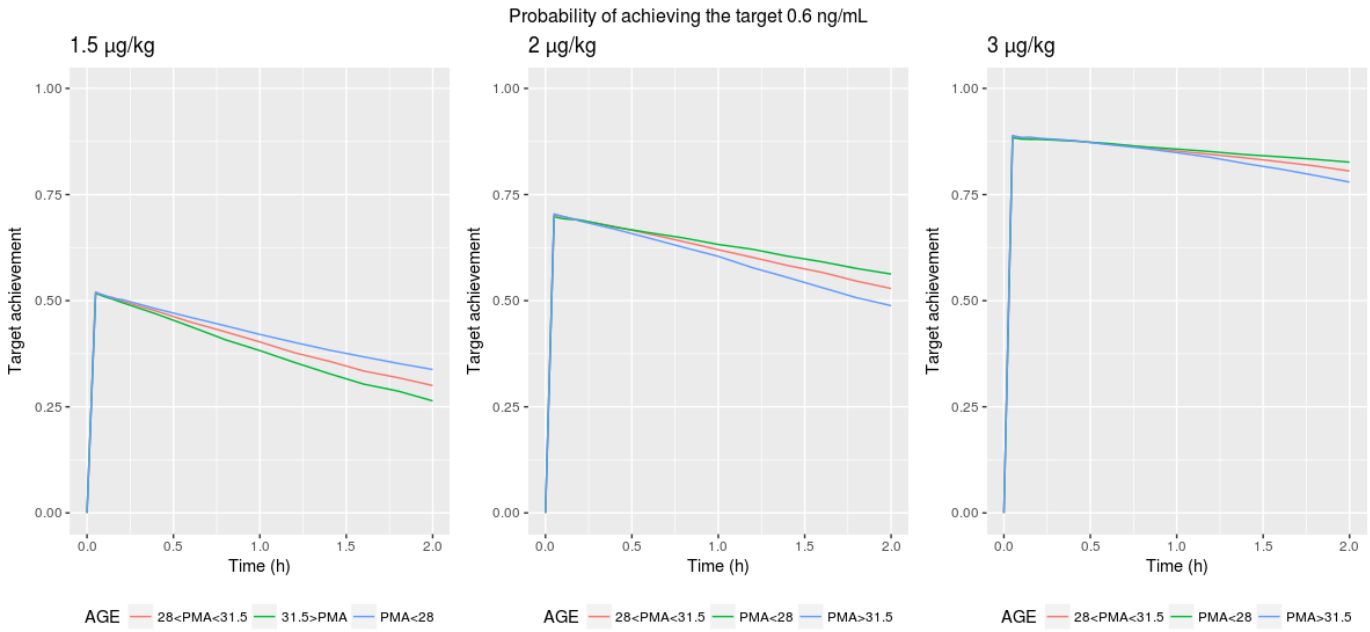

Figure 14: Probability of achieving the target concentration of 0.6 ng/mL plotted against time stratify by dose. Each line represents the simulated probability of target achievement for different PMA ranges.

Figure 14 shows that only 51% of the patients reaches the target concentration few minutes after the dose administration of 1.5 $\mu g/kg$. This percentage decreases progressively to reach 25% after 2h for the preterm babies with a PMA over 31.5 weeks. Around 70% of the patients reaches the target after receiving 2 $\mu g/kg$ of fentanyl. However this number decreases to 50% 2h following the drug administration. The plot also shows that 90% of the patients reaches the target concentration for a dose of 3 $\mu g/kg$ and this percentage only decreases to a minimal value of 76% 2h post-administration.

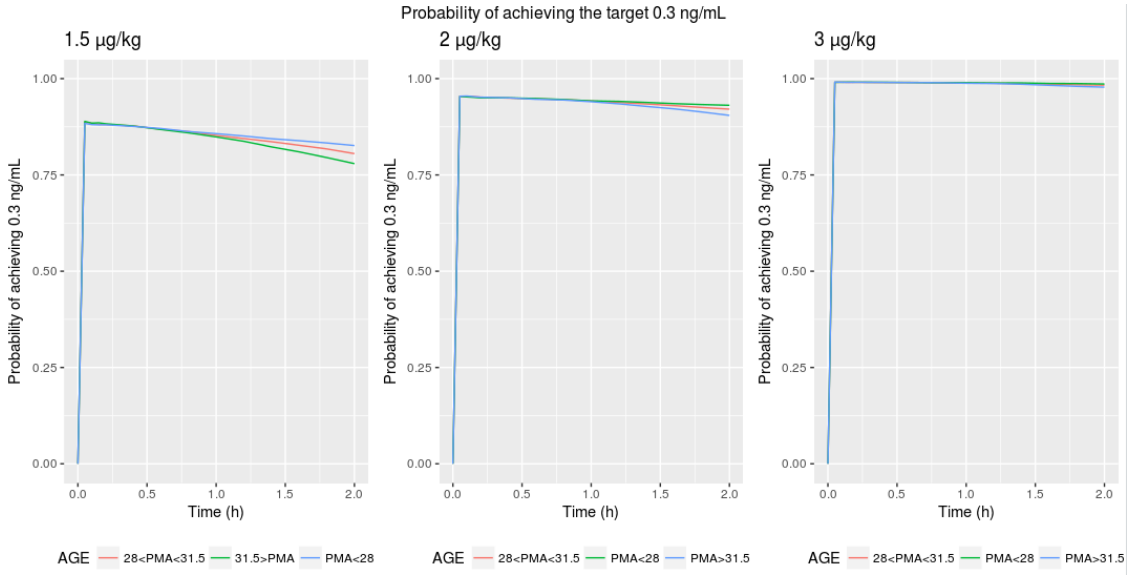

Figure 15: Probability of achieving the target concentration of 0.3 ng/mL plotted against time stratify by dose. Each line represents the simulated probability of target achievement for different PMA ranges.

Figure 15 shows that the target concentration of 0.3 ng/mL is reached by 87% of the patients receiving a dose of 1.5 $\mu g/kg$ and by more than 90% for the patients receiving higher doses (2 $\mu g/kg$ and 3 $\mu g/kg$)

3.3.6 Model evaluation

The RSE of the final PK and PK/PD models presented in Table 4 and Table 7 are below 61% for all parameters, which indicates that the parameters were well estimated by the models.

The goodness-of-fit plots of DV *vs* PRED and IPRED (Figure 5) show that the model underpredicted the population concentration. However, the correlation between observed and predicted concentrations is improved for the individual predictions which suggests that the inclusion of IIV on CL and V1 improved the model. The points are distributed uniformly around the line of unity, hence the model with IIV seems to adequately describe the data. The plot of CWRES *vs* time shows that the residual points are distributed homogeneously around 0. In addition, the vast majority of the values (>95%) are within -2 and 2, indicating that the model predicted well the fentanyl

concentration. The lowess line for both bottom plots is flat around the value 0, therefore the error model also seems to be appropriate. The histogram in Figure 6 confirms that the CWRES follow a normal distribution. The QQ plot shows that the majority of the points are within -2 and 2 and follows the normal distribution although some extreme points deviate from the normality.

The VPC of both PK (Figure 7) and PK/PD models (Figure 8 and 9) show that more than 90% of the observed data are captured by the prediction interval 95%. Hence, the PK and PK/PD models were successfully evaluated by the VPC, meaning that the model was able to simulate data with similar properties to the observed data.

3.4 Discussion

In this chapter, population PK and PK/PD models have been developed for fentanyl in preterm infants. The final PK model was a two-compartment model with an IIV on clearance and central volume of distribution. Age and weight were included as covariates and the model showed that three genetic variants coding for ABCC1 and ABCC3 had an influence on fentanyl clearance. The final PK/PD model was a proportional odds model with a linear drug effect. Using the final PK/PD model, a target concentration of 0.3 ng/mL was defined for procedural pain in preterm infants.

To our knowledge, the PK model developed in this chapter is the first one to describe fentanyl clearance using an allometric weight scaling and a PMA-based sigmoidal maturation function to include the effect of weight and age in neonates. The clearance and volume of distribution at steady state were estimated by the model at 0.2 L/h and 2.75 L, respectively. The model confirms that the clearance in preterm infants is lower compared to older children. The elimination half life calculated from the final model was 2.3 hours, which is close to the value found in the literature in neonates.

The PK/PG model reveals that three genetic variants (one coding for ABCC1 receptor and two coding for ABCC3 receptor) had a significant effect on fentanyl elimination. The patients who carried these minor allele variants had a higher clearance explaining a part of the large intervariability estimated. Both ABCC1 and ABCC3

are part of the MRP subfamily involved in multi-drug resistance. ABCC1, also called MPR1 is an efflux transporter expressed in most human tissues including the endothelial cells of the BBB. Recently, it has been shown that ABCC1 was involved in the brain disposition of morphine in rodents by modulating opioid efflux in the BBB (137, 138). ABCC3 or MRP3 is also an efflux transporter but it is mainly expressed in the liver and intestine cells. Studies have reported that certain genetic variants of MRP3 were associated with an increase of the formation clearance of both morphine metabolites M3G and M6G (139, 140). The role of ABCC1 and ABCC3 in fentanyl elimination remains unclear. Hence, further research should be done to better understand the impact of these genotypes on the fentanyl clearance.

Ontogeny also influences the expression of transporters such as ABCC1 and ABCC3. Although the maturation of ABCC1 in humans remains unknown, the literature reports that the transporter level of expression in the rat BBB increases during the gestation to reach its highest level at birth (141). The expression level of ABCC3 in rats increases gradually during the gestation and after the birth (142). According to the maturation profiles of both transporters, preterm infants might already have a high level of both transporters. However, more studies are needed to confirm their maturation profiles in humans.

Due to the limited number of patients included in the model, each genotype was tested in the model as a dichotomous covariate in order to simplify the model. Therefore, the model assumed that heterozygous and homozygous mutants had the same effect on the clearance whereas it is not the case for most genes. Further models should include more patients in order to confirm these findings and describe the impact of the genetic variants with more precision by using trichotomous variables.

In this study, the association between analgesia and fentanyl concentration has been tested using four different pain scales: two scales evaluating continuous pain (ALPS-neo and EDIN) and two evaluating procedural pain (PIPP and BIIP). For the procedural scales, the observation time was limited to 6h whereas for scale evaluating continuous pain the observation time was 12h. The PK/PD models were only able to establish a

relationship for one scale: EDIN score. Although all the scales have all been validated in preterm infants, they don't include the same items. Only two items are common for the four scales: facial expression and state of agitation. The differences between the scales might be the reason why the model wasn't able to establish a relationship between fentanyl PK and three of the scales. For instance, ALPS-neo presents the specificity to include items that evaluate stress as well as pain and PIPP scale include physiologic factors which have been discussed in numerous papers because of its lack of specificity for pain. In addition, a smaller number of score observations were available for PIPP and BIIP scales compared to the other scales because the observation time was shorter, which could explain why no relationship was found between the fentanyl concentration and procedural pain scales.

One of the main limits of this PK/PD model is that the scores had to be grouped into 3 categories in order to find a significant concentration-effect relationship. Reducing the number of categories was necessary in this analysis because the observed data were limited due to the small number of patients. The 3 categories can be considered as low pain (score=0-3), middle pain (score=4-6) and high pain (score=7-8). Grouping categories is a model simplification that might cause a loss of information.

Since the EDIN scale used to assess pain and sedation in the NEOFENT chapter does not allow the assessment of oversedation, a target concentration of 0.3 ng/mL (corresponding to 95% probability of having a score in the group defined as low pain) seems more appropriate than 0.6 ng/mL (corresponding to a probability of 100%) in order to take into account the risk of oversedation that can be observed with fentanyl (Figure 11).

Simulation results show that in order to have at least 80% of the patients reaching the target of 0.6 ng/mL, a single dose of fentanyl IV bolus corresponding to 3 $\mu g/kg$ should be administered (Figure 14). However, Figure 13 shows that due to the important interindividual variability in the population, the fentanyl simulated concentrations can reach values over 2 ng/mL for a dose of 3 $\mu g/kg$, which is more than three time higher than the target concentration defined in this chapter. Figure 15 shows that from a dose

of 2 $\mu g/kg$, at least 90% of the patients would reach the target concentration of 0.3 ng/mL.

4 Pharmacokinetic/pharmacodynamic modelling of the results of the SANNI1 trial

4.1 Introduction

4.1.1 Clonidine

Clonidine is an alpha-2-adrenergic receptor agonist first synthesised in 1962. It was initially developed as a nasal decongestant before finding application as an antihypertensive agent in the late 1960s (143). However, serious adverse reactions were observed after long term administration in adults including withdrawal syndrome, hypotension and tachycardia. Hence, clonidine is rarely used today for the treatment of hypertension (144). More recently, its sedative and analgesic properties have been highlighted. Since 2000s, clonidine has become a popular sedative agent in the paediatric population. Studies suggest that clonidine decreases pain, discomfort and agitation in children (145). In addition to pain and sedation management, clonidine can be used to treat attention-deficit/hyperactivity disorder (ADHD), drug withdrawal and neonatal abstinence syndrome (NSA) (146). Clonidine is available in various preparations including IV, oral, intramuscular, transdermal, rectal and intranasal (146). Clonidine formula is C9H9Cl2N3 and its molecular weight is 230.093 g/mol.

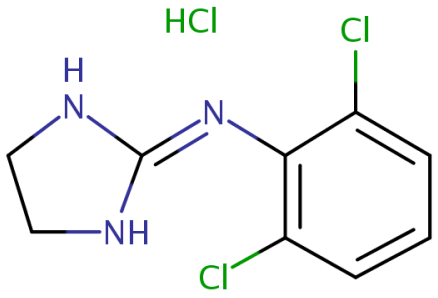

Figure 16: Clonidine structure

4.1.1.0.1 Mechanism of action

Clonidine acts as an agonist with a specificity for the alpha-2-adrenoreceptors which are present in numerous organs including CNS, pancreas and kidney. The stimulation of the alpha 2-adrenoreceptors in the vasomotor centre in the locus coeruleus and in the brain results in an inhibition of the release of excitatory neurotransmitters such as noradrenaline leading to sedation as well as hypotension and bradycardia. The analgesic effect might be the consequence of the stimulation of these receptors located in the substantia gelantinousa of the dorsal horn (147, 148, 143). The full mechanism behind the drug effects remains unclear (143). Studies have suggested that part of the analgesic effect could be due to an hyperpolarisation of the neuronal membrane decreasing the neuronal excitability and repolarization time (146).

Clonidine limits the stress response by suppressing the increase of both sympathetic outflow and vasoconstrictors such as noradrealine, vasopressin and angiotensin. In addition, the drug acts on the neuroendocrine system by inhibiting the release of cortisol and ACTH (143). Hence, clonidine prevents organ failure of heart or kidney which can be observed in children after surgery (149, 150, 151).
Some studies have shown that clonidine is associated with neuroprotective effects which might be related to the inhibition of glutamate and aspartate releases (152).

4.1.1.0.2 Clonidine toxicity

Clonidine has shown an excellent safety profile in children. Rare cases of overdose, bradycardia and hypotension have been observed (4). Minor adverse reactions such as dry mouth have been reported at the beginning of treatment but tend to disappear after a prolonged exposure (153). In case of overdose, clonidine can cause respiratory depression in addition with bradycardia and hypotension. Although the safety profile of clonidine is reassuring, more studies are necessary in order to evaluate the risk of long term exposure particularly in critically ill patients (154).

4.1.1.0.3 Clonidine pharmacokinetics

Clonidine has a high oral biovailability between 75 and 100% and is therefore almost

totally absorbed. Hence, clonidine is ideal for oral administration (143, 148). Clonidine plasma protein binding is only around 30-40%. Due to its lipophilic properties, the drug is rapidly distributed to fat tissues and diffuses through BBB to reach the CNS as well as placenta barrier (143, 147).

Around 50% of clonidine is metabolised in the liver where the compound undergoes a 4-hydroxylation by CYP2D6 to produce p-hydroxyclonidine, its main inactive metabolite. Clonidine is mainly eliminated in the urine of which 50% is unchanged (143, 148). Like most drugs, clonidine clearance is affected by the immaturity of the elimination pathways. Compared to adults, the drug clearance is reduced at birth and increases gradually and significantly during the first month of life (21).

Clonidine has a long elimination half life (that has been estimated around 17 hours in neonates). Hence, a loading dose is required in order to reach therapeutic steady state concentrations in less than 24 hours (155).

4.1.1.0.4 Previously published models

The PK of clonidine in children and neonates has been well described by models published by Potts *et al.* (156) and Larsson *et al.* (148). To describe the influence of weight on PK parameters, both models used an allometric weight scaling with an allometric exponent of 0.75 for clearance and 1 for volumes. The age related changes on clearance was included in both models using different maturation functions. Potts *et al.* used the PNA to describe these changes whereas Larsson *et al.* used a sigmoidal maturation function driven by the PMA. The clearance in neonates has been estimated at approximately one third of that is expected in adults (based on allometric scaling) due to immature elimination pathways (156).

Few PD studies of clonidine can be found in the literature. Hall *et al.* have published PD models using both EEG (BIS score) and pain scores (OAA/S, VAS) to evaluate the sedative effect of clonidine (157). The results suggest that clonidine is an effective sedative agent in adults. The efficacy of clonidine has been confirmed in children by Kleiber *et al.* in a recent study using the COMFORT-B score to assess the level of

sedation (158).

There is no PK/PD model published to date describing the relationship between clonidine concentration and effect.

4.1.2 Hypothermic treatment for perinatal asphyxia

Asphyxia is the consequence of multiple causes in neonates and can occur either intrauterine or during the delivery (perinatal). Perinatal asphyxia is characterised by a reduced oxygenation of the body that might result in vital organ failure. Because the brain is still in development during the first weeks of life, the CNS is particularly vulnerable to perinatal oxygen deficit. For this reason, the CNS is routinely monitored after birth for Hypoxic Ischemic encephalopathy (HIE). Newborns suffering from asphyxia are monitored using EEG in order to prevent neurodepression and seizure.

Asphyxia is commonly treated in the NICU using hypothermic treatment, a technique which has proven its efficacy for moderate and severe HIE. The body temperature is maintained at 33.5 degree Celsius for 72h before a gradual rewarming of 14h (159). An EEG is performed during the hypothermia as well as before the hypothermic treatment in order to decide when/if to start the treatment. An MRI is also used after the hypothermic treatment to evaluate the brain lesions.

Analegesics and sedatives are prescribed during hypothermia in order to minimise the distress of the child. It has been proven that the hypothermic treatment is more efficient if the patient's pain is adequately managed (159). A combination of morphine and midazolam is traditionally used during hypothermia. However, recently it is frequently replaced by a combination of fentanyl and clonidine due to their numerous advantages including a neuroprotective effect and a reduction of opioid need (160).

The effect of hypothermic treatment on the drug PK depends on several factors: the characteristics of the drug (Log P, molecular weight, protein binding), the patient (weight, age, illness) and the ADME (161).

The effect of hypothermic treatment on pharmacodynamics has not been extensively described in the literature. A large variability regarding the impact of hypothermia on

pharmacodynamic parameters was observed between the drug studied (162).

4.1.3 Effect of perinatal asphyxia and hypothermic treatment on ADME

ABSORPTION

Drug absorption is affected by both perinatal asphyxia and hypothermic treatment. Perinatal asphyxia induces an increase of the intestinal permeability, therefore the absorption of drugs administered orally might be higher compared to healthy neonates. It has been shown that hypothermic treatment is associated with a lower arterial flow which can also decrease the drug absorption (161).

DISTRIBUTION

Although hypothermic treatment has a minor effect on protein binding, studies have shown that hypothermia affects the blood pH by inducing a decrease of carbon dioxide partial pressure in the blood. Therefore, the pH of the neonates receiving hypothermic treatment is higher than for the uncooled children (161). In addition, hypothermia causes peripheral vasoconstriction leading to a decrease of the drug distribution in muscles, skin and fat. As a result, the volume of distribution of some drugs such as fentanyl can be reduced (163). The severity of the perinatal asphyxia can also be a factor affecting the drug distribution since it can induce changes in plasma protein composition (161). Furthermore, the rewarming of the body can influence the drug distribution. For instance, drugs with a large volume of distribution that are administrered before the hypothermic treatment can get trapped in the peripheral tissues during hypothermia and then released in the blood circulation during the rewarming causing an increase of the drug concentration.

METABOLISM

The activity of metabolism enzymes such as CYP450 is reduced during the cooling leading to a drug accumulation. In vitro studies have shown that the activity of the CYP3A4 is decreased to 69% at 32 degrees Celsius (164). Therefore the drug clearance is also reduced, the elimination half life is longer and the drug concentrations higher

(163). In addition, hypothermic treatment causes a decrease of the hepatic blood flow. As a result, hypothermia has a more important effect on the metabolic clearance of the drugs with a high hepatic extraction ratio such as propofol (161). During the rewarming, the activity of the metabolism enzymes undergoes a rapid change to return to its baseline value leading to an increase of the drug clearance.

ELIMINATION

Studies have shown that perinatal asphyxia and hypothermic treatment both reduced the elimination of drugs excreted by glomerular filtration. This might be due to the reduced blood flow in the kidney. However, the reasons explaining the reduced renal drug excretion have not been fully explored (161).

4.1.4 Rationale

Hypothermic treatment can alter the PK and PD of analgesics and sedatives. Because their body is still in development, the neonatal population is particularly vulnerable to the numerous adverse reactions of these drugs. Therefore, it is essential to study the impact of hypothermia in asphyxiated neonates receiving hypothermic treatment in order to adapt the doses and decrease the risk of toxicity.

Few PK studies have been previously done to describe the effect of the hypothermic treatment on analgesics and sedatives PK in asphyxiated infants. A multicenter study called PharmaCool was conducted in order to optimise the doses of antibiotics, analgesics, sedatives and anti-epileptic drugs in asphyxiated newborns receiving hypothermic treatment using PK and PK/PD modelling (165). The PK analyses published in 2019 showed that the clearance of morphine and midazolam metabolite (1-hydroxymidazolam) were both reduced by hypothermia (166, 167). These findings confirm the influence of hypothermia on morphine that was shown by Frymoyer *et al.* (168) in 2016. The PharmaCool study also showed that the hypothermic treatment did not influence the elimination of phenobarbital and midazolam (167). These results are supported by the phenobarbital PK model developed by Shellhaas *et al.* (169) and the midazolam PK analysis published by Welzing *et al.* (170). No PK/PD result from the PharmaCool trial

has been published to date. A recent study conducted by Mcadamms *et al.* (171) showed that the elimination half-life of dexmedetomidine was markedly lower in newborns treated with hypothermic treatment compared to the uncooled newborns. However, these findings should be interpreted carefully because only 7 patients were included in the analysis.

Although the influence of hypothermia has been explored for some analgesics and sedatives, the effect of hypothermic treatment on clonidine and fentanyl PK has not been studied. In addition, no previous analysis included PD data in order to establish the relationship between concentration and effect during hypothermia.

For these reasons, it is essential to conduct PK and PK/PD studies in order to determine if the cooling has an effect on the parameters and optimise the doses of both clonidine and fentanyl in this vulnerable population.

4.1.5 Aim

The overall aim of the SANNI1 project was to determine the optimal doses of clonidine and fentanyl given in combination in asphyxiated newborns treated using hypothermia. To reach this aim, the first objective of the project was to develop a PK model for clonidine and fentanyl in this population in order to identify the covariates (such as hypothermia) that influence the PK. The second objective was to use PK/PD modelling to establish a relationship between the concentrations of both drugs and analgesic/sedative effect assessed using pain/sedation scores. These models were then used to performed simulations in order to suggest an optimal dose for both drugs.

4.2 Methods

4.2.1 Study population

The SANNI1 study was a non randomized prospective observational study. The asphyxiated newborns included in the study received hypothermia as routine treatment in the NICU. Because of the limited number of patients in each hospital, a multicenter

trial was chosen. The study took place in three different NICU in Sweden: Kånes University Hospital in Lund and Karolinska University Hospital Solna and Huddinge in Stockholm. The combination of fentanyl and clonidine is routinely prescribed in these NICU to provide analgesia and sedation during hypothermic treatment.

To be included in the study, the patients had to be term infants receiving hypothermic treatment following perinatal asphyxia and in need of analgesics and sedatives according to the Thomsons and ALPS-neo scores. In addition, the newborn infants should have an existing arterial or venous catheter for blood sampling and a parental consent was required. The exclusion criteria were the following: AV-block I-III or a heart rate below 70, serious congenital heart disease that require surgery and a mean arterial blood pressure below 35 mmHg.

The infants with perinatal asphyxia were admitted in the NICU following their birth. The patient physiological parameters and aEEG/EEG were monitored immediately. The hypothermic treatment was started at a maximal PNA of 6h. The temperature was maintained at 33.5 degrees Celsius for 72h before proceeding to a rewarming for approximately 14h (0.5 degrees Celsius/h).

The study started 30 minutes before the beginning of the hypothermic treatment and ended once the temperature was back to baseline (normothermia). The study could reach a maximal period of 7 days.

As clinical routine during the study, several variables were monitored: encephalopathy degree assessed using the Thompson score, physiological functions (heart rate, mean arterial blood pressure and peripheral oxygen saturation), cerebral perfusion using NIRS score and aEEG/EEG. In addition, cerebral ultrasound were performed during the first 24h of the study and an echocardiography was done directly after reaching the hypothermia and the normothermia post hypothermic treatment. A MRI was also performed after the rewarming. Pain and sedation were assessed using two different pain scales (ALPS-neo and COMFORT-Neo sore) and the skin conductance algesimetry to register the galvanic skin response of the patient.

Fentanyl and clonidine were administered intravenously following an algorithm based

on pain and sedation scores. A loading dose of 1 $\mu g/kg$ for both drugs was given over 10 minutes before the start of the continuous infusion 30 minutes after. The starting dose of the infusion was fixed to 1 $\mu g/kg/h$ for fentanyl and 0.1 $\mu g/kg/h$ for clonidine. Both drugs were not administrered at the same time. It was recommended to give fentanyl first followed by clonidine 1 hour later. The doses could be adapted following the dosing algorithm based on the ALPS-neo score. The maximal infusion dose was 3 $\mu g/kg/h$ for fentanyl and 0.5 $\mu g/kg/h$ for clonidine. The exact time of the starting doses and dose changes for both drugs were carefully recorded. The concomitant medications were also recorded. The patients did not receive any muscle relaxant drug during the hypothermic treatment.

The blood samples used for the PK analyses from which the concentration of fentanyl, nor-fentanyl and clonidine were measured were taken from existing catheters (umbilical, arterial or venous). Dried blood spot was used for the sampling of all compounds. All samples were analysed using LC-MS standard method. The limit of quantification for all compounds was 0.1 ng/mL. Mandatory samples were taken at the following time of the study:

- 5 minutes after starting the loading dose for each drug
- Before starting the maintenance infusion and then at 1, 6, 24, and 48h following the infusion start
- Just before starting both the hypothermic treatment and the rewarming and once the normothermia was reached
- Once every 24h during the 3 days following normothermia

Blood samples were also routinely used to monitor blood gas, albumin and cortisol as well as liver and renal function.

COMFORT-neo and ALPS-neo scores were both used as PD endpoints in order to establish the relationship between drug concentration and the analgesic/sedative effect. Both scores were recorded approximately every hour during the entire time of the study.

4.2.2 Pharmacokinetic model building

Two separate population PK models were built in order to describe the concentrations of clonidine and fentanyl in the population studied and identify the covariates that influence the PK parameters.

To define the structural model of both drugs, one and two-compartment models were tested.

An additive, proportional and combined error model was tested for each drug in order to describe the residual variability.

Body weight and age using PMA were included a priori in both models using the standard method including an allometric scaling and a maturation function as described in section 1.2.3. The parameters of the maturation function were estimated by the model or fixed to values estimated in previous models published by Larsson et *al.* (148) for clonidine and Anderson *et al.* (134) for fentanyl.

The observed values below the limit of quantification of 0.1 ng/mL were implemented in the database by dividing the BLQ by 2 or using the M3 method.

The samples taken before the drug administration were included in the model and used to estimate the baseline concentration values.

Once the structural models of both drugs were defined, the influence of body temperature was tested on each parameter as continuous covariates using a centred multiplicative model as follows:

$$CL_i = CL_T \cdot \left(\frac{WT_i}{70}\right)^n \cdot \frac{PMA_i^{Hill}}{PMA_{50}^{Hill} + PMA_i^{Hill}} \cdot \left(\frac{TEMP}{MTEMP}\right)^{index}$$

Where CL_i is the drug clearance in an individual, CL_T is the typical CL for a 70 kg adult, WT is body weight, n the allometric weight exponent, PMA_{50} is the PMA (weeks) for CL to reach 50% maturation. $Hill$ is the shape parameter, $TEMP$ is the body temperature, $MTEMP$ the median temperature and $index$ the temperature exponent.

The values of temperature missing were implemented in the final database by

calculating the mean between the previous and the next temperature observed using a linear slope to take into account the time difference between the samples.

4.2.3 Pharmacokinetic/pharmacodynamic model building

All the PK/PD models were built using a sequential method. For both clonidine and fentanyl, two separate PK/PD models were developed (one for ALPS-neo and one for COMFORT-neo) in order to describe the relationship between drug concentration and analgesic/sedative effect.

For both scales, PK/PD models were developed using two steps; a PK/PD model for each drug was built then a joint model including data from both drugs was developed. First, the PD data were treated as continuous and an inhibitory sigmoid Emax model was tested. The inclusion of an effect compartment in the continuous Emax model was also tested. Then, the data were treated as categorical variables and two categorical models were tested: a proportional odds model and a bounded integer model (with and without Markov effect).

The Emax model tested was an inhibitory sigmoid model with and without effect compartment. The maximal effect Emax was fixed to 1. A logit scale was used in order to limit the prediction in the scale interval. The influence of PMA and temperature was tested using a centred multiplicative covariate model. The scores recorded before the drug administration were used to estimate the baseline score value in logit scale. The exponent of the Emax model corresponding to the shape parameter HILL was either fixed to 1 or estimated by the model. In the joint continuous model, the effects of both drugs on the scores were combined using an additive model. Therefore the model estimated separate parameters for the Emax model of each drug and a common baseline for both drugs.

In the inhibitory Emax sigmoid joint models, the drug effect of clonidine (CEF) and fentanyl (FEF) were combined using an additive model as follows:

$$CEF = \frac{E_{max}c \cdot C_p c^{nc}}{EC_{50}c^{nc} \cdot C_p c^{nc}}$$

$$FEF = \frac{E_{max}f \cdot C_p f^{nf}}{EC_{50}f^{nf} \cdot C_p f^{nf}}$$

$$TEF = B0 - (B0 * CEF * FEF)$$

Where TEF is the total effect, $E_{max}c$ corresponds to the maximum effect for clonidine, $EC_{50}c$ is the clonidine concentration for 50% Emax effect and $C_p c$ is the clonidine concentration. $E_{max}f$ corresponds to the maximum effect for fentanyl, $EC_{50}f$ is the fentanyl concentration for 50% Emax effect and $C_p f$ is the fentanyl concentration. nc and nf represent the slope for clondine and fentanyl, respectively. $B0$ is the baseline effect.

A proportional odds model as described in section 2.2.4 was also built for each scale and drug. In addition to the drug effect, the predictors tested were PMA and temperature. Each predictor was tested using a linear and Emax model. The categories corresponding to the scores missing in the database were ignored in the model. No score were grouped into categories. If the proportional odds model was chosen as final model, the target concentration was determined graphically using the model results. In the joint proportional odds model tested, the drug effects of clonidine and fentanyl were both used as predictor in the same model.

The last model developed was a BI model. In this model, the probability of the kth category of a patient i was defined as:

$$P_{i,j}(k) = \phi(\frac{Z_{k/n} - f(\theta, \eta_i, t, X_{i,j}}{g(\sigma, \eta_{i,g}, t, X_{i,g})}) - \phi(\frac{Z_{(k-1)/n} - f(\theta, \eta_i, t, X_{i,j}}{g(\sigma, \eta_{i,g}, t, X_{i,g})})$$

where $f(.)$ is a function of fixed effect θ, random effect for individual i η_i, time t and covariate X. $g(.)$ is the variance function. Together, the two functions define the following normal distribution: $N(f(.), g(.))$. ϕ corresponds to the cumulative distribution of the normal distribution.

Since the model uses cumulative distribution, the first category is in the interval $[-\infty, Z_{1/n}]$ and corresponds to the equation:

$$P_{i,j}(1) = \phi(\frac{Z_{1/n} - f(\theta, \eta_i, t, X_{i,j}}{g(\sigma, \eta_{i,g}, t, X_{i,g})})$$

whereas the last category is in the interval $[Z_{(n-1)/n}, \infty]$ and was defined as:

$$P_{i,j}(1) = 1 - \phi(\frac{Z_{(n-1)/n} - f(\theta, \eta_i, t, X_{i,j}}{g(\sigma, \eta_{i,g}, t, X_{i,g})})$$

A Markov effect was included in the model if the addition of the Markov element induced a significant decrease of the OFV.

If the observation $Y_{i,j}$ is similar to the previous observation $Y_{i,j-1}$, the probability of a score k for a patient i at a time j follows the equation:

$$P_{i,j}(k|Y_{i,j-1} = k) = \frac{P_{k,i,j} + PM}{1 + PM}$$

When $Y_{i,j-1}$ and $Y_{i,j}$ are different, the equation becomes:

$$P_{i,j}(k|Y_{i,j-1} \neq k) = \frac{P_{k,i,j}}{1 + PM}$$

The parameter PM includes in the model that there is a higher probability for a score to have the similar value that the previous score observed. PM estimates the balance between the component of the model given by f and g and the component corresponding to the previous observation. The model does not predict that two scores with low probabilities and very close in time should be similar. Therefore, it is able to describe large score jumps of observation with more precision. In addition, the Markov element is implemented such as the markovian properties decrease in time, resulting on higher probabilities of having two consecutive same scores with time.

The Markov effect $Meff$ was implemented in the BI model as follows:

$$Meff = BASE + PMAX \cdot (1 - e^{-Ln(2)/HL \cdot TIME})$$

Where $BASE$ is the baseline score estimate of the latent variable, $PMAX$ is the

maximal Markov effect and HL is the half life of the Markov effect.

4.2.4 Simulations

To determine the optimal dose of clonidine and fentanyl in asphyxiated infants receiving hypothermic treatment, simulations were performed using the final PK and PK/PD models. A database of 1000 patients was used as described in section 2.2.5. The simulations were done for a time period of 96 h. In order to follow the study design, the temperature in the simulated database was fixed to 33.5 degrees Celsius during the first 72h and 37 degrees Celsius for the last 24h.The simulations did not take into account that the rewarming is done gradually over 14h in clinical practice.

The simulated doses of clonidine were:

- Loading dose of 1 $\mu g/kg$ followed by a continuous infusion of 0.1, 0.5, 1 $\mu g/kg/h$
- Loading dose of 2 $\mu g/kg$ followed by a continuous infusion of 0.1, 0.5, 1 $\mu g/kg/h$
- Loading dose of 3 $\mu g/kg$ followed by a continuous infusion of 0.1, 0.5, 1 $\mu g/kg/h$
- Loading dose calculated using the target concentration at steady state followed by a continuous infusion of 0.5 and 1 $\mu g/kg/h$

The simulated doses of fentanyl were:

- Loading dose of 1 $\mu g/kg$ followed by a continuous infusion of 1 $\mu g/kg/h$
- Loading dose of 2 $\mu g/kg$ followed by a continuous infusion of 1, 2 $\mu g/kg/h$
- Loading dose of 3 $\mu g/kg$ followed by a continuous infusion of 1, 2, 3 $\mu g/kg/h$
- Loading dose calculated using the target concentration at steady state followed by a continuous infusion of 1,2,3 $\mu g/kg/h$

4.2.5 Model evaluation

RSE, goodness-of-fit plots and PC-VPC were used to evaluate the PK and PK/PD models built in this chapter, as described in section 2.2.6. PWRES plotted against time were also used as goodness-of-fit plot to evaluate the BI models.

In addition, the Akaike information criterion (AIC) was used to compare the models. For a model of m parameter, the AIC can be calculated as follows:

$$AIC = OFV + 2m$$

4.3 Results

4.3.1 Study population

Thirty-one patients who received a combination of clonidine and fentanyl during hypothermic treatment were included in the PK and PK/PD analyses. The demographic characteristics of the population are summarised in Table 8.

Table 8: Table summarising the demographic characteristics of the SANNI1 cohort.

	Median (Range)
Birth weight (kg)	3.7 (2.5 - 4.7)
Gestational age (weeks)	40 (35 - 42)
Postnatal age (days)	3 (0 - 6)
Postmenstrual age (weeks)	40 (36 - 42)

4.3.2 Pharmacokinetic models

4.3.2.1 Clonidine

In total, 267 samples were used to build the clonidine final PK model. The observed clonidine concentrations are presented in Figure 17.

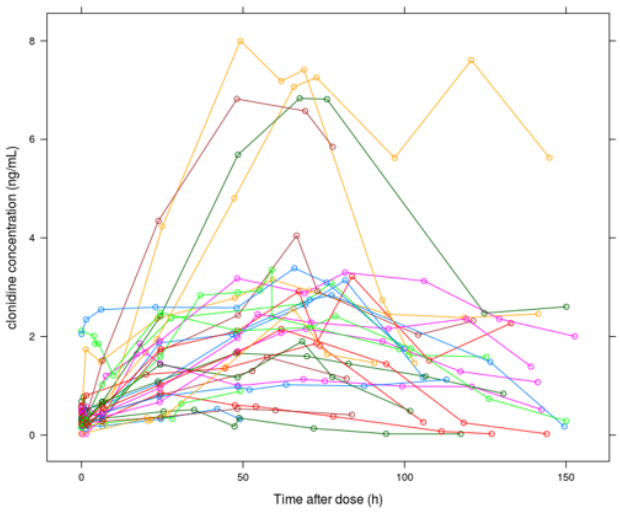

Figure 17: Observed concentrations of clonidine plotted against time after dose administration (TAD). Each line represents a patient.

Clonidine PK data were best described by a one-compartment model with IIV on clearance (CL) and central volume of distribution (V1). The error model that best described the residual error was a combined error model. The BLOQ were included in the model by dividing the BLQ by 2 (BLOQ $< 5\%$). When trying to estimate the parameters of the maturation function, the model estimated PK parameters to non plausible values. Therefore the parameters of the maturation function were fixed to the values estimated by the model published by Larsson *et al.* (148). A significant effect of the temperature was found on the clearance inducing an OFV decrease of 4.7 points. The estimates of the final clonidine PK parameters and the RSE corresponding are presented in Table 9.

Table 9: Estimates from the final clonidine PK model.

Parameter	Estimate	RSE (%)	Bootstrap estimate (95% CI)
CL (L/h/70kg)	14.3	19	15.2 (9.2-18.9)
V1 (L/70kg)	276	9	273 (234-325)
TEMP INDEX	2.61	78	2.54 (-0.65 - 7.58)
IIV CL (%)	76.4	44	71.4 (50.9-102.9)
IIV V1 (%)	35.4	38	33.1 (19.7-45.2)
Err prop (%)	27.5	23	27.2 (20.9-31.1)
Err add (ng/mL)	0.0185	36	0.017 (0.011-0.035)
PMA_50	61.6 FIX	-	-
Hill	2.42 FIX	-	-

CL is the clearance, V1 is the central volume of distribution, RSE is the relative standard error (from NONMEM covariance step), IIV is the interindividual variability. PMA_50 is the PMA (weeks) for CL to reach 50% maturity, and Hill is the shape parameter. TEMP index is the estimate corresponding to the temperature as covariate. FIX means that the value of the parameter was fixed a priori in the model. Err prop and Err add correspond to the estimates of the proportional and additive error model, respectively.

Basic goodness-of-fit plots and VPC used to evaluated the final clonidine PK model are presented in Figure 18 and Figure 19, respectively.

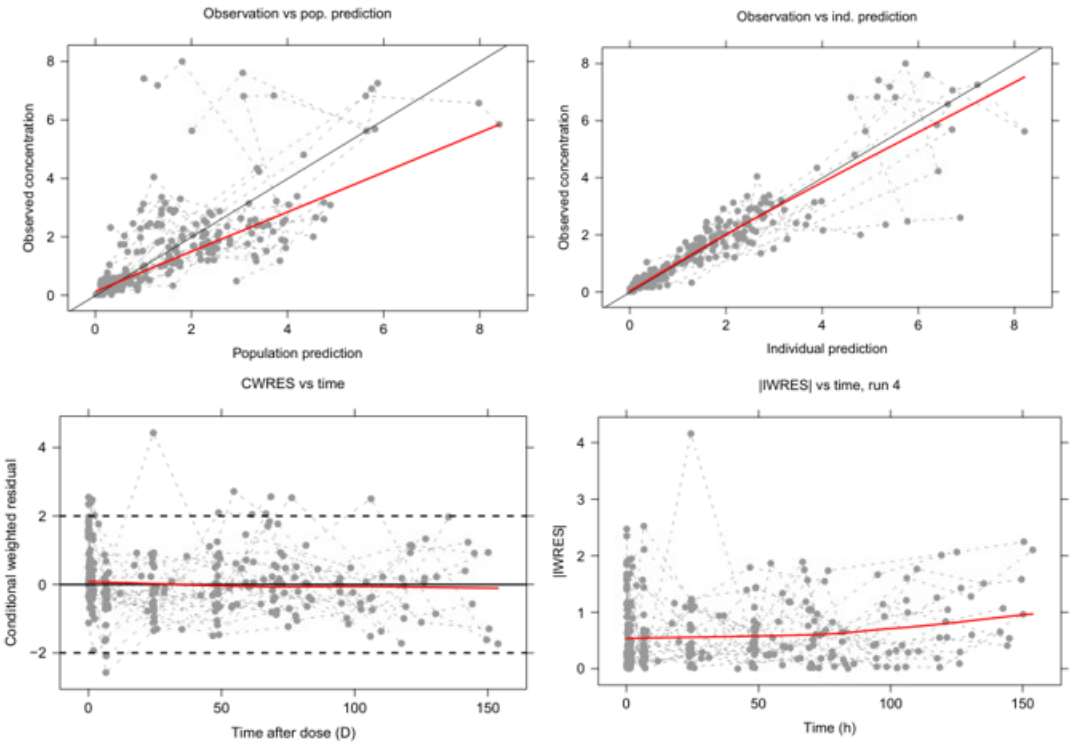

Figure 18: Goodness-of-fit plots of the final clonidine PK model. Plots of the observed concentration vs population predicted concentration (top left) and vs individual predicted concentration (top right), the CWRES versus time after dose (bottom left) and plot of the IWRES vs time after dose (bottom right) from the final clonidine population PK model. The red line is the lowess line and the black line is the line of unity.

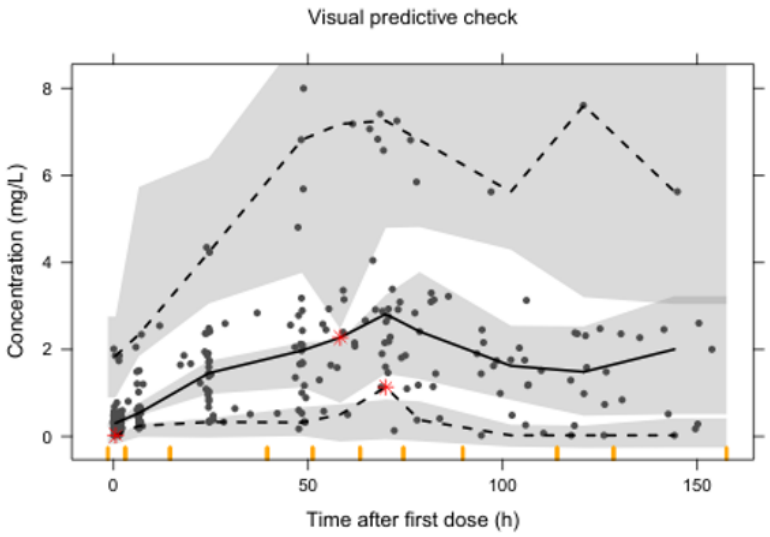

Figure 19: Visual Predictive Check produced using the parameters estimated by the final clonidine PK model. The shaded grey area is the 95 percent prediction interval. The black solid line is the median of the observed data; the black dashed lines are the 5 th and 95 th percentiles of the observed data.

Figure 20 shows the change in percentage of the clonidine individual clearances estimated by the final PK model plotted against the temperature.

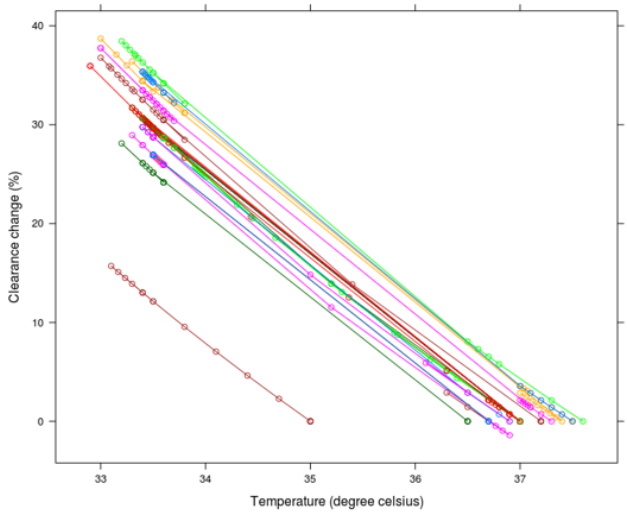

Figure 20: Percentage of clonidine clearance change plotted against the temperature. Each line represents a patient.

Figure 20 shows that the clonidine clearance can be reduced up to 40% during the hypothermic treatment (at 33 degrees Celsius).

4.3.2.2 Fentanyl

In total, 290 samples were used to develop the fentanyl final PK model. The observed concentrations of fentanyl plotted against time are presented in Figure 21.

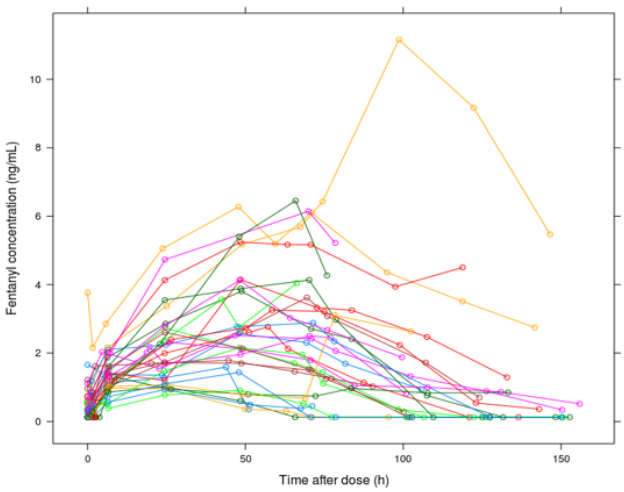

Figure 21: Observed concentration of fentanyl plotted against time after dose administration (TAD). Each line represents a patient.

Fentanyl observed concentrations were best described by a one-compartment model with IIV on clearance (CL) and central volume of distribution (V1). The BLOQ were included in the model using the M3 method. The final residual model was an additive error model. The model could not estimate the parameter of the maturation function, therefore they were fixed to values previously estimated by Anderson *et al.* (134). The change of temperature was found to be a significant covariate on fentanyl clearance. Table 10 summarises the parameter estimates from the final fentanyl PK model.

Table 10: Estimates from the final fentanyl PK model.

Parameter	Estimate	RSE (%)	Bootstrap estimate (95% CI)
CL (L/h/70kg)	135	16	137 (107-178)
V1 (L/70kg)	480	15	472.6 (370-647)
TEMP INDEX	3.94	24	4.01 (1.72-6.24)
IIV CL (%)	73.1	31	73.4 (53.8-92.2)
IIV V1 (%)	52.3	40	48.9 (26.4-62.4)
Err add (ng/mL)	0.477	29	0.469 (0.243-0.688)
PMA_50	73.6 FIX	-	-
Hill	3 FIX	-	-

CL is the clearance, V1 is the central volume of distribution, RSE is the relative standard error (from NONMEM covariance step), IIV is the interindividual variability. PMA_50 is the PMA (weeks) for CL to reach 50% maturity, and Hill is the shape parameter. TEMP index is the estimate corresponding to the temperature as covariate. FIX means that the value of the parameter was fixed a priori in the model. Err add corresponds to the additive error estimate.

Figure 22 shows the goodness-of-fit plots of the final fentanyl model.

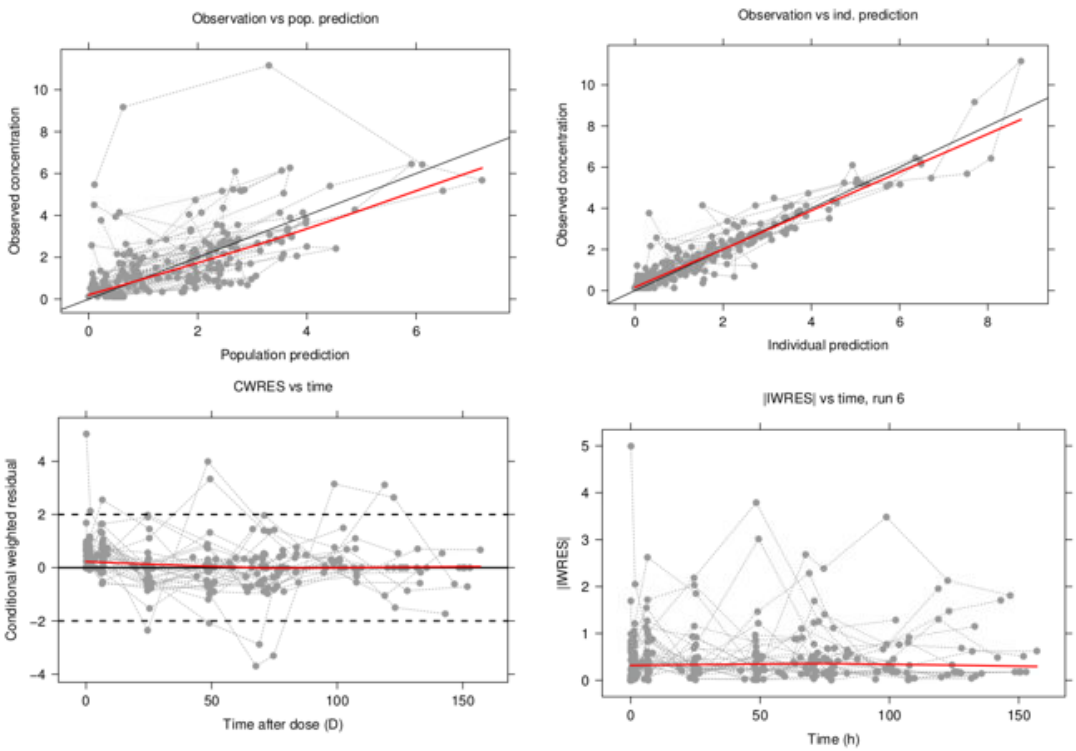

Figure 22: Goodness-of-fit plots of the final fentanyl PK model. Plots of the observed concentration vs population predicted concentration (top left) and vs individual predicted concentration (top right), the CWRES versus time after dose (bottom left) and plot of the IWRES vs time after dose (bottom right) from the final fentanyl population PK model. The red line is the lowess line and the black line is the line of unity.

The VPC used to evaluate the fentanyl model are presented in Figure 23.

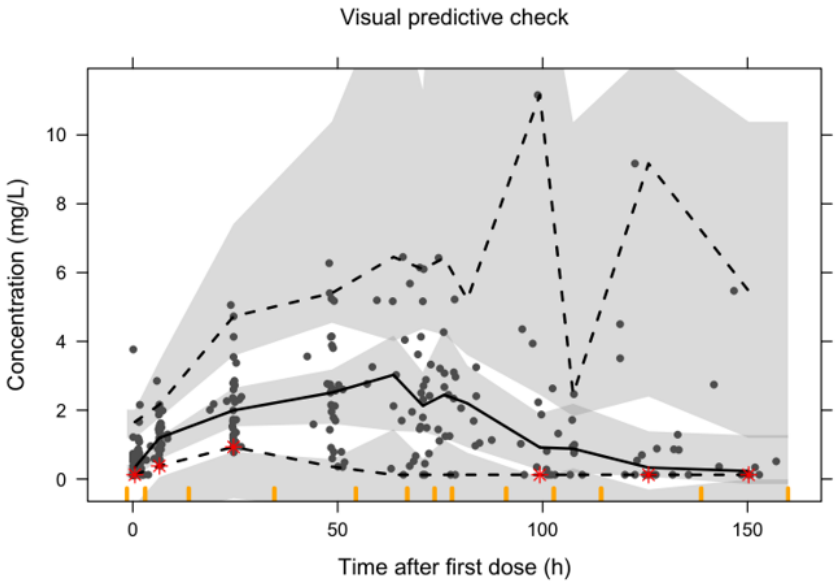

Figure 23: Visual Predictive Check produced using the parameters estimated by the final fentanyl PK model. The shaded grey area is the 95 percent prediction interval. The black solid line is the median of the observed data; the black dashed lines are the 5 th and 95 th percentiles of the observed data.

Figure 24 shows the relationship between temperature and individual clearances estimated by the final PK model.

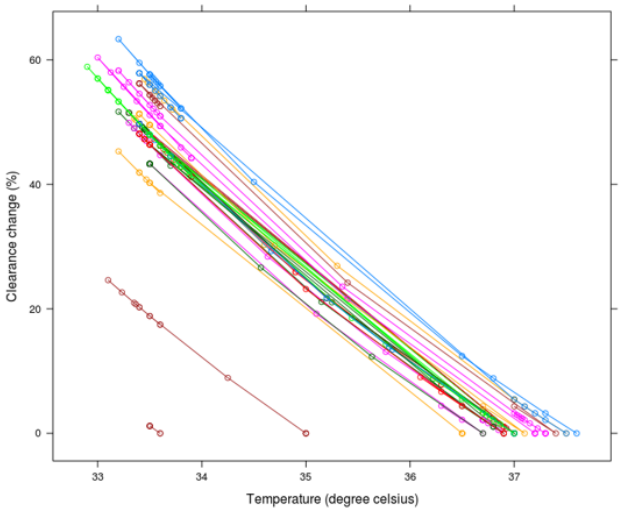

Figure 24: Percentage of fentanyl clearance change plotted against temperature. Each line represents a patient.

Figure 24 shows that the fentanyl clearance can be reduced up to 60% during the

hypothermic treatment (at 33 degrees Celsius).

4.3.3 Pharmacokinetic/pharmacodymamic models

4.3.3.1 ALPS-neo score

The histogram presented in Figure 25 shows the distribution of ALPS-neo scores.

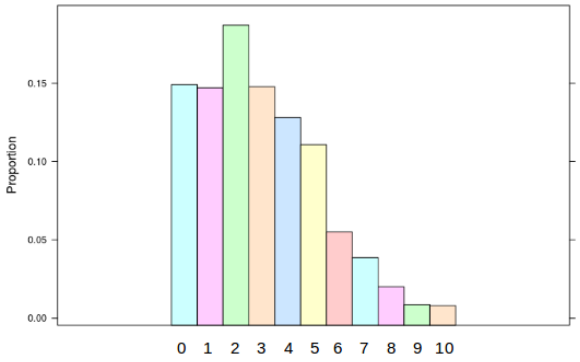

Figure 25: Proportion of ALPS-neo score

The graph shows that the scores are not distributed uniformly. The proportions of scores higher than 6 are considerably lower than the others. In addition, the histogram shows that the proportion of score 0 corresponding to no pain at all is one of the highest.

4.3.3.1.1 Clonidine

All the 31 patients were included in the PK/PD models. In total, 2999 ALPS-neo scores were used to build the models. The relationship between the observed score and clonidine concentration is presented in Figure 26.

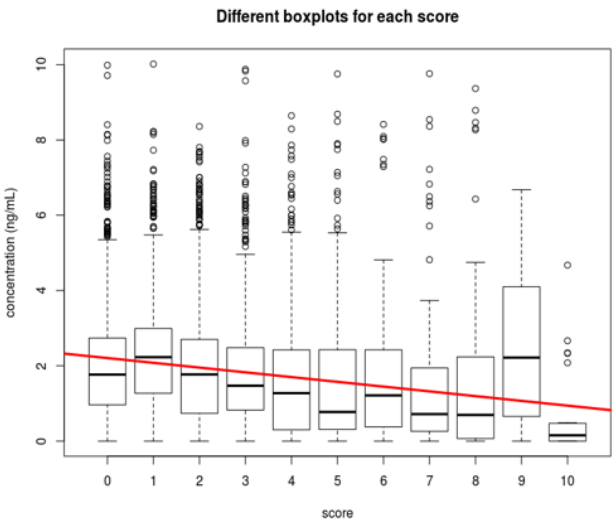

Figure 26: Observed clonidine concentration plotted against boxplot of ALPS-neo scores. The red line is the regression line.

The graph in Figure 26 shows that the ALPS-neo scores seem to decrease when the clonidine concentrations increase.

Emax model

The continuous Emax model that best described the clonidine data was an inhibitory sigmoid Emax model with IIV on EC50 and the baseline B0. The inclusion of an effect compartment did not induce a significant decrease of the OFV. The best error model was an additive error model. A significant influence of age and temperature was found on EC50 and baseline (B0), respectively (ΔOFV=12.4). The parameter estimated by the Emax model and the RSE corresponding are summarised in Table 11.

Table 11: Estimates from the ALPS-neo Emax clonidine PK/PD model.

Parameter	Estimate	RSE (%)	Bootstrap estimate (95% CI)
EC50 (ng/mL)	3.7	14	3.7 (2.9-7.0)
HILL	2.5	7	2.4 (1.6-2.7)
EMAX	1 FIX	-	-
B0	0.42	8	0.43 (0.37-0.56)
PMA EC50	-1.5	118	-1.5 (-6.9 - 4.9)
TEMP B0	-0.66	132	-0.65 (-2.2 - 0.56)
IIV EC50 (%)	53.2	42	51.9 (33.2-76.8)
IIV B0 (%)	64.1	36	59.1 (44.3-86.6)
Err add	0.59	9	0.58 (0.49-0.67)

EMAX is the maximal effect, EC50 is the concentration to reach 50% of the maximal effect in logit scale. B0 is the baseline score in logit scale. HILL is the shape parameter. TEMP B0 and PMA EC50 are the index corresponding to the effect of the temperature on the baseline and PMA on EC50, respectively. IIV is the interindividual variability. Err add is the error in logit scale.

Goodness-of-fit plots for the Emax model linking clonidine concentration and ALPS-neo scores are presented in Figure 27.

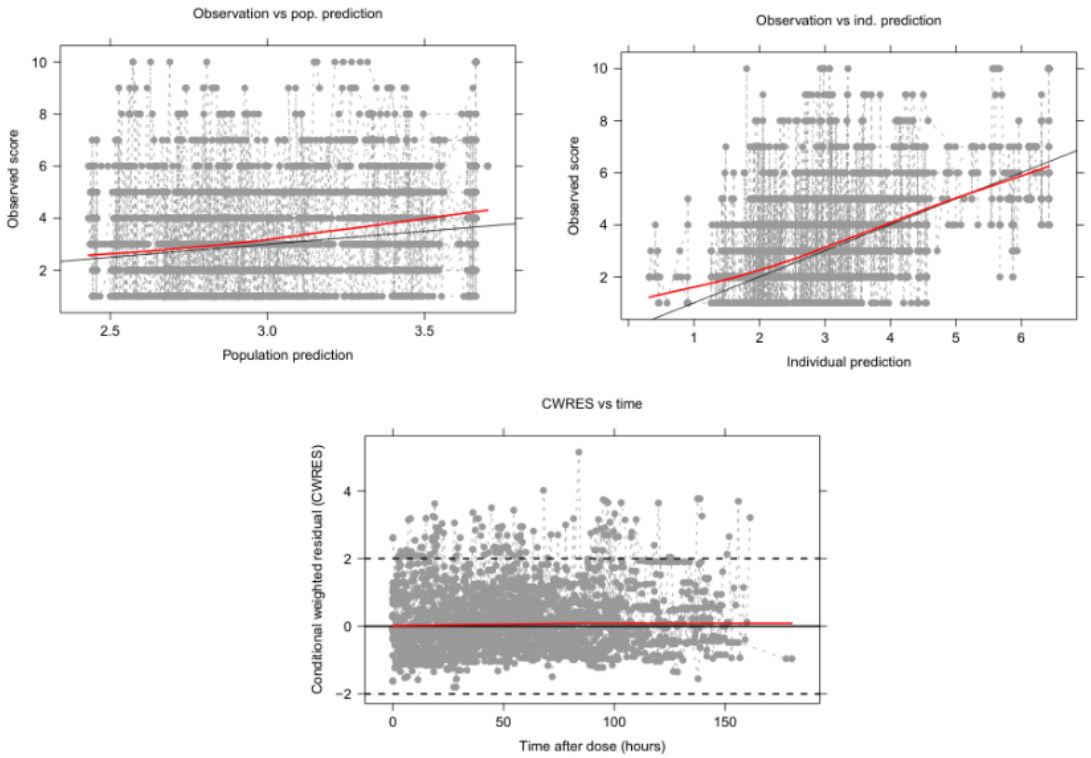

Figure 27: Goodness-of-fit plots of the clonidine Emax model. Plots of the observed scores vs population predicted scores (top left) and vs individual predicted scores (top right) and the CWRES versus time after dose (bottom) from the clonidine Emax model. The red line is the lowess line and the black line is the line of unity.

Figure 28 shows the PC-VPC used to evaluate the clonidine Emax model.

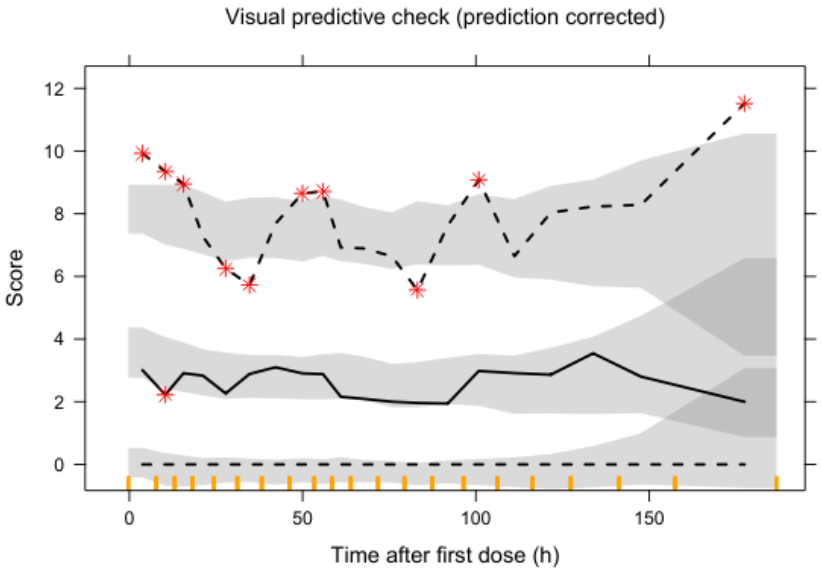

Figure 28: Visual Predictive Check produced using the parameters estimated by the clonidine Emax model. The shaded grey area is the 95 percent prediction interval. The black solid line is the median of the observed data; the black dashed lines are the 5 th and 95 th percentiles of the observed data.

Proportional odds model

A significant effect of the clonidine concentration as predictor on the ALPS-neo score was found using a proportional odds model (ΔOFV=29.3). An Emax model was used to describe the drug effect because it induced a higher decrease of the OFV than the linear model (OFV=11663.4 for the linear model compared to 11681.6 for the Emax model). Change in temperature was also a significant predictor (ΔOFV=33.9). Its effect was described using a linear model. The estimates of the proportional odds model are presented in Table 12.

Table 12: Estimates from the ALPS-neo proportional odds clonidine PK/PD model.

Parameter	Estimate	RSE (%)	Bootstrap estimate (95% CI)
B1	6.97	41	6.64 (1.22-10.9)
B2	-1.09	10	-1.09 (-1.30 - -0.89)
B3	-1.02	9	1.0 (-1.2 - -0.89)
B4	-0.78	11	-0.78 (-0.95 - -0.65)
B5	-0.78	10	-0.77 (-0.94 - -0.65)
B6	-0.92	12	-0.94 (-1.1 - -0.76)
B7	-0.71	14	-0.69 (-0.89 - -0.54)
B8	-0.83	18	-0.81 (-1.1 - -0.57)
B9	-0.83	24	-0.80 (-1.32 - -0.53)
B10	-0.77	38	-0.75 (-1.64 - -0.42)
EC50 (ng/mL)	0.77	76	0.94 (0.13-3.3)
EMAX	0.92	56	1.10 (0.33-2.60)
TEMP	-0.12	7	-0.11 (-0.24 – 0.05)
IIV	1.38	33	1.35 (0.76-2.1)

B are the baseline for each category. EMAX is the maximal effect, EC50 is the concentration to reach 50% of the maximal effect in logit scale. TEMP is the index corresponding to the effect of the temperature. IIV is the interindividual variability.

The model was evaluated using categorical VPC showing the proportion of the observed scores plotted against time in Figure 29 and the same proportion plotted against clonidine concentration in Figure 30.

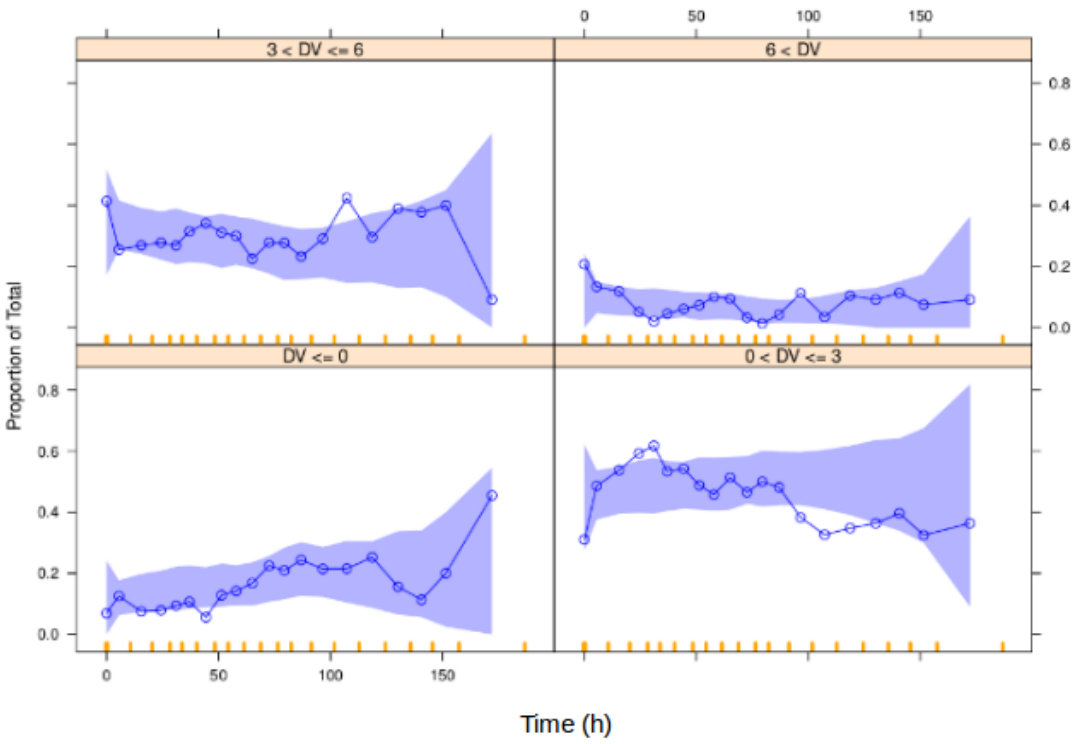

Figure 29: Categorical VPC produced using the parameters estimated by the proportionnal odds PK/PD model (score proportion vs time). The shaded blue area is the 95 percent prediction interval. The blue solid line is the median proportion of the observed scores. DV corresponds to the observed scores and the VPC were stratified by scores.

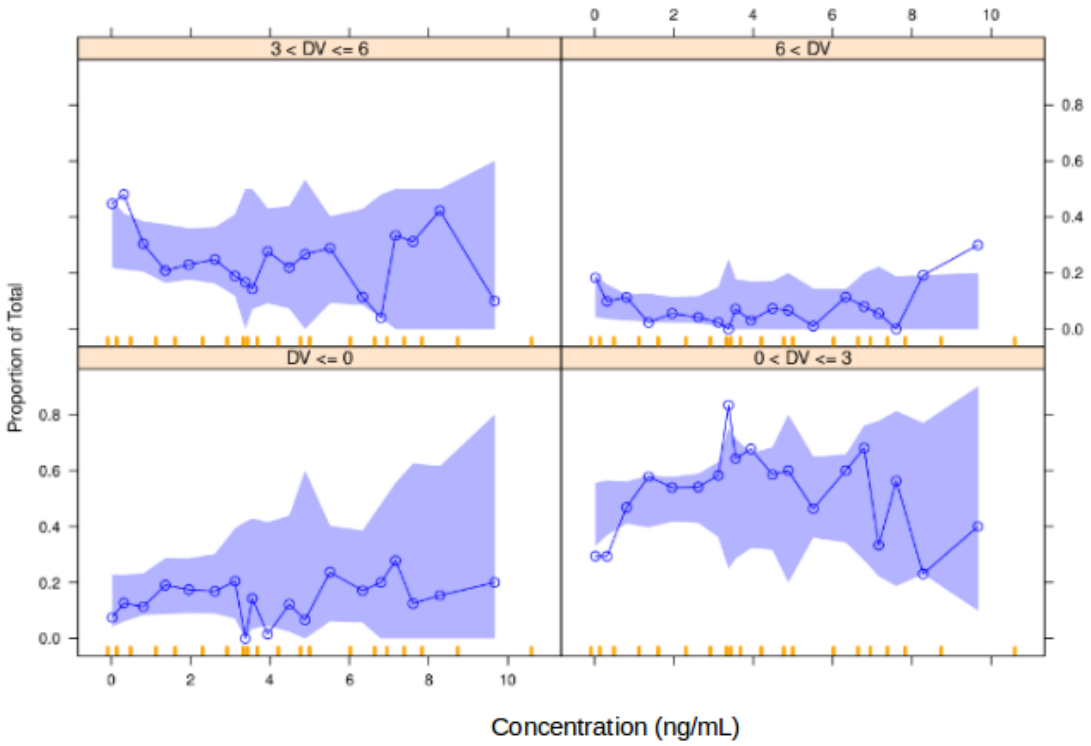

Figure 30: Categorical VPC produced using the parameters estimated by the proportionnal odds PK/PD model (score proportion vs concentration). The shaded blue area is the 95 percent prediction interval. The blue solid line is the median proportion of the observed scores. DV corresponds to the observed scores and the VPC were stratified by scores.

Bounded integer model

A BI model was developed to describe the relationship between clonidine concentration and ALPS-neo score. An Emax model was used to describe the drug effect. The addition of a Markov element significantly improved the model (ΔOFV=1791.1), therefore the parameter was included in the model with an IIV on the baseline score estimate (BASE). The parameters estimated by the BI model are summarised in Table 13.

Table 13: Estimates from the ALPS-neo BI clonidine PK/PD model.

	Parameter	Estimate	RSE (%)	Bootstrap estimate (95% CI)
	EC50 (ng/mL)	1.29	56	1.21 (0.32-3.47)
DRUG EFFECT	EMAX	0.40	42	0.47 (0.22-0.88)
	HILL	1 FIX	-	-
	SD	0.57	5	0.56 (0.52-0.61)
	BASE	-0.57	35	-0.64 (-1.0 - -0.36)
MARKOV EFFECT	PMAX	0.22	104	0.30 (0.05-0.79)
	HL	0.082	90	0.079 (0.022-0.36)
	PM	0.63	13	0.62 (0.48-0.77)
	IIV BASE (%)	0.11	45	0.09 (0.042-0.17)

EMAX is the maximal effect, EC50 is the concentration to reach 50% of the maximal effect in logit scale. HILL is the shape parameter. IIV is the interindividual variability. SD is the residual error. PM is the markov element, BASE is the baseline score estimate of the latent variable, PMAX is the maximal Markov effect and HL is the half life of the Markov effect.

Figure 31 and 32 show the goodness-of-fit plots of the PWRES used to evaluate the

model including the clonidine drug effect without and with a Markov effect, respectively.

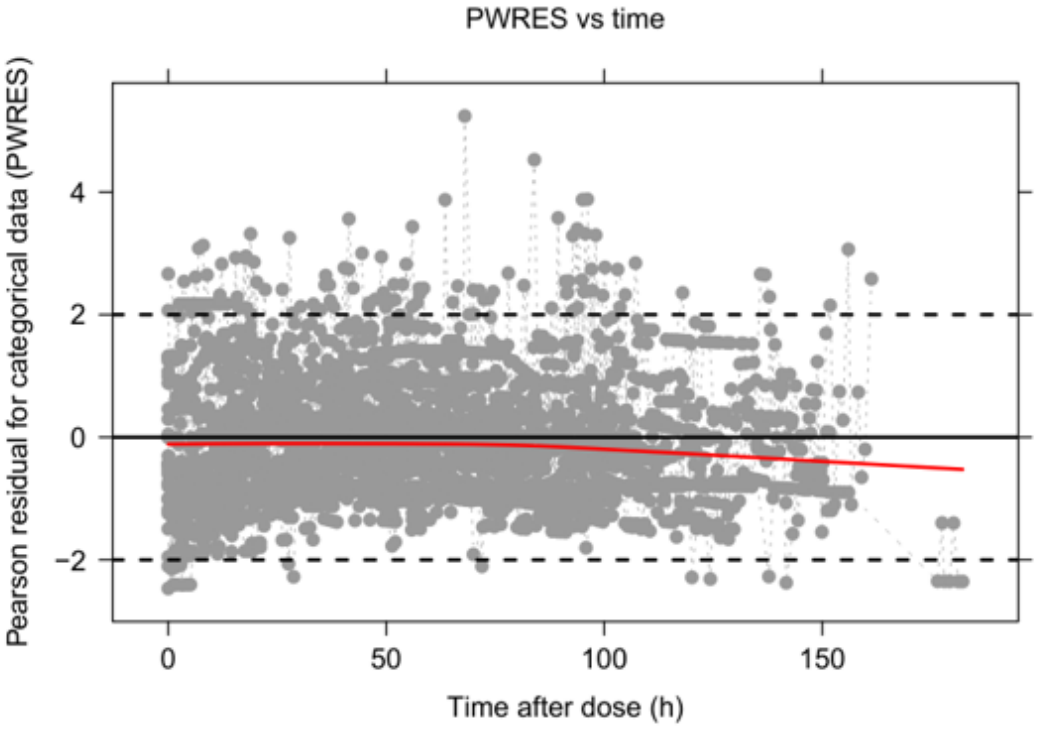

Figure 31: Goodness-of-fit plot of the clonidine BI model without Markov effect. Plot of the Pearson residual for categorical data (PWRES) vs time after dose. The red line is the lowess line and the black line is the line of unity.

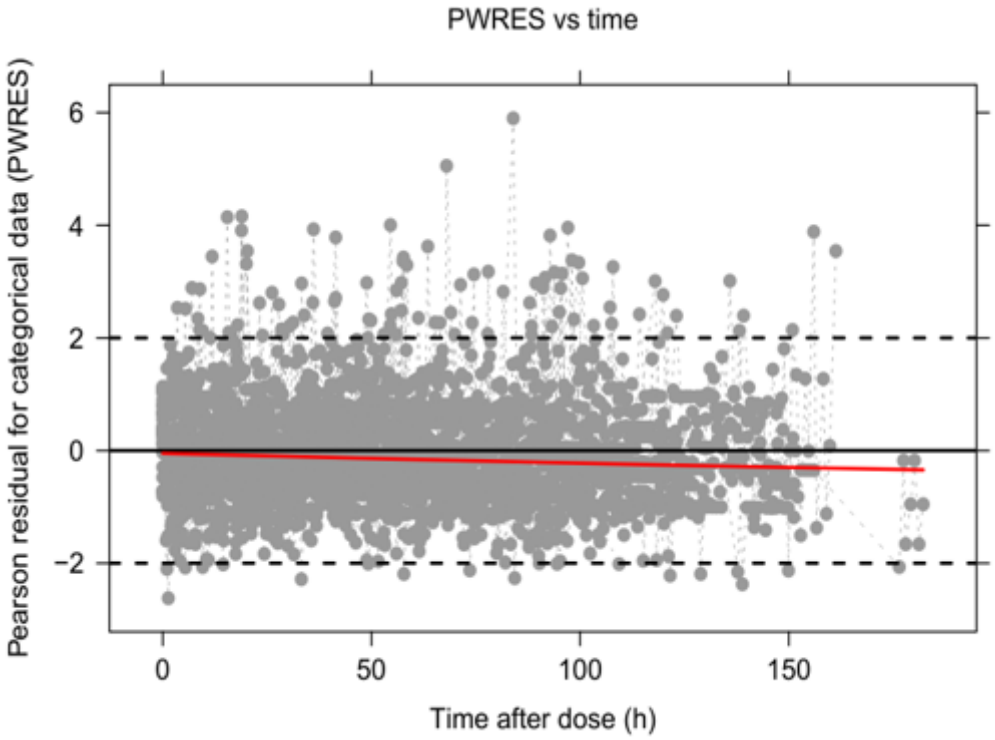

Figure 32: Goodness-of-fit plot of the clonidine BI model with Markov element. Plot of the Pearson residual for categorical data (PWRES) vs time after dose. The red line is the lowess line and the black line is the line of unity.

The relationship between clonidine concentration and probability to observe an ALPS-neo score calculated using the final BI model is presented Figure 33. The graph shows that at 2.5 ng/mL, there is a probability around 70% to have a score below 4 corresponding to a low level of pain. At 2.5 ng/mL, there is also a probability of 80% to get a score below 5.

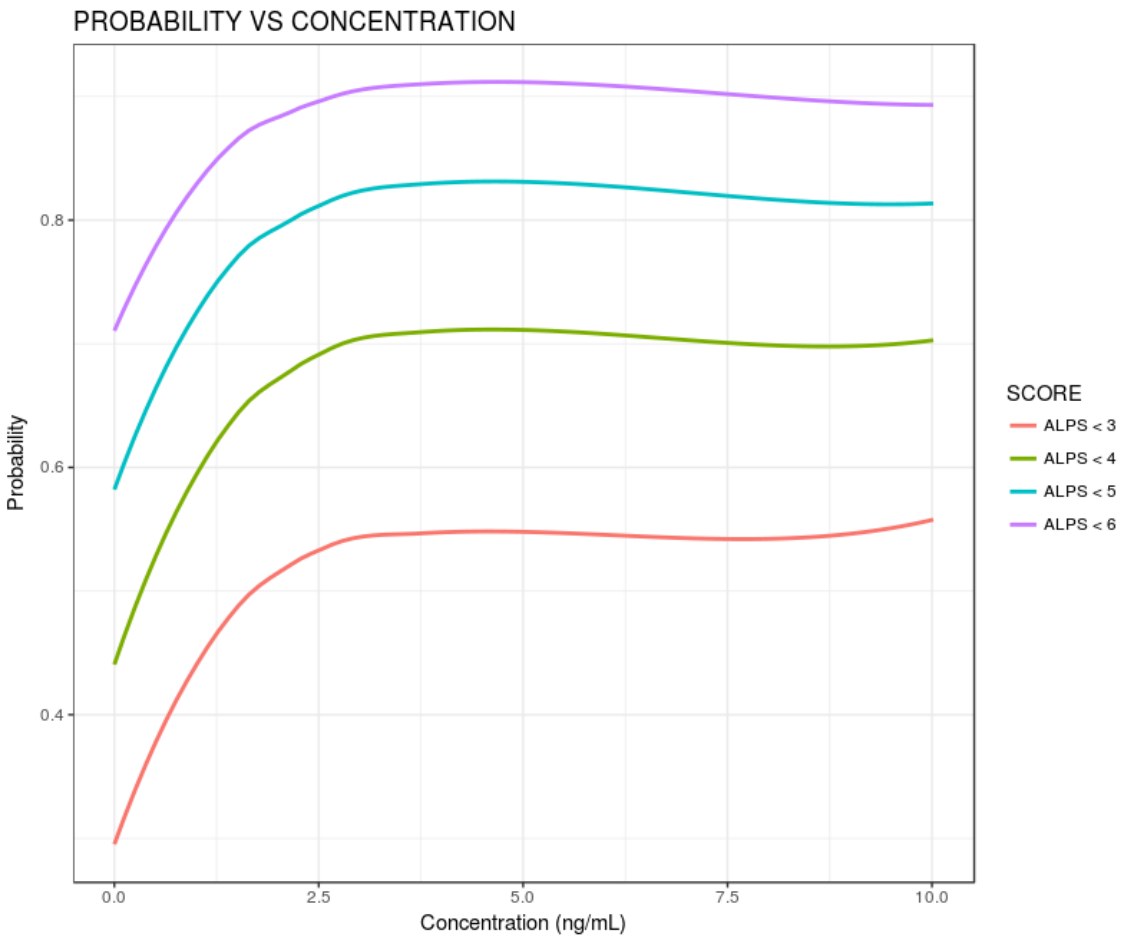

Figure 33: Probability to observe a score plotted against clonidine concentration. The solid lines are smooth lines for different category group.

4.3.3.1.2 Fentanyl

All the 31 patients were also included in the PK/PD models to describe the relationship between fentanyl PK and ALPS-neo score. In total, 3237 scores were used to develop each model. Figure 34 shows the relationship between observed score and fentanyl concentration.

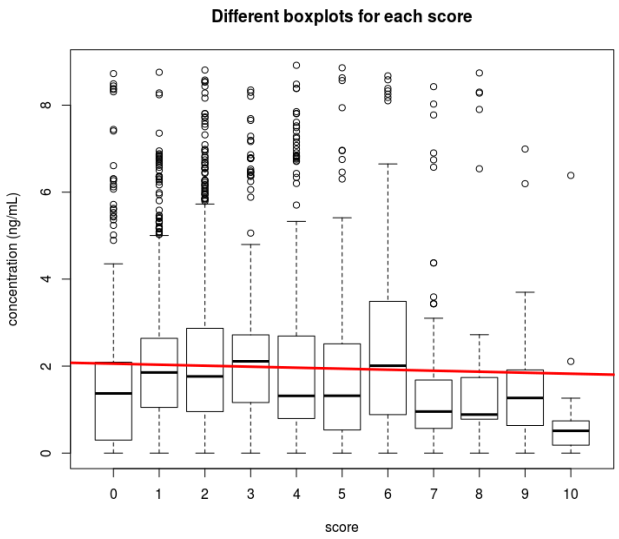

Figure 34: Observed fentanyl concentration plotted against ALPS-neo score. The red line is the regression line.

The graph in Figure 34 does not show a clear relationship between ALPS-neo score and fentanyl concentration.

Emax model

The Emax model that adequately described the fentanyl data was also an inhibitory sigmoid Emax model with IIV on EC50 and the baseline B0 and an additive error model. The inclusion of an effect compartment was not significant. A significant effect of hypothermia was found on both EC50 and B0 (ΔOFV = 159.7). The estimates from the Emax model and the RSE corresponding are presented in Table 14.

Table 14: Estimates from the ALPS-neo Emax fentanyl PK/PD model.

Parameter	Estimate	RSE (%)	Bootstrap estimate median
EC50 (ng/mL)	4.6	19	5.1
HILL	1.8	9	1.7
EMAX	1 FIX	-	-
B0	0.48	9	0.46
TEMP EC50	-4.3	22	-4.4
TEMP B0	29.3	73	32.3
IIV EC50 (%)	85.2	46	94.8
IIV B0 (%)	65.4	27	64.0
Err add	0.56	9	0.53

EMAX is the maximal effect, EC50 is the concentration to reach 50% of the maximal effect in logit scale. B0 is the baseline score in logit scale. HILL is the shape parameter. TEMP B0 and TEMP EC50 are the index corresponding to the effect of the temperature on the baseline and EC50, respectively. IIV is the interindividual variability. Err add is the error in logit scale.

Goodness-of-fit plots for the fentanyl ALPS-neo Emax model are presented in Figure 35.

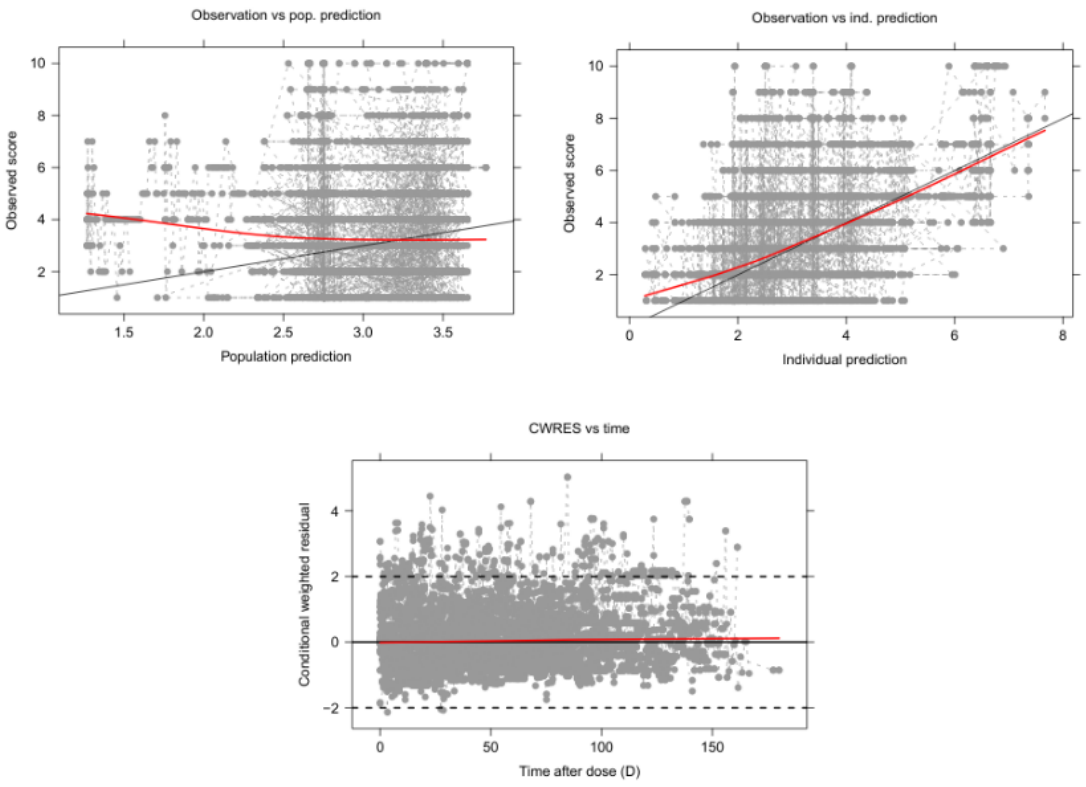

Figure 35: Goodness-of-fit plots of the fentanyl Emax model. Plots of the observed score vs population predicted score (top left) and vs individual predicted score (top right) and the CWRES versus time after dose (bottom) from the fentanyl Emax model. The red line is the lowess line and the black line is the line of unity.

Figure 36 shows the PC-VPC used to evaluate the fentanyl Emax model.

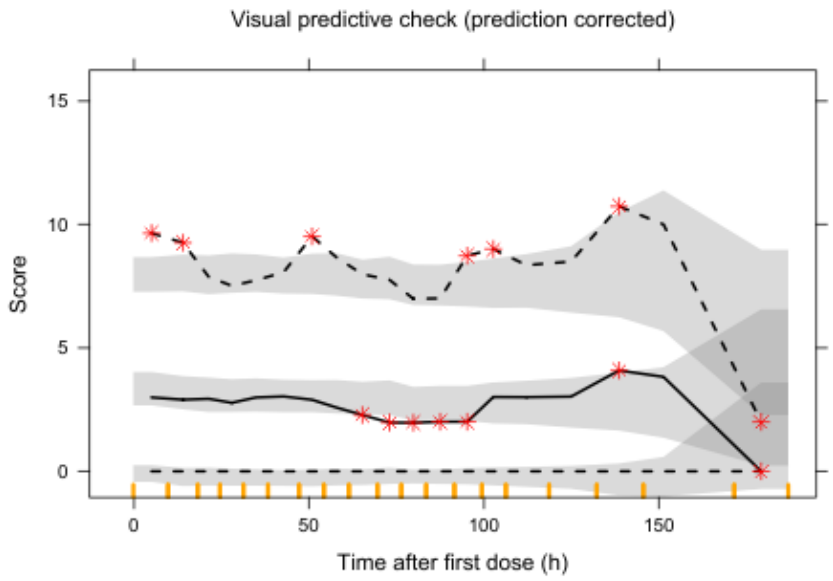

Figure 36: Visual Predictive Check produced using the parameters estimated by the fentanyl Emax model. The shaded grey area is the 95 percent prediction interval. The black solid line is the median of the observed data; the black dashed lines are the 5 th and 95 th percentiles of the observed data.

Proportional odds model

The addition of fentanyl concentration as predictor in the proportional odds model describing the ALPS-neo scores was not found significant with an OFV decrease below 3.84 points (ΔOFV=0.4).

Bounded integer model

A BI model was built in order to describe the relationship between fentanyl concentration and ALPS-neo score. An Emax model was used to describe the drug effect. IIV were added on EC50 and BASE. The addition of a Markov effect increased the instability of the model which was not able to estimate the parameters. The parameter estimates and RSE corresponding are presented in Table 15.

Table 15: Estimates from the ALPS-neo BI fentanyl PK/PD model.

Parameter	Estimate	RSE (%)	Bootstrap estimate (95% CI)
EC50 (ng/mL)	0.16	1512	0.16 (0.0067-1.99)
EMAX	0.88	22171	0.86 (0.70-1.18)
HILL	1.03	33	1.04 (0.99-1.34)
SD	0.574	642	0.564 (0.425-1.434)
IIV EC50 (%)	21.8	880	21.3 (2.8-40.7)
IIV BASE (%)	0.122	436	0.101 (0.0347-0.180)

EMAX is the maximal effect, EC50 is the concentration to reach 50% of the maximal effect in logit scale. HILL is the shape parameter. IIV is the interindividual variability. SD is the residual error.

Goodness-of-fit plot of the PWRES used to evaluate the BI model with an Emax drug effect is presented in Figure 37.

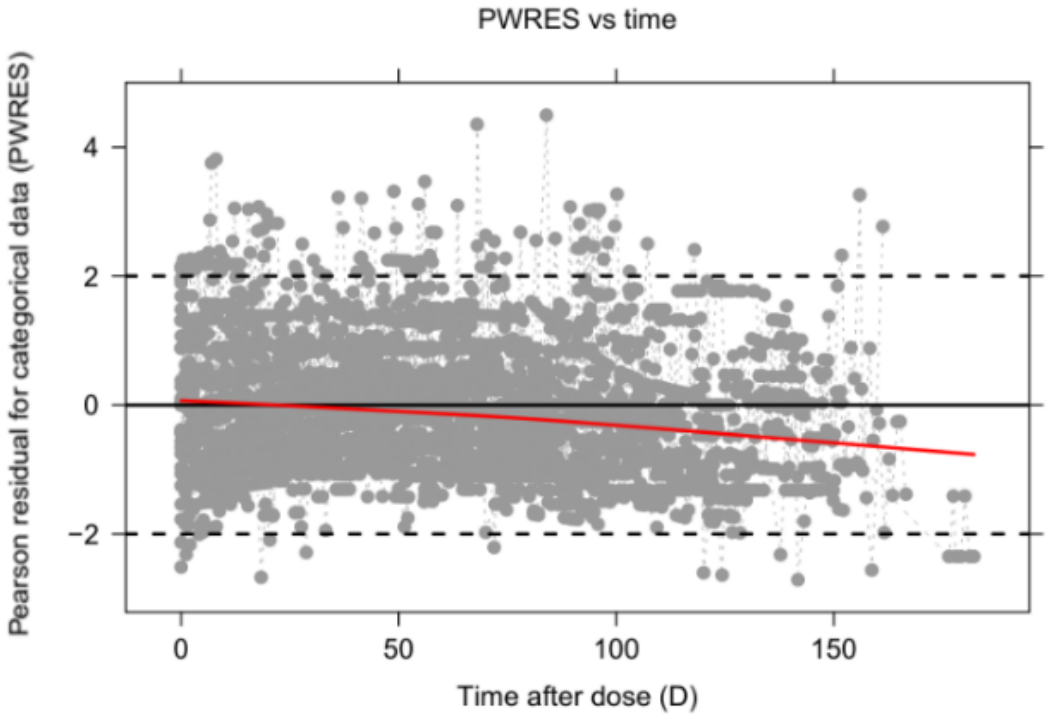

Figure 37: Goodness-of-fit plot of the fentanyl BI model. Plot of the Pearson residual for categorical data (PWRES) vs time after dose. The red line is the lowess line and the black line is the line of unity.

4.3.3.1.3 Joint models

Emax model

A joint Emax model describing the relationship between ALPS-neo score and both drugs was developed. IIV were added on the EC50 of both drugs and the error model used was an additive error model. A significant influence of the hypothermia was found on the baseline B0 (common for both drugs) and the fentanyl EC50 (ΔOFV=154.3). The parameters estimated by the joint Emax model are presented in Table 16.

Table 16: Estimates from the ALPS-neo joint Emax PK/PD model.

Parameter	Estimate	RSE (%)	Bootstrap estimate (95% CI)
CLO EC50 (ng/mL)	6.11	20	6.33 (4.65-58.01)
CLO HILL	1.78	9	1.82 (0.50-2.04)
FENT EC50 (ng/mL)	2.53	12	2.56 (1.42-4.09)
FENT HILL	1.99	11	1.91 (0.66-6.66)
EMAX	1 FIX	-	-
B0	0.418	8	0.410 (0.359-0.473)
TEMP BO	-2.03	43	-1.96 (-2.83 - -0.677)
FENT TEMP EC50	28.9	15	31.4 (25.7-289.9)
CLO IIV EC50 (%)	101	40	104 (69-451)
FENT IIV EC50 (%)	60.1	41	64.0 (44.7-812.4)
IIV B0	65.2	36	57.4 (18.4-494.9)
Err add	0.59	9	0.59 (0.51-0.67)

CLO corresponds to clonidine and FENT to fentanyl. EMAX is the maximal effect, EC50 is the concentration to reach 50% of the maximal effect in logit scale. B0 is the baseline score in logit scale. HILL is the shape parameter. TEMP BO and FENT TEMP EC50 are the index corresponding to the effect of the temperature on B0 and EC50, respectively. IIV is the interindividual variability. Err add is the error in logit scale.

Goodness-of-fit plots and PC-VPC used to evaluate the joint Emax model are presented in Figure 38 and 39, respectively.

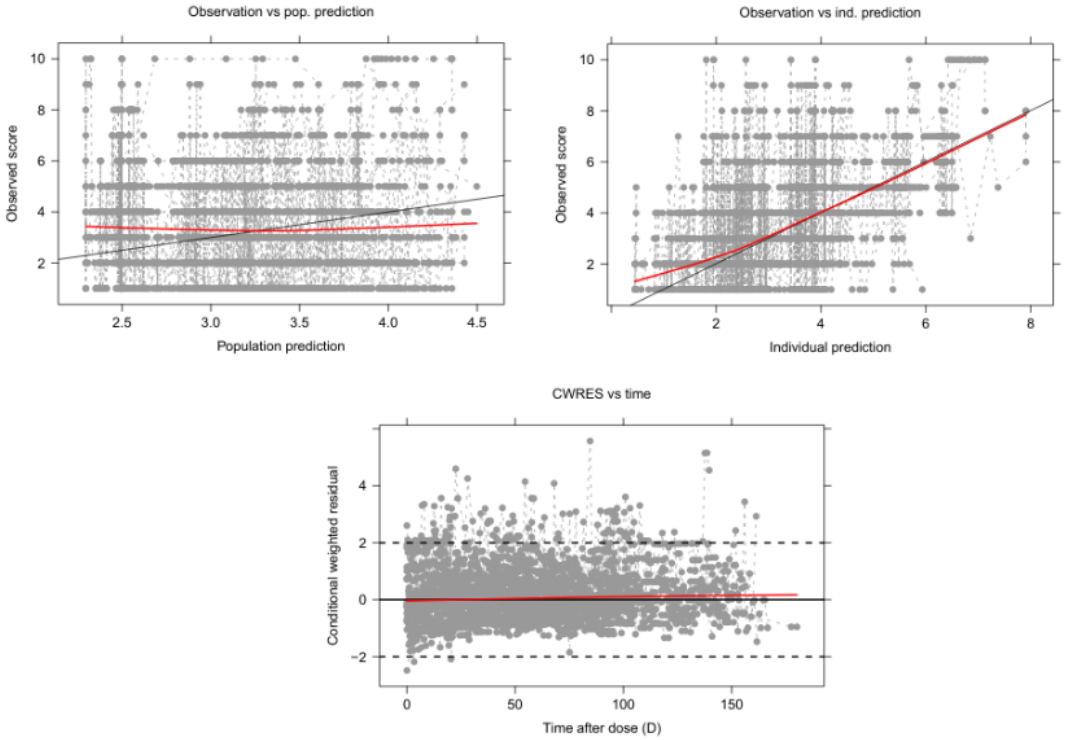

Figure 38: Goodness-of-fit plots of the joint Emax model. Plots of the observed score vs population predicted score (top left) and vs individual predicted score (top right) and the CWRES versus time after dose (bottom) from the joint Emax model. The red line is the lowess line and the black line is the line of unity.

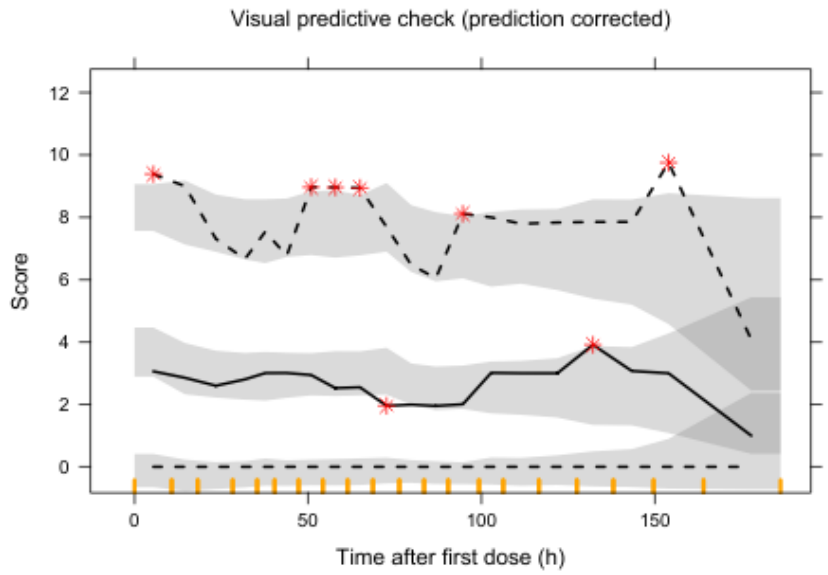

Figure 39: Visual Predictive Check produced using the parameters estimated by the joint Emax model. The shaded grey area is the 95 percent prediction interval. The black solid line is the median of the observed data; the black dashed lines are the 5 th and 95 th percentiles of the observed data.

Proportional odds model

A significant effect of both predictors corresponding to clonidine and fentanyl concentrations was found on the ALPS-neo score using a joint proportional odds model (ΔOFV=69.2). The clonidine drug effect was best described using an Emax model (ΔOFV=5.4) whereas a linear model was used to describe the fentanyl drug effect. The Emax model tested to describe the fentanyl concentration did not induce a significant decreased of the OFV and estimated an EC50 to non plausible value. The change in temperature was also a significant predictor (ΔOFV=41.1). The estimates from the joint proportional odds model are summarised in Table 17.

Table 17: Estimates from the ALPS-neo proportional odds joint PK/PD model.

Parameter	Estimate	RSE (%)	Bootstrap estimate (95% CI)
B1	2.71	14	2.37 (2.15-3.43)
B2	-1.09	11	-1.11 (-1.27 - -0.91)
B3	-1.02	9	-1.02 (-1.19 - -0.89)
B4	-0.778	11	-0.784 (-0.919 - -0.618)
B5	-0.779	10	-0.776 (-0.938 - -0.643)
B6	-0.923	12	-0.944 (-1.125 - -0.766)
B7	-0.706	14	-0.707 (-0.882 - -0.539)
B8	-0.824	18	-0.836 (-1.081 - -0.587)
B9	-0.831	24	-0.803 (-1.280 - -0.552)
B10	-0.767	38	-0.739 (-1.711 - -0.375)
CLO EC50 (ng/mL)	0.946	70	1.05 (0.23 – 3.16)
CLO EMAX	1.26	52	1.413 (0.545-2.740)
FENT SLP	0.0929	102	0.105 (-0.085 - 0.275)
TEMP INDEX	3.32	68	3.20 (-0.69 – 6.47)
IIV	1.32	36	1.35 (0.70 – 2.068)

CLO corresponds to clonidine and FENT to fentanyl. B are the baseline for each category. EMAX is the maximal effect, EC50 is the concentration to reach 50% of the maximal effect in logit scale. TEMP INDEX is the index corresponding to the effect of the temperature. IIV is the interindividual variability.

The categorical VPC showing the proportion plotted against time used to evaluate the model are presented in Figure 40, 41 and 42. Figure 41 and 42 show the categorical VPC of the proportion plotted against the concentration of clonidine and fentanyl, respectively.

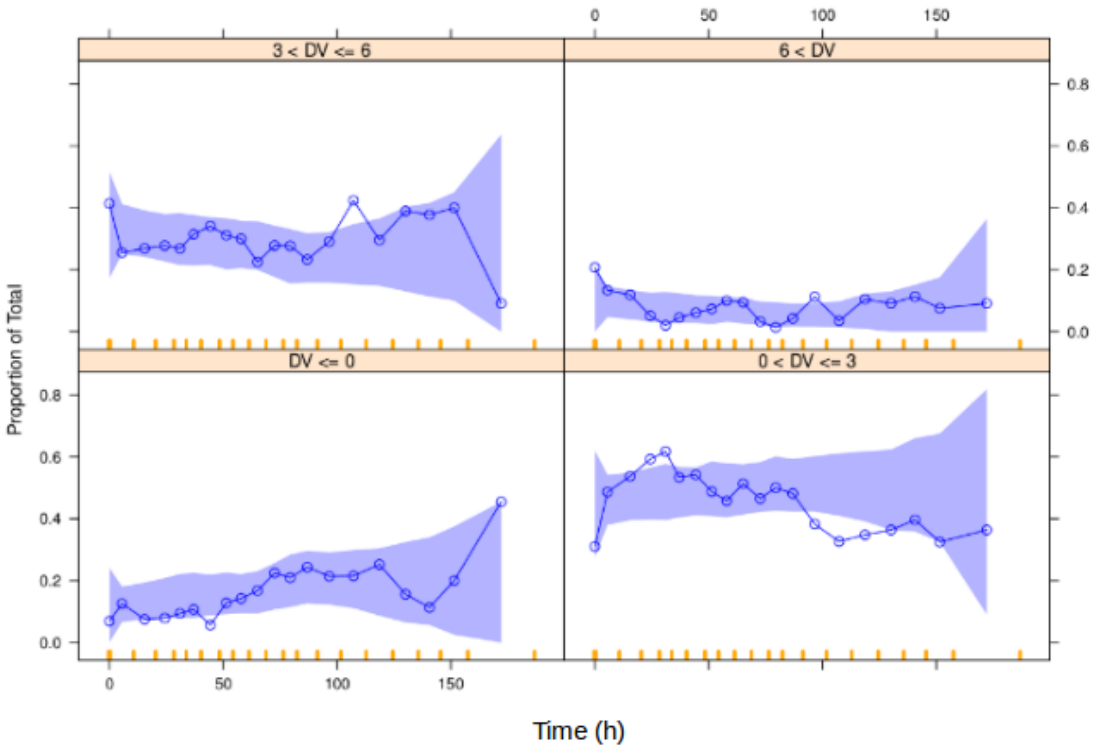

Figure 40: Categorical VPC for both drugs produced using the parameters estimated by the joint proportionnal odds PK/PD model (score proportion vs time). The shaded blue area is the 95 percent prediction interval. The blue solid line is the median proportion of the observed scores. DV corresponds to the observed scores and the VPC were stratified by scores.

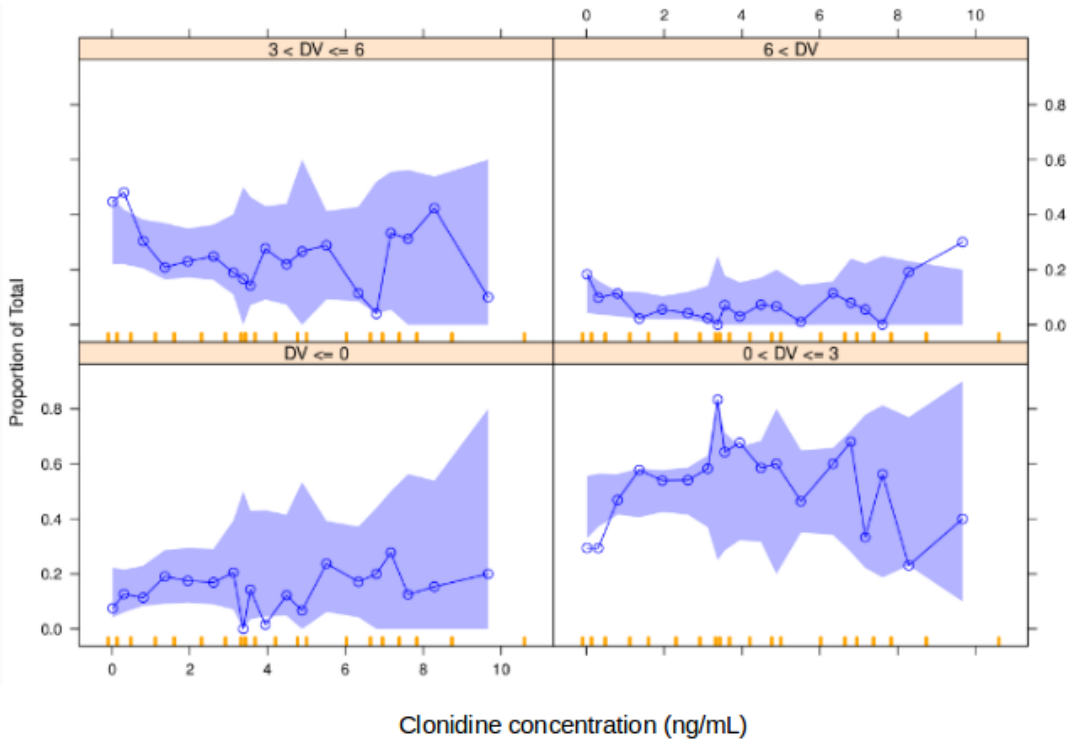

Figure 41: Categorical VPC for clonidine produced using the parameters estimated by the joint proportionnal odds PK/PD model (score proportion vs clonidine concentration). The shaded blue area is the 95 percent prediction interval. The blue solid line is the median proportion of the observed scores. DV corresponds to the observed scores and the VPC were stratified by scores.

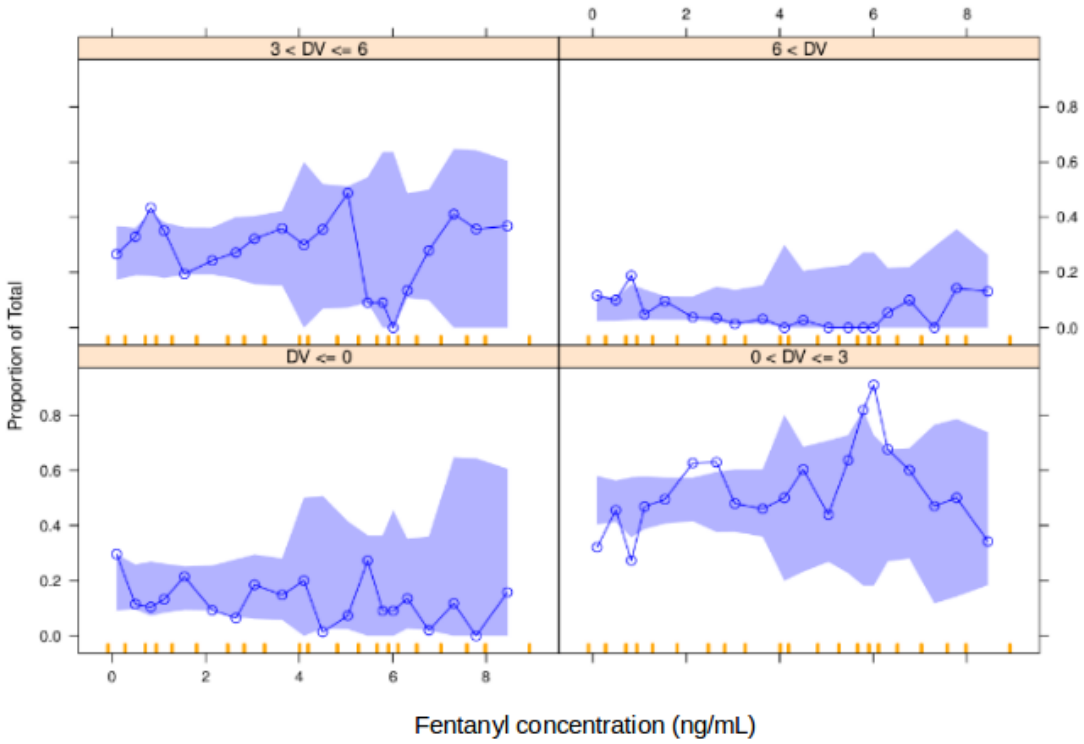

Figure 42: Categorical VPC for fentanyl produced using the parameters estimated by the joint proportionnal odds PK/PD model (score proportion vs fentanyl concentration). The shaded blue area is the 95 percent prediction interval. The blue solid line is the median proportion of the observed scores. DV corresponds to the observed scores and the VPC were stratified by scores.

The relationship between the fentanyl concentration and the probability to observe an ALPS-neo score is presented Figure 43. The graph shows that at 2.6 ng/mL, there is a probability around 80% to have a score below 5 corresponding to a low level of pain. At the same value, there is also a probability of 67% to get a score below 4.

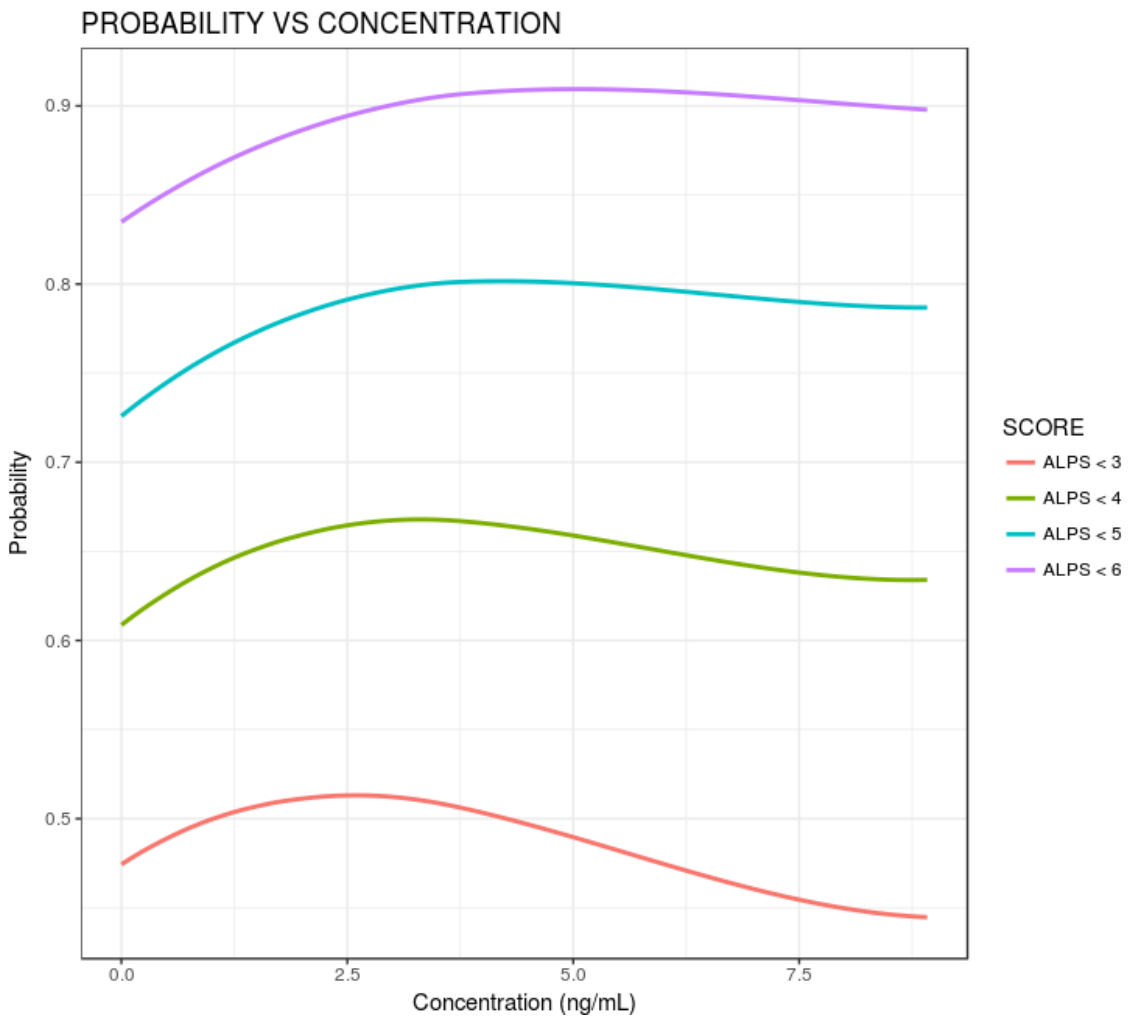

Figure 43: Probability to observe a score plotted against fentanyl concentration. The solid lines are smooth lines for different category group.

Bounded integer model

The joint BI model was not able describe the relationship between ALPS-neo score and concentration of clondine and fentanyl. The BI model estimated parameters of both drugs to non plausible values.

4.3.3.2 COMFORT-neo score

4.3.3.2.1 Clonidine

Twenty-nine patients were included in the clonidine COMFORT-neo PK/PD models. In order to develop the models, 2809 COMFORT-neo scores were used. Figure 44

shows the relationship between the observed scores and clonidine concentrations using boxplots.

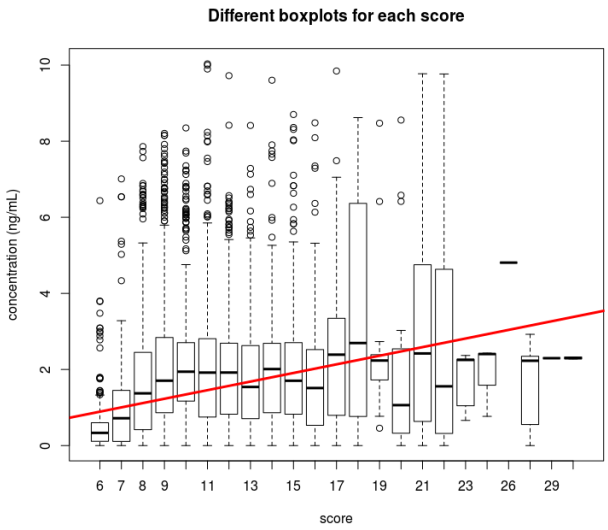

Figure 44: Observed clonidine concentration plotted against COMFORT-neo scores. The red line is the regression line.

Figure 44 shows that the COMFORT-neo score seems to increase when the clonidine concentrations increase. This can be explain by the Simpson's paradox (172).

Emax model

The Emax model that best fitted the data was an inhibitory sigmoid Emax model with additive error model and IIV on clonidine EC50 and baseline B0. The inclusion of an effect compartment did not induce a significant decrease of the OFV. A significant effect of the covariate temperature was found on B0 (ΔOFV=29.6). The estimates produced by the Emax model and the RSE corresponding are summarised in Table 18.

Table 18: Estimates from the COMFORT-neo Emax clonidine PK/PD model.

Parameter	Estimate	RSE (%)	Bootstrap estimate (95% CI)
EC50 (ng/mL)	4.45	22	5.15 (3.23-76.51)
HILL	1.99	18	1.68 (0.66-2.48)
EMAX	1 FIX	-	-
B0	0.244	10	0.249 (0.217-0.300)
TEMP B0	1.27	99	1.01 (-1.19 – 3.23)
IIV EC50 (%)	79.1	54	98.4 (51.1-665.4)
IIV B0 (%)	51.1	46	55.6 (35.3-91.1)
Err add	0.430	11	0.421 (0.335-0.497)

EMAX is the maximal effect, EC50 is the concentration to reach 50% of the maximal effect in logit scale. B0 is the baseline score in logit scale. HILL is the shape parameter. TEMP B0 is the index corresponding to the effect of the temperature on the baseline. IIV is the interindividual variability. Err add is the error in logit scale.

Goodness-of-fit plots and the PC-VPC used to evaluate the clonidine Emax model are presented in Figure 45 and 46, respectively.

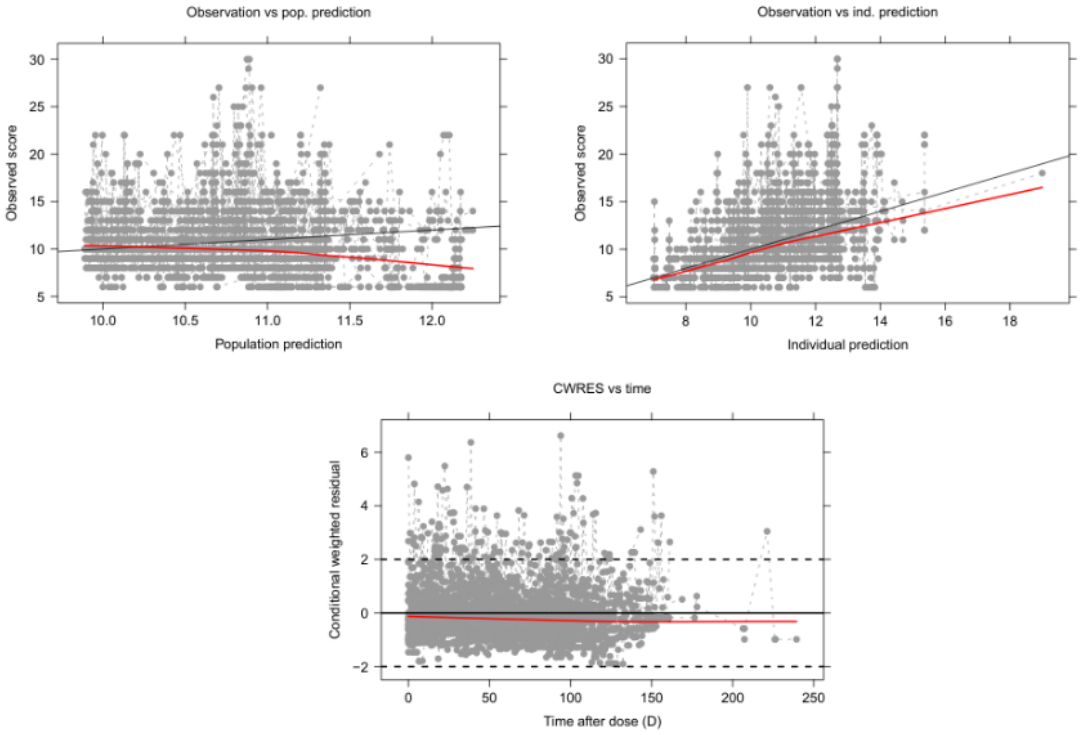

Figure 45: Goodness-of-fit of the clonidine COMFORT-neo Emax model. Plots of the observed score vs population predicted score (top left) and vs individual predicted score (top right) and the CWRES versus time after dose (bottom) from the joint Emax model. The red line is the lowess line and the black line is the line of unity.

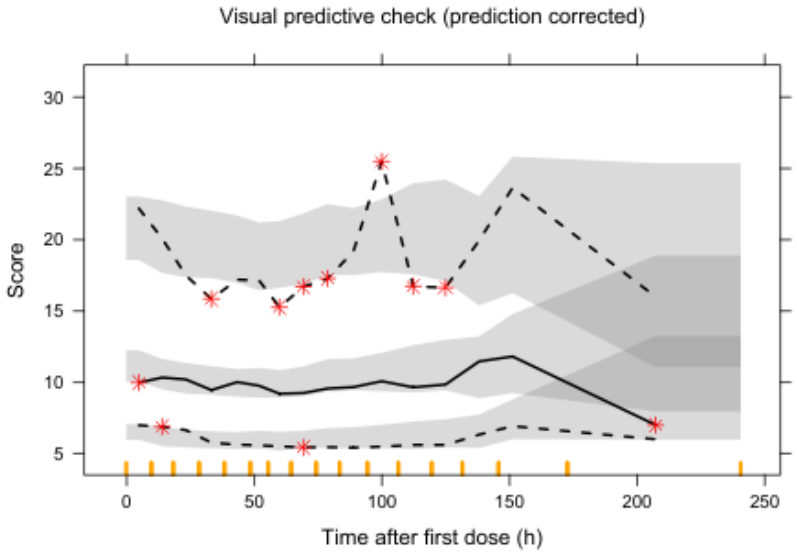

Figure 46: Visual Predictive Check produced using the parameters estimated by the clonidine COMFORT-neo Emax model. The shaded grey area is the 95 percent prediction interval. The black solid line is the median of the observed data; the black dashed lines are the 5 th and 95 th percentiles of the observed data.

Proportional odds model

A proportional odds model for the COMFORT-neo score was also developed. Clonidine concentration was a significant predictor in the model (ΔOFV=18.4). However, the model estimated the EC50 to a non plausible value therefore the model did not fit well the data.

Bounded integer model

A BI model was developed to describe the relationship between COMFORT-neo score and clonidine concentration. The drug effect was described using an Emax model. The addition of a drug effect and a Markov element in the baseline BI model induced a significant decrease of the OFV (ΔOFV= 4140.7 for the drug effect and ΔOFV=6085.8 for the Markov effect). However, the goodness-of-fit plots used to evaluate the model after addition of a drug or Markov effect (PWRES *vs* time) show that the lowess line of the PWRES is higher than 0, indicating the the model did not fit well the data.

4.3.3.2.2 Fentanyl

The 31 patients were included in the PK/PD models developed in order to describe the relationship between COMFORT-neo score and fentanyl concentration. To build the model, 3044 observed scores were used. Figure 47 shows the observed fentanyl concentrations plotted against boxplot of COMFORT-neo scores.

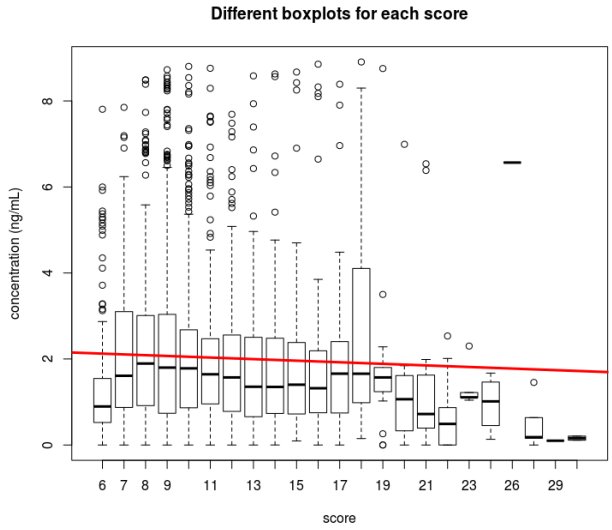

Figure 47: Observed fentanyl concentration plotted against COMFORT-neo scores. The red line is the regression line.

The graph presented in Figure 47 does not show a clear relationship between the COMFORT-neo scores and fentanyl concentrations.

Emax model

An inhibitory sigmoid Emax model with an additive error model and an IIV on EC50 and B0 adequately described the relationship between fentanyl concentration and COMFORT-neo score. The covariate temperature was found significant on the EC50 and B0 (ΔOFV=415.7). The parameters estimated by the Emax model are presented in Table 19.

Table 19: Estimates from the COMFORT-neo Emax fentanyl PK/PD model.

Parameter	Estimate	RSE (%)	Bootstrap estimate median
EC50 (ng/mL)	1.72	54	1.68
HILL	0.87	32	0.92
EMAX	1 FIX	-	-
B0	0.385	11	0.366
TEMP EC50	22.5	48	25.7
TEMP B0	-4.86	30	-5.17
IIV HILL (%)	79.4	32	80.6
IIV EC50 (%)	185.2	145	181.4
IIV B0	61.8	36	59.9
Err add (ng/mL)	0.36	9	0.36

EMAX is the maximal effect, EC50 is the concentration to reach 50% of the maximal effect in logit scale. B0 is the baseline score in logit scale. HILL is the shape parameter. TEMP B0 and TEMP EC50 is the index corresponding to the effect of the temperature on B0 and EC50, respectively. IIV is the interindividual variability. Err add is the error in logit scale.

Goodness-of-fit plots and PC-VPC used to evaluate the fentanyl Emax model are presented in Figure 48 and 49, respectively.

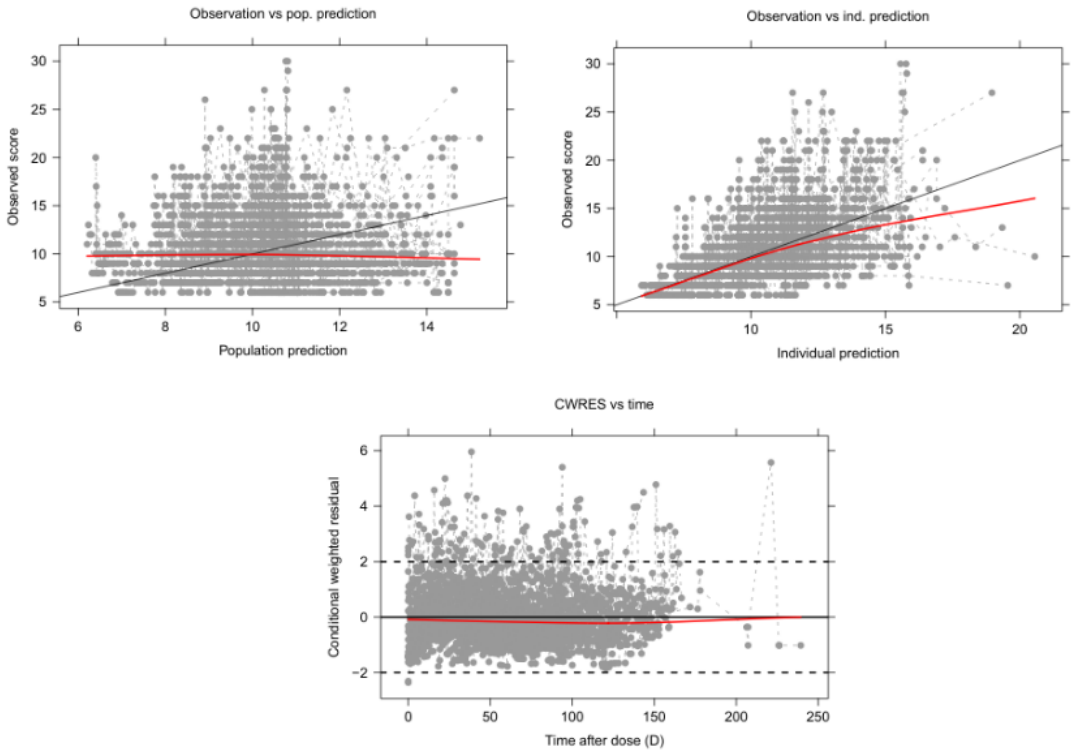

Figure 48: Goodness-of-fit plots of the COMFORT-neo fentanyl Emax model. Plots of the observed score vs population predicted score (top left) and vs individual predicted score (top right) and the CWRES versus time after dose (bottom) from the joint Emax model. The red line is the lowess line and the black line is the line of unity.

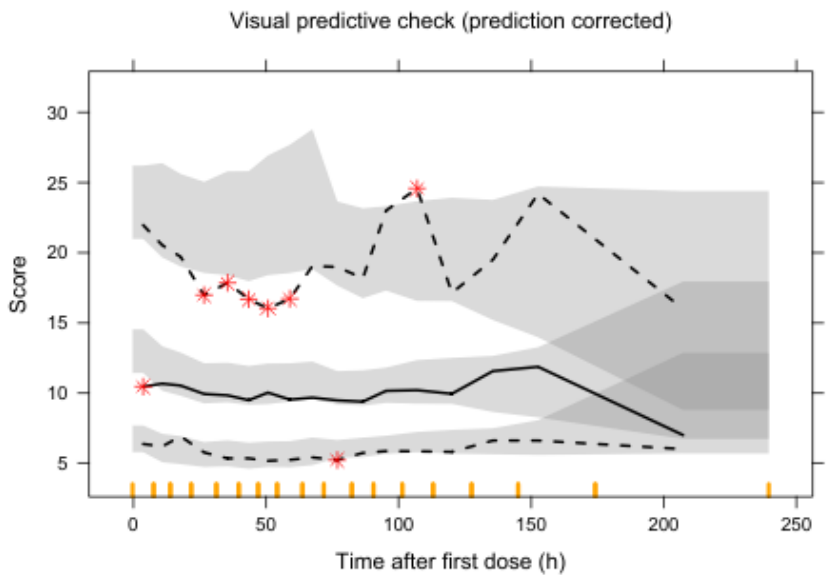

Figure 49: Visual Predictive Check produced using the parameters estimated by the COMFORT-neo fentanyl Emax model. The shaded grey area is the 95 percent prediction interval. The black solid line is the median of the observed data; the black dashed lines are the 5 th and 95 th percentiles of the observed data.

Proportional odds model

The addition of the predictor corresponding to the fentanyl concentration in the proportional odds model describing the COMFORT-B score induced a significant decrease of the OFV (ΔOFV=92.3). However, the model estimated the EC50 to an non plausible value. Therefore, the model did not fit well the data.

Bonded integer model

A BI model was built in order to describe the relationship between COMFORT-neo score and fentanyl concentration. The drug effect was described using an Emax model. As for the clonidine model, the addition of a drug as well as a Markov effect in the baseline BI model induced a significant decreased of the OFV (ΔOFV=6032.6 for the drug effect and ΔOFV=4247.2). However, the goodness-of-fit plots (PWRES *vs* time) used to evaluate the models showed that it did not adequately described the data with a lowess line higher than 0.

4.3.3.2.3 Joint model

Emax model

A joint Emax model describing the relationship between the concentrations of both drugs and COMFORT-neo score was built. The model included an IIV on the baseline B0 and the EC50 of both drugs. The residual error used was an additive error model. A significant effect of hypothermia was found on the fentanyl EC50 (ΔOFV=114.6). The estimates from the joint Emax model and the RSE corresponding are summarised in Table 20.

Table 20: Estimates from the COMFORT-neo Emax joint PK/PD model.

Parameter	Estimate	RSE (%)	Bootstrap estimate (95% CI)
CLO EC50 (ng/mL)	2.78	13	2.84 (2.26-89.5)
CLO HILL	3.60	14	3.59 (0.46-4.46)
FENT EC50 (ng/mL)	2.72	44	2.81 (0.85-37.80)
FENT HILL	0.92	3	0.91 (0.75-1.05)
EMAX	1 FIX	-	-
B0	0.235	7	0.237 (0.204-0.269)
FENT TEMP EC50	11.9	26	13.6 (10.3-244.9)
CLO IIV EC50 (%)	31.2	43	32.7 (20.9-656.5)
FENT IIV EC50 (%)	264.3	36	291.0 (185.4-952.8)
IIV B0	47.8	45	42.4 (24.5-61.6)
Err add	0.436	10	0.433 (0.352-0.532)

CLO corresponds to clonidine and FENT to fentanyl. EMAX is the maximal effect, EC50 is the concentration to reach 50% of the maximal effect in logit scale. B0 is the baseline score in logit scale. HILL is the shape parameter. TEMP EC50 is the index corresponding to the effect of the temperature on EC50. IIV is the interindividual variability. Err add is the error in logit scale.

Figure 50 shows the goodness-of-fit plots of the joint Emax model.

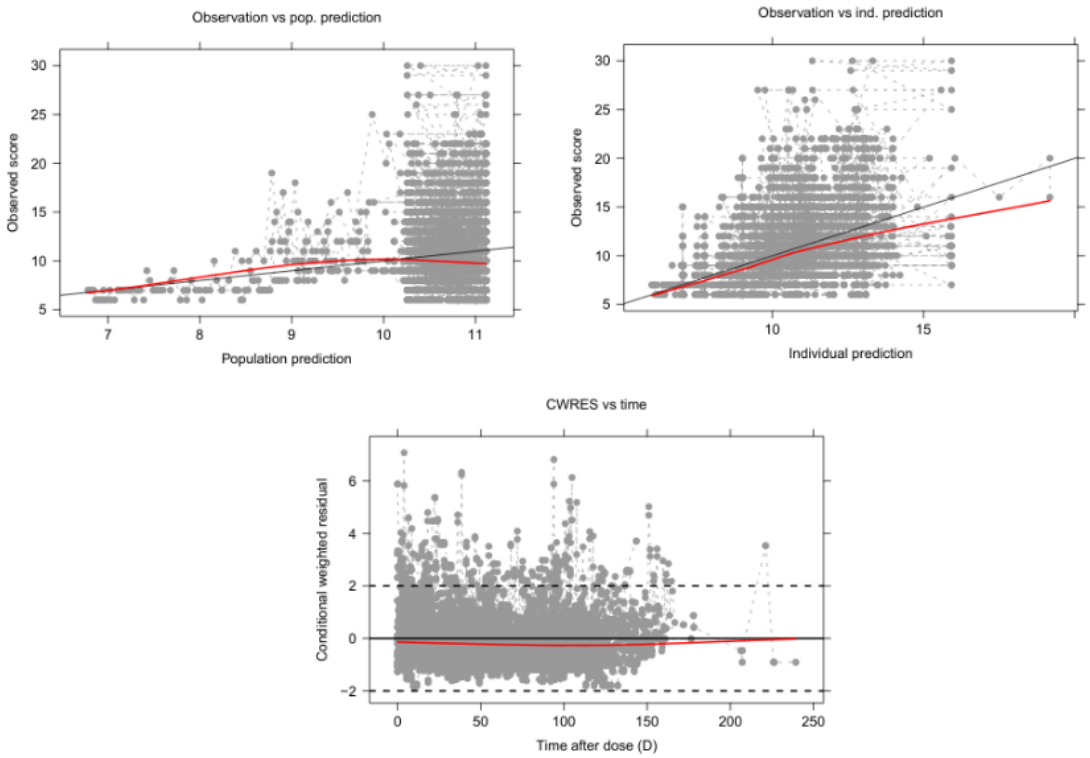

Figure 50: Goodness-of-fit plots of the joint Emax model. Plots of the observed score vs population predicted score (top left) and vs individual predicted score (top right) and the CWRES versus time after dose (bottom) from the joint Emax model. The red line is the lowess line and the black line is the line of unity.

The PC-VPC used to evaluate the joint Emax model are presented in Figure 51.

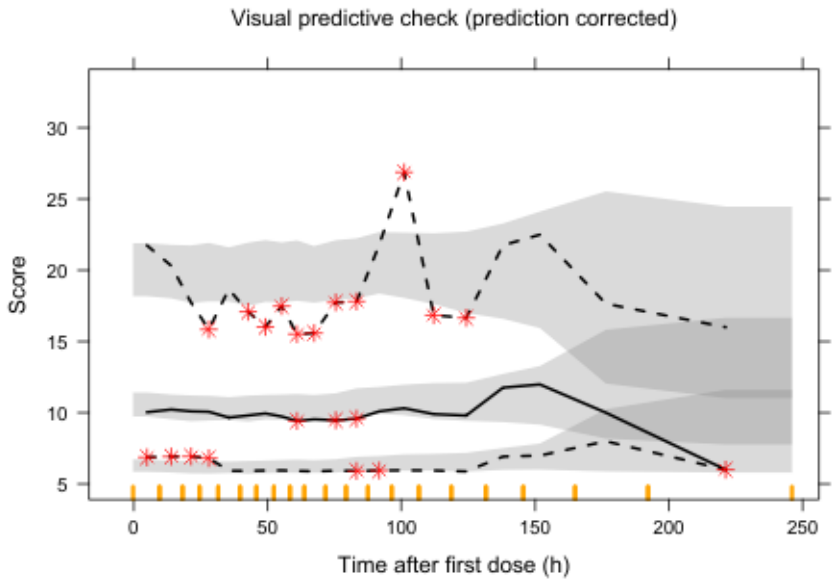

Figure 51: Visual Predictive Check produced using the parameters estimated by the COMFORT-neo joint Emax model. The shaded grey area is the 95 percent prediction interval. The black solid line is the median of the observed data; the black dashed lines are the 5 th and 95 th percentiles of the observed data.

Proportional odds model

The inclusion of both predictors corresponding to the concentration of fentanyl and clonidine in the joint proportional odds model used to describe the COMFORT-neo score induced an overparametrization. Therefore the model was not able to fit the data or estimate the parameters.

Bounded integer model

The joint BI model estimated most of the parameters to non plausible values, therefore the model was not able to adequately describe the data.

4.3.4 Simulations

4.3.4.1 Clonidine

A loading dose of 11 $\mu g/kg$ was calculated using the EC50 (2.78 ng/mL) of the clonidine COMFORT-neo model. To reach the target concentration defined graphically using the ALPS-neo model (2.5 ng/mL), a target concentration of 10 $\mu g/kg$ was calculated.

The simulated concentration of clonidine after a loading dose of 2 and 11 $\mu g/kg$ followed by a continuous infusion of 0.5 or 1 $\mu g/kg/h$ are presented in Figure 52.

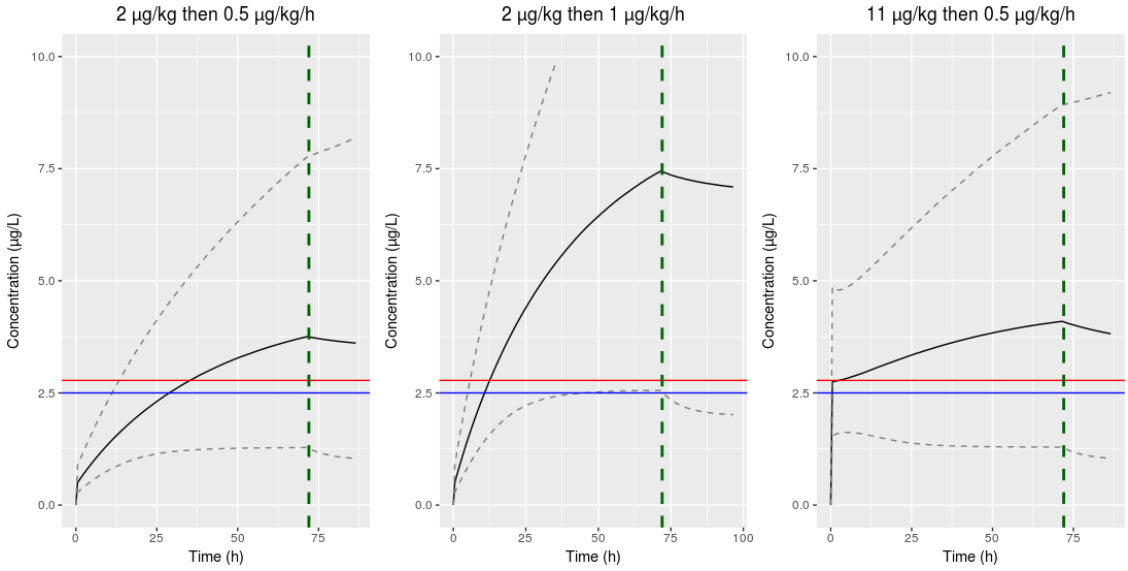

Figure 52: Simulated plasma clonidine concentrations stratify by dose. The blue line represents the target concentration defined graphically using the BI ALPS-neo PK/PD model. The red line corresponds to the EC50 defined using the joint Emax COMFORT-neo PK/PD model. The black line is the predicted median concentration and the dotted line represents the 95 percent confidence interval. The vertical green line corresponds to the starting time of the rewarming.

Figure 52 shows that a loading dose of 11 $\mu g/kg$ is necessary in order for the predicted median to reach the targets defined by the models during the first hour post-administration. After a loading dose of 2 $\mu g/kg$ followed by a continuous infusion of 0.5 $\mu g/kg/h$, the predicted median reaches the targets only 30h post-administration. When the continuous infusion is increased to 1 $\mu g/kg/h$, the predicted median reaches the same targets 12h post-administration. It can also be observed that the slope corresponding to the concentration increase is more abrupt after a continuous infusion of 1 $\mu g/kg/h$ compared to 0.5 $\mu g/kg/h$. All plots presented in Figure 52 show a high interindividual variability.

Figure 53 presents the probability of achieving the clonidine target concentration graphically defined using the BI ALPS-neo model.

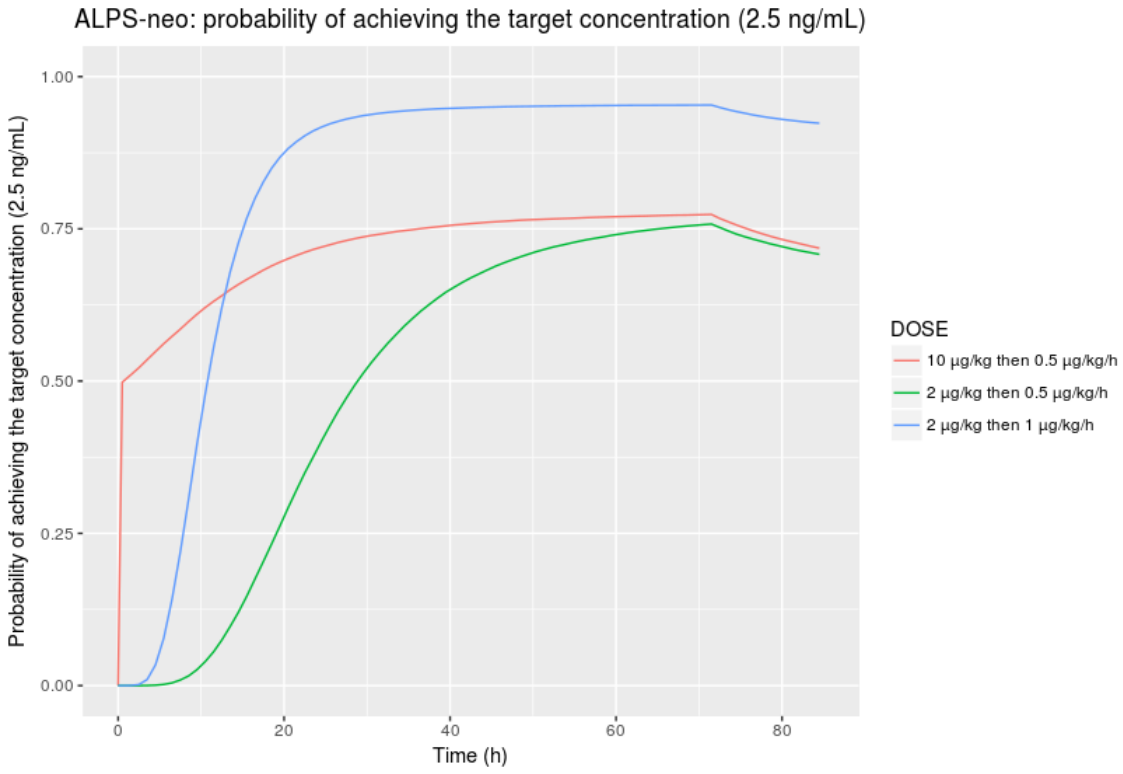

Figure 53: Simulated probability of achieving the clonidine target concentration for ALPS-neo (2.5 ng/mL). Each line (each colour) represents the probability for a different dose.

Figure 53 shows that the probability of achieving the target concentration for ALPS-neo reaches 50% after receiving a loading dose of 10 $\mu g/kg$. This probability increases to 75% 40h post-administration. For a dose of 2 $\mu g/kg$ followed by 0.5 $\mu g/kg/h$, the probability reaches 50% after 25h. For the patients who are given a continuous infusion of 1 $\mu g/kg/h$, the probability increases rapidly to reach 50% 10h post-administration.

Figure 54 shows the probability of achieving the EC50 estimated by the joint COMFORT-neo model.

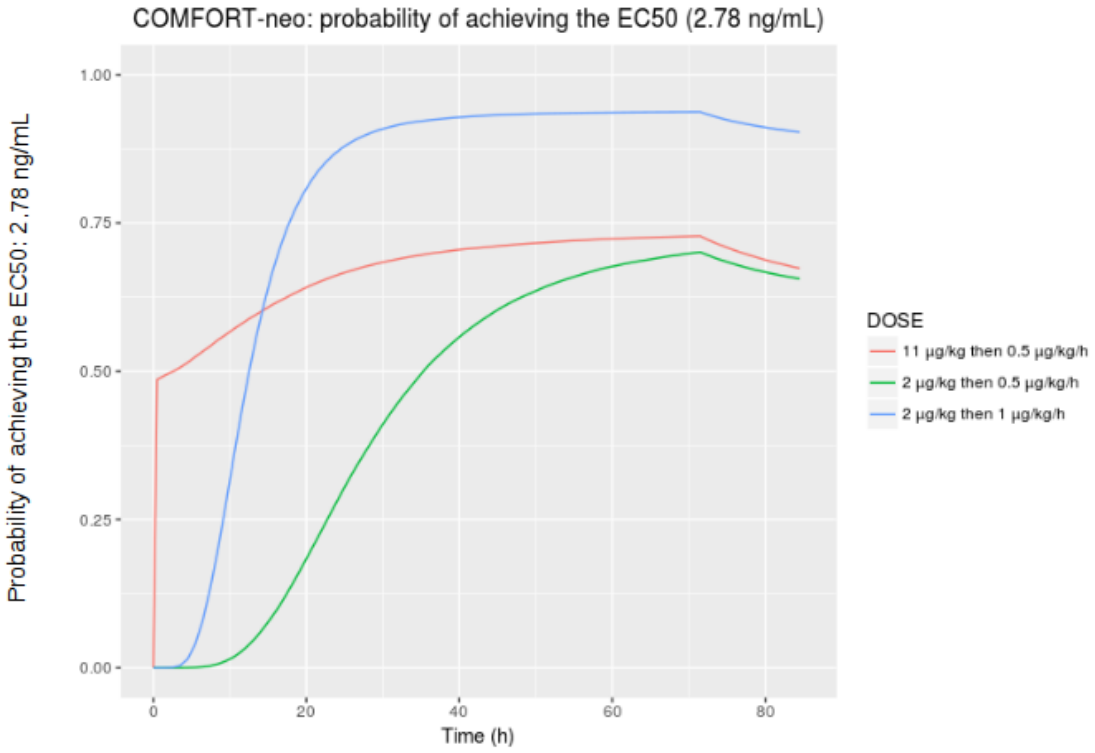

Figure 54: Simulated probability of achieving the clonidine EC50 for COMFORT-neo (2.78 ng/mL). Each line (each colour) represents the probability for a different dose.

Figure 54 shows that there is a probability of 50% of instantly achieving the EC50 estimated by the COMFORT-neo model for a loading dose of 11 $\mu g/kg$. This probability increases slowly to reach a maximum of 70% 40h post-administration. A dose of 2 $\mu g/kg$ followed by 1 $\mu g/kg/h$ is necessary to have at least 90% of the patients achieving the EC50. However this percentage is only reached 50h post-administration.

4.3.4.2 Fentanyl

The simulated fentanyl concentrations for a loading dose of 2, 2.5, 3 $\mu g/kg$ followed by continuous infusion of 2, 2.5, 3 $\mu g/kg/h$ are presented in Figure 55.

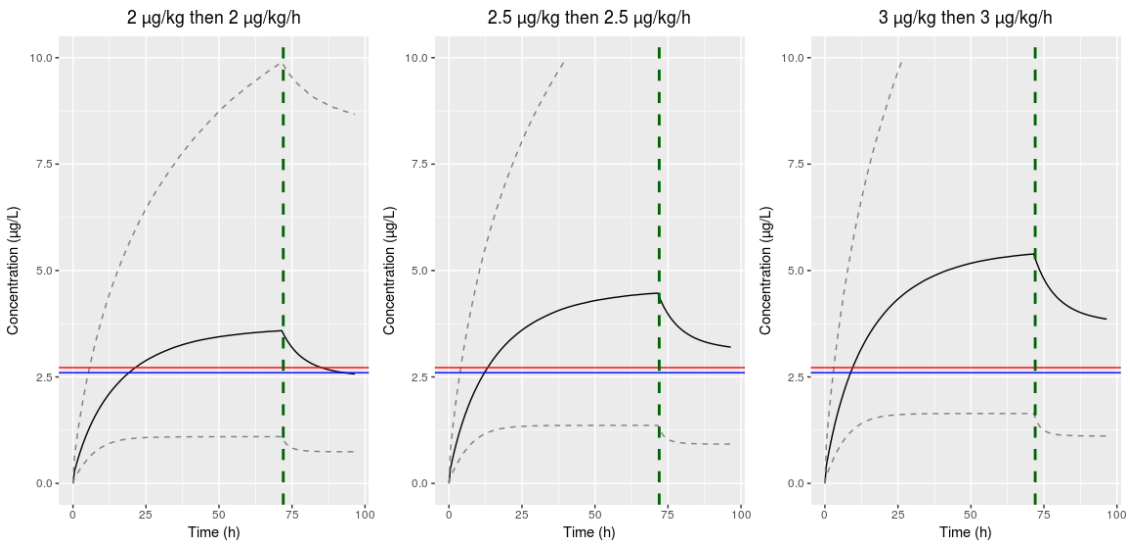

Figure 55: Simulated plasma fentanyl concentration stratify by dose. The blue line represents the target concentration defined graphically using the proportional odds ALPS-neo PK/PD model. The red line corresponds to the EC50 defined using the joint Emax COMFORT-neo PK/PD model. The black line is the predicted median concentration and the dotted line represents the 95 percent prediction interval. The vertical green line corresponds to the starting time of the rewarming.

Figure 55 shows that the predicted median concentration reaches the target concentration 22h following the administration of a 2 $\mu g/kg$ loading dose followed by 2 $\mu g/kg/h$. The target is reached faster with a loading dose of 2.5 $\mu g/kg$ followed by 2.5 $\mu g/kg/h$ (12h). The graphs show that in order for the predicted median to achieve the target before 10h, a dose of 3 $\mu g/kg$ followed by 3 $\mu g/kg/h$ is necessary.

Figure 56 presents the probability of achieving the fentanyl target concentration graphically defined using the joint ALPS-neo proportional odds model.

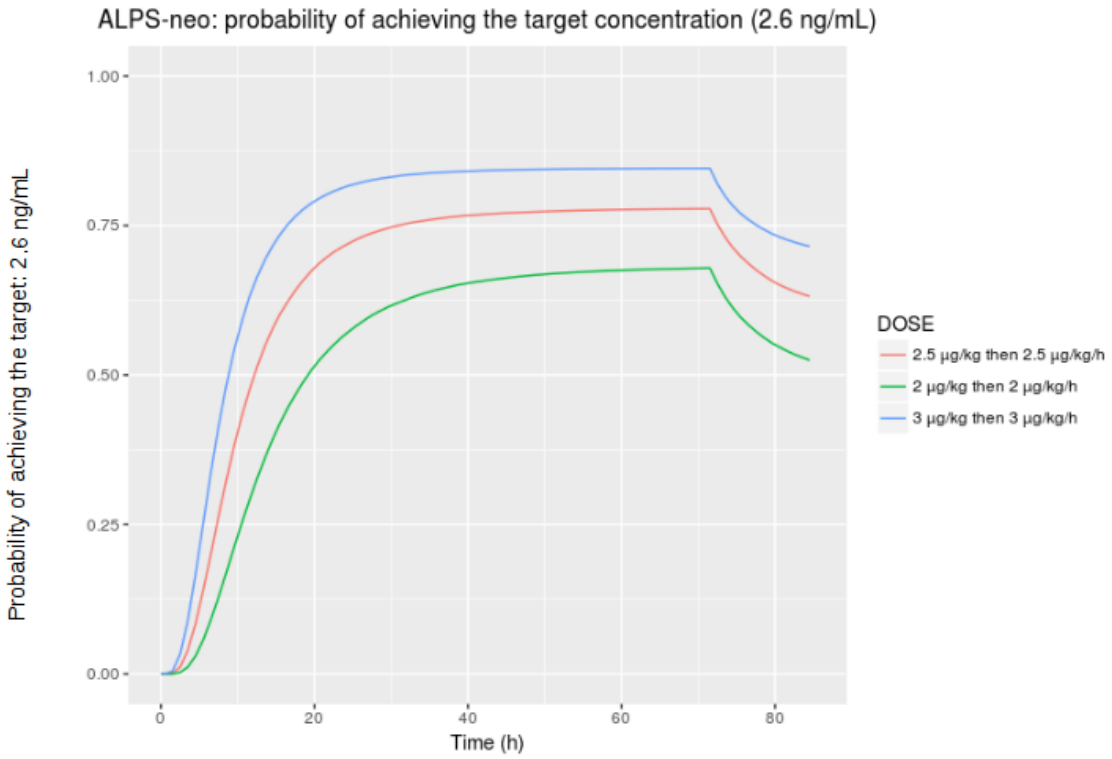

Figure 56: Simulated probability of achieving the fentanyl target concentration for ALPS-neo (2.6 ng/mL). Each line (each colour) represents the probability for a different dose.

Figure 56 shows that the probability of achieving the target concentration gradually increases to reach a maximum of 65% for a loading dose of 2 $\mu g/kg$ followed by 2 $\mu g/kg/h$, 72% for a dose of 2.5 $\mu g/kg$ followed by 2.5 $\mu g/kg/h$ and 90% for a dose of 3 $\mu g/kg$ followed by 3 $\mu g/kg/h$. 10h post-administration, the probability of achieving the target is only of 25%, 40% and 55% for the dose of 2, 2.5 and 3 $\mu g/kg$, respectively.

The probability of achieving the EC50 estimated by the joint COMFORT-neo model is presented in Figure 57.

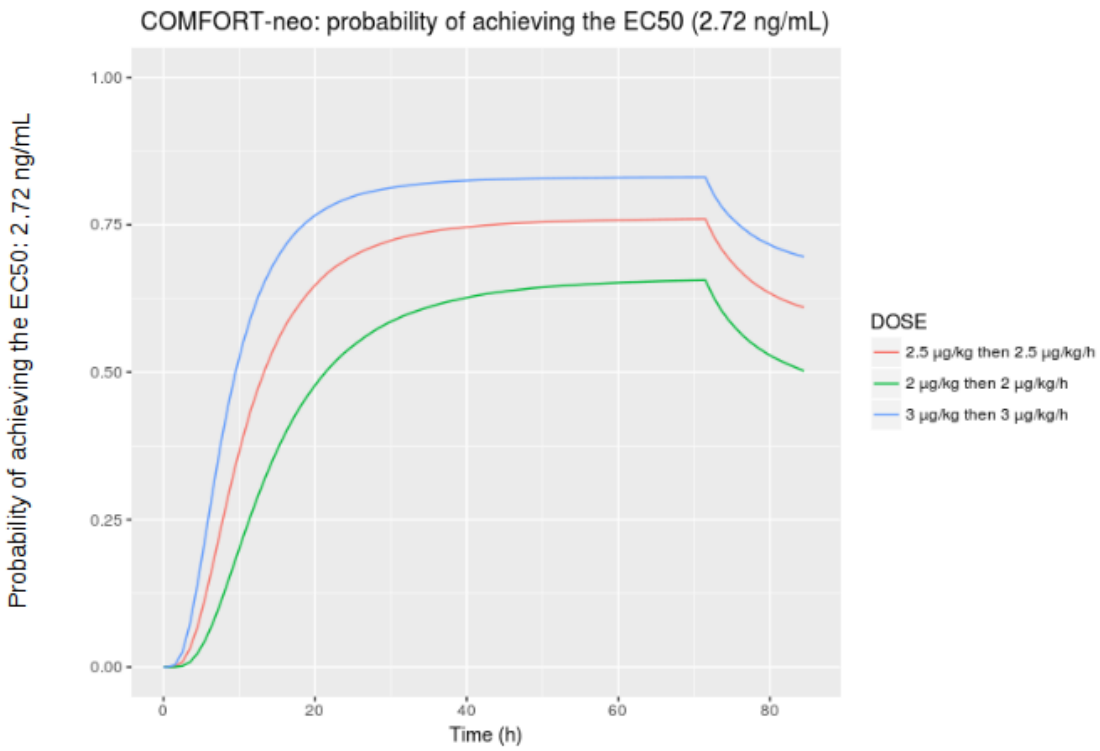

Figure 57: Simulated probability of achieving the fentanyl EC50 COMFORT-neo (2.72 ng/mL). Each line (each colour) represents the probability for a different dose.

Figure 57 shows that the probability to reach the EC50 for the COMFORT-neo score increases gradually to reach a maximum that differs for each dose (85% for 3 $\mu g/kg$, 75% for 2.5 $\mu g/kg$ and 64% for 2 $\mu g/kg$). To have at least 50% of the patient achieving the EC50 10h post-administration, a dose of 3 $\mu g/kg$ followed by $3\mu g/kg/h$ is necessary.

4.4 Discussion

PK/PD models for both ALPS-neo and COMFORT-neo scores have been developed. Models treating the data as continuous or categorical have been tested. The final model for the COMFORT-neo was an inhibitory sigmoid Emax joint model. For ALPS-neo score, the final clonidine model was a BI model with Markov effect and the final fentanyl model was a joint proportional odds model.

4.4.1 Pharmacokinetic models

Population PK models describing the concentrations of clonidine and fentanyl were developed. For each drug, the model that best fitted the data was a one-compartment model. Both models included the influence of weight and age on the CL. Both models show that the hypothermic treatment significantly decrease the CL.

The RSE, goodness-of-fit plots and VPC used to evaluate the clonidine and fentanyl PK model show that both models adequately described the PK data.

The RSE of the parameters presented in Table 9 and 10 are all below 50% except for the RSE evaluating the parameter corresponding to the effect of hypothermia on the clonidine clearance (78%). The medians produced by the bootstrap analysis were close to the parameter estimates.

The goodness-of-fit plots (Figure 18 and 22) presenting the observed concentrations plotted against the predicted concentrations show that both models slightly overpredicted the concentrations. However, the graphs presenting the observed concentrations plotted against the individual predictions show that the inclusion of the IIV improved both models. Most of the CWRES used to evaluate the models are between -2 and 2 and no trend can be observed with a lowess line flat around 0, indicating that both models fit well the data.

The final models of clonidine and fentanyl were also successfully evaluated by the VPC presented in Figure 19 and 23, respectively.

4.4.2 Pharmacokinetic/pharmacodynamic models

4.4.2.1 Comparison of the modelling techniques tested

There is no rule for the choice of model that should be used to treat ordinal categorical data. The choice between treating the data as continuous or categorical (with a proportional odds or BI model) can be made based on different aspects such as parsimony, run time and parameter uncertainty. These aspects depend mainly on the size of the scale which is therefore a key information for the model choice.

Treating pain and sedation score as continuous variable is the most common approach

in peadiatric population because the scales are often composed of more than 10 categories. This model presents the advantage to be simple to implement, easy to interpret and requires less parameter estimations. However, this approach ignores the integer nature of the data which might be an issue at the boundaries of the scale. If not restrained, the residual error can give predictions outside the scale range. To correct this problem, logistic transformation or beta regression can be used. However, such methods only predict the extreme values asymptotically (110).

In addition, when modelling scores as continuous variable, the parameters can be estimate using a first-order conditional method which is more robust than the Laplacian method used to estimate categorical data (110). One limitation to consider with this type of model is the important run time due to the number of observations and estimations of the interindividual variabilities (173).

The proportional odd model respects the categorical nature of the data, but requires a large number of parameters which can be an inconvenient for large scales (110). Overparameterization can occur when using a proportional odds model since the model estimates the probability of the baseline for each score as well as the parameters corresponding to the predictors. For this reason, the proportional odds model is generally not used to analyse large scales with more than 11 categories such as COMFORT-neo score. Only few studies used an ordered categorical based model to analyse scale with scores superiors or equal to 7 (173). In addition, the number of observations required for the proportional odds model increases with the number of categories in order to adequately estimate the parameters. If some categories of the scales are not observed in the data, the proportional odds model is not able to estimate their probabilities. The probability of such score would need to be ignored or categories would need be merged into groups. One of the limit of the proportional odds model is the assumption that the random effect as well as the predictor effect is the same for all categories. Changing this assumption would require to increase the model size considerably and therefore increase the risk of overparameterization (110).

Compared to the proportional odds model, the BI model presents the advantage to

be able to analyse scales of any category number and predict scores that are not observed in the database. Additionally, the BI model predicts that there is a lower probability to get an extreme score. This assumption requires for the data to be distributed in an unimodal way, which might not be the case depending on the scale analysed. Unimodal distribution are observed more frequently in rating scale using verbal expression instead of numerical values to identify categories (110).

To choose the right model it is important to consider the possibility that two consecutive observations may not be independent because of clinical reasons and database characteristics such as collection frequency. For this reason, it is useful to test if the inclusion of a Markov element leads to a model improvement. It has been shown that applying a proportional odds model to data with markovian properties can lead to model misspecification and therefore poor performance and inaccurate prediction. If the Markov feature of a data is not negligible, the proportional odds model should be avoid and Markov elements should be taken into account by using Markov models or other ordinal categorical models that include markov components such as BI model. Unlike the proportional odds model, the BI model allows the inclusion of Markov elements in the model (109).

In conclusion, the continuous model is easy to develop but takes a long time to run and does not respect the integer nature of the data unlike categorical models such as proportional odds and BI models. Compared to the proportional odds model, the BI model presents the advantage to be flexible, it requires less parameter estimates and allows the addition of Markov elements. However, both categorical models are more complex to implement than continuous models (173).

4.4.2.2 Model evaluation

4.4.2.2.1 ALPS-neo score

Clonidine

The Emax model describing the relationship between clonidine concentration and ALPS-neo score was successfully evaluated using the PC-VPC as shown in Figure 28

and the bootstrap presented in Table 11. However, the RSE presented in Table 11 show that the model was not able to adequately estimate the parameters corresponding to the covariate index ($PMAEC50$ and $TEMPB0$) with RSE>100%. Although the majority of the CWRES presented in Figure 27 are within -2 and 2 and the lowess line is flat around 0, the goodness-of-fit plots show that some CWRES values are over 2.

The proportional odds model describing the ALPS-neo score using the clonidine effect and the temperature as predictors was also successfully evaluated by the categorical VPC presented in Figure 29 and 30. Based on the RSE and the bootstrap summarised in Table 12, the model estimated with precision most parameters. However, the estimate corresponding to the EC50 has a RSE > 70%.

The RSE evaluating the parameters estimated by the BI model summarised in Table 13 show that although the BI model adequately estimated most parameters, it was not able to estimate with precision two parameters describing the Markov effect (PMAX and HIL). However, all the parameter estimates fall within the 95% confidence interval produced by the bootstrap evaluation. The goodness-of-fit plots presented in Figure 31 and 32 show that the majority of the PWRES of the model with and without Markov effect are between -2 and 2. However, the graphs also show that that some PWRES reach a value between 4 and 6. Figure 31 shows that the lowess line of the PWRES is flat around 0 for the first 70h after the first dose administration, however after 70h a trend below 0 can be observed. This trend is improved on the graph presented in Figure 32 evaluating the model including a Markov element. This indicates that the inclusion of a Markov effect improved the model by improving the description of the data observed after 70h following the first dose administration.

Fentanyl

The RSE and bootstrap results suggest that the model was able to adequately estimate most parameters. The RSE presented in Table 14 are below 50% except for the parameter corresponding to the temperature index on the baseline. In addition, the median generated by the bootstrap evaluation are close to the parameter estimates. The goodness-of-fit plot of the observed concentrations plotted against the population

predictions in Figure 35 shows that without inclusion of the IIV, the model did not fit well the data. The inclusion of IIV highly improved the model as it is shown on the plot presenting the observed concentrations *vs* individual predictions in Figure 35. The CWRES graph shows that the lowess line is around 0 and no trend can be observed. The Emax model was successfully evaluated by the PC-VPC presented in Figure 36.

Most of the RSE used to evaluate the BI model summarised in Table 15 are over 400%. However, the parameter estimates fall within the 95% confidence interval produced by the bootstrap evaluation and the median is close to the estimates obtained with the BI model. The majority of the PWRES presented in Figure 37 are between -2 and 2. However a clear trend of the lowess line can be observed.

Joint models

The joint Emax model describing the relationship between ALPS-neo score and both drug concentrations was successfully evaluated by the PC-VPC presented in Figure 39. Based on the RSE and the bootstrap results presented in Table 16, the model estimated with precision all the parameters. The goodness-of-fit plots (Figure 38) show that the inclusion of IIV on the parameters considerably improved the model. The lowess line of the CWRES is flat around 0 and no trend can be observed indicating that the model fit well the data.

The joint proportional odds model was also successfully evaluated by the categorical VPC shown in Figure 40, 41 and 42. Although the RSE corresponding to the slope of the fentanyl linear drug model (FENT SLP), the EC50 of the clonidine Emax drug model (CLO EC50) and the index of the temperature effect (TEMP INDEX) are over 60%, the bootstrap show that the model was able to estimate with precision all the parameters (Table 16).

4.4.2.2.2 COMFORT-neo score

Clonidine

Based on the RSE and bootstrap results summarised in Table 18, the Emax model built to describe the relationship between clonidine concentration and COMFORT-neo

score estimated all the parameters with precision except the parameter corresponding to the temperature effect (TEMP B0) for which the RSE was close to 100%. The goodness-of-fit plots in Figure 45 show that the IIV improved the model. Although most of the CWRES are between -2 and 2, the graph of the CWRES shows that some CWRES points are over 2, reaching the values of 6 in certain cases. The PC-VPC presented in Figure 46 successfully evaluated the model even though some points are outside the prediction interval.

Fentanyl

Based on the RSE summarised in Table 19, the fentanyl Emax model described all parameters with precision except the parameter corresponding to the EC50. However, all parameters are close to the median obtained with the bootstrap analysis. The goodness-of-fit plots show that the model was also improved by the the inclusion of IIV. However the graph presented in Figure 48 shows that the model did overpredict the observed scores higher than 12. Some CWRES values are over 2 even though the lowess line seems to be flat around 0. Most of the observations are within the 90% prediction interval produced by the PC-VPC presented in Figure 49.

Joint model

The RSE and bootstrap results show that the joint Emax model estimated with precision all the parameters (Table 20). The goodness-of-fit plots presented in Figure 50 show that the inclusion of IIV considerably improved the model. Although some CWRES points are over 2, the lowess line of CWRES is flat around 0. The PC-VPC (presented in Figure 51) show that some points are outside the PC-VPC prediction interval.

4.4.2.3 Choice of the final pharmacokinetic/pharmacodynamic models

The choice of the final model for each score was based on model evaluation, AIC and relevance of the type of model.

4.4.2.3.1 ALPS-neo score

For a scale of 10 categories such as ALPS-neo, a categorical model is preferred because it respects the categorical nature of the data unlike the continuous Emax model. For this reason, even though the Emax models were successfully evaluated, they were not selected as final models for both drugs.

Even though the AIC of the clonidine BI model without Markov effect (AIC = 11746) was higher than the one corresponding to the proportional odds model (AIC = 11659), the inclusion of a Markov element in the BI model induced an important decrease of the OFV and AIC (AIC = 9962). In addition, it would be logical to include a Markov effect to describe pain and sedation scores when possible. For these reasons and based on the RSE and PWRES goodness-of-fit plot used to evaluated the model, the BI model including a drug effect and a Markov element was chosen to be the final clonidine model.

The inclusion of fentanyl concentration as predictor in the fentanyl proportional odds model was not significant. The AIC of the BI model (AIC = 12703) was higher than the AIC of the joint ALPS-neo proportional model (AIC = 11653). In addition, the RSE estimated by the fentanyl BI model were higher than 100%. Therefore, the joint proportional odds model was chosen as final model to describe the concentration-effect relationship of fentanyl with ALPS-neo score.

4.4.2.3.2 COMFORT-neo score

Since the COMFORT-neo score is a large scale with more than 20 categories, the proportional odds is not the most adequate model to describe the data because of the risk of overparameterization which can increase the instability of the model. In addition, the proportional model odds model is not able to include the COMFORT-neo score categories that are not observed in the population studied. Because its respect the categorical nature of the PD data, a BI model would be preferred compared to a continuous Emax model. However, the Emax model presents the advantage to be easy to develop and combine into a joint PK/PD model for both drugs.

The model evaluation techniques show that both categorical models (proportional

odds and BI models) were not able to adequately describe the data. For each drug, the separate continuous Emax models provided a good fit. Based on the model evaluation, the separate Emax model were improved when they were combined into a joint Emax model including the effect of both drugs. In addition, a joint model is more relevant since both drugs were administered in combination. For these reasons, the joint PK/PD Emax model was chosen as final model to describe relationship between the COMFORT-neo score and both drugs.

4.4.2.4 General discussion points on the PK/PD models

The hypothermia explained a part of the IIV observed in the final joint proportional odds model chosen to link ALPS-neo and fentanyl. In addition, a significant effect of the temperature was found on the fentanyl EC50 estimated by the final joint Emax model for the COMFORT-neo but not on the clonidine EC50. This result might be explained by the differences in terms of pharmacodynamics between the two drugs. The pathways and receptors involved in fentanyl mechanism of action might be more affected by hypothermia than the ones involved in clonidine response.

The final models were used to define the target concentrations for both drugs. For the ALPS-neo score, the target concentrations of fentanyl and clonidine were defined graphically to a value of 2.5 ng/mL for clonidine and 2.6 ng/mL for fentanyl. These values as well as the EC50 estimated by the joint COMFORT-neo Emax model were used to perform simulations in order to determine the optimal dose of both drugs and suggest dose regimens for this particular population.

One of the main limitations of the PK/PD analysis is that a Markov effect could not be tested on the final joint proportional odds model for ALPS-neo as well as on the final joint Emax model for COMFORT-neo. The inclusion of a Markov element in the model as it was done for the final BI model linking ALPS-neo and clonidine might improve the model and therefore describe with more precision the relationship between drugs concentration and scores.

Both PK and PK/PD models will be updated by including the data of the 50

newborns once all the patients have been recruited. Including more patients in the analyses should not induce important changes in the findings presented in this chapter. However, it should improve the models and therefore the precision of the estimations.

4.4.3 Simulations

Based on the clonidine simulation results for the ALPS-neo score (Figure 53), a clonidine loading dose of 10 $\mu g/kg$ should be administered in order to have 50 % of the patients reaching the target concentration during the first hour post-administration. For the COMFORT-neo score (Figure 54), a loading dose of 11 $\mu g/kg$ should be given to have 50% of the patients reaching the EC50 in less than an hour. When using the EC90 as target concentration for the COMFORT-neo score, this dose should be increased by a factor 2 in order to obtain the same results. These doses are considerably higher than the doses routinely used in the NICU, therefore the clonidine adverse effects have to be considered. Although the incidence of adverse effects reported after clonidine administration is low in most studies, cases of hypotension and bradycardia in children have been observed. A recent study has shown that after administration of loading doses up to 2 $\mu g/kg$ followed by continuous infusions up to 2 $\mu g/kg/h$, severe bradycardia and systolic hypotensionsion were observed in 40% and 50% of the PICU patients, receptively (174). Due to the lack of information on clonidine safety, prescribing loading doses over 10 $\mu g/kg$ may not be feasible in the NICU. Therefore, the simulation results suggest that clonidine should be used in combination with other sedatives in order to adequately manage pain and sedation in asphyxiated newborns treated with hypothermia.

Fentanyl simulation results (Figure 56 and 57) suggest that a loading dose of 3 $\mu g/kg$ followed by a continuous infusion of 3 $\mu g/kg$ should be administered in order to have at least 80% of the patients reaching the target concentration for ALPS-neo and the EC50 for COMFORT-neo. However, this percentage is only reached after 20h. 5h post-administration, only 25% of the patients would reach the target. To increase the probability of achieving the target during the first hours post-administration, a

higher loading dose should be given. However, because of the well known side effects of fentanyl that can occur even at low doses in neonates, increasing the dose would not be feasible.

5 Pharmacokinetic/pharmacodynamic modelling of the results of the CloSed trial

5.1 Introduction

5.1.1 Drugs studied

5.1.1.1 Midazolam

Midazolam is a short acting benzodiazepine that provides anxiolysis, sedation, amnesia as well as muscle relaxation (21). It is mainly used in combination with opioids as sedative for pain management during post-operative and procedural settings (175). Midazolam is the sedative most commonly prescribed in the NICU because it presents some advantages such as stopping seizures and causing anterograde amnesia that minimizes the child's painful memories (176). Compared to other benzodiazepines, midazolam acts faster and has a shorter effect duration with less active metabolites (21). It can be administered using various routes such as oral, IV, intranasal and intramuscular (177). Midazolam formula is C18H13ClFN3 and its molecular weight is 325.78 g/mol.

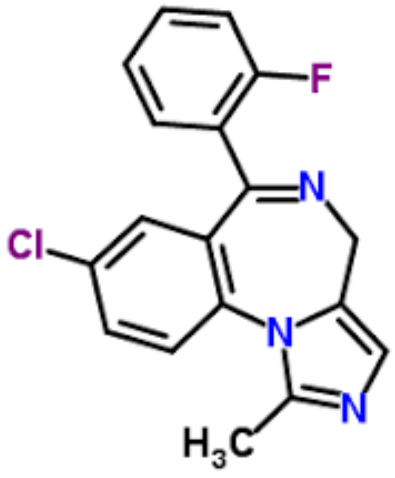

Figure 58: Midazolam structure

5.1.1.1.1 Mechanism of action

The midazolam effect is due to its action on the neuronal inhibitory pathways mediated by gamma-aminobutyric acid (GABA), a major inhibitory neurotransmitter of the central nervous system. Midazolam potentiates the inhibitory action of GABA by binding a receptor complex called GABA-A which cause the opening of the membrane chloride channels leading to a hyperpolarisation of the membrane cell. Both midazolam and GABA bind the same complex receptor GABA-A at different sites. This mechanism is responsible for most clinical effects of the drug including sedation and amnesia (175, 176, 178).

5.1.1.1.2 Midazolam toxicity

Despite its good efficacy/safety ratio, midazolam can cause numerous adverse reactions. Therefore its use in children should be carefully monitored. The most common adverse effects of midazolam include hiccough, cough, nausea, and vomiting (175). In case of overdose, midazolam can induce respiratory depression and infusion syndrome in which case continuous ventilator support is required (179, 175). Studies have reported that the risk of respiratory depression is significantly higher when midazolam is given in combination with opioids such as morphine and fentanyl (180). The long term administration of midazolam induces a high rate of tolerance in children and adults, in which case the dose should be increased in order to maintain the therapeutic effects. As all benzodiazepines, its long term use can also induce a dependence, leading to a withdrawal syndrome if the drug is stopped abruptly. Midazolam is known for its heamodynamic safety, however the literature has reported some cases of modest reduction of arterial blood pressure and increase of heart rate (180). Other adverse effects include memory loss, pseudo-seizure and myoclonic jerking (181). In preterm and term newborns, adverse neurological effects have been observed after administration of midazolam such as impaired level of consciousness, abnormal movements and vision. However, the long term consequences of these effects on the immature brain remains unknown (178).

5.1.1.1.3 Midazolam pharmacokinetics

When given orally, midazolam has a good permeability but a low bioviailabiliy as a result of an important first pass metabolism.

Midazolam has a relatively large volume of distribution and is rapidly distributed after IV administration (180). Thanks to its lipophilic properties, it can easily cross the BBB to reach its main target: the central nervous system. Approximately 97% of the drug is bound to plasma proteins.

Midazolam is metabolised in the liver where the drug undergoes an hydroxylation by CYP3A4 and CYP3A5 to form two metabolites, 1-hydroxymidazolam and 4-hydroxymidazolam (176, 180). These active metabolites contribute to 10% of the sedative effect of the drug. They are then glucuronidated and excreted into urine (176).

Studies have reported a large interindividual variability of the midazolam clearance in children (182). The clearance is significantly reduced in neonates compared to older children due to the immaturity of the renal function and liver enzymes involved in the drug metabolism (176). Both CYP3A4 and 3A5 undergo important developmental changes during the first year of life. CYP3A4 appears in the liver during the first weeks following the birth, whereas CYP3A4 is already present at birth. Both enzymes reach their adult activity after 1 year of life. The immaturity of the elimination pathways are more important is preterm newborns, increasing the drug elimination half-life up to 22h compared to 6h in term newborns (176).

5.1.1.1.4 Previously published models

Several PK models describing midazolam concentration in children have been published in the literature. Anderson *et al.* (134) developed a sigmoidal maturation model for midazolam that takes into account the influence of age and size using published clearance estimates after IV administration. This model can be used in combination with an allometric scaling in order to estimate the clearance in various peadiatric populations. The authors estimated a maturation half-life around 70 weeks of postmentrual age. More recently, Kos *et al.* (183) developed a different model in order to describe the pharmacokinetics of midazolam in critically ill children with severe bronchiolitis. This

model also used a sigmoidal maturation function to describe the population clearance, however the authors estimated a maturation half-life shorter around 45 weeks of PMA. Such differences might be explained by the type of population studied.
In addition to the influence of age and weight on midazolam clearance, few models studied the effect of severe illness on the PK (184, 185). These models showed that critical illness in children significantly affect the midazolam clearance. This effect is probably the consequence of inflammation causing a reduction of the CYP3A4/5 activity (185).

Few PK/PD models have been published in the literature describing the relationship between midazolam concentration and sedative effect in children. In 2002, Johson *et al.* (186) developed the first model that linked the concentration of midazolam and its active l-hydroxy metabolite to the sedation effect using a binary sedation scale (awake/asleep). The model predicted the adequate scores in 86% of the cases and showed that the metabolite effect should be taken into account since it was able to compensate the decrease effect of the parent after metabolism. Peeters *et al.* (103) developed a more complex PK/PD model in 2006 describing the relationship between midazolam concentration and sedation using the COMFORT-B score in non ventilated infants after major surgery. The authors included a postanesthesia effect in order to take into account the influence of drugs administered during the surgery on the sedative effect observed. Simulation were performed using the model in order to determine the optimal dose of midazolam in this population. More recently, Valkenburg *et al.* (187) built a model to compare the PK and PD of IV midazolam after cardiac surgery between children with and without Down syndrome. Unlike Peeters *et al.* (103), they found a minimal effect of the drug concentration on the COMFORT-B score.

5.1.1.2 Morphine

Morphine which is extracted from the *Papaver somniferum*, is one of the opioids most commonly prescribed in the PICU and NICU. It is used as reference to compare the efficacy and safety of other opioids (122). Because of its strong analgesic properties,

morphine is indicated for pain management in post-operative settings and during invasive procedures. It is also suitable for mechanically ventilated children (30). Morphine formula is C17H19NO3 and its molecular weight is 285.34 g/mol. It can be administered by IV, oral, intramuscular as well as subcutaneous routes (122).

The analgesic effect of morphine is mainly due to its binding to the opioids μ receptors in the central nervous system leading to a stimulation of the descending inhibitory pathways (21)

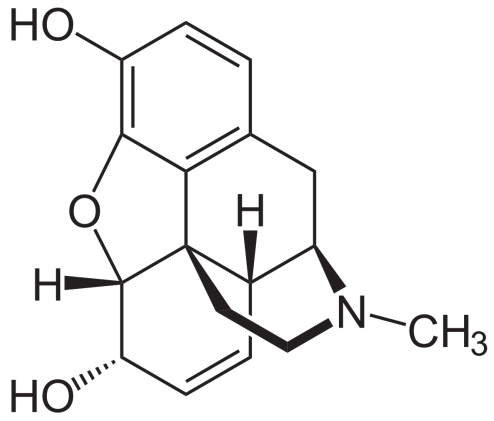

Figure 59: Morphine structure

5.1.1.2.1 Morphine toxicity

Morphine can cause various adverse effects such as miosis, pruritus, constipation, increased biliary pressure, urinary retention, and hypotension. Respiratory depression is the major adverse effect observed in children after administration of morphine limiting its indication in certain cases. The literature reports that the risk of respiratory depression is higher in neonates and infants under 1 year old. A recent trial that aimed to evaluate morphine efficacy for procedural pain in preterm infants had to be stop early because of the high incidence of respiratory depression observed in the preterm population. Other factors increasing this risk include severity of illness and co-medication (other sedatives). In addition, long term use of morphine can induce tolerance and dependence and therefore withdrawal syndrome if the dose is not gradually decreased (122).

5.1.1.2.2 Morphine pharmacokinetics

When administered orally, morphine undergoes a high first pass metabolism resulting in a limited biovailability around 40% (188).

Despite its poor lipophilic properties, morphine has a large volume of distribution. However, its penetration in the CNS is delayed compared to other opioids since it has more difficulties to cross the BBB due to its low solubility in lipid tissues. Therefore, the analgesia effect of the drug only occurs 20 minutes after IV administration (188). Only 20 to 40% of morphine is bound to plasma proteins. This value is decreased in neonates but the impact on the drug distribution is minimal given the limited percentage of protein binding in older children (117). The morphine volume of distribution increases gradually to reach its adult value around 6 months of life. However, studies show that the volume of distribution is higher in preterm infants compared to term newborns. This can be due to different factors including percentage of fat and size of the immature organs (122).

Morphine is almost entirely metabolised (90%) in the liver by glucuronidation in two major metabolites: morphine-3-glucuronide (M3G) and morphine-6-glucuronide (M6G). M3G is considered inactive and is produced in higher proportion compared to M6G (around 50%). M3G does not bind opioid receptors, however it does stimulate the CNS via other receptors that does not induce analgesia. After IV administration, the highest concentrations of M3G are observed after 15 minutes. M6G binds the opioid receptors and is highly active with an analgesic effect more potent than morphine. This metabolite reaches its concentration peak after 45 minutes post IV administration and is produced in lower amount (around 15%) (188). Both metabolites have a high water solubility and are excreted in the urine. Morphine clearance is significantly reduced in young children due to the immaturity of the liver and kidney. Preterm and term newborns are able to produce M3G from birth, however concentration of M6G can only be found after 2 days of life which explains the unpredictable analgesia effect and numerous adverse effects reported in preterm population (122, 117).

5.1.1.2.3 Previously published models

Since morphine was one of the first analgesic commercialised, its pharmacokinetic and pharmacodynamic properties have been studied more extensively than other analgesics in preterm and term newborns, infants and older children. Most analyses published in the literature have used a non-compartimental approach, however more recently few PK compartmental models have been developed in order to determine the factors that contribute to the large interindividual variability of the drug PK in children (122). These models show that age, weight and critical illness affect the morphine elimination leading to a clearance reduction due to the immaturity and/or dysfunction of both liver and kidney (189).

Few models have described the effect of organ maturation on morphine clearance. Anand *et al.* (190) developed a model that includes a sigmoidal maturation function using the PMA in order to describe the morphine clearance. However, this model didn't include any metabolite data. Using a different PK model, Bouwmeester *et al.* (191) were able to describe the metabolite clearances for both metabolites with an exponential maturation function using the postnatal age. Recently, both maturation functions were used by Knosgaard *et al.* (192) in order to developed a meta-model which described the drug PK in preterm and term neonates. In addition to the effect of age on clearance, some models found a significant effect of organ maturation on the central volume of distribution of the parent (191), however these findings have been discussed in numerous studies.

The relationship between effect and morphine concentration has not been clearly established using PK/PD modelling. In their study, Knosgaard *et al.* were not able to describe the effect of morphine on PIPP score in neonates. Recently, Valkenburg *et al.* (193) developed a PK/ PD model describing the relationship of morphine concentration and oversedation in young children after cardiac surgery using the COMFORT-B score.

5.1.2 Rationale for the CloSed trial

Clonidine is frequently used instead of intravenous midazolam in children because of its better safety including a lower incidence of delirium, agitation, withdrawal syndrome

and respiratory depression (144). Clonidine presents some additional advantages compared to opioids and benzodiazepines: it prevents organ dysfunction, it does not affect the natural sleep and does not cause neurotoxic effects, tolerance or dependance (154). It is often prescribed in combination with opioids such as morphine and fentanyl. Studies have shown that when given with fentanyl, the dose of both drugs could be reduced providing a lower risk of toxicity (146). The combination of opioids and clonidine seems to be a better alternative to the common use of opioids and midazolam (194).

There are limited data supporting the non inferiority of clonidine compared to midazolam. Wolf *et al.* (194) tried to compared both drugs in a double blind randomised controlled trial called SLEEP. However, the study was terminated due to enrolment issues. Although the authors conclude to the non inferiority of clonidine, these results have to be interpreted with caution since the analysis had a low statistical power due to the limited number of patients included. Wolf *et al.* (194) identified that the main reason for the challenging recruitment was the reluctance of parents and clinicians to give their consent to a sedation study in critically ill infants.

Unfortunately, there is a lack of efficacy and safety data informing the clonidine use as sedative agent in children. In their pilot study, Duffet *et al.* (195) tried to prove the efficacy of clonidine in a double-blind, randomised controlled trial of oral clonidine *vs* placebo. However, the authors were not able to find a significant difference of efficacy between the two groups. When given in combination with midazolam, two studies published in the literature have reported that clonidine was safe and effective (196, 197). Hünseler *et al.* (198) have shown that clonidine reduced the need of opioids and benzodiazpines in a double blind randomised controlled trial comparing the requirement of fentanyl and midazolam with and without clonidine.

There is no study published to our knowledge that describes the relationship between clonidine and sedative effect using PK/PD modelling. The target concentration and adequate dose regimens for clonidine in children have not been yet determined. For these reasons, additional PK and PK/PD studies are needed.

5.1.3 Aim

The initial aim of the CloSed (CLOnidine compared with midazolam for SEDation of paediatric patients in the intensive care unit) trial was to provide necessary data in order to obtain a Paediatric Use Marketing Authorisation (PUMA) for clonidine use in PICU. However, the trial was terminated early due to recruitment issues and therefore this aim could not be achieved.

A secondary endpoint of the CloSed trial was to develop PK/PD models for clonidine and midazolam. This chapter therefore focussed on developing these models in the patients who were recruited.

To reach this goal, the first objective of this chapter was to develop PK models for clonidine, midazolam and morphine in order to identify the covariates influencing the PK of the three drugs (e.g. weight, age, genetic variants). The second objective was to developed PK/PD models for clonidine and midazolam to establish the relationship between drug concentration and sedative effect for both drugs using COMFORT-B score.

5.2 Methods

5.2.1 Study population

Data for the PK and PK/PD analyses were collected from the European trial CloSed (EudraCT: 2014-003582-24, Clinicaltrials.gov: NCT02509273). The CloSed trial was a double blind, multicentre, phase III randomised controlled trial with two parallel groups (children were randomly allocated to clonidine or midazolam arm). The trial ran from May 2016 to October 2018. Ethical approval was obtained for each participating centre.

Patients were recruited from five different European countries (Czech Republic, Germany, Italy, The Netherlands and Sweden). Children were included in the CloSed trial if the following criteria were met: age between birth and 18 years old, expected admission to the PICU, expected indication for mechanical ventilation and need for a continuous sedation for at least 24 hours. Informed consent from the parents or the

legal guardians was necessary in order to enrol a child in the study.

The patients were not included in the study if they had a gestational age below 34 weeks, or if they had severe organ insufficiencies, brain injuries, acute asthma, severe bradycardia and arterial hypertension. Other exclusion criteria included pregnancy, CPAP or ECMO treatment and known hypersensitivity to any of the drugs prescribed in the trial. In addition, the patient could not have received clonidine during the 7 days prior to the admission and not have had sedation for more than 72 hours prior to the screening.

Clonidine and midazolam which correspond to the investigational medical product (IMP) were administered for a maximal period of 7 days. The patients received loading doses of 15 minutes followed by maintenance continuous infusions. The starting doses of IMP were a loading dose of 2 $\mu g/kg$ followed by a continuous infusion of 1 $\mu g/kg/h$ for clonidine and a loading dose of 200 $\mu g/kg$ followed by 100 $\mu g/kg/h$ for midazolam. The doses were halved in neonates younger than 28 days old. The maintenance infusion rates were then adjusted following a dosing algorithm based on the sedation levels assessed using both COMFORT-B score and Nurses Interpretation of Sedation Score (NISS). Three formulations of IMP with different strength (low, medium and high) depending on the child's weight were available.

In addition to the IMP, all patients received IV continuous infusion of morphine as background drug for pain. The dose of morphine was adjusted individually based on the pain scores assessed using the Numerical Rating Scale (NRS). Propofol could also be administered as bridging sedative therapy before and until the 30 minutes following the initiation of the IMP treatment. Bolus of ketamine were allowed as additional analgesic when needed. Additionally, some patients included in the study were transferred to the PICU after undergoing major surgery during which they received anaesthetic drugs. The time, date and duration of surgery as well as every co-medication given before and during the IMP treatment were carefully documented.

In summary, the dose adjustment of IMP and morphine was done as follows:

- NRS score >= 4: increase of morphine

- NRS score < 4: no increase of morphine
- COMFORT-B score > 22: increase sedative agent
- COMFORT-B score <= 22 - >= 11, NISS score 1: increase of sedative agent
- COMFORT-B score <= 22 - >= 11, NISS score 2: maintain sedation
- COMFORT-B score <= 22 - >= 11, NISS score 3: decrease of sedative agent
- COMFORT-B score < 11: decrease of sedative agent

The trial can be divided using the following periods of time: screening, baseline, treatment period, completion, post-dose monitoring period and 14 day follow up visit .

Pain and sedation were assessed using the COMFORT-B, NISS and NRS score every 3 hours during the study period. Additional assessments were also done 30 minutes after an increase of IMP dose and an adjustment of morphine dose. The pain scores always took precedent over the sedation scores.

In addition to the pain and sedation assessment, a physical examination was performed before and after the IMP treatment and the vital signs including blood pressure, heart rate (supine pulse rate), respiratory rate, occurrence of apnoea and peripheral arterial oxygen saturation were recorded during the entire time of the trial. The vital signs were recorded every 15 minutes during the first two hours following the IMP administration, then these variables were measured every 3 hours at the same time as the pain and sedation assessment.

The type of ventilation received by the patient and the fluid balance were recorded from the baseline period. The severity of illness including organ dysfunction, neurodevelopmental long term effects and withdrawal symptoms were also assessed during the trial.

Blood gas, heamatology, coagulation and clinical chemistry were recorded from the beginning of the study. Clinical chemistry assessment included the measure of parameters describing the kidney function (creatinine) and the liver function such as aspartate aminotransferase (ASAT), alanine aminotransferase (ALAT), gamma-glutamyl transferase (GGT) and bilirubine.

Two blood samples used to measure the drug concentrations for the PK study were

mandatory: the first one was taken after the first loading dose and the second just before the end of the IMP treatment. Additional PK blood samples were taken during routine clinical procedures with a maximum number of six samples per patient. Ideally, the samples were taken once a day. In order to define the baseline concentration of the drugs, a mandatory blood sample was taken just before starting the IMP treatment for the patients who received clonidine or midazolam within 5 days before the screening. The samples were collected using arterial or central venous catheters or by vein or arterial puncture. The samples had a volume between 0.6 and 1.0 mL. The concentration of clonidine, midazolam, morphine and their main metabolites (1-OH midazolam, M3G and M6G) were measured using plasma extracted from each PK blood sample.

The genetic variants tested on the PK came from genes coding for enzymes of the metabolism and specific receptors involved in the mechanism of each drug (clonidine, midazolam and morphine). The genes coding for metabolism enzymes were CYP3A4, CYP3A5, CYP2D6, UGT2B7, POR, COMT and MC1R. The genes coding for the receptors were ABCB1, GABA, MDR1, MRP1, MRP2, MRP4, BRCP, ADRA2A, OPRM1, OCT1, ABCC3, IL-1Ra, IL-1b, ARRB2 and STAT6.

The COMFORT-B scores were used as PD endpoints in the PK/PD modelling in order to establish a relationship between sedation and concentration of clonidine or midazolam. To evaluate the safety of clonidine, heart rate and blood pressure were used to build PK/PD models describing the correlation between clonidine concentration and adverse effects.

5.2.2 Primary endpoint of the CloSed trial

The primary objective of the CloSed trial was to assess the non inferiority of continuous intravenous clonidine compared with continuous intravenous midazolam in mechanically ventilated children in the PICU. Therefore, the primary endpoint was sedation success or failure.

Sedation failure was defined using pain and sedation scores as follows:

- NRS < 4 / COMFORT-B > 22

- NRS < 4 / 11 <= COMFORT-B >= 22 / NISS = 1

The analysis was done using logistic regression with treatment, centre and age group as covariates at a one-sided significance level of alpha corresponding to 2.5%.

The statistical hypotheses were defined as follows:

- H0: OR <= δOR
- H1: OR > δOR

With

$$OR = \frac{pC \cdot (1 - pM)}{(1 - pC) \cdot pM)}$$

. H0 is the null hypothesis and H1 is the alternative hypothesis.

pC and pM are the probabilities of sedation success in the clonidine group and midazolam group, respectively. δOR is the non-inferiority margin which was predefined as 0.583.

5.2.3 Pharmacokinetic model building

Three separate population NLME models were developed in order to describe the concentration of the three drugs administered in this study: clonidine, midazolam and morphine. For clonidine, a one- and two-compartment models were tested to define the basic structural model. For midazolam and morphine a model with one compartment for the parent and separate compartments for the metabolites were tested.

If the clearance of the main compartment could not be estimated by the model, it was assumed that the parent (midazolam or mophine) was entirely metabolised therefore the clearance of the parent was ignored. This assumption could be made because more than 90% of midazolam and morphine is metabolised in the liver. The parameters of the model were estimated by the model or fixed using previously published values.

In order to describe the residual variability for each model, an additive, proportional and combined error model was tested for the parent compartments and the metabolite compartments.

Body weight was included *a priori* on the parameters of the three models using

allometric scaling with the allometric exponent fixed to 0.75 for the clearances and 1 for the volumes.

Age was included in the models also *a priori* using different maturation functions depending on the drug and the type of parameters. A bibliography research was undertaken in order to select previous PK models published that were able to adequately describe the effect of age on clearances and volumes using maturation functions. These maturation functions were then used in the models developed in this chapter.

A standard sigmoidal maturation function using PMA as described in section 1.2.3 was used to describe the influence of age on the parent clearances and the formation clearances of the metabolites (1-OH-midazolam, M3G and M6G). This function was also used to include age as covariate on the elimination clearance of 1-OH-midazolam.

For the morphine model, additional maturation functions were used on the elimination clearances of both metabolites and on the central volume of distribution. Effect of age on the metabolite clearances of both M3G and M6G was included in the model using the following maturation function (MFM) (199):

$$MFM = 1 - 0.832 \cdot e^{-PNA \cdot \frac{log(2)}{129}}$$

To describe the morphine central volume of distribution , PNA was included in the maturation function (MFV) as follows (199):

$$MFV = 1 + 0.391 \cdot e^{-PNA \cdot \frac{log(2)}{26.3}}$$

In addition to age and weight, the effect of covariates reflecting the kidney functions (creatinine) and the liver function (ASAT, ALAT, GGT and bilirubin) were tested and included in the model if it induced a OFV decrease of more than 3.64 points. The covariates corresponding to the liver function were tested on each parameter using a centred multiplicative covariate model. Creatinine was included in the model using a maturation function (MSCR) published by Cerrioti *et al.* as follows:

$$MSCR = -2.37330 - 12.91367 \cdot Ln(AGEY) + 23.93581 \cdot AGEY^{0.5}$$

Where $AGEY$ is the age in years calculated dividing PNA by 365.25.

The concentration values below the limit of quantification of 0.05 ng/mL were implemented in the database of the three models by dividing the BLQ by 2.

5.2.4 Pharmacokinetic/pharmacogenetic model building

The effect of genetic variants on the clearances of the three drugs was tested as describe in section 2.2.3.

5.2.5 Pharmacokinetic/pharmacodynamic model building of the efficacy variables

The PK/PD models were built using a sequential method. Different PK/PD models (for each drugs) were tested in order to establish the relationship between drug concentration and sedative/analgesic effect assessed using COMFORT-B score. The data were first treated as continuous variables using an Emax model, then the data were treated as ordered categorical variable and a proportional odds model as well as a BI model were tested.

5.2.5.1 Continuous model

Firstly the data were treated as continuous and an inhibitory sigmoid Emax model with and without effect compartment was tested in order to describe the IMP effect of both drugs (IMPEFF).

Then, the addition of a post-surgery effect in the Emax model for the patients who underwent surgery before starting the IMP treatment was tested as described in the PK/PD model published by Peeters *et al.* (103).

For the patients who had major surgery, the post-surgery effect (PS) was implemented using an Emax model as follows:

$$PS = BASE + PAEFF$$

$$PAEFF = \frac{PAEMAX \cdot TPS}{TPS50 + TPS}$$

$$PAEMAX = SMAX - BASE$$

Where $BASE$ is the score at the end of the surgery and $PAEFF$ is the postanethesia effect. $SMAX$ corresponds to the maximal score obtained once the effect of the anesthetic used for the surgery is gone, $PAEMAX$ is the maximal postanesthesia effect from $BASE$ (difference between $BASE$ and $SMAX$), TPS is the time post-surgery in hours and $TPS50$ is the time post-surgery at half maximum postanesthesia effect in hours.

In order to reflect the complete anesthesia induced during the surgery the BASE parameter was fixed to 6 which corresponds to the minimal COMFORT-B score.

For the patients who did not undergo surgery before starting the IMP treatment, the baseline score ($B0$) was either estimated or set to the observed values in the database for each individual in a separate column in order to simplify the model.

The effect of the comedication (morphine, propofol and ketamine) on the COMFORT-B score ($CMEFF$) was also tested one by one using an additive model.

In order to test the effect of morphine, the concentrations and doses of morphine were added in the database and the PK parameters were fixed in the model to the values estimated by the morphine PK model developed in this chapter. The effect of morphine was implemented using an Emax model.

The concentration of ketamine and propofol were not collected, therefore only the doses of both drugs were added in the PK/PD database. Since the PK parameters could not be estimated, an Emax K-PD model was used to test the influence of both drugs on the sedation score as described by the following equation:

$$CMEFF = \frac{EMAX_{CM} \cdot (KDE \cdot A_{CM})}{EC50_{CM} + (KDE \cdot A_{CM})}$$

where $CMEFF$ is the effect of the comedication (ketamine or propofol), $EMAX_{CM}$

corresponds the the maximal effect of the co-medication, $EC50_{CM}$ is the concentration of co-medication to reach 50% of the maximal effect and A_{CM} is the quantity of drug in the co-medication compartment. KDE is the parameter estimated by the model corresponding to the elimination rate constant describing the equilibrium between dose rate and observe effect (first order).

The total effect on the COMFORT-B score (EFFECT) was characterised as follows:

- For the patients who underwent surgery:

$$EFFECT = PS - IMPEFF - CMEFF$$

- For the patients who did not undergo surgery:

$$EFFECT = B0 - IMPEFF - CMEFF$$

Where PS is the post-surgery effect, $IMPEFF$ is the IMP effect and $CMEFF$ is the co-medication effect. $B0$ corresponds to the baseline score which was estimated or fixed.

Once both separate PK/PD models for clonidine and midazolam were developed, a joint model was tested in order to improve the precision of the parameter estimates. The common parameter for both drugs was the time post-surgery at half maximum postanesthesia effect ($TPS50$). The parameters that could not be estimated by the joint model were fixed to the values estimated by the separate models developed previously in this chapter. The effect of both drugs on the scores were combined using an additive model.

5.2.5.2 Categorical models

The data were then treated as categorical and a proportional odds model as well as a BI model were tested in order to describe the relationship between both drugs and COMFORT-B score. The models were developed as described in section 3.2.3.

The predictors tested in the proportional odds model were the drug concentration

(using an Emax or a linear model) and the post-surgery effect (using a linear model). To include a post-surgery effect in the model, a binary categorical variable was implemented in the database with 0 corresponding to the patients who did not undergo surgery before starting the trial and 1 corresponding to the children who underwent surgery before receiving the IMP.

In the BI model tested, the drug effect was included using an Emax model. A Markov effect was included in the model if it induced a significant decrease of the OFV. The Markov component was implemented in the model as described in section 3.2.3. The post-surgery effect was tested in the Emax model as described in the previous section.

5.2.6 Pharmacokinetic/pharmacodynamic model building of the safety variables

The safety PK/PD models were also built using a sequential method. Two PK/PD models were developed in order to describe the relationship between clonidine concentration and adverse effects using heart rate (HR) and mean arterial pressure (MAP). The PK/PD models tested were Emax models with or without effect compartment. The values of HR and MAP recorded before IMP were used as baseline values in the models.

5.2.7 Simulations

Simulations were performed in order to determine the optimal dose of clonidine and midazolam necessary to reach the target concentrations defined by the PK/PD models. A database of 1000 patients was used for the simulations as described in section 2.2.5.

Separate simulations were done for the patients who underwent surgery before receiving IMP and for those who do not need surgery. For the children receiving surgery, separate simulations were performed for a time post-surgery corresponding to 1, 2 and 3h.

All simulations were limited to 12h. For each dose and each drug, the graphs

simulated the drug concentrations and the COMFORT-B scores corresponding for two age groups (neonates younger than 28 days old and children older than 28 days old). Plots presenting target achievement over time were also generated using the simulations results.

The simulated dose of clondine for the neonates younger than 28 days old were:

- Loading dose of 1 $\mu g/kg$ followed by a continuous infusion of 0.75, 1 and 1.5 $\mu g/kg/h$
- Loading dose of 2 $\mu g/kg$ followed by a continuous infusion of 1, 1.5 and 2 $\mu g/kg/h$
- Loading dose of 3 $\mu g/kg$ followed by a continuous infusion of 1.5, 2 and 2.5 $\mu g/kg/h$
- Loading dose of 5 $\mu g/kg$ followed by a continuous infusion of 2, 3 and 4 $\mu g/kg/h$

The simulated dose of clondine for the children older than 28 days old were:

- Loading dose of 2 $\mu g/kg$ followed by a continuous infusion of 1, 1.5 and 2 $\mu g/kg/h$
- Loading dose of 4 $\mu g/kg$ followed by a continuous infusion of 2, 3 and 4 $\mu g/kg/h$
- Loading dose of 6 $\mu g/kg$ followed by a continuous infusion of 3, 4 and 5 $\mu g/kg/h$
- Loading dose of 10 $\mu g/kg$ followed by a continuous infusion of 3, 4 and 5 $\mu g/kg/h$

The simulated dose of midazolam for the neonates younger than 28 days old were:

- Loading dose of 100 $\mu g/kg$ followed by a continuous infusion of 50, 75 and 100 $\mu g/kg/h$
- Loading dose of 150 $\mu g/kg$ followed by a continuous infusion of 50, 75 and 100 $\mu g/kg/h$
- Loading dose of 200 $\mu g/kg$ followed by a continuous infusion of 75, 100, 150 $\mu g/kg/h$

The simulated dose of midazolam for the children older than 28 days old were:

- Loading dose of 200 $\mu g/kg$ followed by a continuous infusion of 100, 150 and 200 $\mu g/kg/h$
- Loading dose of 300 $\mu g/kg$ followed by a continuous infusion of 150, 200 and 250 $\mu g/kg/h$
- Loading dose of 400 $\mu g/kg$ followed by a continuous infusion of 250, 300, 350 $\mu g/kg/h$

5.2.8 Model evaluation

The PK and PK/PD models developed in this chapter were evaluated using RSE, bootstrap, goodness-of-fit and VPC as described in section 2.2.6.

5.3 Results

5.3.1 Study population

In total, 28 patients were included in the study. Thirteen of them received midazolam and 15 received clonidine. Morphine was administered to all the patients as background for pain. In addition, 10 children from the clonidine arm and 6 from the midazolam arm received propofol as bridging sedative via IV continuous infusion or bolus prior to enrolment. The dose of propofol in the clonidine group was higher than in the midazolam group. The demographic data of the cohort (by type of drug administered) are summarized in Table 21.

Table 21: Table summarising the demographic characteristics of the CloSed cohort.

	All drugs Median (Range)	Clonidine Median (Range)	Midazolam Median(Range)
Birth weight (kg)	3.8 (2.0 - 16.7)	4 (2.7 - 16.1)	3.3 (2.0 - 16.7)
Gestational age (weeks)	40 (36.3 - 40)	-	-
Postnatal age (days)	26 (0 - 2023)	41 (0 - 1419)	4 (0 - 2023)
Postmenstrual age (weeks)	43.6 (36.3 - 371.9)	45.9 (36.7 - 242.7)	40.1 (36.3 - 371.9)
Sex (M/F)	14/14	9/6	5/8
surgery (yes/no)	18/10	7/8	11/2
bridging propofol (yes/no)	16/12	10/15	6/7

5.3.2 Primary endpoint of the CloSed trial

The result of the primary endpoint of the trial are summarised in Table 22. Although there were sedation failures in both arms, the table shows that there was a higher number of sedation failure in the clonidine group.

Table 22: Results of the primary endpoint of the CloSed trial.

Endpoint	Clonidine	Midazolam
Success	8	11
Failure	4	2
Non assessable	3	0

The logistic regression analysis of the primary endpoint between treatment groups adjusted by centre and age was not significant therefore the null hypothesis H0 was rejected at 2.5% significance level. However due to the limited number of patients, these results have to be interpreted carefully.

5.3.3 Pharmacokinetic modelling

5.3.3.1 Clonidine

In total, 36 samples were used to develop the clonidine PK model. The 15 patients who received clonidine were included in the model. The observed concentration of clonidine plotted against time are presented in Figure 60. The graph shows that the PK data were limited with a number of samples between 2 and 4 by patient. Only one child received clonidine before starting the IMP treatment. The concentration recorded before the first dose was included as baseline in the model. The values corresponding to BLOQ were below 5%.

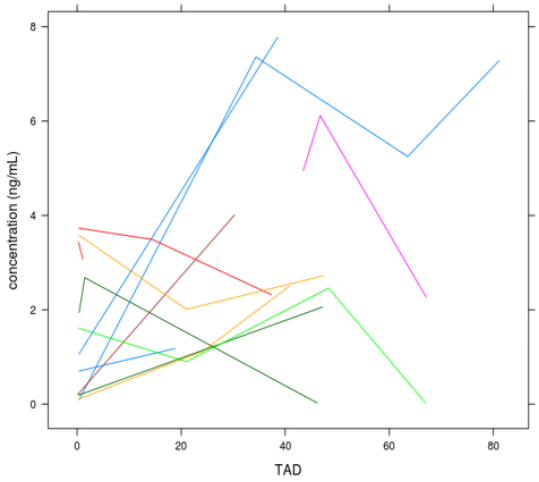

Figure 60: Observed concentration of clonidine plotted against the time after dose administration (TAD). Each line represents a patient.

The PK data were best described by a one-compartment model with IIV on clearance and central volume of distribution. The final residual model was a proportional error model. The model was not able to estimate the parameters of the maturation function,

therefore they were fixed to values estimated by a previous clonidine model published by Larsson *et al.* (148). No other covariates had a significant influence on the PK parameters.

The parameter estimates from the final clonidine PK model and the RSE corresponding are presented Table 23.

Table 23: Estimates from the final clonidine PK model.

Parameter	Estimate	RSE (%)	Bootstrap Median(5-95)
CL (L/h/70kg)	28.0	20	28.1 (19.2 - 37.1)
V (L/70kg)	202.4	24	202.2 (122.8 - 289.3)
IIV CL (%)	49.6	47	46.9 (20.7 - 65.6)
IIV V1 (%)	87.7	32	85.0 (57.4 - 106.8)
Err prop (%)	43.6	7	43.6 (20.7 - 56.6)
PMA_50	61.6 FIX	-	-
Hill	2.42 FIX	-	-

CL is the clearance, V1 is the central volume of distribution, RSE is the relative standard error (from NONMEM covariance step), IIV is the interindividual variability. PMA_50 is the PMA (weeks) when the maturation has reach 50%, and Hill is the shape parameter. FIX means that the value of the parameter was fixed a priori in the model. Err prop correspond to the proportional error estimate.

Basic goodness-of-fit plots are shown in Figure 61.

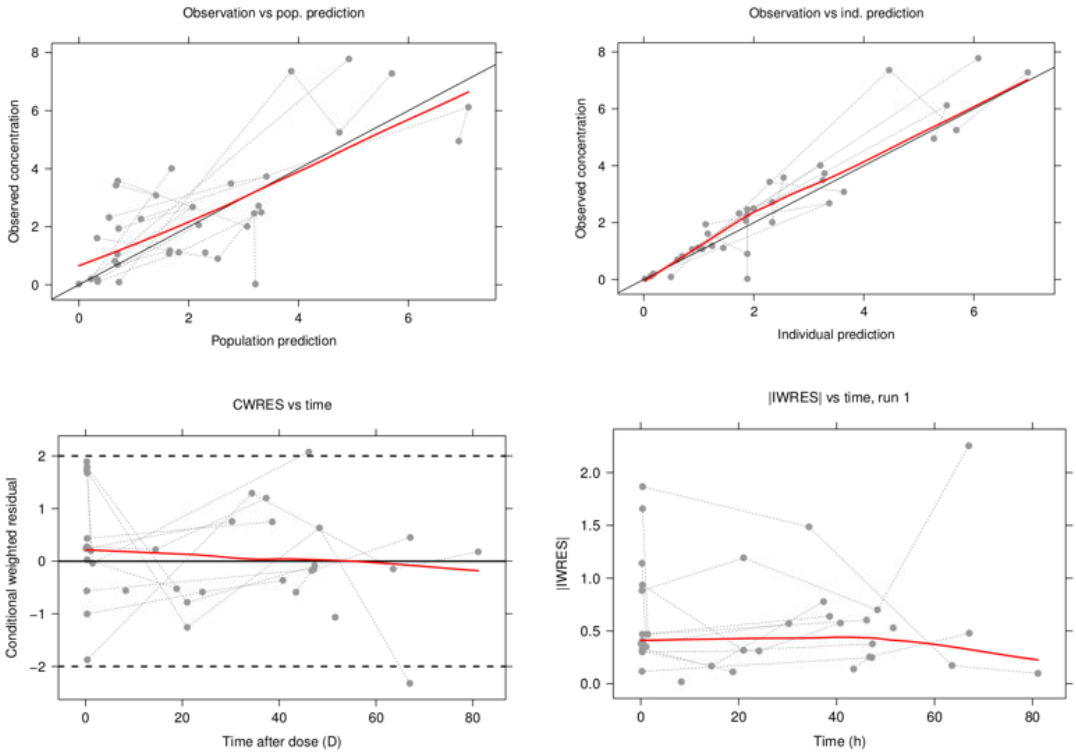

Figure 61: Goodness-of-fit plots of the final clonidine PK model. Plots of the observed concentration vs population predicted concentration (top left) and vs individual predicted concentration (top right), the CWRES versus time after dose (bottom left) and plot of the IWRES vs time after dose (bottom right) from the final fentanyl population PK model. The red line is the lowess line and the black line is the line of unity.

The VPC used to evaluate the final clonidine model are presented in Figure 62.

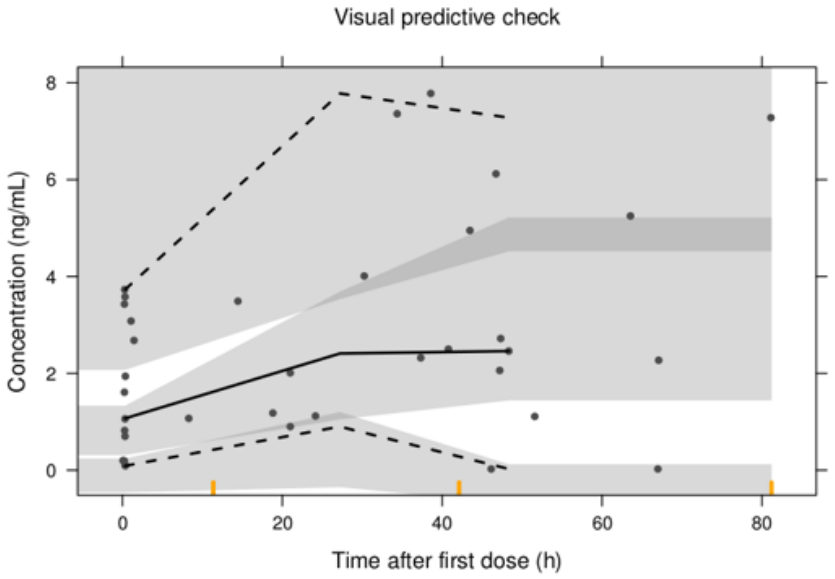

Figure 62: Visual Predictive Check produced using the parameters estimated by the final clonidine PK model. The shaded grey area is the 95 percent prediction interval. The black solid line is the median of the observed data; the black dashed lines are the 5 th and 95 th percentiles of the observed data.

5.3.3.2 Midazolam

Thirty-seven samples were used to build the midazolam PK model, each sample given a concentrations of midazolam and its main metabolite 1-OH-midazolam. No patient was excluded from the analysis, therefore the data from all 13 patients receiving midazolam were used to develop the model. The observed concentrations of midazolam and 1-OH-midazolam are presented in Figure 63. The number of samples by patient was between 2 and 4. Four patients had baseline concentrations of midazolam and its metabolite before starting the IMP treatment. These concentrations were included in the model.

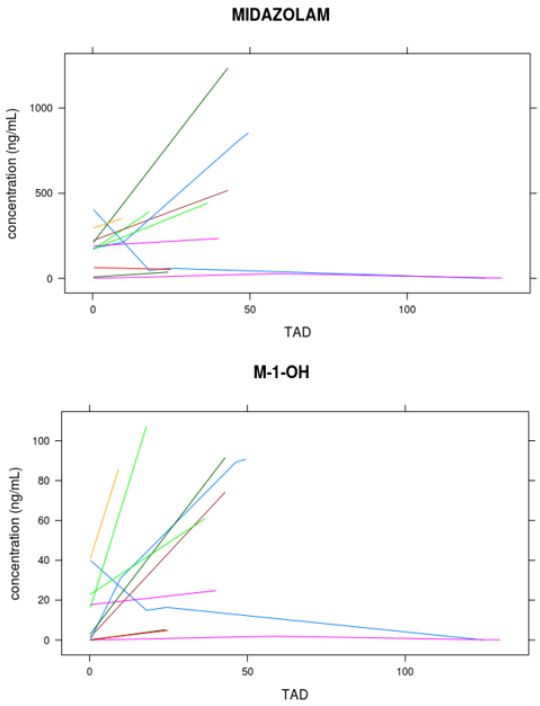

Figure 63: Observed concentration of midazolam and its main metabolite 1-OH-midazolam plotted against the time after dose administration (TAD). Each line represents a patient.

The model that best fitted the data was a one-compartment model for midazolam and its metabolite with IIV on the central volume of distribution (V1) and the formation clearance of 1-OH-midazolam (CLm). The best residual model was a combined error model for both midazolam and metabolite compartments. The model was not able to estimate the parent clearance, therefore it was assumed in the model that midazolam was entirely metabolised in 1-OH-midazolam. The compartmental structure of the final model is presented in Figure 64.

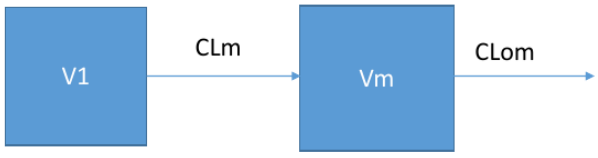

Figure 64: Representation of the final midazolam model

The model was not able to estimate the parameters of the maturation function (non plausible values of clearance estimated), therefore they were fixed using values

estimated by a maturation model for midazolam clearance published by Anderson *et al.* (134). The same values were used for the maturation function of the metabolite formation clearance (CLm) and the metabolite elimination clearance (Clom). Age and weight were the only covariates that had a significant effect on the PK parameters.

The estimates of the final PK parameters and the RSE corresponding are presented in Table 24.

Table 24: Estimates from the final midazolam PK model.

Parameter	Estimate	RSE (%)	Bootstrap Median(5-95)
V1 (L/70kg)	85.8	30	75.6 (37.7 - 124.5)
CLm (L/h/70kg)	33.4	32	35.3 (22.3 - 61.7)
Vm (L/70kg)	90.8	67	87.3 (39.0 - 222.9)
CLom (L/h/70kg)	211.6	12	214.7 (178.5 - 295.5)
IIV CLm (%)	91.7	41	84.9 (42.4 - 113.1)
IIV V1 (%)	133.4	54	131.1 (66.3 - 236.2)
Err prop parent (%)	46.9	39	45.8 (22.4 - 58.3)
Err add parent (ng/mL)	1.24	69	1.25 (0.24 - 1.79)
Err prop metab (%)	57.4	31	57.4 (42.4 - 72.8)
Err add metab (ng/mL)	0.023	23	0.023 (0.014 - 0.037)
PMA_50	73.6 FIX	-	-
Hill	3 FIX	-	-

V1 is the central volume of distribution, CLm the metabolite formation clearance,

Vm the volume of the metabolic compartment and CLom the clearance out of the metabolic compartment. RSE is the relative standard error (from NONMEM covariance step), IIV is the interindividual variability. PMA_50 is the PMA (weeks) when the maturation has reach 50%, and Hill is the shape parameter. FIX means that the value of the parameter was fixed a priori in the model.Err prop and Err add correspond to the error proportional and additive, respectively.

Basic goodness-of-fit plots evaluating the model for both midazolam and 1-OH-midazolam are presented in Figure 65.

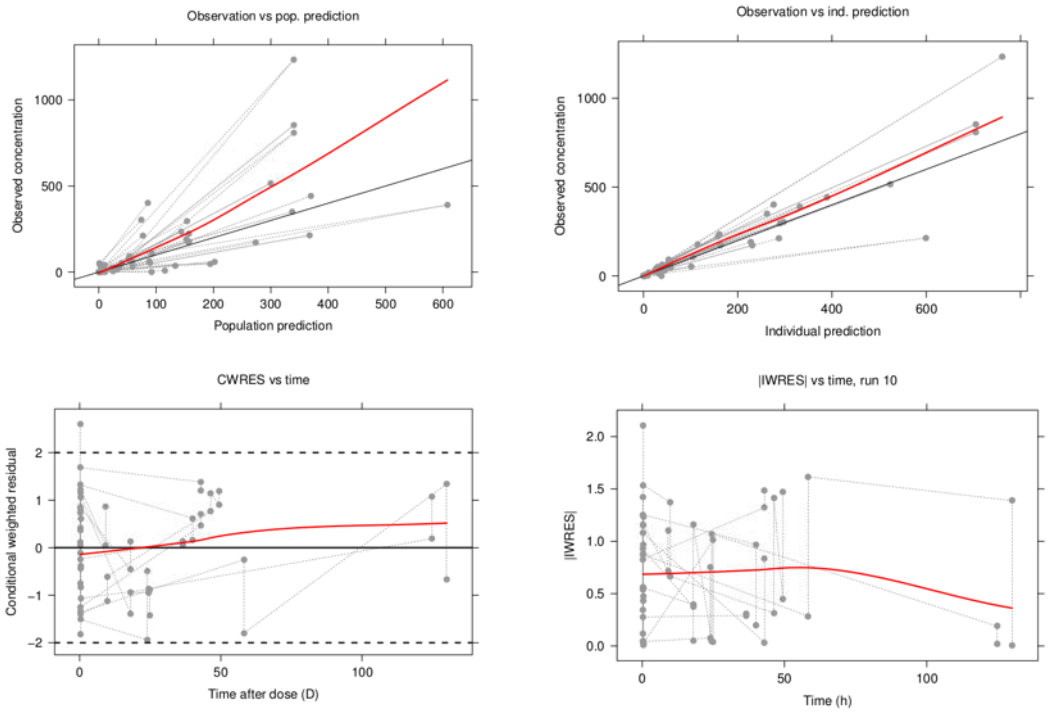

Figure 65: Goodness-of-fit plots of the final midazolam PK model. Plots of the observed concentration vs population predicted concentration (top left) and vs individual predicted concentration (top right), the CWRES versus time after dose (bottom left) and plot of the IWRES vs time after dose (bottom right) from the final midazolam population PK model. The red line is the lowess line and the black line is the line of unity.

The VPC for the final model are presented in Figure 66. Figure 67 shows the VPC stratified by compounds (midazolam and its metabolite).

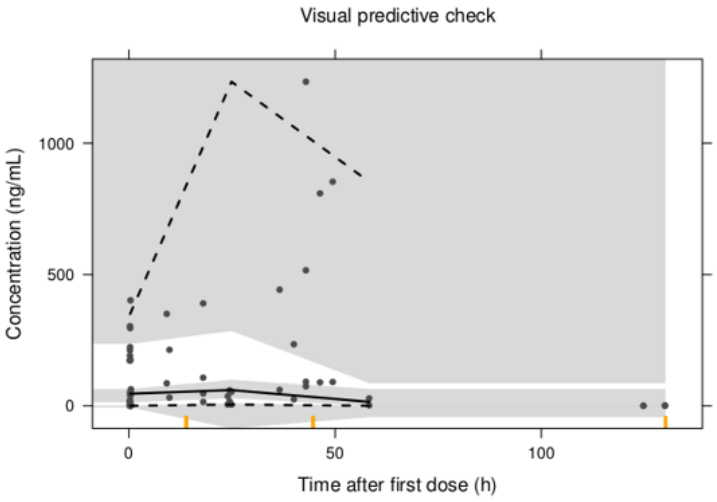

Figure 66: Visual Predictive Check produced using the parameters estimated by the final midazolam PK model. The shaded grey area is the 95 percent prediction interval. The black solid line is the median of the observed data; the black dashed lines are the 5 th and 95 th percentiles of the observed data.

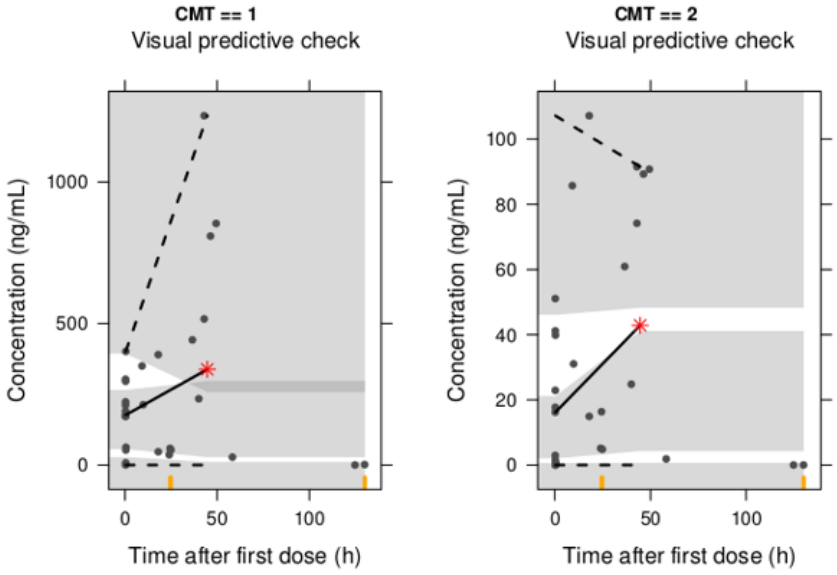

Figure 67: VPC produced using the parameters estimated by the final midazolam PK model. The VPC are stratified by compounds: midazolam (left) and 1-OH-Midazolam (right). The shaded grey area is the 95 percent prediction interval. The black solid line is the median of the observed data; the black dashed lines are the 5 th and 95 th percentiles of the observed data.

5.3.3.3 Morphine

In total, 65 samples were used to developed the morphine PK model. Each sample provided a concentration of morphine and the two main metabolites M3G and M6G. One patient was excluded of the PK analysis because a dose was missing. Hence, 27 children were included to build the final model. The observed concentration of morphine, M3G and M6G are shown in Figure 68. The number of samples by patient was between 2 and 5. Three children had positive concentration of morphine and metabolites before starting the IMP treatment. These data were used in the model as baseline concentrations.

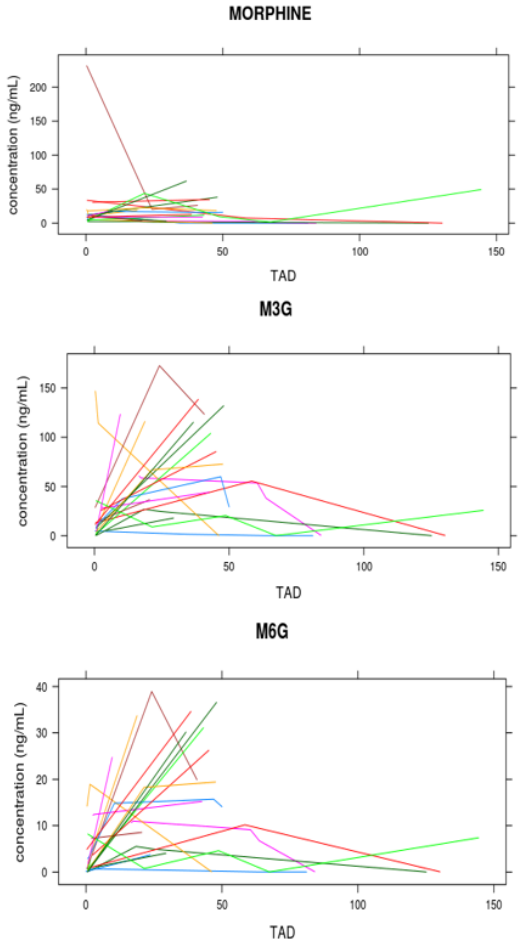

Figure 68: Observed concentration of morphine and its main metabolites M3G and M6G plotted against the time after dose administration (TAD). Each line represents a patient.

The PK data were best described by a one-compartment model for morphine and one-compartment model for each metabolite (M3G and M6G). IIV was added on central

volume of distribution (V1), formation clearance of M3G (CL3M) and M6G (CL6M), M3G volume of distribution (V3) and the metabolite clearance of M3G (CLom3). A combined error model for each compartment was used to describe the residual error. The model was not able to estimate the morphine clearance (parameter estimated to non plausible values), therefore the model assumed that morphine was entirely metabolised to M3G and M6G. The compartmental structure of the final model is presented in Figure 69.

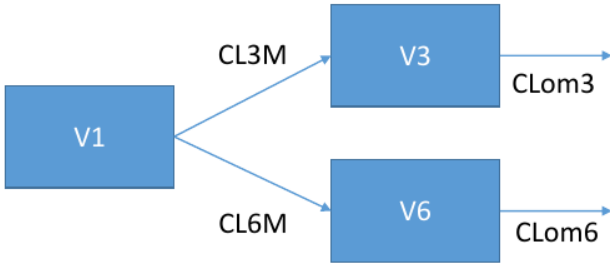

Figure 69: Representation of the final morphine compartmental model

The parameter estimates from the final morphine PK model and the RSE corresponding are presented in Table 25.

Table 25: Estimates from the final morphine PK model.

Parameter	Estimate (RSE (%))	IIV (RSE (%))	Bootstrap median(5-95)
V1 (L/70kg)	103.6 (34)	116.6 (47)	110.3 (61.2 - 172.2)
CL3M (L/h/70kg)	81.8 (31)	117.4 (31)	83.8 (54.6 - 117.6)
V3 (L/70kg)	38.4 (26)	134.5 (46)	42.1 (24.3 - 67.8)
CLom3 (L/h/70kg)	16.3 (23)	99.4 (35)	15.7 (10.4 - 20.7)
CL6M (L/h/70kg)	6.5 (21)	48.9 (45)	6.8 (5.0 - 9.3)
V6 (L/70kg)	30 FIX (-)	-	-
CLom6 (L/h/70kg)	5.5 (23)	-	5.5 (3.9 - 9.6)
Crea CL3M	-1.3 (15)	-	-1.3 (-2.0 - 0.9)
Crea CLom6	2.0 (25)	-	1.9 (0.5 - 3.0)
Err prop parent (%)	54.7 (35)	-	52.0 (33.2 - 65.6)
Err add parent (ng/mL)	0.025 (6)	-	0.025 (0.024 - 0.025)
Err prop M3G (%)	54.7 (32)	-	50.9 (36.1 - 61.6)
Err add M3G (ng/mL)	0.30 (59)	-	0.24 (0.020 - 0.47)
Err prop M6G (%)	76.8 (90)	-	68.6 (34.6 - 183.3)
Err add M6G (ng/mL)	0.062 (60)	-	0.057 (0.018 - 0.092)

V1 is the central volume of distribution, CL3M and CL6M are the formation clearances of M3G and M6G, respectively. V3 and V6 correspond to the volume of the metabolic compartments. CLom3 and CLom6 are the clearance out of the metabolic

compartment of M3G and M6G, respectively. Crea CL3M and Crea CLom6 are the index corresponding to the effect of creatinine level on CL3M and Clom6, respectively. RSE is the relative standard error (from NONMEM covariance step), IIV is the interindividual variability. Err prop and Err add correspond to the error proportional and additive, respectively.

The estimation of the M6G volume of distribution induced an instability of the model leading an estimation to non plausible values for all parameters. Hence this parameter was fixed to a value published previously in a morphine model developed in children by Knibbe *et al.* (200).

The parameters of the sigmoidal maturation function used to describe the formation clearances of both metabolites (CL3M and CL6M) were fixed to values published by Anand *et al.* (190). Those used to estimate the metabolite clearances (CLom3 and CLom6) and central volume of distribution (V1) were fixed to values estimated by the morphine model developed by Bouwmeester *et al.* (191).

In addition to weight and age, the model also found a significant influence of creatinine level on CL3M and CLom6.

Basic goodness-of-fit plots evaluating the model for morphine and both metabolites together are shown in Figure 70.

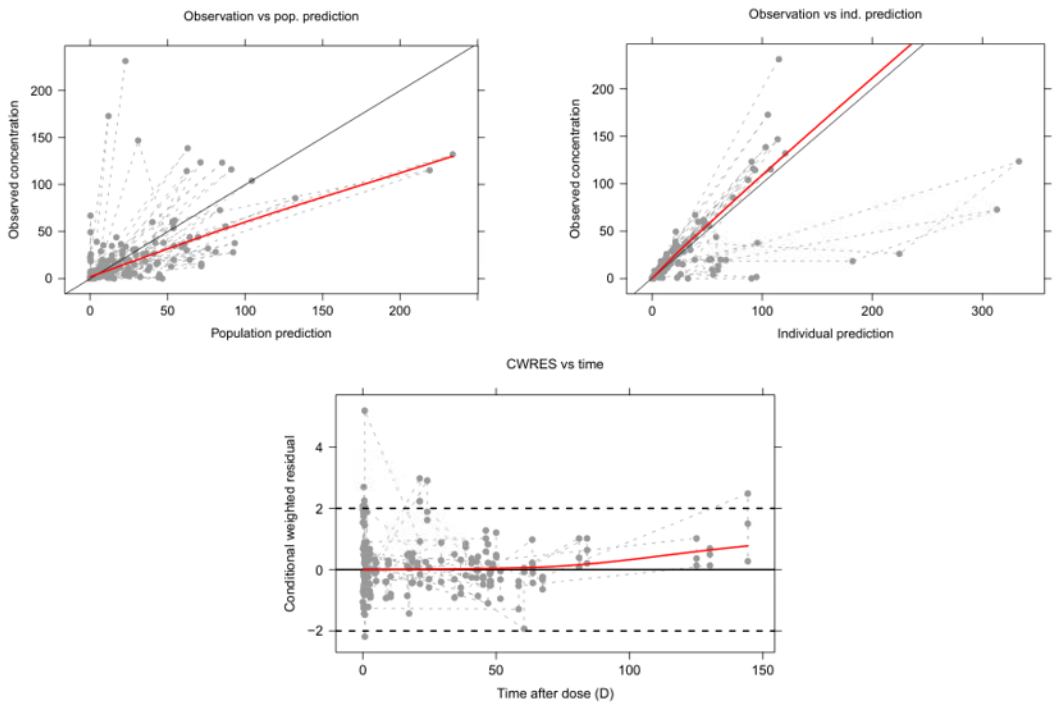

Figure 70: Goodness-of-fit plots of the final morphine PK model. Plots of the observed concentration vs population predicted concentration (top left) and vs individual predicted concentration (top right), the CWRES versus time after dose from the final morphine population PK model. The red line is the lowess line and the black line is the line of unity.

The VPC used to evaluate the final model are shown in Figure 71. Figure 72 presents the VPC stratified by compounds (morphine, M3G, M6G).

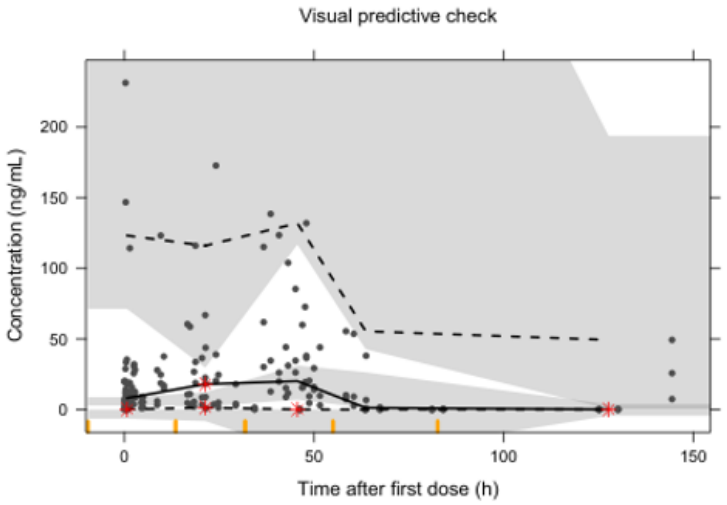

Figure 71: Visual Predictive Check produced using the parameters estimated by the final morphine PK model. The shaded grey area is the 95 percent prediction interval. The black solid line is the median of the observed data; the black dashed lines are the 5 th and 95 th percentiles of the observed data.

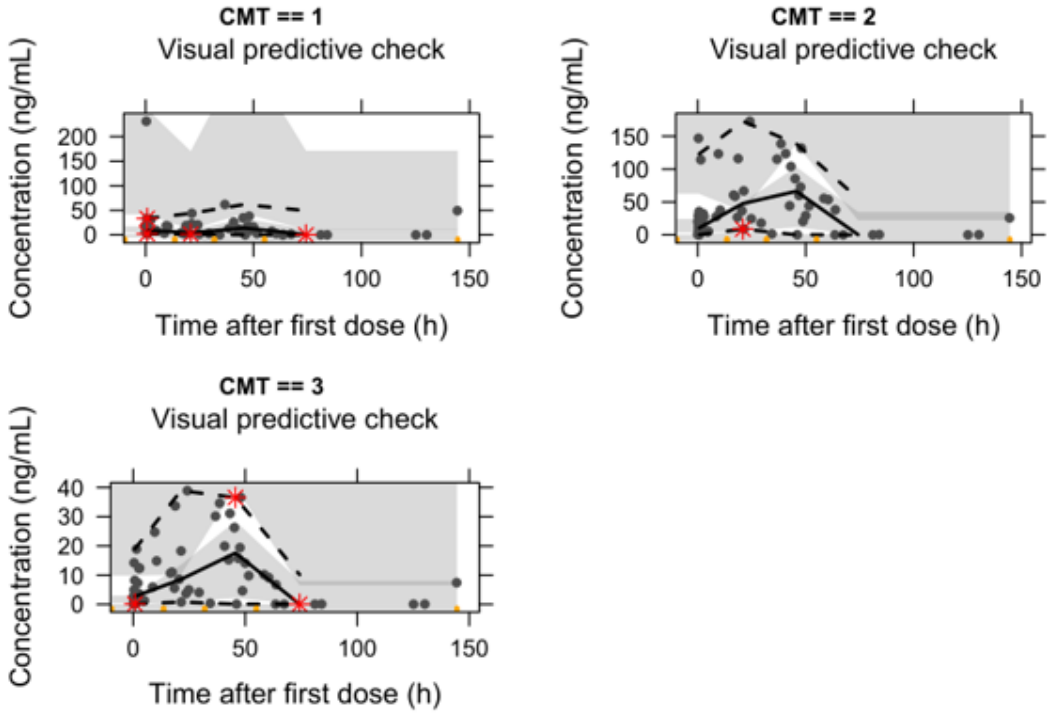

Figure 72: VPC produced using the parameters estimated by the final morphine PK model. The VPC are stratified by compounds: morphine (top left), M3G (top right) and M6G (bottom left). The shaded grey area is the 95 percent prediction interval. The black solid line is the median of the observed data; the black dashed lines are the 5 th and 95 th percentiles of the observed data.

5.3.4 Pharmacokinetic/pharmacogenetic modelling

No significant association between genetic variants and individual clearances was found during the screening process. Therefore no gene was tested in the PK model with NONMEM.

5.3.5 Pharmacokinetic/pharmacodynamic modelling of the efficacy variables

5.3.5.1 Data

All the patients who received the IMP treatment were included in the PK/PD models (13 for midazolam and 15 for clonidine). The characteristics of the COMFORT-B score by patient used in the PK/PD model to evaluate the sedation effect of the drugs are summarised in Table 26.

Table 26: Table summarising the characteristics of the COMFORT-B data by patient and by drug.

	Clonidine Median (Range)	Midazolam Median (Range)
Score	13 (6 - 27)	12 (6 - 26)
Number of data point	25 (9 - 47)	23 (18 - 38)
Assessment time (h)	62.5 (13.5 - 107.3)	62.7 (33.2 - 91.6)

In total, 317 observed scores were used to build the midazolam PK/PD model and 306 were used to develop the clonidine PK/PD model. The observed COMFORT-B scores plotted against midazolam and clonidine concentrations are presented in Figure 73 and Figure 74, respectively. The plots do not show any obvious relationship between score and concentration.

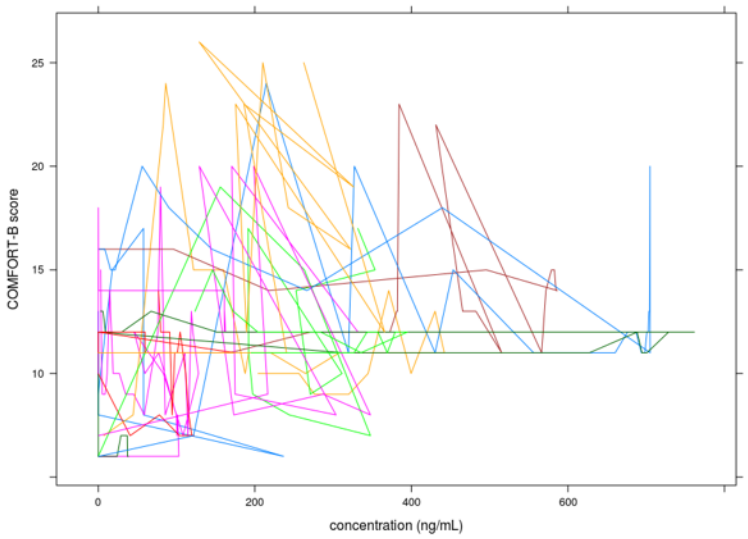

Figure 73: COMFORT-B score plotted against midazolam concentration. Each line represents a patient.

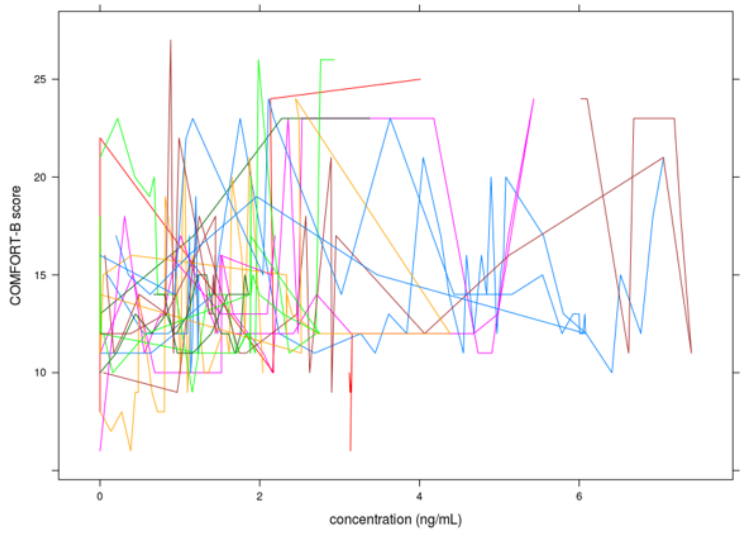

Figure 74: COMFORT-B score plotted against clonidine concentration. Each line represents a patient.

Individual plots regrouping drug concentration, COMFORT-B score, IMP dose and doses of the different co-drug administered (morphine, propofol) for clonidine and midazolam are shown in Figure 75 and 76, respectively.

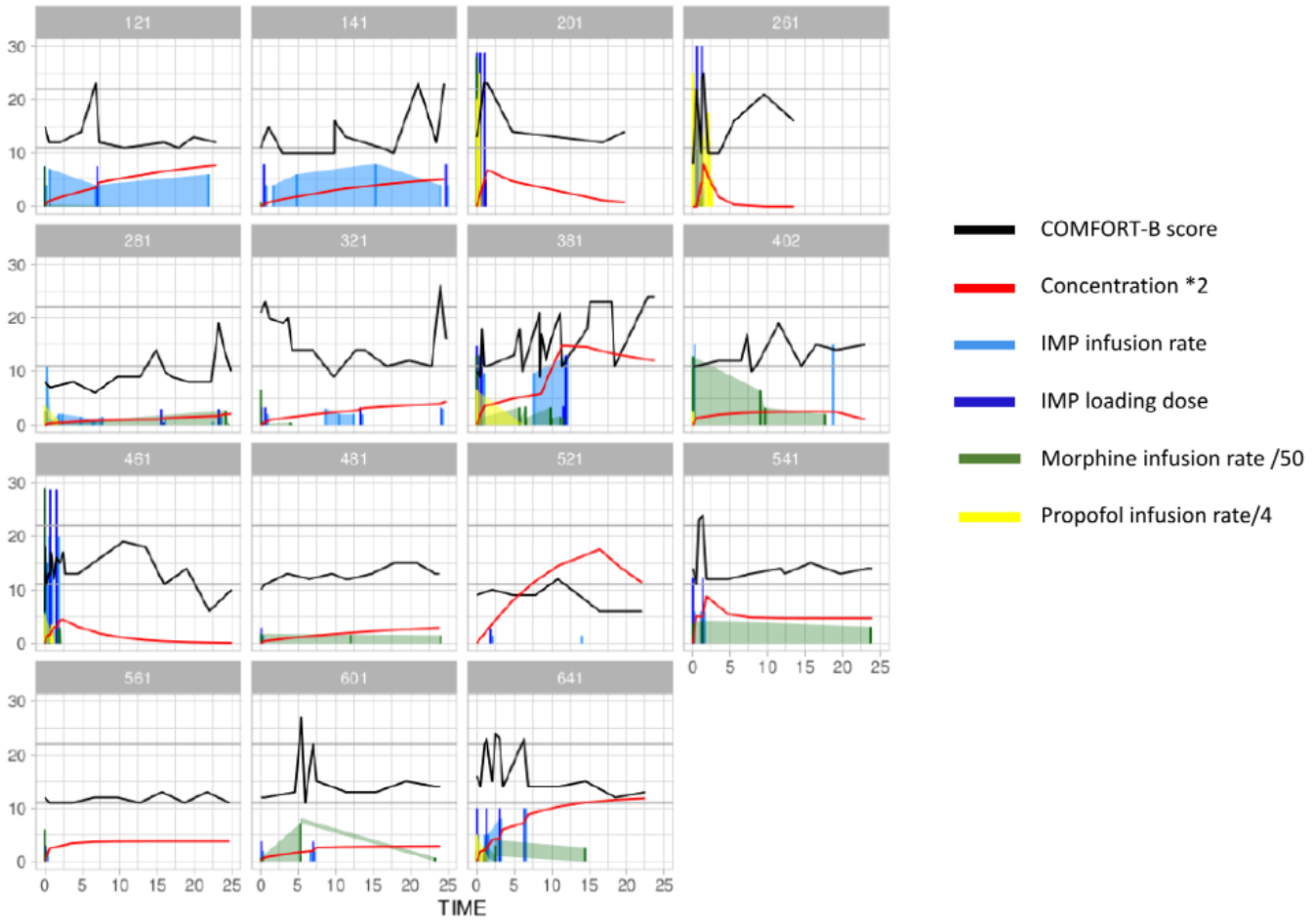

Figure 75: Individual plots of the patients receiving clonidine regrouping drug concentration (red line), COMFORT-B score (black line), clonidine loading dose (vertical dark blue line), clonidine infusion rate (blue shaded area), morphine infusion rate (green shaded area) and propofol infusion rate (yellow shaded area)

The individual plots presented in Figure 75 show a clear relationship between clonidine concentration and COMFORT-B score for the patients 201, 161, 521 and 641. However, there is no clear concentration-effect relationship that can be observed for the other patients. Additional clonidine loading doses seem to induce a drop of the COMFORT-B score as it can be seen for patients 121 and 141.

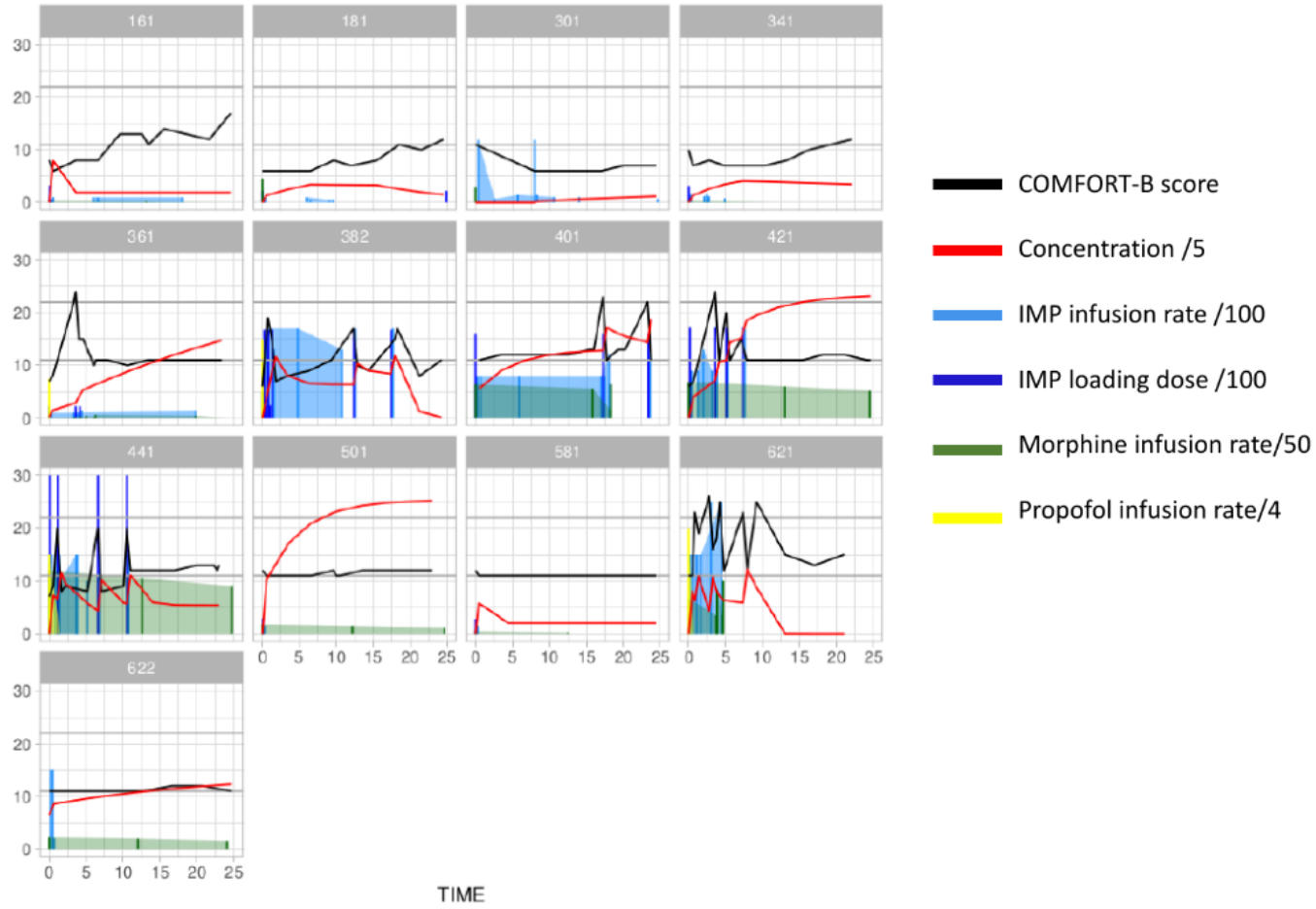

Figure 76: Individual plots of the patients receiving midazolam regrouping drug concentration (red line), COMFORT-B score (black line), midazolam loading dose (vertical dark blue line), midazolam infusion rate (blue shaded area), morphine infusion rate (green shaded area) and propofol infusion rate (yellow shaded area)

The midazolam individual plots presented in Figure 76 show that for most patients the scores seems to decrease when the concentrations increase (e.g. patient 121,181). However, no relationship between midazolam concentration and score can be observed for few patients (e.g. 501, 581, 622).

Eleven of the 13 patients in the midazolam arm underwent surgery before starting the IMP treatment whereas only 7 of the 15 patients of the clonidine group had surgery before receiving clonidine.

5.3.5.2 Continuous model

5.3.5.2.1 Midazolam

The inhibitory sigmoid Emax model with no post-anesthesia effect estimated the midazolam EC50 parameter to a non plausible value. Although the inclusion of an effect compartment induced a significant decreased of the OFV (68.5 points), the model did not improve the estimation of the EC50 parameter. The inclusion of the post-anesthesia effect in the model for the patients who underwent major surgery increased the stability of the model that was able to estimate with precision the parameters. In addition, it induced a significant decreased of the OFV corresponding to 28.1 points. The final model included an IIV on EC50 and the best residual model was a proportional error model.

The model was not able to estimate the maximal effect of midazolam (EMAX), therefore this parameter was fixed to the value 6, as it has been previously done in the PK/PD model developed by Peeters *et al.* (103).

The model could not estimate the baseline score before administration of the IMP treatment (B0), hence the baseline scores were set to the observed values in the database for each individual in a separate column in order to simplify the model.

A significant effect of propofol included using an Emax K-PD model was found on the COMFORT-B score (ΔOFV = 21.1). The propofol maximal effect (Emax) and EC50 were fixed to values published in the propofol PK/PD model developed in children by Peeters *et al.* (201). The propofol KDE parameter was estimated by the model.

No significant effect of other co-medication (morphine or ketamine) was found.

The parameter estimates from the final midazolam PK/PD model and the RSE corresponding are presented in Table 27.

Table 27: Estimates from the final midazolam PK/PD model.

Parameter	Estimate	RSE (%)	Bootstrap Median(range)
EC50 (ng/mL)	186.0	61	258.9 (33.8 - 1692.8)
PAEMAX	9.3	11	9.3 (7.0 - 10.9)
TPS50 (h)	0.11	43	0.11 (0.03 - 0.60)
BASE	6 FIX	-	-
EMAX	6 FIX	-	-
KDE	9.6	19	9.2 (5.4 - 12.1)
IIV EC50 (%)	246.6	55	252.4 (161.2 - 446.1)
Err prop (%)	24.9	15	24.3 (21.1 - 28.1)

BASE is the score at the end of the surgery, PAEMAX is the maximal postanesthesia effect from BASE and $TPS50$ is the time post-surgery at half maximum postanesthesia effect in hours. EMAX is the maximal effect, EC50 is the concentration to reach 50% of the maximal effect and IIV is the interindividual variability.

Basic goodness-of-fit plots are presented in Figure 77.

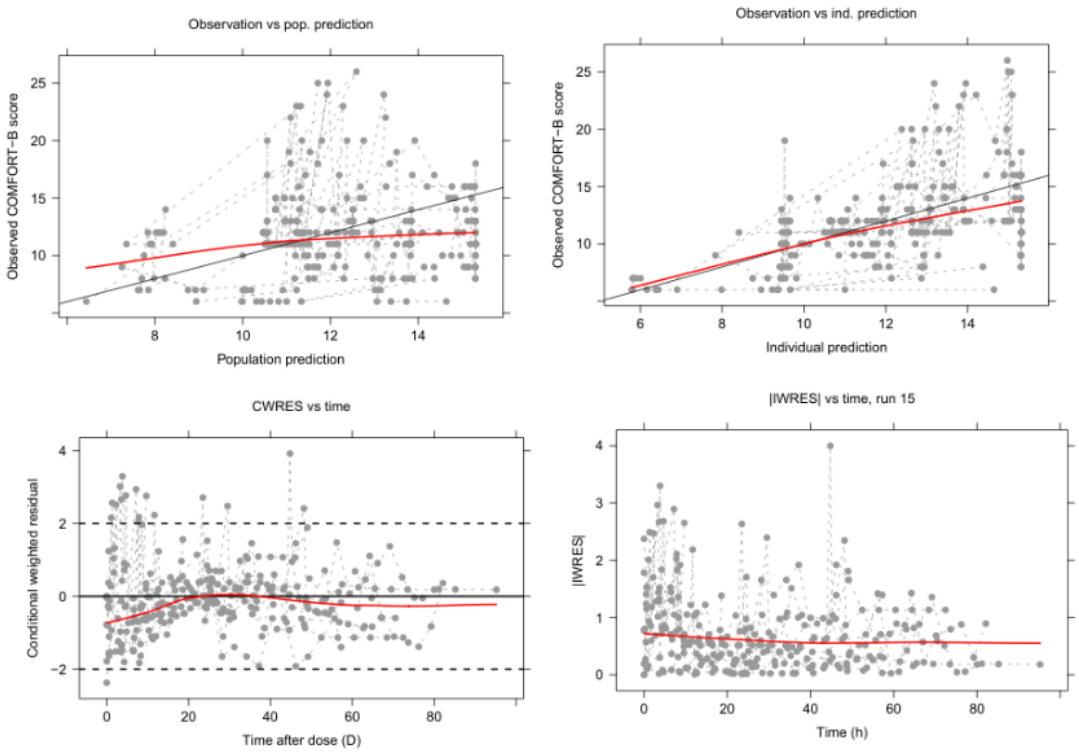

Figure 77: Goodness-of-fit plots of the final midazolam PK/PD model. Plots of the observed score vs population predicted score (top left) and vs individual predicted score (top right) CWRES versus time after dose (bottom left) and plot of the IWRES vs time after dose (bottom right). The red line is the lowess line and the black line is the line of unity.

The VPC evaluating the final model are shown in Figure 78.

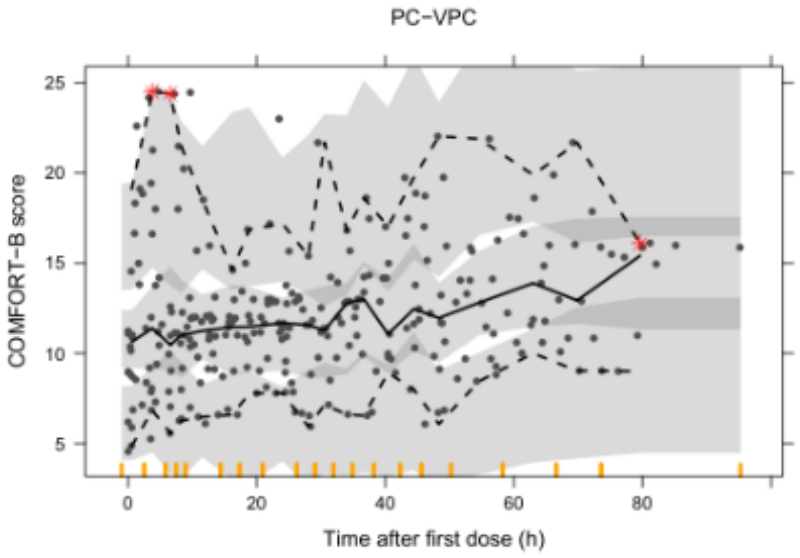

Figure 78: VPC produced using the parameters estimated by the final midazolam PK/PD model. The shaded grey area is the 95 percent prediction interval. The black solid line is the median of the observed data; the black dashed lines are the 5 th and 95 th percentiles of the observed data.

5.3.5.2.2 Clonidine

The inhibitory sigmoid Emax model withour post-surgery effect estimated a non plausible value of EC50, therefore the model was not able to adequately describe the data. The inclusion of an effect compartment was not significant and did not improve the estimation of the clonidine EC50. The inclusion of a post-anesthesia effect in the inhibitory sigmoid Emax model for the patients who underwent surgery during which they received complete anesthesia improved the model fit by estimating with precision the parameters and decreasing the OFV by 361 points. An IIV was added on the EC50. The model that best described the residual error was a proportional error model.

The estimation of the maximal effect of clonidine (EMAX) induced an instability of the model leading to non plausible parameter estimates. Hence this parameter was fixed to 6, as it has been done in the midazolam PK/PD model. The same issue occurred with PAEMAX that could not be estimated by the model, therefore a sensitivity analysis was done in order to fix the parameter to a rational value that improved the stability of the model.

No significant effect of co-medications (morphine, ketamine and propofol) was found.

The estimates of the clonidine PK/PD parameters and the RSE corresponding are presented in Table 28.

Table 28: Estimates from the final clonidine PK/PD model.

Parameter	Estimate	RSE (%)
EC50 (ng/mL)	2.73	7
PAEMAX	11.8 FIX	-
TPS50 (h)	0.069	228
BASE	6 FIX	-
EMAX	6 FIX	-
B0	15.6	4
IIV EC50 (%)	525	56
Err prop (%)	28	26

BASE is the score at the end of the surgery, PAEMAX is the maximal postanesthesia effect from BASE and $TPS50$ is the time post-surgery at half maximum postanesthesia effect in hours. EMAX is the maximal effect, EC50 is the concentration to reach 50% of the maximal effect and IIV is the interindividual variability.

5.3.5.2.3 Joint model

In order to improve both models, a joint PK/PD model combining the data of both midazolam and clonidine was built. This model was similar to the ones developed for the individual drugs. Apart from the parameter TPS50 which was common for both drugs, the other parameters were specific to each drug.

Since the model was not stable enough to estimate all parameters, the midazolam parameters (except TPS50) were fixed to the values estimated by the midazolam PK/PD model developed in this chapter.

The parameter estimates from the final joint PK/PD model and the RSE corre-

sponding are presented Table 29.

Table 29: Estimates from the final joint PK/PD model.

Drugs	Parameter	Estimate	RSE (%)	Bootstrap Median(range)
	EC50 (ng/mL)	186.0 FIX	-	-
	PAEMAX	9.3 FIX	-	-
MIDAZOLAM	KDE	9.6 FIX	-	-
	IIV EC50 (%)	246.6 FIX	-	-
	Err prop (%)	24.9 FIX	-	-
	TPS50 (h)	0.11	68	0.13 (0.03 - 0.36)
BOTH DRUGS	BASE	6 FIX	-	-
	EMAX	6 FIX	-	-
	EC50 (ng/mL)	2.73	9	5.23 (0.41 - 31.8)
	PAEMAX	11.8 FIX	-	-
CLONIDINE	B0	15.6	4	15.6 (14.3 - 16.6)
	IIV EC50 (%)	525	52	473 (225 - 1355)
	Err prop (%)	28.2	14	28.1 (23.6 - 31.6)

BASE is the score at the end of the surgery, PAEMAX is the maximal postanesthesia effect from BASE and $TPS50$ is the time post-surgery at half maximum postanesthesia effect in hours. EMAX is the maximal effect, EC50 is the concentration to reach 50% of the maximal effect and IIV is the interindividual variability.

Because the joint model improved the precision of the clonidine parameter estimates, this model was chosen as final PK/PD model for clonidine.

The basic goodness-of-fit plots used to evaluate the clonidine data from the joint model are presented in Figure 79.

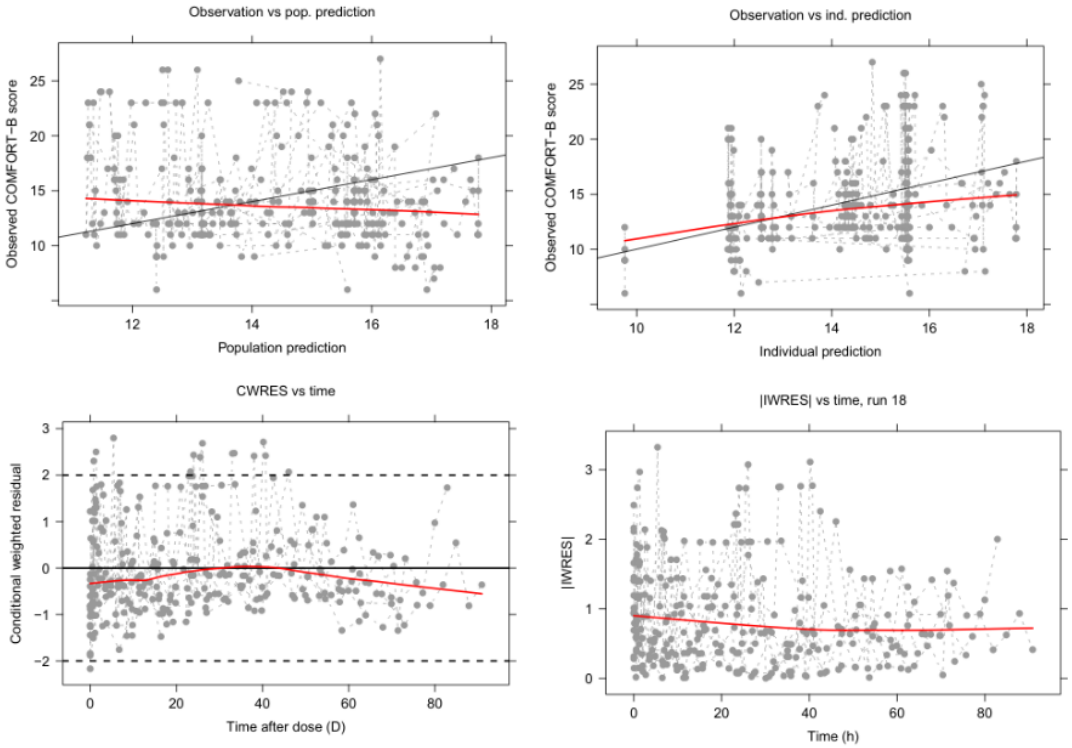

Figure 79: Goodness-of-fit plots of clonidine using the final joint PK/PD model. Plots of the observed score vs population predicted score (top left) and vs individual predicted score (top right), CWRES versus time after dose (bottom left) and plot of the IWRES vs time after dose (bottom right). The red line is the lowess line and the black line is the line of unity.

The VPC of clonidine from the final joint PK/PD model are shown in Figure 80.

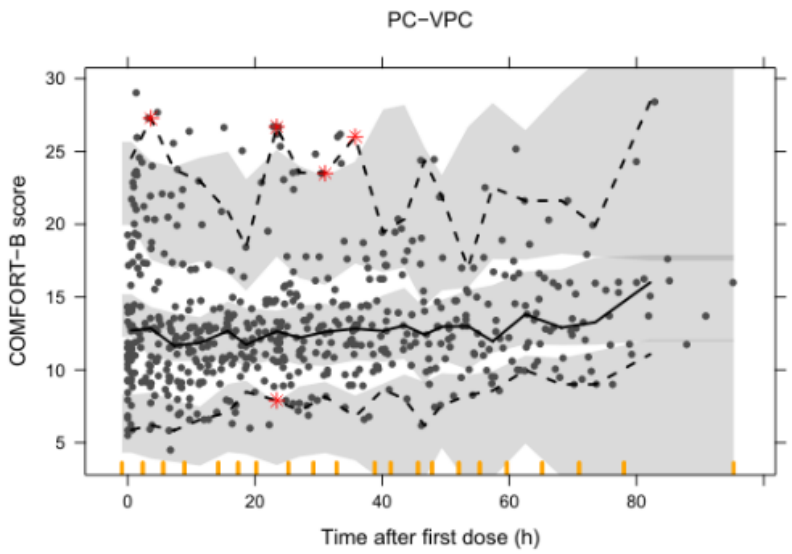

Figure 80: VPC of clonidine produced using the parameters estimated by the final joint PK/PD model. The shaded grey area is the 95 percent prediction interval. The black solid line is the median of the observed data; the black dashed lines are the 5 th and 95 th percentiles of the observed data.

5.3.5.2.4 Categorical model

5.3.5.2.5 Proportional odds model

In the proportional odds model developed for clonidine, non of the predictors had a significant effect on the COMFORT-B score.

In the proportional odds model developed for midazolam, the predictor corresponding to the drug effect did not induce a significant decrease of the OFV. However, the post-surgery effect was a significant predictor inducing an OFV decrease of 5.6 points.

5.3.5.2.6 Bounded integer model

The BI models developed for both drugs were not able to adequately describe the relationship between drug concentrations and COMFORT-B score. The parameters corresponding to Emax and EC50 of each drug were estimated by the model to non plausible values. For both drugs, the Markov effect was not found significant in the BI models developed.

5.3.6 Pharmacokinetic/pharmacodynamic modelling of safety variables

All patients who received clonidine were included in the safety analysis in order to develop PK/PD models describing the relationship between clonidine concentration and adverse effects using HR and MAP data.

In total, 963 measures of HR and 801 measure of MAP were used to build the PK/PD models.

The observed HR and MAP data plotted against clonidine concentration are presented in Figure 81 and Figure 82, respectively. The plots show that the vital signs (HR or MAP) seems to decrease with the clonidine concentration.

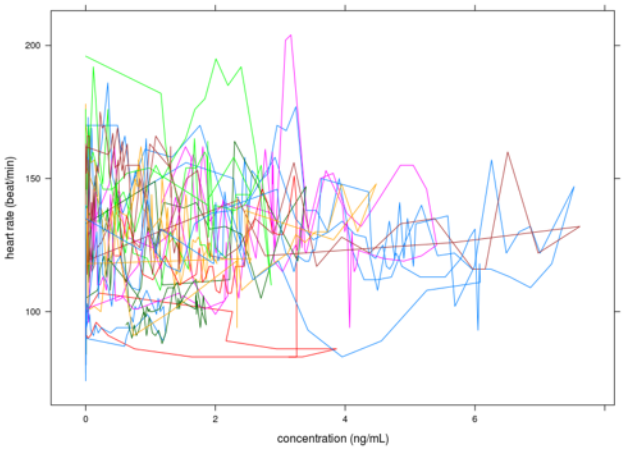

Figure 81: Heart rate plotted against clonidine concentration. Each line represents a patient.

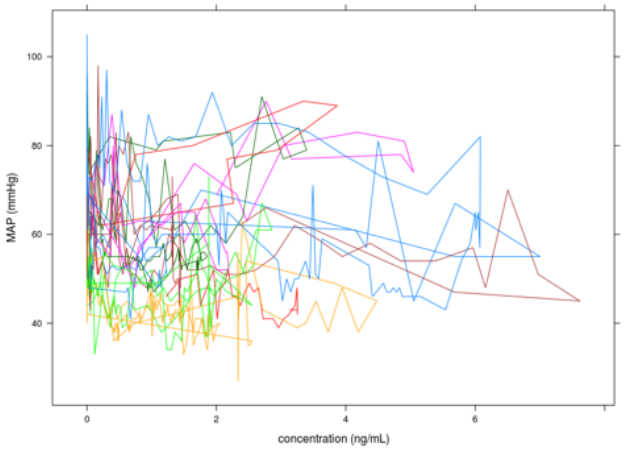

Figure 82: MAP plotted against clonidine concentration. Each line represents a patient.

No significant relationship between clonidine PK and both HR and MAP was found using a continuous Emax model. The models were unstable and estimated the EC50 parameters to non plausible values.

5.3.7 Simulations

The graphs generated using the simulated midazolam concentration in neonates younger than 28 days old for a loading dose of 100 $\mu g/kg$ following by an infusion of 100 $\mu g/kg/h$ are presented in Figure 83. Figure 84 shows the simulation plots of midazolam in children older than 28 days old for a loading dose of 200 $\mu g/kg$ following by an infusion of 200 $\mu g/kg/h$.

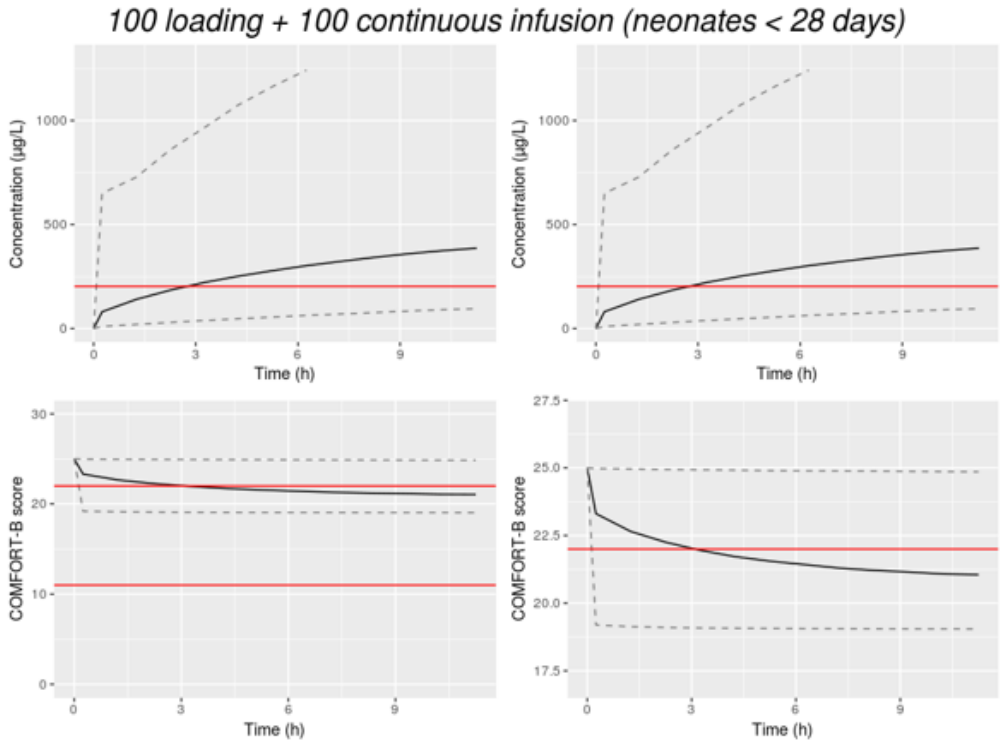

Figure 83: Plots generated using the simulated midazolam concentration in neonates younger than 28 days old for a loading dose of 100 mcg/kg followed by an infusion of 100 mcg/kg/h. Both graphs on the top present the simulated concentration of midazolam where the red line represents the EC50 defined using the PK/PD model. The graph on the bottom left shows the change in COMFORT-B score following the simulated concentration produced using the final PK/PD model. The red lines are the scores between which the level of sedation was considered as adequate. A zoom of this graph is presented on the bottom right. For all the graphs, the black line is the predicted median concentration and the dotted line represents the 95 percent prediction interval.

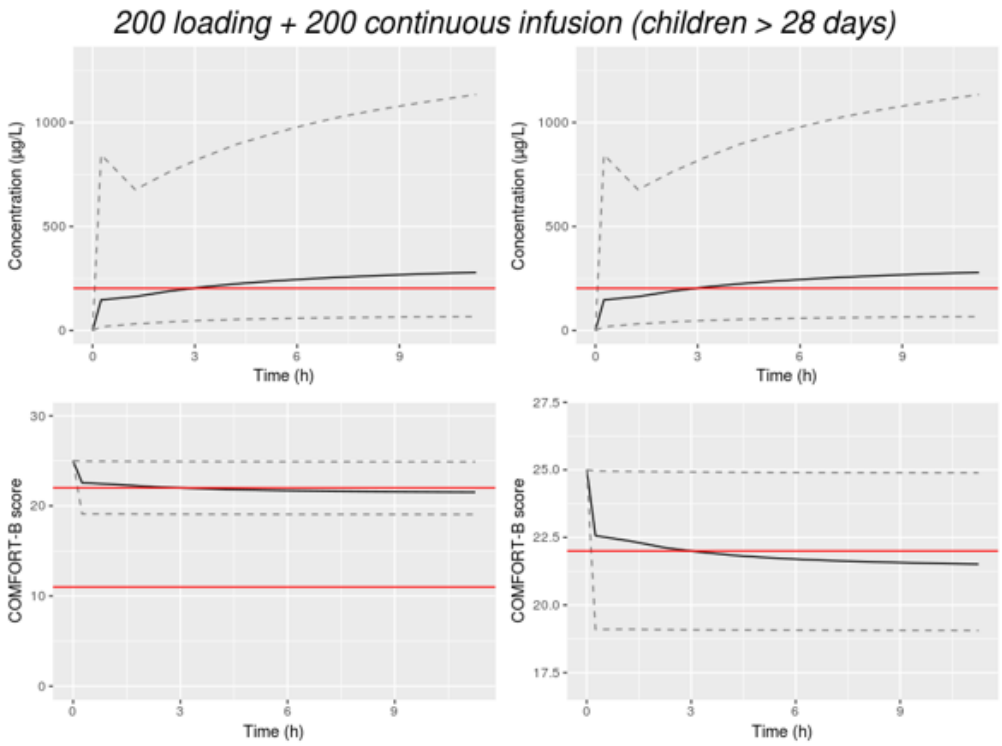

Figure 84: Plots produced using the simulated midazolam concentration in children older than 28 days old for a loading dose of 200 mcg/kg followed by an infusion of 200 mcg/kg/h

The simulated midazolam concentration plot presented in Figure 84 shows that the predicted median for the children older than 28 days old reaches the EC50 estimated by the PK/PD model 3h after receiving a loading dose of 200 $\mu g/kg$ followed by 200 $\mu g/kg/h$. Figure 83 shows that this dose should be divided by two in order to obtain the same results in neonates younger than 28 days old.

Figure 85 shows the graphs produced using the simulated clonidine concentrations in children younger than 28 days old for a loading dose of 2 $\mu g/kg$ followed by an infusion of 1.5 $\mu g/kg/h$. The simulated clonidine concentrations in children older than 28 days old for a loading dose of 4 $\mu g/kg$ followed by an infusion of 3 $\mu g/kg/h$ are presented in Figure 86.

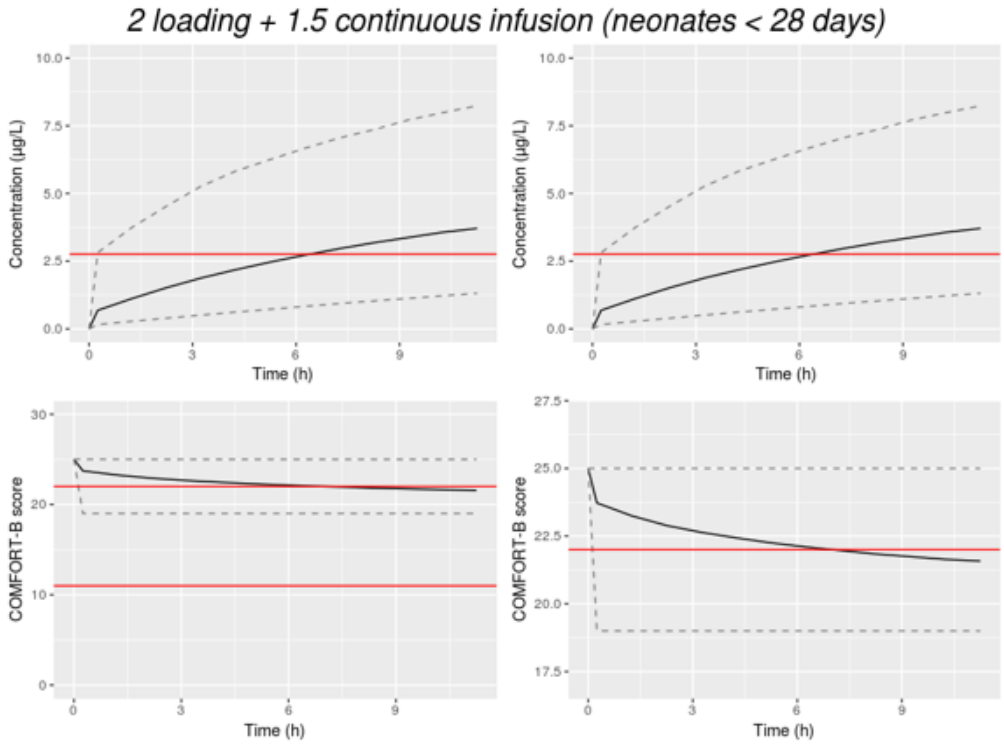

Figure 85: Plots produced using the simulated clonidine concentration in children younger than 28 days old for a loading dose of 2 mcg/kg following by an infusion of 1.5 mcg/kg/h.

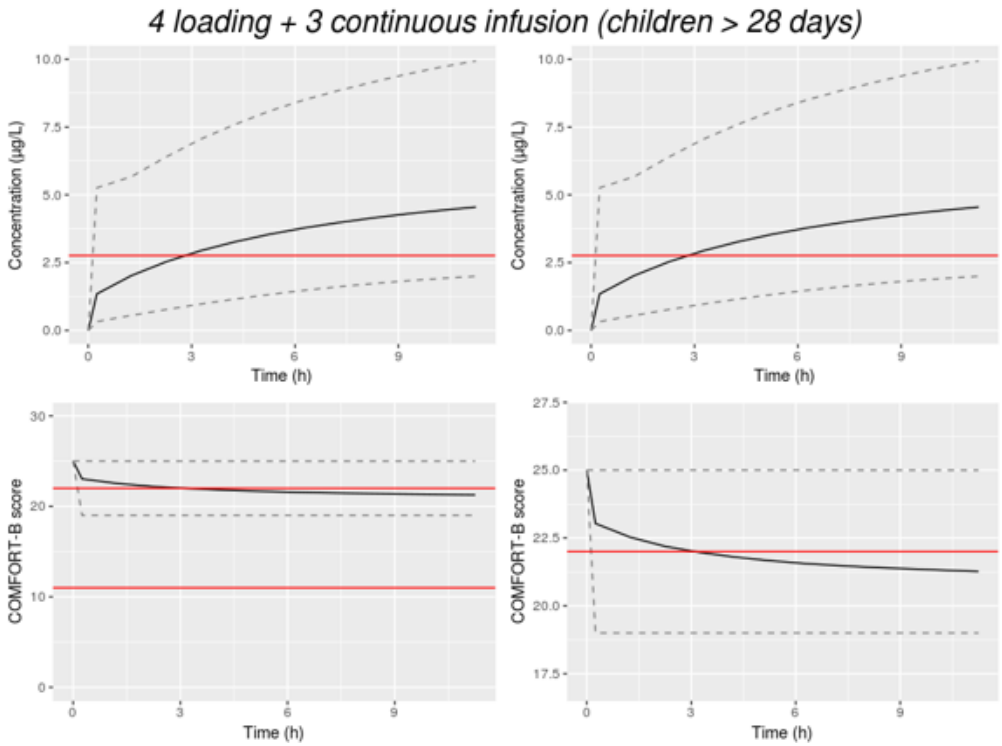

Figure 86: Plots produced using the simulated clonidine concentration in children older than 28 days old for a loading dose of 4 mcg/kg following by an infusion of 3 mcg/kg/h.

Figure 86 shows that the predicted median concentration for children older then 28 days reaches the EC50 3h after receiving a loading dose of 4 $\mu g/kg$ followed by a continuous infusion of 3 $\mu g/kg/h$. When this dose is divided by 2 for the neonates younger that 28 days (Figure 85), the same results are obtained after 6h.

A high variability in term of concentration and COMFORT-B score is predicted for both age groups and both drugs (Figure 83, 84, 85 and 86). All figures show that a decrease of 3 points in the COMFORT-B score is reached by 50% of the patients 3h after the dose administration (6h for neonates receiving clonidine).

The probability of achieving the midazolam EC50 is shown in Figure 87. The dose simulated was 200 $\mu g/kg$ followed by 200 $\mu g/kg/h$. This dose was halved in newborn younger than 28 days old as it was designed in the trial.

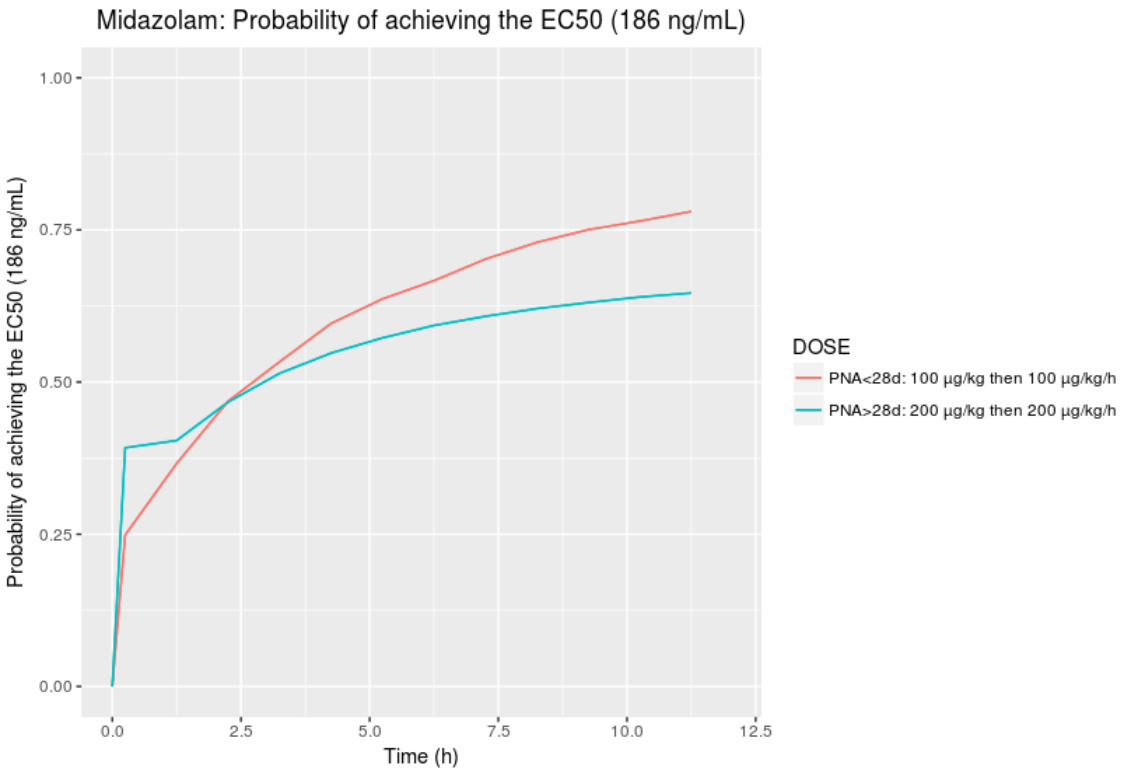

Figure 87: Simulated probability of achieving the midazolam EC50. Each line represents a different dose depending on PNA range.

Figure 87 shows that more than 75% of the newborns younger than a month reaches the EC50 12h post-administration of 100 $\mu g/kg$ followed by100 $\mu g/kg/h$ whereas only 65% of the older children reaches the same value 12h after receiving a dose of 200 $\mu g/kg$ followed by an infusion of 200 $\mu g/kg/h$. For both age groups, 50% of the patients reaches the EC50 2.5h after the drug administration.

Figure 88 presents the simulated probability of achieving clonidine EC50. The dose simulated was 4 $\mu g/kg$ followed by 3 $\mu g/kg/h$. This dose was halved in neonates with a PNA<28 days.

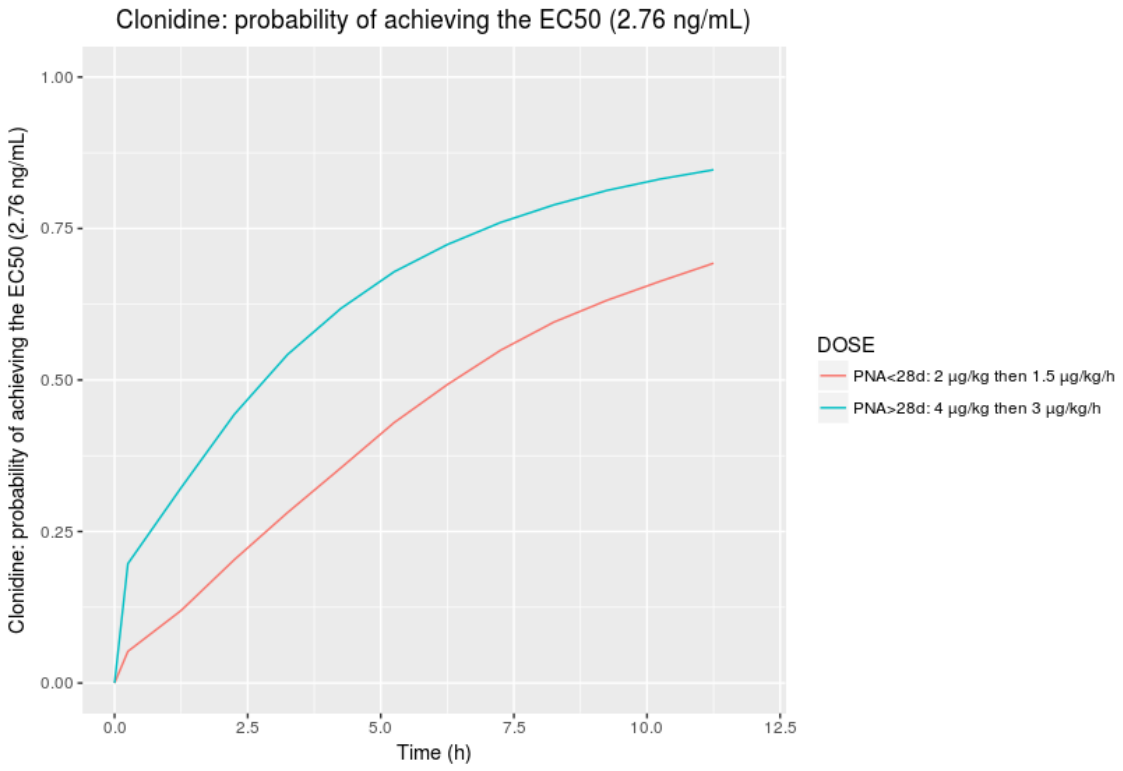

Figure 88: Simulated probability of achieving the clonidine EC50. Each line represents a different dose depending on PNA range.

Figure 88 shows that 80% of the infants older than 28 days receiving a clonidine dose of 4 $\mu g/kg$ followed by 3 $\mu g/kg/h$ reaches the EC50 after 12h and 70% of the neonates who receive half this dose reaches the target after 12h. 2.5h post-administration, only 25% of the newborns younger than 28 days reaches this target whereas this percentage corresponds to 50% for the older infants.

5.4 Discussion

The CloSed trial was stopped early by the data safety monitoring committee because the recruitment rate was too slow and there was no prospect of meeting the primary endpoint. However, double blind data were collected in 28 patients and PK as well as PK/PD models were developed accounting for clonidine, midazolam and morphine.

5.4.1 Pharmacokinetic models

Three PK models have been developed to describe the concentration of clonidine, midazolam and morphine and their metabolites (1-OH-midazolam, M3G and M6G). For each drug, the PK data were best described by a one-compartment model for the parent and each metabolite. The influence of weight and organ maturation on the drug clearances were included as covariates in all PK models.

Based on the different techniques of model evaluation, the final clonidine PK model seemed to adequately describe the data. The RSE presented in Table 23 were all below 40% and the medians produced by the bootstrap analysis were close to the parameter estimates. The goodness-of-fit plots presented in Figure 61 show that the model adequately predicted the observations. In addition, the clonidine PK model was successfully evaluated by the VPC presented in Figure 62.

The RSE and bootstrap presented in Table 24 successfully evaluated the precision of the parameter estimated by the final midazolam PK model. The goodness-of-fit plots presented in Figure 65 show that the model underpredicted the observed concentrations of midazolam and its metabolite. However, the inclusion of IIV seemed to improve the model since the individual predictions are close to the observed concentrations. Although a large majority of the values of CWRES are between -2 and 2, the lowess line is not completely flat around 0. The VPC (Figure 66 and 67) shows that more than 90% of the observed data are captured by the prediction interval 95%, indicating that the model fit well the data.

The RSE and bootstrap evaluating the morphine PK model presented in Table 25 shows that the model was able to estimate with precision most of the model parameters even though the estimates corresponding to the M6G error model have RSE superior or equal to 60%. The goodness-of-fit plots show that the model underpredicted the observed concentrations of morphine and metabolites. Although the inclusion of IIV improves the model, the plot of individual prediction *vs* concentration shows that the model still underpredicted some concentrations. The final model was evaluated successfully by the VPC even if some points seem to be outside the prediction interval.

The parameters estimated by the morphine PK model built in this chapter are compared to values estimated by previous models found in the literature in Table 30. These parameter estimates are close to those published in the morphine model developed by Bouwmeester *et al.* (191). When added together, the formation clearance of both metabolites is similar across the previous published studies (80 L/h/70kg). The morphine model developed in this chapter was not able to estimate the volume of distribution of M6G which was fixed to a value estimated by Bouwmeester *et al.* (191) in order to simplify and improve the stability of the model. Additional concentration data of M6G are necessary for the model to be able to adequately estimate the parameters of the M6G compartment.

Table 30: Comparison of morphine PK parameter estimates.

Parameter	Our model	Bouwmeester et al.	Anand et al.
V1 (L/70kg)	104.0	136.0	122
CL3M + CL6M (L/h/70kg)	88.2	67.9	84.2
V3 (L/kg)	38.4	23 FIX	-
CLom3 (L/h/kg)	16.3	17.4	-
V6 (L/kg)	30 FIX	30 FIX	-
CLom6 (L/h/kg)	5.5	5.8	-

V1 is the central volume of distribution and CL3M and CL6M the formation clearance of M3G and M6G, respectively. V3 and V6 correspond to the volume of the metabolic compartments. CLom3 and CLom6 are the clearance out of the metabolic compartment of M3G and M6G, respectively.

Creatinine is a marker of the glomerular filtration rate and therefore it can be used to evaluate the kidney function. Serum creatinine was a significant covariate of CL3M and CLom6 in the morphine model. These findings suggest that impaired kidney function affects the metabolite clearances, which was expected since the majority of morphine metabolites is eliminated in the urine.

Since the trial was terminated early, the number of patients and data available to develop the PK models was limited. Hence, the model was not able to estimate the parameters corresponding to the parent clearance for the midazolam and morphine models. For this reason, it was assumed that both midazolam and morphine were entirely metabolised in the liver in order to simplify the models.

5.4.2 Pharmacokinetic/pharmacodynamic models

Two PK/PD models (one for clonidine and one for midazolam) were developed in order to characterise the relationship between drug concentration and analgesic/sedative

effect assessed using COMFORT-B score. For each drug, the model that provided the best fit was an inhibitory sigmoid model including a postanesthesia effect for the patients who underwent major surgery before the treatment. The clonidine model was improved using a joint model fixing the midazolam parameters to the estimates obtained with the midazolam PK/PD model developed in this chapter. To our knowledge, this is the first blinded study establishing a relationship between clonidine concentration and sedative effect and therefore the first model suggesting a target concentration for clonidine.

The RSE for the midazolam model presented in Table 27 are all below 65% indicating that the model adequately estimated the parameters. The clonidine model was not able to estimate with precision TPS50 parameter as shown in Table 28 (RSE = 228%). However, this parameter was well estimated by the joint model presented in Table 29 (RSE = 68%), indicating that the joint model improved the fit of the clonidine data. Although the parameters estimated by the midazolam and the joint PK/PD models are all between the prediction interval produced by the bootstrap, the estimates of EC50 for both drugs is lower than the median generated by the bootstrap.

The goodness-of-fit plots of both models presented in Figure 77 and 79 show that the models underpredicted the observed scores below 14 and overpredicted the observed scores over 14. However, the correlation between observed and predicted concentrations is considerably improved for the individual predictions which suggests that the inclusion of IIV on the EC50 improved both models. Although the lowess line of the CWRES is not completely flat around the value 0, the vast majority of the CWRES values are between -2 and 2 and the points seem to be distributed homogeneously around 0.

The midazolam and joint models were both successfully evaluated by the PC-VPC (Figure 78 and 80).

The midazolam model published by Peeters *et al.* in 2006 (103) was used as reference to develop both clonidine and midazolam PK/PD models in this chapter. In their model, the authors also included a postanethesia effect in order to describe the relationship between drug concentration and COMFORT-B score in non ventilated children after

craniofacial surgery. As in the model developed here, they used an Emax model to describe the midazolam effect and the parameter corresponding to the maximal effect ($EMAX$) was also fixed to 6 (the lowest possible score). Unlike the model built by Peeter *et al.* (103), the model developed in this chapter was not able to estimate the baseline score during the surgery which was therefore fixed to the minimal COMFORT-B score.

The main limit of the PK/PD models is that some parameters had to be fixed to the previously published. The data could not be treated as categorical since the proportional odds and the BI models were not able to describe the data. The lack of stability of the models could be explained by the numerous adverse events (non related to clonidine or midazolam) experienced by most patients as well as the co-medications frequently needed in both arms. Therefore, the drugs investigated were not the only factors affecting the COMFORT-B score. Unfortunately, the instability of the models made it impossible to use a logit function in the Emax model in order to limit the prediction in the COMFORT-B scale range. The adverse events that occurred in both arms might explain the large IIV estimated on the $EC50$ of both drugs. Further studies should be done in order to determine the covariates that can explain a part of this variability. Adverse events affecting the scores occurred more frequently in the clonidine group, which can be the reason why the model was not able to estimate the clonidine $PAEMAX$ unlike midazolam.

In the clonidine arm, 8 patients did not have surgery whereas only 2 patients did not undergo major surgery in the midazolam group. Therefore more data defining the baseline score for patients without surgery were available in the clonidine group. For this reason, the clonidine model was able to estimate B0 with precision which was not the case for the midazolam model.

Propofol had a significant effect on the COMFORT-B score in the midazolam model but not in the clonidine model. This result was surprising considering that more patients in the clondine group received propofol. This might be the consequence of the instability of the clonidine model making it unable to estimate with precision the parameter KDE.

This can be explained by the fact that more adverse events not drug related occurred in the clonidine group inducing an important noise in the model.

Furthermore, a significant effect of morphine and its metabolites would have been expected on the sedation score. However, it was not the case. Several reasons can explain this result: the dose of morphine might be too low to have a significant effect, the morphine effect might be less important for patients who used morphine for a long period of time, finally the COMFORT-B score might not be the ideal score to assess the analgesic effect of morphine.

The PK/PD model with a maximal effect ($EMAX$) fixed to 6 provided the best fit for both drugs. Hence, they both induced a light sedation with a modest decrease of the COMFORT-B score. For this reason, midazolam and clonidine might need to be given in combination with other sedatives when a higher sedation level is required.

The safety models developed in this chapter were not able to establish a relationship between clonidine concentrations and adverse effects using heart rate and blood pressure as PD safety endpoints. This result could be explained by the dose regimen used in the CloSed trial that might be too low to induce severe adverse effects. One limitation of the model tested is that it did not take into account the influence of age on both heart rate and blood pressure. Alternative models such as an indirect response model could be explored to describe the effect of clonidine and fentanyl on both safety endpoints.

5.4.3 Simulations

The simulation results suggest that a dose of 4 $\mu g/kg$ followed by a continuous infusion of 3 $\mu g/kg/h$ for clonidine and a dose of 200 $\mu g/kg$ followed by 200 $\mu g/kg/h$ for midazolam should be used in children in order to have at least 70% of the patients achieving the EC50 12h post-administration (Figure 87 and 88). These dose should be halved in newborn younger than one month old. Even at these doses, only 50% of the patient would reach the EC50 in less than 3h. This percentage is decrease to 25% for the neonates younger than 28 days receiving clonidine.

6 Discussion

Although pain and sedation management in children has improved over the years, the optimal doses of most analgesics and sedatives routinely prescribed have not yet been determined in the paediatric population. These drugs (such as the ones studied in this thesis) are therefore prescribed in an "off label" fashion in the intensive care. The work done in this thesis used PK and PK/PD modelling to inform on the appropriate use of fentanyl, clonidine and midazolam in specific paediatric populations.

6.1 Clonidine models

The clonidine PK in children has been well described by models published in the literature by Potts *et al.* (156) and Larsson *et al.* (148). The clearance estimated by the clonidine model developed in the SANNI chapter (14.3 L/h/70kg) is close to the one estimated by the models developed by Larsson *et al.* (148) and the one published by Potts *et al.* (156) corresponding to 14.6 L/h/70kg and 17.9 L/h/70kg, respectively. Although the clonidine clearance estimated in the CloSed chapter (28 L/h/70kg) is higher, the 95% confidence interval produced by the bootstrap used to evaluate the clearance estimate [19.2-37.1] overlaps the one evaluating the clearance estimated by Larsson *et al.* (148) [16.0-20.3], therefore the clonidine clearance estimated in the CloSed chapter is also in line with the literature.

Although the PK of clonidine is well known, the target concentration and dose regimens that should be administered in children have not yet been defined. A variety of doses are routinely used in research as well as in clinical practice (155). The PK/PD models developed for clonidine in Chapter 4 and 5 are the first one describing the relationship between clonidine concentration and sedative effect using pain scales. These models inform on the target concentration which differs for each scale. For the COMFORT score, both PK/PD models developed in Chapter 4 and 5 estimated a similar EC50 (2.78 for the SANNI chapter and 2.73 for the CloSed chapter) using a continuous Emax model.

The simulations performed using the final PK/PD models presented in both chapters show that a loading dose of clonidine higher than the ones routinely prescribed should be administered in order to provide an adequate sedation during the first hours post-administration. This finding confirms the necessity of increasing the clonidine dose in children that was suggested in the PK simulation study published by Hayden *et al.* (155). Since the doses suggested for clonidine are considerably higher than the ones routinely administered in the PICU, additional safety studies are needed. The work in this thesis highlight the inconvenient of clonidine due to its long elimination half life. The clonidine models developed suggest that the drug might need to be given in combination with other sedatives in order to provide an adequate pain and sedation management in children.

6.2 Fentanyl models

Few models published in the literature have described fentanyl PK in children (Table 2). In their previously published study, Norman *et al.* (124) analysed the PK data from 14 of the 25 patients included in the model built for the NEOFENT chapter to conduct a non-compartmental analysis. The values of clearance and volume at steady state estimated by the compartmental model (Cl_{ss}=0.20 $L/h/kg$, V_{ss}=2.74 L/h) are close to those found with the non-compartmental analysis (Cl_{ss}=0.23 $L/h/kg$, V_{ss}=3 L/h), suggesting that the model adequately described the data for this specific population. In their model, Norman *et al.* excluded infants with two or less concentration samples which explains why only 14 of the 25 newborns were included in their study. A compartmental approach was preferred for the analysis in the NEOFENT chapter because it allows the inclusion of patients with limited blood samples (two or less) and the identification of covariates explaining the IIV.

The CLss estimated by the model published by Völler *et al.* (123) in preterm infants was 0.42 L/h. This value is twice as high as the one estimated by the model developed in the NEOFENT chapter (0.20 L/h). This difference might be explained by the demographic characteristics of the two populations. The clearance was thus

calculated using the Völler model with the NEOFENT demographic data, resulting in a clearance of 0.38 L/h which is close to the value estimated by Voller *et al.* The value estimated in preterm infants is reduced compared to the clearances estimated in full term newborns (1.7-4 L/h). This difference of factor 10 suggests that the immaturity of the elimination pathways plays a major role in the drug elimination.

The clearance at steady state estimated by the final fentanyl model in the SANNI chapter corresponds to 2.05 L/h. This value is in line with the values of clearance estimated by previous published models in term neonates presented in Table 2.

The PK modelling undertaken in chapter 3 and 4 improves our knowledge on the adequate use of fentanyl by identifying covariates that affect the fentanyl PK (e.g. genetic variants, hypothermic treatment). The results from the NEOFENT chapter highlight the importance of genetic variants to explain a part of the variability on the PK parameters. Even though the genetic variants explained a part of the IIV estimated on the clearance (15%) for the NEOFENT cohort, this variability remains high in preterm infants (82%). Therefore, further research should be done in order to identify the other covariates that could explain this variability. The effect of genetic variants on fentanyl PK will also be explored in the SANNI cohort after the recruitment of all patients.

The PK/PD models developed in Chapter 3 and 4 are the first ones describing the relationship between fentanyl concentration and analgesic effect. These models were used to optimise the dose of fentanyl by defining target concentrations and dose regimens in specific peadiatric populations. The target concentration defined in the NEOFENT chapter (0.3 ng/mL) is lower than the one defined in the SANNI chapter (2.6 for the ALPS-neo score). This difference might be explained by the demographic differences between the two populations (preterm infants *vs* term asphyxiated newborns) and the scales used to assess the analgesic effect (EDIN scale for NEOFENT *vs* ALPS-neo for SANNI). Studies have shown that preterm infants have a lower expression level of opioid transporters such as P-gp. As a result, a larger concentration of fentanyl is able to cross the BBB (202). In addition, preterm babies have an increased expression rate

of opioid receptors during the three first weeks of life, therefore the fentanyl potency is higher compared to older children or adults (203). These physiological differences might explain why the target concentration is lower in preterm infants since they have higher potency and fentanyl concentration in their developing brain.

The simulations performed in both chapters show that a higher dose of fentanyl than the ones prescribed in the trials are necessary in order to have at least 80% of the patients reaching the target concentration. Because fentanyl can cause numerous severe adverse effects, increasing the dose in children should be closely monitored.

6.3 Midazolam model

Midazolam PK and PK/PD have been described by few previous published models in the literature. The estimation of the midazolam clearance (0.14 L/h/kg) is similar to the one estimated in the maturation model for midazolam clearance developed by Anderson *et al.* (134) (0.13 L/h/kg). Since Anderson *et al.* (134) used published clearance estimates to construct their maturation model, only the parameter corresponding to the clearance was estimated in the paper.

In the literature, it has been shown that critical illness has a significant impact on midazolam PK (185, 61). Therefore, it would be relevant to test the influence of critical illness marker such as CRP level in the PK model as covariate. However the CRP level data were limited in the CloSed study making it challenging to test it as covariate in the PK model.

A comparison of the PK/PD parameters estimated by the midazolam PK/PD model built in the CloSed chapter and the one developed by Peeters *et al.* (103) is presented in Table 31. The $EC50$ and $PAEMAX$ estimates are close in both analyses. The IIV on the $EC50$ is considerably higher in the IMP model, which might be explained by the smaller number of patients included in the model (13 compared to 24). TPS50 is higher in the model developed by Peeters *et al.* (103), which reflects the difference of design between both studies; the time post-surgery before midazolam administration was longer in their study.

Table 31: Comparison of midazolam PK/PD parameter estimates.

	Our model	Peeters et al.
EC50 (ng/mL)	186.0	188.9
PAEMAX	9.3	9.8
TPS50 (h)	0.11	8.9
BASE	6 FIX	10.2
EMAX	6 FIX	6 FIX
IIV EC50 (%)	246.6	89

BASE is the score at the end of the surgery, PAEMAX is the maximal postanesthesia effect from BASE and TPS50 is the time post-surgery at half maximum postanesthesia effect in hours. EMAX is the maximal effect, EC50 is the concentration to reach 50% of the maximal effect and IIV is the interindividual variability.

The simulations performed in the CloSed chapter suggest doses higher than the ones administered in the CloSed trial. However, these doses are still within the range of those used in clinical practice. When increasing the dose, the adverse effects of the drug should be considered particularly in neonates and young infants for which studies have reported a higher incidence of midazolam adverse effects. When considering the EC90 as target concentration, the simulations suggest that the dose should be considerably increased (> factor 5) which may not be feasible in the PICU because of the risk of adverse events.

6.4 Effect of hypothermic treatment on the drug studied

To our knowledge, the models developed in the SANNI chapter are the first ones to study the effect of hypothermia on both PK and PD parameters in asphyxiated newborns after administration of clonidine and fentanyl. Both models show that the hypothermic

treatment has a significant impact on clonidine and fentanyl clearances. These results were expected since previous studies have shown that the PK of other opioids (e.g morphine) and alpha-2-adrenergic receptor agonists such as dexmedetomidine are also affected by hypothermia (168, 171).

6.5 Pain and sedation scales

The lack of specificity and sensitivity of the available assessment tools make it challenging to objectively evaluate the drug sedative and analgesic effect. There is no consensus on which tool should be used to best assess the drug efficacy. In this thesis, different scales have been used as PD endpoints (EDIN, COMFORT-B, COMFORT-neo and ALPS-neo) making it challenging to compare the target concentration obtained for the same drug across studies and scales. For instance, in the SANNI chapter different target concentrations were defined for fentanyl and clonidine depending on which scale was used to build the model: APLS-neo or COMFORT-neo scales. Although some items included in both scales are similar (e.g. body activity, facial expression/tension), both scales are different as described in section 1.3.2. In addition, the ALPS-neo scale has been developed in order to assess pain and stress whereas COMFORT-neo assesses pain and sedation. Since the scales have not be designed to assess the same effect, it is expected for the target concentration of the drugs to be different.

In addition, scales such as ALPS-neo and EDIN are not able to assess oversedation unlike the COMFORT scales since the lowest score possible (0) corresponds to "no pain at all". Hence, using such scales as PD endpoint could lead to a misinterpretation of pain and sedation levels and therefore incorrect dose optimisation.

6.6 Maturation model on drug clearance

The PK models developed in this thesis present some limits; due to the limited number of patients, the models were not able to estimate the parameters of the maturation function. For fentanyl, these parameters were fixed using a maturation

model for midazolam clearance. Both fentanyl and midazolam are mainly metabolised by CYP3A4 which explains why the midazolam maturation function provided a good estimation of the fentanyl clearance maturation. However, a part of the fentanyl metabolism involves other enzymes of which the maturation is not taken into account in the midazolam maturation function.

For clonidine and midazolam, published maturation models developed to describe the clearance of these drugs in young infants and children have been used. However, although the effect of ontogeny for clonidine and midazolam has been well described in the literature, additional data are needed for the model to be able to estimate these parameters in the specific population studied in this thesis. The PK model developed in the SANNI chapter will be updated once all the 50 patients will be included in the study and the maturation parameters will be re-estimated.

6.7 Probability of target achievement

To determine the optimal dose, the probability of target achievement is commonly used in PK/PD modelling because it allows a comparison between the doses of the number of patients reaching the target. For instance, most antibiotic models published in the literature include a probability of target achievement using the MIC. Such graphs are not presented in papers describing PK/PD models developed for analgesics and sedatives. Due to the high interindividual variability observed when using pain scores as PD endpoints, a large prediction interval of simulated concentrations is generated by the simulations. For this reason, the probability of target achievement has to be interpreted carefully because it does not take into account the risk of adverse effects that can occurred when the concentration increase. It is also challenging to simulate the risk of oversedation since it would depend on the level of pain assessed before the drug administration which is highly variable between patients. In addition, most of the scales such as ALPS-neo are not able to assess the oversedation.

6.8 Limitation of the modelling performed in this thesis

The modelling work performed in this thesis presents several limitations. First, the modeller was not involved in the data collection nor the study design planning which might have helped for the understanding of the data used in the models and therefore the modelling work. Secondly, due to recruitment issues the data available to perform the modelling work were limited making it challenging to use advanced modelling techniques or estimate with precision all parameters. This aspect can lead to model misspecification and impact the simulations results. Finally, the drug toxicity was not modelled successfully, making it challenging to recommend a dose increase in clinical practice as suggested by the simulations. In the CloSed and SANNI trial, toxicity measures were available which was not the case for the NEOFENT trial. However, the safety profiles were not explored in the SANNI chapter and the safety PK/PD modelling done in the CloSed chapter was not able to describe the data which might be due to the fact that the model tested was not appropriate and/or that age was not taken into account in the model.

6.9 Strengths and limitations of the trials

As mention in section 1.1.4, running a clinical trial in children can be challenging. Except for the SANNI trial, the two other trials presented in this thesis (NEOFENT and CloSed) had to be stopped early. This is mainly due to patient recruitment issues resulting in a limited sample size and therefore limited data.

Moreover, it is challenging to run a comparison trial in children. In the CloSed study, most patients needed rescue medications such as propofol and ketamine and numerous adverse events non related to the drugs were observed. For ethical reasons, providing rescue medications in children is essential, however it can highly affect the scores used to assess pain and sedation. In addition, the frequency and severity of adverse events as well as rescue medications needed being different in both arms, it is challenging to compare the efficacy of both drugs.

Although the three trials presented in this thesis had planned to study the influence of genetic variants on the drug PK, developing PK/PG models with a limited number of patients can be challenging because in most cases the model does not have enough data to establish a relationship between drug PK and genetic variants. This can explain why no SNPs had a significant effect on clonidine and fentanyl clearances in the CloSed chapter. Therefore further analyses including more patients should be done in order to find a significant effect of SNPs on the PK parameters in the CloSed chapter and to confirm the genetic results found in the NEOFENT chapter.

The design of the CloSed trial presented an important strength compared to the other trials of this thesis. Since it was double blinded and randomised, the risk of bias in the results was minimized. In addition, the fact that the trial was double blind allowed the clinicians to objectively compare the doses and frequency of rescue medications such as propofol needed in both arms.

Finally one of the main strength of the three trials was that the pain and sedation scores were assessed regularly providing rich PD data by patient to build the PK/PD models.

6.10 Safety considerations

The simulations performed in all chapters suggest that the doses of clonidine, fentanyl and midazolam should be increased in the specific population studied in order to provide adequate pain and sedation management. However when contemplating increasing the dose of analgesics and sedatives, it is necessary to consider dose-related adverse effects.

Increasing the clonidine dose would increase the risk of adverse effects including severe bradycardia and hyotension. A low incidence of side effects has been observed in the majority of the published studies conducted in children. However, these studies did not use a loading dose over 3 $\mu g/kg$ nor an infusion dose over 3 $\mu g/kg/h$. In addition, since the doses suggested in the SANNI and CloSed chapter are considerably higher than the one used in the actual clinical practice, the clinicians might be reluctant to prescribe it.

With regard to fentanyl, based on the simulation results of the NEOFENT chapter and the fact that fentanyl is known to cause numerous adverse reactions in preterm infants even at low doses, the dose of 2 $\mu g/kg$ instead of 3 $\mu g/kg$ seemed more appropriate. Even though the dose of 2 $\mu g/kg$ is within the range of fentanyl dose routinely prescribed in the NICU for preterm infants (0.5 $\mu g/kg$ - 2 $\mu g/kg$), further research is needed in order to establish the relationship between drug adverse effect and concentration.

6.11 Further work

Further modelling work is needed on a larger sample size of patients in order to improve the robustness of the models and therefore obtain models that would be able to estimate both PK and PK/PD parameters with high precision. Since patient recruitment is challenging for clinical peadiatric studies, data from separate trials (e.g CloSed combined with SANNI) could be combined in order to increase the sample size. Building robust PK and PK/PD models for fentanyl and clonidine would be necessary in order to use the TCI technique in the PICU for these drugs and therefore facilitate the dosing in clinical practice.

This thesis highlights that using observational scales as PD endpoints to assess pain and sedation might not be ideal since most scales are not able to measure oversedation and the target concentration defined using PK/PD modelling differs depending on the scales. Therefore further analysis could be done using more objective PD endpoints such as EEG. Developing PK/PD models to characterise the relationship between fentanyl/clonidine concentration and pain/sedation effect using EEG is part of the future work expected in the SANNI study.

In addition, all models developed in this thesis estimated a large IIV on the parameters. A part of this variability is explained by the hypothermic treatment and genetic variants for SANNI and NEOFENT chapter, respectively. Even though the large IIV estimated could be explained by the limited number of patients included in the analyses, further research should be done with additional covariates (such as marker of critical illness) that could be tested to explain a part of this variability.

The results of the NEOFENT chapter show that three genetic variants coding for ABCC1 and ABCC3 have a significant influence on fentanyl clearance. However, the role of both transporters in the fentanyl mechanism of action is unknown. Therefore further studies should be done (*in vitro* or *in vivo*) to investigate their roles in fentanyl elimination in order to better understand the impact of such genetic variants on the clearance.

The optimal doses of fentanyl and clonidine suggested in this thesis are considerably higher than the ones routinely prescribed in clinical practice. However, there is limited information regarding the safety of both drugs in the literature and the safety models developed in this thesis were not able to describe the relationship between drug concentrations and safety endpoints. Therefore, further investigations are needed to improve our knowledge on the safety of clonidine and fentanyl. One of the first step to achieve this goal could be to use the data provided by the CloSed and SANNI studies to try an indirect response model instead of an Emax model and include the influence of age as covariate in order to describe the relationship between clonidine concentration and heart rate as well as blood pressure. In addition, safety studies including higher doses than the ones routinely prescribed for clonidine ad fentanyl need to be conducted in order to characterise the drug adverse effects. The design of these studies could include a gradual increase of the doses as well as a close monitoring of the safety endpoints and adverse events. These studies should include enough patients to be able to develop robust safety PK/PD models that could be used to establish a clear relationship between doses and side effects.

6.12 Summary

In summary, the modelling done in this thesis has been used to improve the pain and sedation management in children. Different PK/PD models have been developed to optimise the dose regimens of analgesics and sedatives needed to provide an adequate effect in specific paediatric populations.

APPENDIX A

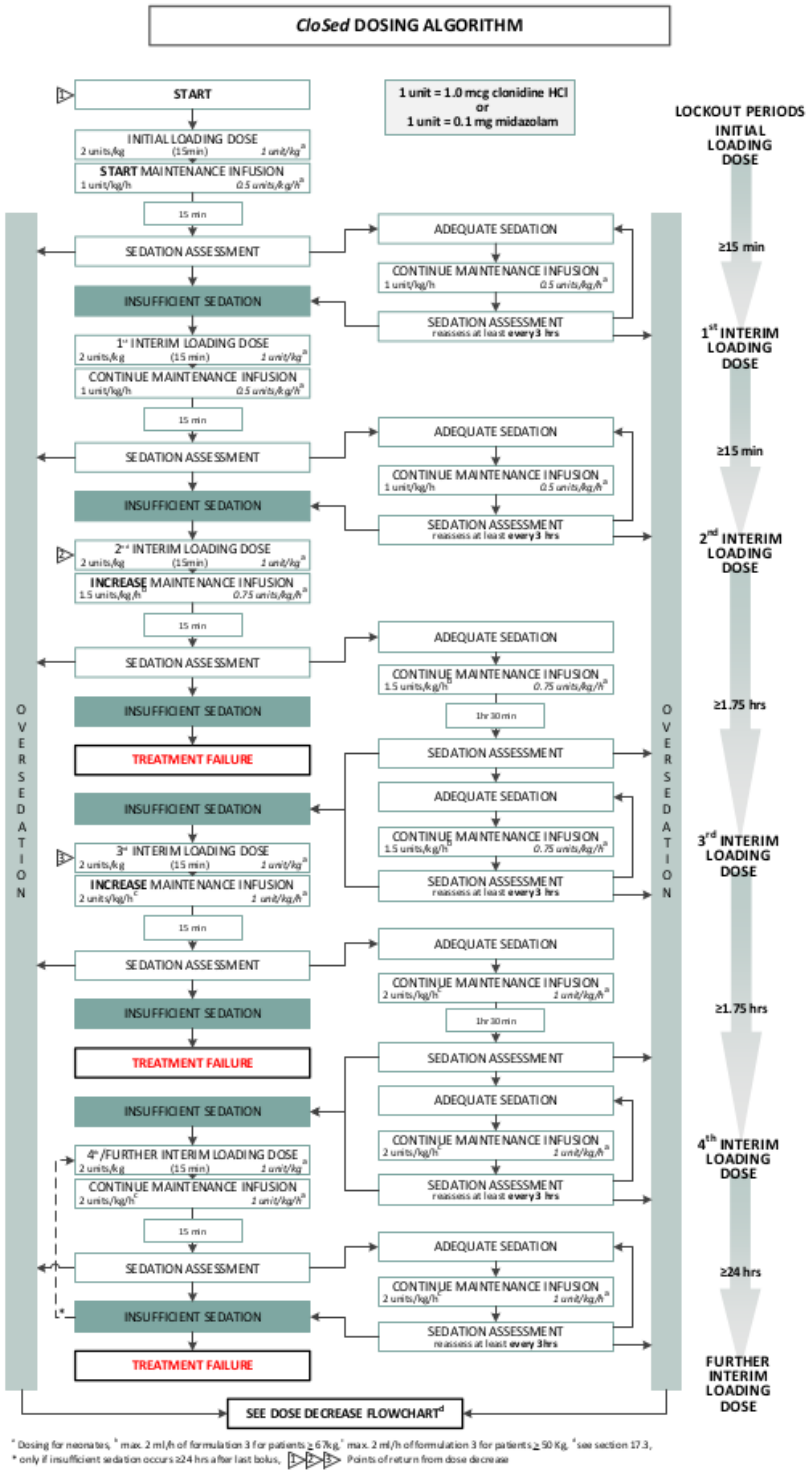

Figure 89: Appendix A: CloSed dosing algorithm

APPENDIX B

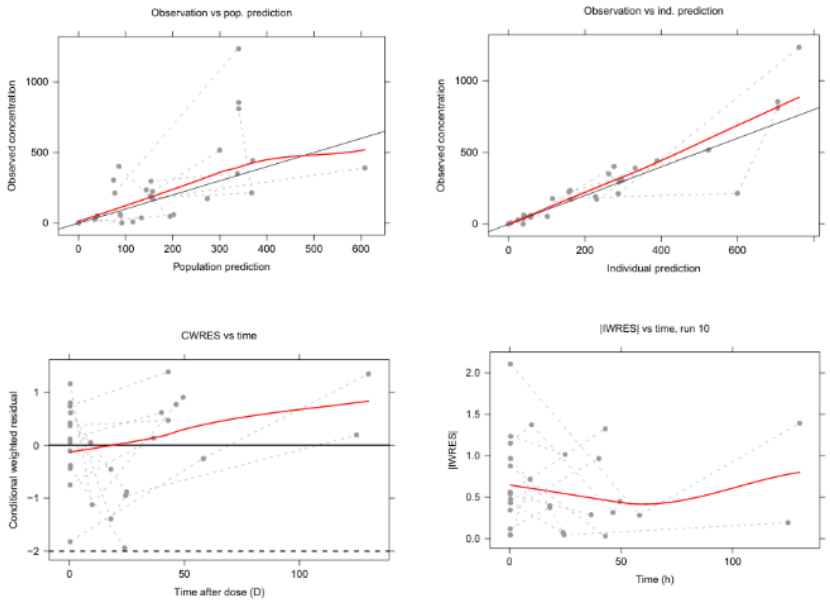

Figure 90: Appendix B: Goodness-of-fit plots of midazolam (parent) used to evaluate the midazolam PK model for CloSed trial

APPENDIX C

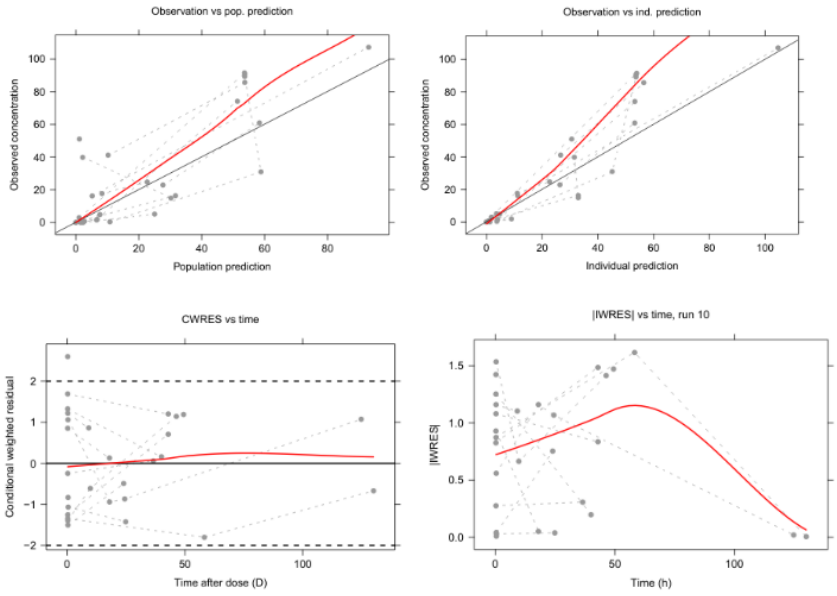

Figure 91: Appendix C: Goodness-of-fit plots of midazolam metabolite used to evaluate the midazolam PK model for CloSed trial

APPENDIX D

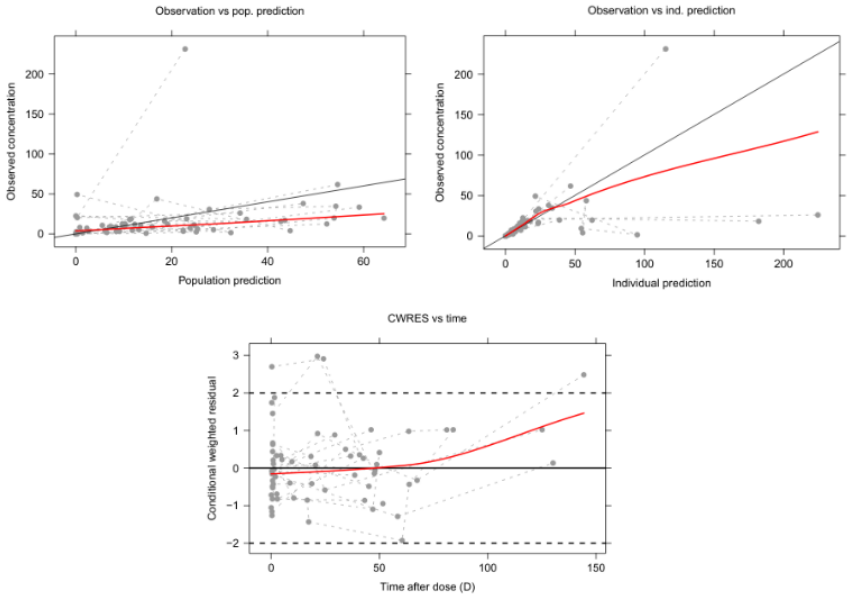

Figure 92: Appendix D: Goodness-of-fit plots of morphine (parent) used to evaluate the morphine PK model for CloSed trial

APPENDIX E

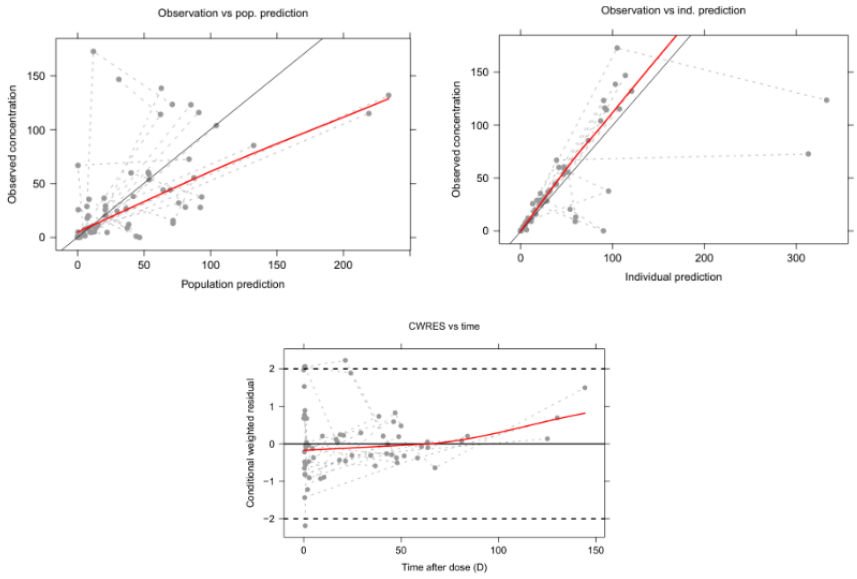

Figure 93: Appendix E: Goodness-of-fit plots of M3G used to evaluate the morphine PK model for CloSed trial

APPENDIX F

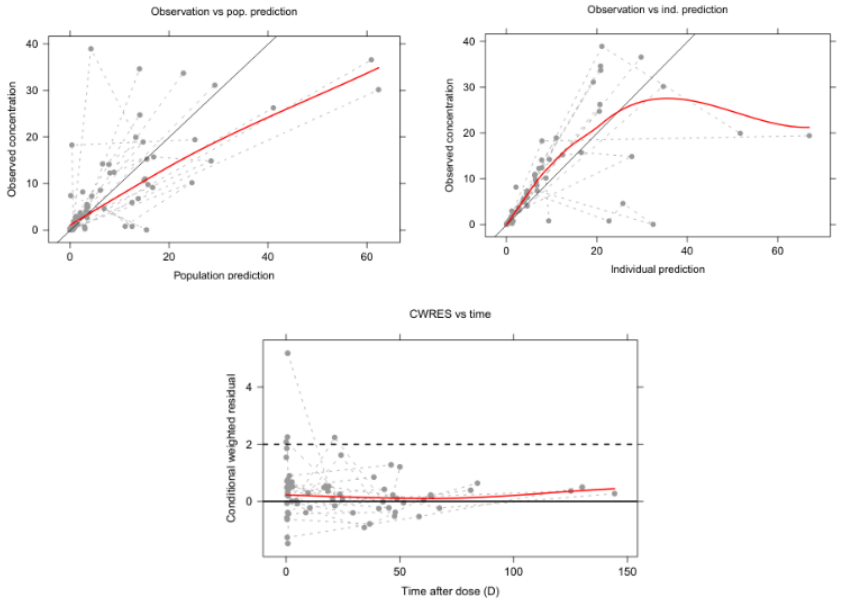

Figure 94: Appendix F: Goodness-of-fit plots of M6G used to evaluate the morphine PK model for CloSed trial

Bibliography

1. *Classification of chronic pain: Descriptions of chronic pain syndromes and definitions of pain, part iii: Pain terms, a current list with definitions and notes on usage.* (IASP Press, 1994).

2. *The recognition and assessment of acute pain in children: Update of full guideline.* (Royal College of Nursing, 2009).

3. Walker, S. M. Neonatal pain. *Paediatr Anaesth* **24**, 39–48 (2014).

4. Walker, T. & Kudchadkar, S. R. Pain and Sedation Management: 2018 Update for the Rogers' Textbook of Pediatric Intensive Care. *Pediatr Crit Care Med* **20**, 54–61 (2019).

5. Walker, S. M. Long-term effects of neonatal pain. *Semin Fetal Neonatal Med* **24**, 101005 (2019).

6. Duerden, E. G. *et al.* Early Procedural Pain Is Associated with Regionally-Specific Alterations in Thalamic Development in Preterm Neonates. *J. Neurosci.* **38**, 878–886 (2018).

7. McGrath, P., Stevens, B., Walker, S. & Zempsky, W. *Oxford textbook of paediatric pain:* (Oxford Univ. Press, 2014).

8. Moultrie, F., Slater, R. & Hartley, C. Improving the treatment of infant pain. *Curr Opin Support Palliat Care* **11**, 112–117 (2017).

9. Taddio, A., Katz, J., Ilersich, A. L. & Koren, G. Effect of neonatal circumcision on pain response during subsequent routine vaccination. *Lancet* **349**, 599–603 (1997).

10. Grunau, R. V., Whitfield, M. F., Petrie, J. H. & Fryer, E. L. Early pain experience, child and family factors, as precursors of somatization: a prospective study of extremely premature and fullterm children. *Pain* **56**, 353–359 (1994).

11. Barnes, S., Yaster, M. & Kudchadkar, S. R. Pediatric Sedation Management. *Pediatr Rev* **37**, 203–212 (2016).

12. Meredith, J. R., O'Keefe, K. P. & Galwankar, S. Pediatric procedural sedation

and analgesia. *J Emerg Trauma Shock* **1**, 88–96 (2008).

13. Cravero, J. P. & Havidich, J. E. Pediatric sedation–evolution and revolution. *Paediatr Anaesth* **21**, 800–809 (2011).

14. Sheta, S. A. Procedural sedation analgesia. *Saudi J Anaesth* **4**, 11–16 (2010).

15. Vet, N. J. *et al.* Optimal sedation in pediatric intensive care patients: a systematic review. *Intensive Care Med* **39**, 1524–1534 (2013).

16. Walker, S. M. Translational studies identify long-term impact of prior neonatal pain experience. *Pain* **158 Suppl 1**, S29–S42 (2017).

17. Yuki, K. *et al.* Pediatric Perioperative Stress Responses and Anesthesia. *Transl Perioper Pain Med* **2**, 1–12 (2017).

18. Ancora, G. *et al.* Evidence-based clinical guidelines on analgesia and sedation in newborn infants undergoing assisted ventilation and endotracheal intubation. *Acta Paediatr.* **108**, 208–217 (2019).

19. Harris, J. *et al.* Clinical recommendations for pain, sedation, withdrawal and delirium assessment in critically ill infants and children: an ESPNIC position statement for healthcare professionals. *Intensive Care Med* **42**, 972–986 (2016).

20. Schiller, R. M. *et al.* Analgesics and Sedatives in Critically Ill Newborns and Infants: The Impact on Long-Term Neurodevelopment. *J Clin Pharmacol* **58 Suppl 10**, S140–S150 (2018).

21. Donato, J., Rao, K. & Lewis, T. Pharmacology of Common Analgesic and Sedative Drugs Used in the Neonatal Intensive Care Unit. *Clin Perinatol* **46**, 673–692 (2019).

22. Ceci, A. *et al.* Medicines for children licensed by the European Medicines Agency (EMEA): the balance after 10 years. *Eur. J. Clin. Pharmacol.* **62**, 947–952 (2006).

23. Barker, C. I. S. *et al.* Pharmacokinetic studies in children: recommendations for practice and research. *Arch. Dis. Child.* **103**, 695–702 (2018).

24. Costa, H. T. M. L., Costa, T. X., Martins, R. R. & Oliveira, A. G. Use of off-label and unlicensed medicines in neonatal intensive care. *PLoS ONE* **13**, e0204427

(2018).

25. De Cock, R. F. *et al.* The role of population PK-PD modelling in paediatric clinical research. *Eur. J. Clin. Pharmacol.* **67 Suppl 1**, 5–16 (2011).

26. Mason, K. P. & Seth, N. Future of paediatric sedation: towards a unified goal of improving practice. *Br J Anaesth* **122**, 652–661 (2019).

27. Hakim, M. *et al.* Acetaminophen pharmacokinetics in severely obese adolescents and young adults. *Pediatric Anesthesia* **29**, 20–26 (2018).

28. Playne, R., Anderson, B. J., Frampton, C., Stanescu, I. & Atkinson, H. C. Analgesic effectiveness, pharmacokinetics, and safety of a paracetamol/ibuprofen fixed-dose combination in children undergoing adenotonsillectomy: A randomized, single-blind, parallel group trial. *Paediatr Anaesth* **28**, 1087–1095 (2018).

29. Hannam, J. A., Anderson, B. J. & Potts, A. Acetaminophen, ibuprofen, and tramadol analgesic interactions after adenotonsillectomy. *Paediatr Anaesth* **28**, 841–851 (2018).

30. Ismail, A. *et al.* Pain management interventions in the Paediatric Intensive Care Unit: A scoping review. *Intensive Crit Care Nurs* **54**, 96–105 (2019).

31. Marzuillo, P., Calligaris, L., Amoroso, S. & Barbi, E. Narrative review shows that the short-term use of ketorolac is safe and effective in the management of moderate-to-severe pain in children. *Acta Paediatr.* **107**, 560–567 (2018).

32. Rodieux, F. *et al.* When the Safe Alternative Is Not That Safe: Tramadol Prescribing in Children. *Front Pharmacol* **9**, 148 (2018).

33. Anderson, B. J., Thomas, J., Ottaway, K. & Chalkiadis, G. A. Tramadol: keep calm and carry on. *Paediatr Anaesth* **27**, 785–788 (2017).

34. Baarslag, M. A., Allegaert, K., Knibbe, C. A., Dijk, M. van & Tibboel, D. Pharmacological sedation management in the paediatric intensive care unit. *J. Pharm. Pharmacol.* **69**, 498–513 (2017).

35. Ng, E., Taddio, A. & Ohlsson, A. Intravenous midazolam infusion for sedation of infants in the neonatal intensive care unit. *Cochrane Database Syst Rev* **1**, CD002052

(2017).

36. Giovannitti, J. A., Thoms, S. M. & Crawford, J. J. Alpha-2 adrenergic receptor agonists: a review of current clinical applications. *Anesth Prog* **62**, 31–39 (2015).

37. Schug, S., Palmer, G., Scott, D., Halliwell, R. & Trinca, J. *Acute pain management: Scientific evidence*. (ANZCA & FPM, 2015).

38. Choi, B. M. *et al.* Population pharmacokinetic and pharmacodynamic model of propofol externally validated in children. *J Pharmacokinet Pharmacodyn* **42**, 163–177 (2015).

39. Rigouzzo, A. *et al.* The relationship between bispectral index and propofol during target-controlled infusion anesthesia: a comparative study between children and young adults. *Anesth. Analg.* **106**, 1109–1116 (2008).

40. Khosravi, S., Hahn, J. O., Dumont, G. A. & Ansermino, J. M. A monitor-decoupled pharmacodynamic model of propofol in children using state entropy as clinical endpoint. *IEEE Trans Biomed Eng* **59**, 736–743 (2012).

41. Hahn, J. O., Dumont, G. A. & Ansermino, J. M. A direct dynamic dose-response model of propofol for individualized anesthesia care. *IEEE Trans Biomed Eng* **59**, 571–578 (2012).

42. Lamond, D. W. Review article: Safety profile of propofol for paediatric procedural sedation in the emergency department. *Emerg Med Australas* **22**, 265–286 (2010).

43. Davidson, A. & Flick, R. P. Neurodevelopmental implications of the use of sedation and analgesia in neonates. *Clin Perinatol* **40**, 559–573 (2013).

44. Ing Lorenzini, K., Daali, Y., Dayer, P. & Desmeules, J. Pharmacokinetic-pharmacodynamic modelling of opioids in healthy human volunteers. a minireview. *Basic Clin. Pharmacol. Toxicol.* **110**, 219–226 (2012).

45. Martini, C., Olofsen, E., Yassen, A., Aarts, L. & Dahan, A. Pharmacokinetic-pharmacodynamic modeling in acute and chronic pain: an overview of the recent literature. *Expert Rev Clin Pharmacol* **4**, 719–728 (2011).

46. Yang, H., Feng, Y. & Xu, X. S. Pharmacokinetic and pharmacodynamic modeling for acute and chronic pain drug assessment. *Expert Opin Drug Metab Toxicol*

10, 229–248 (2014).

47. Morse, J. D., Hannam, J. & Anderson, B. J. Pharmacokinetic-pharmacodynamic population modelling in paediatric anaesthesia and its clinical translation. *Curr Opin Anaesthesiol* **32**, 353–362 (2019).

48. Kern, S. E. Challenges in conducting clinical trials in children: approaches for improving performance. *Expert Rev Clin Pharmacol* **2**, 609–617 (2009).

49. Haslund-Krog, S. S. *et al.* Challenges in conducting paediatric trials with off-patent drugs. *Contemp Clin Trials Commun* **23**, 100783 (2021).

50. Guarracino, F. *et al.* Target controlled infusion: TCI. *Minerva Anestesiol* **71**, 335–337 (2005).

51. Anderson, B. J. & Hodkinson, B. Are there still limitations for the use of target-controlled infusion in children? *Curr Opin Anaesthesiol* **23**, 356–362 (2010).

52. Johnson, T. N. Modelling approaches to dose estimation in children. *Br J Clin Pharmacol* **59**, 663–669 (2005).

53. Germovsek, E., Barker, C. I. S., Sharland, M. & Standing, J. F. Correction to: Pharmacokinetic-Pharmacodynamic Modeling in Pediatric Drug Development, and the Importance of Standardized Scaling of Clearance. *Clin Pharmacokinet* **58**, 139 (2019).

54. Strolin Benedetti, M., Whomsley, R. & Baltes, E. L. Differences in absorption, distribution, metabolism and excretion of xenobiotics between the paediatric and adult populations. *Expert Opin Drug Metab Toxicol* **1**, 447–471 (2005).

55. Vetterly, C. & Howrie, D. A Pharmacokinetic and Pharmacodynamic Review. In: Munoz R, Morell V, Cruz E, Vetterly C, editors. *Critical Care of Children with Heart Disease* **9**, 83–7 (2010).

56. Lu, H. & Rosenbaum, S. Developmental pharmacokinetics in pediatric populations. *J Pediatr Pharmacol Ther* **19**, 262–276 (2014).

57. Alcorn, J. & McNamara, P. J. Pharmacokinetics in the newborn. *Adv. Drug Deliv. Rev.* **55**, 667–686 (2003).

58. Allegaert, K., Mian, P. & Anker, J. N. van den Developmental Pharmacokinetics in Neonates: Maturational Changes and Beyond. *Curr Pharm Des* **23**, 5769–5778

(2017).

59. Anker, J. van den, Reed, M. D., Allegaert, K. & Kearns, G. L. Developmental Changes in Pharmacokinetics and Pharmacodynamics. *J Clin Pharmacol* **58 Suppl 10**, S10–S25 (2018).

60. Rhodin, M. M. *et al.* Human renal function maturation: a quantitative description using weight and postmenstrual age. *Pediatr. Nephrol.* **24**, 67–76 (2009).

61. Brussee, J. M. *et al.* Children in clinical trials: towards evidence-based pediatric pharmacotherapy using pharmacokinetic-pharmacodynamic modeling. *Expert Rev Clin Pharmacol* **9**, 1235–1244 (2016).

62. Stephenson, T. How children's responses to drugs differ from adults. *Br J Clin Pharmacol* **59**, 670–673 (2005).

63. Mulla, H. Understanding developmental pharmacodynamics: importance for drug development and clinical practice. *Paediatr Drugs* **12**, 223–233 (2010).

64. Conklin, L. S., Hoffman, E. P. & Anker, J. van den Developmental Pharmacodynamics and Modeling in Pediatric Drug Development. *J Clin Pharmacol* **59 Suppl 1**, S87–S94 (2019).

65. Disma, N. & Hansen, T. G. Pediatric anesthesia and neurotoxicity: can findings be translated from animals to humans? *Minerva Anestesiol* **82**, 791–796 (2016).

66. Paediatric Anaesthetists of Great Britain, A. of & Ireland *Good practice in postoperative and procedural pain management, 2nd edition.* (Paediatr Anaesth, 2012).

67. Moor, R. Pain assessment in a children's A&E: a critical analysis. *Paediatr Nurs* **13**, 20–24 (2001).

68. Stinson, J. N., Kavanagh, T., Yamada, J., Gill, N. & Stevens, B. Systematic review of the psychometric properties, interpretability and feasibility of self-report pain intensity measures for use in clinical trials in children and adolescents. *Pain* **125**, 143–157 (2006).

69. Baeyer, C. L. von Children's self-report of pain intensity: what we know, where we are headed. *Pain Res Manag* **14**, 39–45 (2009).

70. Wong, C., Lau, E., Palozzi, L. & Campbell, F. Pain management in children: Part

1 - Pain assessment tools and a brief review of nonpharmacological and pharmacological treatment options. *Can Pharm J (Ott)* **145**, 222–225 (2012).

71. Dijk, M. van, Ceelie, I. & Tibboel, D. Endpoints in pediatric pain studies. *Eur. J. Clin. Pharmacol.* **67 Suppl 1**, 61–66 (2011).

72. Hicks, C. L., Baeyer, C. L. von, Spafford, P. A., Korlaar, I. van & Goodenough, B. The Faces Pain Scale-Revised: toward a common metric in pediatric pain measurement. *Pain* **93**, 173–183 (2001).

73. Tsze, D. S., Baeyer, C. L. von, Bulloch, B. & Dayan, P. S. Validation of self-report pain scales in children. *Pediatrics* **132**, e971–979 (2013).

74. Ambuel, B., Hamlett, K. W., Marx, C. M. & Blumer, J. L. Assessing distress in pediatric intensive care environments: the COMFORT scale. *J Pediatr Psychol* **17**, 95–109 (1992).

75. Carnevale, F. A. & Razack, S. An item analysis of the COMFORT scale in a pediatric intensive care unit. *Pediatr Crit Care Med* **3**, 177–180 (2002).

76. Johansson, M. & Kokinsky, E. The COMFORT behavioural scale and the modified FLACC scale in paediatric intensive care. *Nurs Crit Care* **14**, 122–130 (2009).

77. Dijk, M. van *et al.* The association between physiological and behavioral pain measures in 0- to 3-year-old infants after major surgery. *J Pain Symptom Manage* **22**, 600–609 (2001).

78. Ista, E., Dijk, M. van, Tibboel, D. & Hoog, M. de Assessment of sedation levels in pediatric intensive care patients can be improved by using the COMFORT 'behavior' scale. *Pediatr Crit Care Med* **6**, 58–63 (2005).

79. Boerlage, A. A. *et al.* The COMFORT behaviour scale detects clinically meaningful effects of analgesic and sedative treatment. *Eur J Pain* **19**, 473–479 (2015).

80. Dijk, M. van *et al.* Taking up the challenge of measuring prolonged pain in (premature) neonates: the COMFORTneo scale seems promising. *Clin J Pain* **25**, 607–616 (2009).

81. Bai, J., Hsu, L., Tang, Y. & Dijk, M. van Validation of the COMFORT Behavior scale and the FLACC scale for pain assessment in Chinese children after cardiac surgery.

Pain Manag Nurs **13**, 18–26 (2012).

82. Lundqvist, P. *et al.* Development and psychometric properties of the Swedish ALPS-Neo pain and stress assessment scale for newborn infants. *Acta Paediatr.* **103**, 833–839 (2014).

83. Holsti, L. & Grunau, R. E. Initial validation of the Behavioral Indicators of Infant Pain (BIIP). *Pain* **132**, 264–272 (2007).

84. Debillon, T., Zupan, V., Ravault, N., Magny, J. F. & Dehan, M. Development and initial validation of the EDIN scale, a new tool for assessing prolonged pain in preterm infants. *Arch. Dis. Child. Fetal Neonatal Ed.* **85**, 36–41 (2001).

85. Cowen, R., Stasiowska, M. K., Laycock, H. & Bantel, C. Assessing pain objectively: the use of physiological markers. *Anaesthesia* **70**, 828–847 (2015).

86. McPherson, C., Ortinau, C. M. & Vesoulis, Z. Practical approaches to sedation and analgesia in the newborn. *J Perinatol* (2020).

87. Raeside, L. Physiological measures of assessing infant pain: a literature review. *Br J Nurs* **20**, 1370–1376 (2011).

88. Morton, D. L., Sandhu, J. S. & Jones, A. K. Brain imaging of pain: state of the art. *J Pain Res* **9**, 613–624 (2016).

89. Sciusco, A. *et al.* Effect of age on the performance of bispectral and entropy indices during sevoflurane pediatric anesthesia: A pharmacometric study. *Paediatr Anaesth* 399–408

90. Paisansathan, C., Ozcan, M. D., Khan, Q. S., Baughman, V. L. & Ozcan, M. S. Signal persistence of bispectral index and state entropy during surgical procedure under sedation. *ScientificWorldJournal* **2012**, 272815 (2012).

91. Ranger, M., Johnston, C. C., Limperopoulos, C., Rennick, J. E. & Plessis, A. J. du Cerebral near-infrared spectroscopy as a measure of nociceptive evoked activity in critically ill infants. *Pain Res Manag* **16**, 331–336 (2011).

92. Ette, E. I., Williams, P. J. & Lane, J. R. Population pharmacokinetics III: design, analysis, and application of population pharmacokinetic Studies. *Ann Pharmacother*

38, 2136–2144 (2004).

93. Ette, E. I. & Williams, P. J. Population pharmacokinetics II: estimation methods. *Ann Pharmacother* **38**, 1907–1915 (2004).

94. Standing, J. F. Understanding and applying pharmacometric modelling and simulation in clinical practice and research. *Br J Clin Pharmacol* **83**, 247–254 (2017).

95. Holford, N., Heo, Y. A. & Anderson, B. A pharmacokinetic standard for babies and adults. *J Pharm Sci* **102**, 2941–2952 (2013).

96. Lanao, J. M. *et al.* Pharmacokinetic basis for the use of extended interval dosage regimens of gentamicin in neonates. *J. Antimicrob. Chemother.* **54**, 193–198 (2004).

97. Kimura, T. *et al.* Population pharmacokinetics of arbekacin, vancomycin, and panipenem in neonates. *Antimicrob. Agents Chemother.* **48**, 1159–1167 (2004).

98. Anderson, B. J., Allegaert, K., Van den Anker, J. N., Cossey, V. & Holford, N. H. Vancomycin pharmacokinetics in preterm neonates and the prediction of adult clearance. *Br J Clin Pharmacol* **63**, 75–84 (2007).

99. Germovsek, E., Barker, C. I., Sharland, M. & Standing, J. F. Scaling clearance in paediatric pharmacokinetics: All models are wrong, which are useful? *Br J Clin Pharmacol* **83**, 777–790 (2017).

100. Zhang, L., Beal, S. L. & Sheiner, L. B. Simultaneous vs. sequential analysis for population PK/PD data I: best-case performance. *J Pharmacokinet Pharmacodyn* **30**, 387–404 (2003).

101. Anderson, B. J., Holford, N. H., Woollard, G. A., Kanagasundaram, S. & Mahadevan, M. Perioperative pharmacodynamics of acetaminophen analgesia in children. *Anesthesiology* **90**, 411–421 (1999).

102. Ene, I. & William, J. *Pharmacometrics: The science of quantitative pharmacology.* (John Wiley & Sons Inc, 2015).

103. Peeters, M. Y. *et al.* Pharmacokinetics and pharmacodynamics of midazolam and metabolites in nonventilated infants after craniofacial surgery. *Anesthesiology* **105**, 1135–1146 (2006).

104. Krause, A. & Lowe, P. J. Visualization and communication of pharmacometric

models with berkeley madonna. *CPT Pharmacometrics Syst Pharmacol* **3**, e116 (2014).

105. Louizos, C., Yanez, J. A., Forrest, M. L. & Davies, N. M. Understanding the hysteresis loop conundrum in pharmacokinetic/pharmacodynamic relationships. *J Pharm Pharm Sci* **17**, 34–91 (2014).

106. Kjellsson, M. C., Zingmark, P. H., Jonsson, E. N. & Karlsson, M. O. Comparison of proportional and differential odds models for mixed-effects analysis of categorical data. *J Pharmacokinet Pharmacodyn* **35**, 483–501 (2008).

107. Sheiner, L. B. A new approach to the analysis of analgesic drug trials, illustrated with bromfenac data. *Clin Pharmacol Ther* **56**, 309–322 (1994).

108. Colin, P. J. *et al.* Dexmedetomidine pharmacokinetic-pharmacodynamic modelling in healthy volunteers: 1. Influence of arousal on bispectral index and sedation. *Br J Anaesth* **119**, 200–210 (2017).

109. Schindler, E. & Karlsson, M. O. A Minimal Continuous-Time Markov Pharmacometric Model. *AAPS J* **19**, 1424–1435 (2017).

110. Wellhagen, G. J., Kjellsson, M. C. & Karlsson, M. O. A Bounded Integer Model for Rating and Composite Scale Data. *AAPS J* **21**, 74 (2019).

111. Bergstrand, M., Hooker, A. C., Wallin, J. E. & Karlsson, M. O. Prediction-corrected visual predictive checks for diagnosing nonlinear mixed-effects models. *AAPS J* **13**, 143–151 (2011).

112. Thigpen, J. C., Odle, B. L. & Harirforoosh, S. Opioids: A Review of Pharmacokinetics and Pharmacodynamics in Neonates, Infants, and Children. *Eur J Drug Metab Pharmacokinet* (2019).

113. Anand, K. J. & Hall, R. W. Pharmacological therapy for analgesia and sedation in the newborn. *Arch. Dis. Child. Fetal Neonatal Ed.* **91**, F448–453 (2006).

114. Stanley, T. H. The fentanyl story. *J Pain* **15**, 1215–1226 (2014).

115. Ziesenitz, V. C., Vaughns, J. D., Koch, G., Mikus, G. & Anker, J. N. van den Pharmacokinetics of Fentanyl and Its Derivatives in Children: A Comprehensive Review. *Clin Pharmacokinet* **57**, 125–149 (2018).

116. Lee, B., Park, J. D., Choi, Y. H., Han, Y. J. & Suh, D. I. Efficacy and Safety

of Fentanyl in Combination with Midazolam in Children on Mechanical Ventilation. *J. Korean Med. Sci.* **34**, e21 (2019).

117. Pacifici, G. M. Clinical pharmacology of fentanyl in preterm infants. A review. *Pediatr Neonatol* **56**, 143–148 (2015).

118. Lammers, E. M. *et al.* Association of fentanyl with neurodevelopmental outcomes in very-low-birth-weight infants. *Ann Pharmacother* **48**, 335–342 (2014).

119. McPherson, C. *et al.* Brain Injury and Development in Preterm Infants Exposed to Fentanyl. *Ann Pharmacother* **49**, 1291–1297 (2015).

120. Drewes, A. M. *et al.* Differences between opioids: pharmacological, experimental, clinical and economical perspectives. *Br J Clin Pharmacol* **75**, 60–78 (2013).

121. Saarenmaa, E., Neuvonen, P. J. & Fellman, V. Gestational age and birth weight effects on plasma clearance of fentanyl in newborn infants. *J. Pediatr.* **136**, 767–770 (2000).

122. Thigpen, J. C., Odle, B. L. & Harirforoosh, S. Opioids: A Review of Pharmacokinetics and Pharmacodynamics in Neonates, Infants, and Children. *Eur J Drug Metab Pharmacokinet* **44**, 591–609 (2019).

123. Völler, S. *et al.* Rapidly maturing fentanyl clearance in preterm neonates. *Arch Dis Child Fetal Neonatal Ed* **104**, F598–F603 (2019).

124. Norman, E. *et al.* Individual variations in fentanyl pharmacokinetics and pharmacodynamics in preterm infants. *Acta Paediatr.* (2019).

125. Gauntlett, I. S. *et al.* Pharmacokinetics of fentanyl in neonatal humans and lambs: effects of age. *Anesthesiology* **69**, 683–687 (1988).

126. Ziesenitz, V. C., Vaughns, J. D., Koch, G., Mikus, G. & Anker, J. N. van den Correction to: Pharmacokinetics of Fentanyl and Its Derivatives in Children: A Comprehensive Review. *Clin Pharmacokinet* **57**, 393–417 (2018).

127. Hagos, F. T. *et al.* Factors Contributing to Fentanyl Pharmacokinetic Variability Among Diagnostically Diverse Critically Ill Children. *Clin Pharmacokinet* **58**, 1567–1576 (2019).

128. Choi, B. M. *et al.* Population pharmacokinetic and pharmacodynamic model of

propofol externally validated in children. *J Pharmacokinet Pharmacodyn* **42**, 163–177 (2015).

129. Encinas, E. *et al.* A predictive pharmacokinetic/pharmacodynamic model of fentanyl for analgesia/sedation in neonates based on a semi-physiologic approach. *Paediatr Drugs* **15**, 247–257 (2013).

130. McPherson, C., Miller, S. P., El-Dib, M., Massaro, A. N. & Inder, T. E. The influence of pain, agitation, and their management on the immature brain. *Pediatr Res* **88**, 168–175 (2020).

131. Norman, E. *et al.* Rapid sequence induction is superior to morphine for intubation of preterm infants: a randomized controlled trial. *J. Pediatr.* **159**, 893–899 (2011).

132. Norman, E., Wikstrom, S., Rosen, I., Fellman, V. & Hellstrom-Westas, L. Premedication for intubation with morphine causes prolonged depression of electrocortical background activity in preterm infants. *Pediatr. Res.* **73**, 87–94 (2013).

133. Matic, M., Wildt, S. N. de, Tibboel, D. & Schaik, R. H. N. van Analgesia and Opioids: A Pharmacogenetics Shortlist for Implementation in Clinical Practice. *Clin Chem* **63**, 1204–1213 (2017).

134. Anderson, B. J. & Larsson, P. A maturation model for midazolam clearance. *Paediatr Anaesth* **21**, 302–308 (2011).

135. Bergstrand, M. & Karlsson, M. O. Handling data below the limit of quantification in mixed effect models. *AAPS J* **11**, 371–380 (2009).

136. Sumpter, A. L. & Holford, N. H. Predicting weight using postmenstrual age–neonates to adults. *Paediatr Anaesth* **21**, 309–315 (2011).

137. Su, W. & Pasternak, G. W. The role of multidrug resistance-associated protein in the blood-brain barrier and opioid analgesia. *Synapse* **67**, 609–619 (2013).

138. Chaves, C., Remiao, F., Cisternino, S. & Decleves, X. Opioids and the Blood-Brain Barrier: A Dynamic Interaction with Consequences on Drug Disposition in Brain. *Curr Neuropharmacol* **15**, 1156–1173 (2017).

139. Chidambaran, V. *et al.* ABCC3 genetic variants are associated with postop-

erative morphine-induced respiratory depression and morphine pharmacokinetics in children. *Pharmacogenomics J* **17**, 162–169 (2017).

140. Venkatasubramanian, R. *et al.* ABCC3 and OCT1 genotypes influence pharmacokinetics of morphine in children. *Pharmacogenomics* **15**, 1297–1309 (2014).

141. Ek, C. J. *et al.* Efflux mechanisms at the developing brain barriers: ABC-transporters in the fetal and postnatal rat. *Toxicol Lett* **197**, 51–59 (2010).

142. Brouwer, K. L. *et al.* Human Ontogeny of Drug Transporters: Review and Recommendations of the Pediatric Transporter Working Group. *Clin Pharmacol Ther* **98**, 266–287 (2015).

143. Neil, M. J. Clonidine: clinical pharmacology and therapeutic use in pain management. *Curr Clin Pharmacol* **6**, 280–287 (2011).

144. Johr, M. Clonidine in paediatric anaesthesia. *Eur J Anaesthesiol* **28**, 325–326 (2011).

145. Romantsik, O., Calevo, M. G., Norman, E. & Bruschettini, M. Clonidine for pain in non-ventilated infants. *Cochrane Database Syst Rev* **4**, CD013104 (2020).

146. Capino, A. C., Miller, J. L. & Johnson, P. N. Clonidine for Sedation and Analgesia and Withdrawal in Critically Ill Infants and Children. *Pharmacotherapy* **36**, 1290–1299 (2016).

147. Khan, Z. P., Ferguson, C. N. & Jones, R. M. alpha-2 and imidazoline receptor agonists. Their pharmacology and therapeutic role. *Anaesthesia* **54**, 146–165 (1999).

148. Larsson, P. *et al.* Oral bioavailability of clonidine in children. *Paediatr Anaesth* **21**, 335–340 (2011).

149. Burch, M. *et al.* Influence of cardiopulmonary bypass on water balance hormones in children. *Br Heart J* **68**, 309–312 (1992).

150. Dorman, T. *et al.* Effects of clonidine on prolonged postoperative sympathetic response. *Crit. Care Med.* **25**, 1147–1152 (1997).

151. Kulka, P. J., Tryba, M. & Zenz, M. Preoperative alpha2-adrenergic receptor agonists prevent the deterioration of renal function after cardiac surgery: results of a

randomized, controlled trial. *Crit. Care Med.* **24**, 947–952 (1996).

152. Laudenbach, V. *et al.* Effects of alpha(2)-adrenoceptor agonists on perinatal excitotoxic brain injury: comparison of clonidine and dexmedetomidine. *Anesthesiology* **96**, 134–141 (2002).

153. Hayden, J. C. *et al.* Efficacy of Î±2-Agonists for Sedation in Pediatric Critical Care: A Systematic Review. *Pediatr Crit Care Med* **17**, 66–75 (2016).

154. Eberl, S., Ahne, G., Toni, I., Standing, J. & Neubert, A. Safety of clonidine used for long-term sedation in paediatric intensive care: A systematic review. *Br J Clin Pharmacol* (2020).

155. Hayden, J. C. *et al.* Optimizing clonidine dosage for sedation in mechanically ventilated children: A pharmacokinetic simulation study. *Paediatr Anaesth* **29**, 1002–1010 (2019).

156. Potts, A. L. *et al.* Clonidine disposition in children; a population analysis. *Paediatr Anaesth* **17**, 924–933 (2007).

157. Hall, J. E., Uhrich, T. D. & Ebert, T. J. Sedative, analgesic and cognitive effects of clonidine infusions in humans. *Br J Anaesth* **86**, 5–11 (2001).

158. Kleiber, N., Rosmalen, J. van, Tibboel, D. & Wildt, S. N. de Hemodynamic Tolerance to IV Clonidine Infusion in the PICU. *Pediatr Crit Care Med* **19**, e409–e416 (2018).

159. Jacobs, S. E. *et al.* Cooling for newborns with hypoxic ischaemic encephalopathy. *Cochrane Database Syst Rev* CD003311 (2013).

160. Sarnat, H. B. & Sarnat, M. S. Neonatal encephalopathy following fetal distress. A clinical and electroencephalographic study. *Arch. Neurol.* **33**, 696–705 (1976).

161. Smits, A., Annaert, P., Van Cruchten, S. & Allegaert, K. A Physiology-Based Pharmacokinetic Framework to Support Drug Development and Dose Precision During Therapeutic Hypothermia in Neonates. *Front Pharmacol* **11**, 587 (2020).

162. Broek, M. P. van den, Groenendaal, F., Egberts, A. C. & Rademaker, C. M. Effects of hypothermia on pharmacokinetics and pharmacodynamics: a systematic

review of preclinical and clinical studies. *Clin Pharmacokinet* **49**, 277–294 (2010).

163. Zanelli, S., Buck, M. & Fairchild, K. Physiologic and pharmacologic considerations for hypothermia therapy in neonates. *J Perinatol* **31**, 377–386 (2011).

164. Fritz, H. G. *et al.* Anesth AnalgThe effect of mild hypothermia on plasma fentanyl concentration and biotransformation in juvenile pigs. *Anesth Analg* **100**, 996–1002 (2005).

165. Haan, T. R. de *et al.* Pharmacokinetics and pharmacodynamics of medication in asphyxiated newborns during controlled hypothermia. The PharmaCool multicenter study. *BMC Pediatr* **12**, 45 (2012).

166. Favié, L. M. A. *et al.* Pharmacokinetics of morphine in encephalopathic neonates treated with therapeutic hypothermia. *PLoS One* **14**, e0211910 (2019).

167. Favié, L. M. A. *et al.* Phenobarbital, Midazolam Pharmacokinetics, Effectiveness, and Drug-Drug Interaction in Asphyxiated Neonates Undergoing Therapeutic Hypothermia. *Neonatology* **116**, 154–162 (2019).

168. Frymoyer, A. *et al.* Decreased Morphine Clearance in Neonates With Hypoxic Ischemic Encephalopathy Receiving Hypothermia. *J Clin Pharmacol* **57**, 64–76 (2017).

169. Shellhaas, R. A., Ng, C. M., Dillon, C. H., Barks, J. D. & Bhatt-Mehta, V. Population pharmacokinetics of phenobarbital in infants with neonatal encephalopathy treated with therapeutic hypothermia. *Pediatr Crit Care Med* **14**, 194–202 (2013).

170. Welzing, L. *et al.* Disposition of midazolam in asphyxiated neonates receiving therapeutic hypothermia–a pilot study. *Klin Padiatr* **225**, 398–404 (2013).

171. McAdams, R. M., Pak, D., Lalovic, B., Phillips, B. & Shen, D. D. Dexmedetomidine Pharmacokinetics in Neonates with Hypoxic-Ischemic Encephalopathy Receiving Hypothermia. *Anesthesiol Res Pract* **2020**, 2582965 (2020).

172. Ameringer, S., Serlin, R. C. & Ward, S. Simpson's paradox and experimental research. *Nurs Res* **58**, 123–127 (2009).

173. Plan, E. L., Elshoff, J. P., Stockis, A., Sargentini-Maier, M. L. & Karlsson, M. O. Likert pain score modeling: a Markov integer model and an autoregressive continuous

model. *Clin Pharmacol Ther* **91**, 820–828 (2012).

174. Kleiber, N. *et al.* Population pharmacokinetics of intravenous clonidine for sedation during paediatric extracorporeal membrane oxygenation and continuous venovenous hemofiltration. *Br J Clin Pharmacol* **83**, 1227–1239 (2017).

175. Blumer, J. L. Clinical pharmacology of midazolam in infants and children. *Clin Pharmacokinet* **35**, 37–47 (1998).

176. Pacifici, G. M. Clinical pharmacology of midazolam in neonates and children: effect of disease-a review. *Int J Pediatr* **2014**, 309342 (2014).

177. Conway, A., Rolley, J. & Sutherland, J. R. Midazolam for sedation before procedures. *Cochrane Database Syst Rev* CD009491 (2016).

178. Ng, E., Taddio, A. & Ohlsson, A. Intravenous midazolam infusion for sedation of infants in the neonatal intensive care unit. *Cochrane Database Syst Rev* **1**, CD002052 (2017).

179. Barends, C. R., Absalom, A., Minnen, B. van, Vissink, A. & Visser, A. Dexmedetomidine versus Midazolam in Procedural Sedation. A Systematic Review of Efficacy and Safety. *PLoS One* **12**, e0169525 (2017).

180. Olkkola, K. T. & Ahonen, J. Midazolam and other benzodiazepines. *Handb Exp Pharmacol* 335–360 (2008).

181. Carter, B. S. & Brunkhorst, J. Neonatal pain management. *Semin Perinatol* **41**, 111–116 (2017).

182. Altamimi, M. I., Sammons, H. & Choonara, I. Inter-individual variation in midazolam clearance in children. *Arch Dis Child* **100**, 95–100 (2015).

183. Kos, M. K. *et al.* Maturation of midazolam clearance in critically ill children with severe bronchiolitis: A population pharmacokinetic analysis. *Eur J Pharm Sci* **141**, 105095 (2020).

184. Brussee, J. M. *et al.* Predicting CYP3A-mediated midazolam metabolism in critically ill neonates, infants, children and adults with inflammation and organ failure. *Br J Clin Pharmacol* **84**, 358–368 (2018).

185. Ince, I. *et al.* Critical illness is a major determinant of midazolam clearance in

children aged 1 month to 17 years. *Ther Drug Monit* **34**, 381–389 (2012).

186. Johnson, T. N., Rostami-Hodjegan, A., Goddard, J. M., Tanner, M. S. & Tucker, G. T. Contribution of midazolam and its 1-hydroxy metabolite to preoperative sedation in children: a pharmacokinetic-pharmacodynamic analysis. *Br J Anaesth* **89**, 428–437 (2002).

187. Valkenburg, A. J. *et al.* Sedation With Midazolam After Cardiac Surgery in Children With and Without Down Syndrome: A Pharmacokinetic-Pharmacodynamic Study. *Pediatr Crit Care Med* (2020).

188. Lugo, R. A. & Kern, S. E. Clinical pharmacokinetics of morphine. *J Pain Palliat Care Pharmacother* **16**, 5–18 (2002).

189. Altamimi, M. I., Choonara, I. & Sammons, H. Inter-individual variation in morphine clearance in children. *Eur J Clin Pharmacol* **71**, 649–655 (2015).

190. Anand, K. J. *et al.* Morphine pharmacokinetics and pharmacodynamics in preterm and term neonates: secondary results from the NEOPAIN trial. *Br J Anaesth* **101**, 680–689 (2008).

191. Bouwmeester, N. J., Anderson, B. J., Tibboel, D. & Holford, N. H. Developmental pharmacokinetics of morphine and its metabolites in neonates, infants and young children. *Br J Anaesth* **92**, 208–217 (2004).

192. Knøsgaard, K. R. *et al.* Pharmacokinetic models of morphine and its metabolites in neonates:: Systematic comparisons of models from the literature, and development of a new meta-model. *Eur J Pharm Sci* **92**, 117–130 (2016).

193. Valkenburg, A. J. *et al.* Exploring the Relationship Between Morphine Concentration and Oversedation in Children After Cardiac Surgery. *J Clin Pharmacol* **60**, 1231–1236 (2020).

194. Wolf, A. *et al.* Prospective multicentre randomised, double-blind, equivalence study comparing clonidine and midazolam as intravenous sedative agents in critically ill children: the SLEEPS (Safety profiLe, Efficacy and Equivalence in Paediatric intensive care Sedation) study. *Health Technol Assess* **18**, 1–212 (2014).

195. Duffett, M. *et al.* Clonidine in the sedation of mechanically ventilated children:

a pilot randomized trial. *J Crit Care* **29**, 758–763 (2014).

196. Ambrose, C. *et al.* Intravenous clonidine infusion in critically ill children: dose-dependent sedative effects and cardiovascular stability. *Br J Anaesth* **84**, 794–796 (2000).

197. Arenas-López, S. *et al.* Use of oral clonidine for sedation in ventilated paediatric intensive care patients. *Intensive Care Med* **30**, 1625–1629 (2004).

198. Hünseler, C. *et al.* Continuous infusion of clonidine in ventilated newborns and infants: a randomized controlled trial. *Pediatr Crit Care Med* **15**, 511–522 (2014).

199. Bouwmeester, N. J., Anderson, B. J., Tibboel, D. & Holford, N. H. Br J AnaesthDevelopmental pharmacokinetics of morphine and its metabolites in neonates, infants and young children. *Br J Anaesth* **92**, 208–217 (2004).

200. Knibbe, C. A. *et al.* Morphine glucuronidation in preterm neonates, infants and children younger than 3 years. *Clin Pharmacokinet* **48**, 371–385 (2009).

201. Peeters, M. Y. *et al.* Propofol pharmacokinetics and pharmacodynamics for depth of sedation in nonventilated infants after major craniofacial surgery. *Anesthesiology* **104**, 466–474 (2006).

202. Lam, J. *et al.* The ontogeny of P-glycoprotein in the developing human blood-brain barrier: implication for opioid toxicity in neonates. *Pediatr Res* **78**, 417–421 (2015).

203. Mulla, H. Understanding developmental pharmacodynamics: importance for drug development and clinical practice. *Paediatr Drugs* **12**, 223–233 (2010).